Propagation effects in atomic systems for ultrashort and long pulses: Control of the optical response

Faheel Hashmi

Université de Toulouse

THÈSE

En vue de l'obtention du

DOCTORAT DE L'UNIVERSITÉ DE TOULOUSE

Délivré par *l'Université Toulouse III - Paul Sabatier*
Discipline ou spécialité : *Physique de la Matière*

Présentée et soutenue par *Faheel-Ather HASHMI*
Le *03 FEVRIER 2009*

Titre : *Effets de propagation dans des systèmes atomiques en régime d'impulsions longues et courtes: Contrôle de la réponse optique*

JURY
M. Kamel BENCHEIKH (Examinateur)
M. Mohamed Aziz BOUCHENE (Directeur de thèse)
M. Daniel BRAUN (Examinateur)
M. Fabien BRETENAKER (Rapporteur)
M. Thomas COUDREAU (Rapporteur)
M. Claude FABRE (Examinateur)
M. Michael FLEISCHHAUER (Examinateur)

Ecole doctorale : *Science de la Matière*
Unité de recherche : *Laboratoire "Collisions Agrégats Réactivité"*
Directeur(s) de Thèse : *M. Mohamed Aziz BOUCHENE*
Rapporteurs :

Acknowledgments

First of all, and most of all, I am grateful to Aziz. I wish to thank the ex and the present directors of the lab LCAR Bertrand GIRARD and Jacques VIGUÉ, the members of the jury, all the people in the lab, the Pakistani community in Toulouse, and friends and family. I wish to thank also the Higher Education Commission of Pakistan for providing funds for this research and to "Société française d'exportation des ressources éducatives" for taking care of my stay in France.

List of Publications

- Chapter 2
  - *Phase control of non-adiabatic optical transitions*,
    F. A. Hashmi and M. A. Bouchene, accepted in Phys. Rev. A (2009).
  - *Application of propagation effects in atomic vapours for the shaping of ultrashort pulses*,
    J. C. Delagnes, F. A. Hashmi and M. A. Bouchene, in Aspects of Optical Sciences and Quantum Information, edited by M. Abdel-Aty, Research Signpost, Kerala (2007).
  - *Spectral and temporal modifications of a weak resonant ultrashort pulse propagating in a two level system driven by a strong non-resonant field*,
    J. C. Delagnes, F. A. Hashmi and M. A. Bouchene, Phys. Rev. A **74**, 053822 (2006).
- Chapter 3
  - *Slowing and storing light processes without a trapping dark state in a duplicated two-level system: Theoretical study*,
    F. A. Hashmi and M. A. Bouchene, submitted to J. Mod. Opt. (2008).
  - *Slowing light through Zeeman coherence oscillations in a duplicated two-level system*,
    F. A. Hashmi and M. A. Bouchene, Phys. Rev. A **77**, 051803(R) (2008).
- Chapter 4
  - *Coherent control of the effective susceptibility through wave mixing in a duplicated two-level system*,
    F. A. Hashmi and M. A. Bouchene, Phys. Rev. Lett. **101**, 213601 (2008).

– *Phase control of medium gain in a duplicated two-level system: From ultrashort to long pulse regime*,
F. A. Hashmi and M. A. Bouchene, Applied Mathematics & Information Science **1**, 305 (2007).

Contents

List of Figures

Introduction

Coherent propagation of light pulses in dense atomic media has been extensively studied in $70's$ and $80's$, and is now a well established domain in optics. In limit of monochromatic waves, and for weak light fields, the response of the medium is determined by the linear susceptibility that describes the absorptive and dispersive properties of the medium. For strong fields, non-linear phenomena like optical bi-stability, intensity-dependent refractive index, saturation induced transparency appear [Boyd92, Allen75]. However, it is often true that the both the dispersion and the non-linear response effects are masked by the strong linear absorption. That is why, the techniques that can modify the optical response of the system, and get rid of strong absorption at resonance, have received a lot attention in the last decade and a half. Spectacular experiments have been performed and have given birth to new research fields in physics. Slow, stored and fast light [Milonni02, Milonni05, Fleischhauer05], and giant Kerr nonlinearity [Schmidt96, Kang03] are some non-exhaustive examples. In parallel the tailoring of the optical

La propagation d'impulsions lumineuses dans des milieux atomiques denses a été étudiée intensivement dans les années 70 et 80, et représente actuellement un domaine bien connu de l'optique. Dans la limite d'une onde monochromatique peu intense, la réponse du milieu est déterminé par la susceptibilité linéaire qui décrit les propriétés d'absorption et de dispersion du milieu. Pour des champs intenses, des phénomènes non linéaires tel que la bi-stabilité optique, l'effet Kerr dynamique, l'autofocalisation, la transparence induite par saturation apparaissent [Boyd92, Allen75]. Cependant, il est souvent vrai que les propriétés dispersives et les effets dus à la réponse non linéaire sont masqués par la forte absorption. C'est pour cela que les techniques permettant de se débarrasser de la forte absorption à résonance ont reçu une attention particulière ces quinze dernières années. Des expériences spectaculaires ont été menées et ont données naissance à de nouveaux domaines de recherche en physique. La lumière lente, rapide, stockée [Milonni02, Milonni05, Fleischhauer05] et l'effet Kerr géant [Schmidt96, Kang03] en sont quelques

response has given rise to negative refractive index physics [Pendry00, Shelby01] which is very promising for realizing a perfect lens. Part of the present thesis deals with the propagation of light pulses in atomic media whose optical response has been modified.

For ultrashort pulse, the propagation effects are entirely different than for the long pulse regime. The key element in their propagation is considered to be the McCall&Hahn theorem [McCall67, McCall69]. It states that the pulse area saturates with the propagation. In strong pulse regime, the theorem led to theoretical studies and experimental realization of a lot of interesting phenomena. Break-up of large pulses into smaller ones [Gibbs70, Lamb71, Slusher72], pulse (self) compression by coherent absorption [Gibbs71], and self induced transparency [Gibbs70, Lamb71, Slusher72, Patel67, Crisp69, Patel70] are some to name. In the weak field regime the theorem predicts vanishing pulse area with the propagation distance and has been studied theoretically [Crisp70] and experimentally [Rothenberg84]. Weak ultrashort pulse develop strong oscillatory structures during propagation to satisfy the vanishing pulse area while maintaining pulse energy, as the significant absorption of the ultrashort pulses can not take place [Eberly81, Felinto04, Dudovich02, Kallmann99, Christov98, Bouchène92, Arlt97a, Arlt97b, Avenel83]. An-

exemples. En parallèle, la mise en forme de la réponse optique a donné naissance à la physiques des milieux à indice négatif [Pendry00, Shelby01] très prometteur pour la réalisation de lentilles parfaites. Une partie de cette thèse traite de la propagation d'impulsions lumineuse dans des milieux atomiques dont on a modifié la réponse optique.

Pour des impulsions ultracourtes, les effets de propagation sont entièrement différents de ceux obtenues en régime d'impulsions longues. L'élément clé dans cette propagation est le théorème de McCall&Hahn [McCall67, McCall69]. Celui-ci indique que l'aire de l'impulsion sature durant la propagation. En régime d'impulsion intense, le théorème a conduit à des études théoriques et à la réalisation expérimentale de nombreux phénomènes intéressants. La fragmentation d'impulsions larges en de plus petites [Gibbs70, Lamb71, Slusher72], l'auto-compression de l'impulsion par absorption cohérente [Gibbs71] et la transparence auto-induite [Gibbs70, Lamb71, Slusher72, Patel67, Crisp69, Patel70] en sont quelques exemples. En régime de champ faible, le théorème prédit la décroissance rapide de l'aire de l'impulsion au cours de la propagation, et a été étudié théoriquement [Crisp70] et expérimentalement [Rothenberg84]. Puisque aucune absorption significative ne peut se produire pour des impulsions ultracourtes, les impulsions ultracourtes et de faible intensité présentent des structures fortement oscillantes durant la propagation afin de satisfaire à la double condition

other part of the thesis deals with the propagation of ultrashort pulses. The propagation effects can be used to probe the atomic dynamics as the two are coupled (through Maxwell Bloch equations), and in the opposite sense, the atomic dynamics can be adjusted (by a strong field) to produce the desired shaping effects. This phenomena in both respects will be presented with the study of propagation effects in strongly driven atomic media.

The study is also the continuation of the research being carried out in the lab by M. A. Bouchene and coworkers. Propagation effects experienced by the femtosecond pulses and the control of these effects have been studied. It has been shown that the propagation effects can be compensated for by using a pulse-shaper that introduces the phase on the spectral components, opposite to the one introduced by dispersion [Delagnes07f]. The propagation effects have been used to probe strongly driven transitions [Delagnes04], and to study the gain-dispersion coupling induced by the transient light-shifts in a driven two-level system [Delagnes07c]. Finally, the double two-level system — for which the modification of the linear response in long pulse regime will be presented in the present thesis — has also been studied in ultrashort pulse regime. The coherent control of the medium gain and the pulse shape [Delagnes07b], the influence of time

d'aire nulle et d'énergie lumineuse constante [Eberly81, Felinto04, Dudovich02, Kallmann99, Christov98, Bouchène92, Arlt97a, Arlt97b, Avenel83]. Une autre partie de cette thèse traite de la propagation d'impulsions ultracourtes. Les effets de propagation peuvent être utilisés pour sonder la dynamique atomique puisque les deux phénomènes sont couplés (à travers les équations de Maxwell), et en sens opposé, la dynamique atomique peut être ajustée (par un champ fort) pour produire l'effet de mise en forme désiré.

L'étude que nous avons mené est aussi la continuation de travaux de recherche antérieurs menés au sein du laboratoire par M. A. Bouchene et ses collaborateurs. Les effets de propagation subis par des impulsions femtosecondes et le contrôle de ces effets ont été étudiés. Il a été montré que les effets de propagation pouvaient être compensé en utilisant un dispositif type "pulse-shaper" qui introduisait une phase spectrales opposé à celle de la dispersion [Delagnes07f]. Les effets de propagation ont été aussi utilisé pour sonder des transitions fortement couplés optiquement [Delagnes04], et pour étudier le couplage gain-dispersion induit par les déplacements lumineux dans un système à deux niveaux couplé au rayonnement [Delagnes07c]. Finalement, le système à deux niveaux double — pour lequel la modification de la réponse linéaire en régime d'impulsions longues sera présenté dans cette thèse — a été aussi étudié

delay [Delagnes07a], and the spin orbit effects [Delagnes07d] have been studied.

en régime d'impulsion ultracourtes. Le contrôle cohérent du gain du milieu ainsi que la forme de l'impulsion [Delagnes07b], l'influence du retard entre impulsions [Delagnes07a] et les effets de spin orbite [Delagnes07d] ont été étudiés.

The organization and the contents of the next Chapters are as follows.

L'organisation et le contenu des chapitres suivants sont comme suit.

In Chapter 1, I present the light interaction with a two-level atomic system in both long and ultrashort pulse regime. I will discuss the basics of propagation effects for the two pulse-duration regimes and derive the expression for the light group-velocity. The Chapter will also be used to establish the formalism and the notation that will be used in the latter Chapters to discuss various results.

Dans le chapitre 1, je présenterai l'interaction de la lumière avec un système atomique à deux niveaux dans le régime d'impulsions longues et courtes. Je discuterai les éléments de base des effets de propagation pour les deux régimes d'impulsions et je dériverai l'expression de la vitesse de groupe de la lumière. Ce chapitre servira aussi à établir le formalisme et les notations qui seront utilisés dans les autres chapitres pour discuter de résultats variés.

Chapter 2, deals with the strongly driven two-level system in ultrashort pulse regime and the probing of the system through resonant propagation effects. Strongly driven two-level systems have been extensively studied and the basic characteristics like Rabi oscillations [Rabi37, Gibbs73], adiabatic following [Grischkowsky73, Grischkowsky72], and Mollow triplet [Mollow72, Wu77] have been established in $70's$. The features that interest us are light-shifts and non-adiabatic transitions introduced by strong non-resonant pulses and described in adiabatic basis [Cohen-Tannoudji98]. The technique developed in [Delagnes04] to probe the light shifts in a three

Le chapitre 2, traite du système à deux niveaux piloté par des impulsions femtosecondes en régime de champ fort et sondé à travers les effets de propagation résonante. Les systèmes à deux niveaux excités en champs fort ont été étudiés de manière intensive et les effets caractéristiques de base tels que les oscillations de Rabi [Rabi37, Gibbs73], l'évolution adiabatique [Grischkowsky73, Grischkowsky72], et le triplet de Mollow [Mollow72, Wu77] ont été établis dans les années 70. Les aspects qui nous intéressent sont les déplacements lumineux et les transitions non adiabatiques induits par des impulsions intenses non résonantes, et décrits

level system will be used in a two level system [Delagnes06] which is paradoxically more complex to analyze. This is also a pulse shaping technique which can work in ultraviolet and picosecond pulse regimes where the traditional pulse-shaping methods [Zeek99, Tull97, Wefers95] can not function efficiently. We also focus on non-adiabatic transitions [Shore90] in the system, and make use of the shape-dependence of these transitions [Berman98] to cause complete population inversion [Vitanov07, Torosov07, Vasilev06] in the adiabatic basis. The novelty in the scheme that will be proposed in the present work is the extreme sensitivity of the asymptotic bare state populations on the relative phase between the exciting pulses. The phenomena is explained in terms of the control of non-adiabatic jump, and rapid adiabatic passage [Melinger92, Liedenbaum89, Allen75] that appears in a specifically well adapted adiabatic basis. With the virtue of this increased sensitivity, this effect can lead to the improvement of the techniques based on interferometry such as lock-in techniques, meteorology, Ramsey spectroscopy, coherent control, pump-probe techniques, and gyro-laser techniques to name some [Demtröder96, Bass01, Diels96]. Finally in the last part of the Chapter we will apply the technique developed in [Delagnes04, Delagnes06] to probe the non-adiabatic jump in real time, which is otherwise not visible in real populations [Vasilev06].

dans la base adiabatique [Cohen-Tannoudji98]. La technique développée en [Delagnes04] pour sonder les déplacements lumineux dans un système à trois niveaux sera étendue dans un système à deux niveaux [Delagnes06] qui est paradoxalement plus complexe à analyser. Cette méthode représente aussi une technique de mise en forme d'impulsions qui peut s'appliquer dans le domaine UV et pour des impulsions picosecondes où les méthodes traditionnelles [Zeek99, Tull97, Wefers95] ne sont pas efficaces. Nous nous focaliserons aussi sur les transitions non-adiabatiques [Shore90] dans le système et nous verrons comment tirer profit de la dépendance en fonction de la forme temporelle [Berman98] pour réaliser une inversion totale de la population [Vitanov07, Torosov07, Vasilev06] dans la base adiabatique. La nouveauté dans le schéma que nous proposons dans le chapitre présent est l'extrême sensibilité à la phase relative entre impulsions excitatrices de la population asymptotique (dans la base diabatique). Le phénomène est expliqué en termes de contrôle de sauts non adiabatiques et de passage adiabatique rapide [Melinger92, Liedenbaum89, Allen75] qui apparaît dans une base adaptée. En raison de cette sensibilité accrue, cet effet peut amener à une amélioration des techniques interféromètriques tels que l'asservissement, la métrologie, la spectroscopie Ramsey, le contrôle cohérent, les techniques pompe-sonde et les techniques liés au gyrolaser [Demtröder96, Bass01, Diels96]. En-

Chapter 3, deals with a new technique [Hashmi08b] that suppress the linear absorption of a driven double two-level system for a linearly polarized probe field in the presence of a much stronger orthogonally polarized control field. The spectral transparency window obtained can be very narrow and can be used to produce slow light. Slow light, besides being a fascinating phenomena, is important from technological point of view as it has tremendous potential for all optical communication. Optical buffering, real-time-delay lines, optical memories, and data synchronization [Gauthier05, Gauthier06] are some to name that can benefit from slow light technology. Ultraslow light has also paved the way for light storage [Liu01] and for quantum memories [Fleischhauer02], for the computing machines of the future. The early realizations of slow light [Kasapi95] were carried out using quantum interference effects in three-level systems associated with *electromagnetic induced transparency*(EIT) [Fleischhauer05, Marangos98, Boller91]. Later, *coherent population oscillations* (CPO) [Boyd88, Boyd81, Schwarz67] in a two level system were used to produce slow light in artificial structures

fin, dans la dernière partie de ce chapitre nous appliquerons la technique développée en [Delagnes04, Delagnes06] pour sonder le saut non adiabatique en temps réel, qui n'est autrement pas visible dans les populations des états diabatiques [Vasilev06].

Le chapitre 3 traite d'une nouvelle technique [Hashmi08b] qui permet de supprimer pour un champ sonde polarisé linéairement l'absorption par un système à deux niveaux dupliqué et ce en présence d'un champ contrôle plus intense et polarisé perpendiculairement. La fenêtre de transparence spectrale obtenue peut être très étroite et peut être utilisé pour ralentir la lumière. La lumière lente en plus d'être un phénomène fascinant, est important d'un point de vue technologique par les potentialités nombreuses qu'elle ouvre pour les communications "tout optique". Les mémoires tampons optiques, les lignes à retard en temps réel, les mémoires optiques, et la synchronisation de données [Gauthier05, Gauthier06] peuvent tous bénéficier des retombées technologiques liées à la lumière lente. La possibilité de ralentir la lumière a ouvert la voie au stockage de lumière [Liu01] et à la réalisation de mémoires quantiques [Fleischhauer02] pour les ordinateurs de demain. Les premières réalisations de lumière lente [Kasapi95] ont été menés en utilisant les interférences quantiques associées à la transparence électromagnétique induite par laser (TEI) dans les systèmes à trois niveaux [Fleischhauer05, Marangos98,

[Bigelow03b, Bigelow03a]. Other techniques that modify the dispersive response of the medium have also been used to produce slow lights. These include stimulated Raman scattering [Kijoon01], stimulated Brillion scattering [Okawachi05], and dispersion in photonic crystals [Gersen05]. The method presented here can be thought of as a hybrid between EIT and CPO as it presents features that are more like EIT and acts in a way which is more like CPO.

Boller91]. Plus tard, les oscillations cohérentes de population (OCP) [Boyd88, Boyd81, Schwarz67] dans un système à deux niveaux ont été utilisés pour produire de la lumière lente dans des structures artificielles [Bigelow03b, Bigelow03a]. D'autres techniques qui modifient les propriétés dispersives ont été aussi utilisées pour produire de la lumière lente. Ceci inclus la diffusion Raman stimulée [Kijoon01], la diffusion Brillouin stimulée [Okawachi05] et la dispersion dans les cristaux photoniques [Gersen05]. La méthode présentée ici peut être considérée comme hybride entre celle basée sur la TEI et celle basée su les OCP car elle présente des caractéristiques assez similaires à la première mais est plus proche dans son principe de la deuxième.

The last Chapter deals with the coherent control of the medium response of the system. The idea of the control of the dynamics of a physical system interacting with coherent laser fields arose in $80's$ and matured by the beginning of the present decade [Shapiro03]. The interaction of mutually coherent light fields with quantum mechanical systems gives rise to different quantum paths. The key idea of the control is to make use of interference between these different quantum paths to suppress or favor specific channels. Several mechanisms in this regard have been explored. The combination of a fundamental frequency and its harmonics [Brumer86], and excitation by time delayed coherent

Le dernier chapitre traite du contrôle cohérent de la réponse optique d'un milieu. L'idée du contrôle de la dynamique d'un système physique interagissant avec des champs lasers cohérents est apparue dans les années 80 et a mûri dans le début de cette dernière décade [Shapiro03]. L'interaction de champs mutuellement cohérents avec le système quantique donne naissance à plusieurs chemins quantiques. L'idée centrale du contrôle est d'utiliser ces interférences entre différents chemins quantiques pour supprimer ou favoriser une voie spécifique. A cet égard, plusieurs mécanismes ont été explorés. La combinaison d'une fréquence fondamentale et ses harmoniques [Brumer86], l'excitation par des impulsions cohérentes

pulses [Scherer90] are some examples. The control comes from the relative optical phase difference between different excitation fields. The advantage in such schemes is the ease and versatility in the control of the relative phase. This can, for instance, be achieved by simply modifying the delay between the sequence of excitation pulses [Blanchet97]. In this last Chapter, I present the control of the medium susceptibility for low optical densities [Hashmi08a]. This can be realized in the same double two-level system discussed in Chapter 3, in connection with the slow light. The techniques that suppress the linear absorption of a medium, make the nonlinear interaction more accessible to study and to control. For example the use of a nonlinear scheme to suppress absorption through EIT and achieve giant Kerr response has been proposed [Schmidt96] and realized [Kang03]. Phase control of EIT [Kapale05] and Kerr nonlinearity [Sun08] have also been demonstrated. Other techniques for the control of the optical response has also been proposed [McCullough00]. In the situation presented in Chapter 4, the result is striking because of the simplicity of the obtained expression of the effective susceptibility. It is just the linear susceptibility times a phase factor that renders gain dispersion coupling. A versatile control of the absorptive and dispersive profiles is thus possible by adjusting the relative phase between the exciting fields. For higher optical depths

décalées en temps [Scherer90] en sont quelques exemples. Le contrôle provient de la différence de phase optique entre différents champs excitateurs. L'avantage dans ces schémas est la facilité et la flexibilité dans le contrôle de la phase relative. Ceci peut être effectué en modifiant simplement le retard entre impulsions excitatrices [Blanchet97]. Dans ce dernier chapitre, je présenterai le contrôle de la susceptibilité pour des densités optiques faibles [Hashmi08a]. Ceci est réalisé dans le même système à deux niveaux double discuté dans le chapitre 3 en connexion avec la lumière lente. Les techniques qui permettent la suppression de l'absorption linéaire d'un milieu, rendent la réponse non linéaire accessible à l'étude et au contrôle. Par exemple, il a été proposé [Schmidt96] et expérimentalement réalisé [Kang03] un schéma d'excitation non linéaire basé sur la suppression de l'absorption par la TEI, ce qui a permis l'obtention d'une réponse Kerr géante. Un contrôle de phase de la TEI [Kapale05] et de la non linéarité Kerr [Sun08] a été aussi démontré. D'autres techniques pour le contrôle de la réponse optique ont été proposés [McCullough00]. Dans la situation de ce chapitre, le résultat est particulièrement frappant à cause de la simplicité de l'expression de la susceptibilité effective obtenue. Elle s'écrit simplement comme le produit de la susceptibilité linéaire par un terme de phase ce qui va donner un couplage gain-dispersion. Un contrôle aisé des profils d'absorption et de dis-

phase saturation takes place with the system changing into an efficient amplifier for the probe and can build the probe from infinitesimally small values [Lukin98].

persion est alors possible en ajustant la phase relative entre champs excitateurs. Pour des densités optiques plus élevées, la saturation de la phase se produit dans le système transformant ce dernier en un amplificateur efficace pour le champ sonde et peut donc reconstruire la sonde à partir de valeurs infimes [Lukin98].

Chapter 1

Light interaction with a Two-level system

In this chapter I will present the interaction and propagation of light in a two-level atomic system. The two-level system is a very convenient, first tool to study light-matter interaction. A lot of real problems in optics can be modeled by simple two-level systems, and such systems, despite being overly simple, provide a deep insight into the nature of the problem. In this regard, the two-level system— interacting with light pulses— has been extensively studied, and is now a text book example. I will recall some basic features of light interaction with the two-level system in different pulse duration regimes. This will also introduce us to the notation and formalism required to discuss the results in next chapters.

Dans ce chapitre, je présenterai l'interaction et la propagation de la lumière dans un système atomique à deux niveaux. Le système à deux niveaux est pratique pour étudier dans une première étape l'interaction lumière-matière. Un grand nombre de problèmes en optique peuvent être modélisés par des systèmes à deux niveaux qui même simple permettent d'avoir une vue approfondie de la nature du problème. C'est pour cela que le système à deux niveaux - interagissant avec des impulsions lumineuses- a été étudié de manière intensive et représente actuellement un cas d'école. Je vais rappeler quelques éléments de base de l'interaction de la lumière avec le système à deux niveaux dans différents régimes d'impulsions. Cela permettra de nous initier aux notations et formalismes requis pour discuter les chapitres sui-

The interaction is studied in the limit of *semiclassical approximation*. In this approximation, the atomic system is treated quantum mechanically with well defined discrete energy levels, whereas the interacting light is given by classical expressions. The approximation is justified as even the weakest light source has such a large number of photons, that, it can be treated classically. Moreover, the interaction terms are written using *dipole approximation*. This suggests that, since the size of an atom is much smaller than the typical wavelength of exciting radiation, the atom does not see any spatial variation of the electric field, and responds only to the instantaneous electric field. Another conventional approximation is *rotating wave approximation*(RWA). This assumes that the laser frequency is the largest possible frequency in the system, and any dynamics going on at still higher frequencies can be averaged out. Finally, *slowly varying envelope approximation* suggests that the variation of the electric field envelope across the time and length scales of one optical period and unit wavelength is negligible.

L'interaction est étudiée dans la limite de l'approximation semiclassique. Dans cette approximation, le système atomique est traité quantiquement avec des niveaux d'énergie discrets bien définis, tandis que la lumière qui interagit est traitée classiquement. L'approximation est justifiée car même des sources de lumière faibles contiennent en général un grand nombre de photons justifiant par là le traitement classique. De plus, les termes d'interaction sont écrits en utilisant l'approximation dipolaire. Cela traduit le fait que comme la dimension de chaque atome est bien plus petite que la longueur d'onde caractéristique de la radiation, l'atome ne peut voir aucune variation spatiale du champ électrique et réponds uniquement à la valeur instantannée du champ. Une autre approximation utilisée est l'approximation de l'onde tournante (RWA). Elle suppose que la fréquence laser est la plus large possible dans le système et toute dynamique à des fréquences plus élevées peut être moyennée. Enfin, l'approximation de l'enveloppe lentement variable suggère que la variation de l'enveloppe du champ électrique sur des échelles de temps et d'espace de l'ordre de la période optique et de la longueur d'onde sont négligeables.

I will present the interaction of coherent light with a closed two-level atomic system in two pulse duration regimes— short and long pulse regimes. In short pulse regime,

Je vais présenter l'interaction de lumière cohérente avec un système à deux niveaux fermé dans deux régimes de durée d'impulsions, courtes et longues. En régime d'impulsions

the relaxation processes can be neglected, and the dynamics are dominated by the transient phenomena. The formalism more adapted to study this regime is that of time dependent Schrödinger equation, and in the limit of strong non-resonant exciting fields, adiabatically dressed basis [Cohen-Tannoudji98] can provide a better insight into the interaction. On the other hand, for long pulses we have to take into account the relaxation processes. Density matrix formalism in this case is more suitable. I will discuss the two formalisms, and then present the propagation of light pulses in the two pulse-duration regimes. Finally, I will discuss the velocity of light propagation in an atomic medium.

courtes, les processus de relaxations peuvent être négligés, et la dynamique est dominée par des phénomènes transitoires. Le formalisme adaptée pour étudier ce régime est celui de l'équation de Schrödinger dépendante du temps et dans la limite de champs forts non-résonants, la base adiabatique [Cohen-Tannoudji98] permet d'avoir une meilleure vision de l'interaction. D'un autre côté, pour des impulsions longues on doit tenir compte des processus de relaxation. Le formalisme de la matrice densité est alors plus adapté. Je discuterai ces deux formalismes, et présenterai alors la propagation d'impulsions lumineuses dans les deux régimes de durée d'impulsions. Finalement, je discuterai la vitesse de propagation dans un système atomique.

1.1 The Two-level system

Consider a two-level atomic system consisting of states $|a\rangle$ and $|c\rangle$ with the energy difference $\hbar\omega_0$ between the states as shown in Fig. 1.1. The system interacts with a classical electrical field given by the expression

$$\vec{E}_c(y,t) = \vec{e}_z A_c f_c(t,y)\, e^{-i(\omega_c t - k_c y)} + cc. \tag{1.1}$$

$\vec{e}_z$ is the polarization unit vector, A_c is the field amplitude, and $f_c(t,y)$ is the field envelope. The field is real at the entrance of the medium (at $y=0$), and the envelope is normalized to unity $\int_\infty^\infty f_c(t,0)\, d(t/\tau_c) = 1$. τ_c is the field duration, *cc* in the above expression denotes the complex conjugate, and the field propagates along y axis. The field is detuned by $\Delta_c = \omega_0 - \omega_c$ from resonance and has the temporal duration τ_c. In the *dipole approximation* the interaction of the field with the atomic system is given by $-\hat{\vec{D}} \cdot \vec{E}_c$, where $\hat{\vec{D}}$ is the instantaneous dipole moment. We define the dipole matrix element as $D = \left\langle a|\hat{\vec{D}} \cdot \vec{e}_z|c\right\rangle$. The Rabi frequency associated with the interaction is

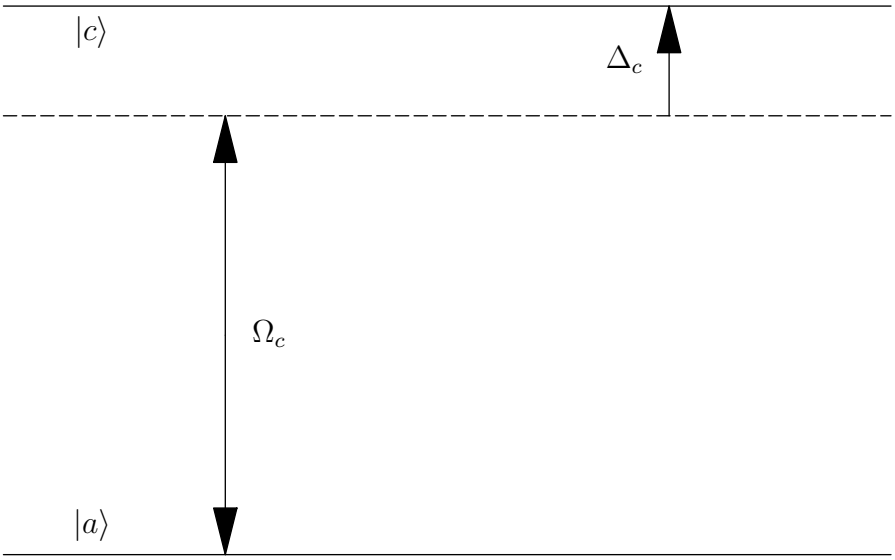

Figure 1.1: A two level system interacting with a laser field.

$\Omega_c = DA_c f_c/\hbar$. The Hamiltonian of the system is given by

$$H = \begin{pmatrix} 0 & -\vec{D}\cdot\vec{E}_c \\ -\vec{D}\cdot\vec{E}_c & \hbar\omega_0 \end{pmatrix}. \tag{1.2}$$

The Hamiltonian contains the components oscillating with $e^{-i\omega_c t}$ and $e^{i\omega_c t}$. We place ourselves in the frame of reference oscillating with $e^{-i\omega_c t}$, and average out the components oscillating with double the frequency using RWA. We next take the case of different pulse duration regimes independently.

1.1.1 Ultrashort pulse regime

For ultrashort pulses, the relaxation processes are not important. These processes take place at the time scale of nanoseconds, and hence for the pulses having the time duration of the order of picoseconds or femtoseconds, these processes can safely be neglected. We write the wavefunction of the system as (simplifying the notation by removing y dependence):

$$|\Psi(t)\rangle = a(t)|a\rangle + c(t)\,e^{-i\omega_c t}|c\rangle. \tag{1.3}$$

The evolution of the system is given by time dependent Schrödinger equation

$$i\hbar\partial_t|\Psi\rangle = H|\Psi\rangle. \tag{1.4}$$

Using Eq. (1.2,1.3) in Eq. (1.4) and after carrying out RWA, we can write the time evolution of the system as

$$i\hbar\partial_t \begin{pmatrix} a \\ c \end{pmatrix}(t) = \tilde{H} \begin{pmatrix} a \\ c \end{pmatrix}(t), \tag{1.5}$$

with

$$\tilde{H} = \hbar \begin{pmatrix} 0 & -\Omega_c^* \\ -\Omega_c & \Delta_c \end{pmatrix}. \tag{1.6}$$

The general solution of Eq. (1.5) is not known and one has to resort to numerical solutions. However, for certain special cases, analytical or approximate solutions can be worked out. We next take up certain such cases.

For resonant excitation $\Delta_c = 0$, and for real field $\Omega_c^* = \Omega_c$, the Eq. (1.5) can be solved analytically. Assuming all the population to be initially in the ground state, the state of the system at a time t is given by

$$a(t) = \cos\left(\int_{-\infty}^{t} \Omega_c\left(\acute{t}\right) d\acute{t}\right), \tag{1.7a}$$

$$c(t) = i\sin\left(\int_{-\infty}^{t} \Omega_c\left(\acute{t}\right) d\acute{t}\right). \tag{1.7b}$$

The populations exhibit well known Rabi oscillations [Rabi37, Gibbs73], and the asymptotic population transfer to the excited state is determined by the pulse area $\int_{-\infty}^{\infty} \Omega_c(t)\, dt$, which is proportional to the Fourier transform of the field at central laser frequency.

For arbitrary detuning and complex fields, one can work out perturbative solutions in the limit of weak field regime. If the field is weak enough such that $\Omega_c \ll \tau_c^{-1}$, then at *zeroth order* with respect to field amplitude, we have $a^{(0)}(t) = 1$ and $c^{(0)}(t) = 0$. At *first order* one gets

$$a^{(1)}(t) \simeq 1, \tag{1.8a}$$

$$c^{(1)}(t) \simeq ie^{-i\Delta_c t} \int_{-\infty}^{t} \Omega_c\left(\acute{t}\right) e^{i\Delta_c \acute{t}} d\acute{t}. \tag{1.8b}$$

The asymptotic population in excited state is determined by $\int_{-\infty}^{\infty} \Omega_c\left(\acute{t}\right) e^{i\Delta_c \acute{t}} d\acute{t}$ which is again proportional to the Fourier transform of the field at atomic frequency.

In both the above cases, the Fourier components at resonance determine the asymptotic population transfer to the excited state. For more general and stronger pulses, the entire pulse spectrum has to be taken into account, and alternative methods are required to study the interaction.

1.1.2 Adiabatic basis

Adiabatic bases [Cohen-Tannoudji98] provide an alternative insight into the light interaction with atomic system, and are particularly well suited in the case of strong pulses. Assuming real field for simplicity, we define a rotation matrix as

$$R(t) = \begin{pmatrix} \cos\theta & \sin\theta \\ -\sin\theta & \cos\theta \end{pmatrix}(t). \tag{1.9}$$

Here θ is the mixing angle. It is defined for real field as

$$\tan(2\theta)(t) = \frac{2\Omega_c(t)}{\Delta_c}, \tag{1.10}$$

and lies between 0 and $\pi/2$. We define the generalized Rabi frequency as $\Omega = \sqrt{\Delta_c^2 + 4{\Omega_c}^2}$ and write some useful relations involving the mixing angle

$$\begin{aligned} &\sin 2\theta = 2\Omega_c/\Omega, && \cos 2\theta = \Delta_c/\Omega, \\ &\sin^2\theta = (\Omega - \Delta_c)/2\Omega, && \cos^2\theta = (\Omega + \Delta_c)/2\Omega. \end{aligned} \tag{1.11}$$

The adiabatic basis are now defined as

$$\begin{pmatrix} |\alpha\rangle \\ |\gamma\rangle \end{pmatrix}(t) = R(t) \begin{pmatrix} |a\rangle \\ e^{-i\omega_c t}|c\rangle \end{pmatrix}. \tag{1.12}$$

The time evolution for the adiabatic wave function

$$|\psi(t)\rangle = \alpha(t)|\alpha\rangle(t) + \gamma(t)|\gamma\rangle(t), \tag{1.13}$$

is given by

$$i\hbar\partial_t \begin{pmatrix} \alpha \\ \gamma \end{pmatrix}(t) = \left(R\tilde{H}R^\dagger - i\hbar R\partial_t R^\dagger\right)\begin{pmatrix} \alpha \\ \gamma \end{pmatrix}(t). \tag{1.14}$$

$R\tilde{H}R^\dagger$ is the adiabatic Hamiltonian. It is diagonal and given by

$$R\tilde{H}R^\dagger = \frac{\hbar}{2}\begin{pmatrix} \Delta_c - \Omega & 0 \\ 0 & \Delta_c + \Omega \end{pmatrix}. \tag{1.15}$$

The two diagonal terms represent light-shifted energy levels. The separation between the levels is given by $\hbar\Omega(t)$ which depends on the shape and the intensity of the field, as well as on detuning. The coupling between the

adiabatic levels is provided by the second term in Eq. (1.14). This second term constitutes non-adiabatic coupling (NAC) and is given by

$$-i\hbar R\partial_t R^\dagger = i\hbar \begin{pmatrix} 0 & 1 \\ -1 & 0 \end{pmatrix} \partial_t \theta. \tag{1.16}$$

The non-adiabatic coupling depends strongly on the shape of the pulse. It is given explicitly as

$$\left(\partial_t \theta\right)(t) = \frac{\Delta_c}{\Omega\left(t\right)^2} \left(\partial_t \Omega_c\right)(t). \tag{1.17}$$

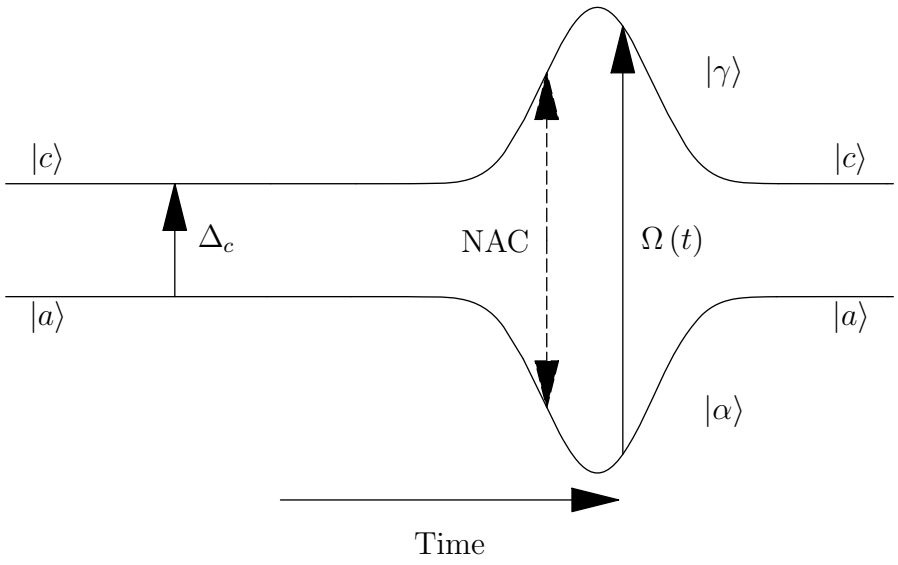

Figure 1.2: Two level system in adiabatic bases. The bare states are separated by Δ_c (after RWA). The strong field stretches the levels apart for transient time. The separation between the levels is proportional to $\Omega\left(t\right)$, and the transitions between the levels are provided by non-adiabatic coupling (NAC)

The system in adiabatic bases is shown in Fig. 1.2. The adiabatic energy levels are stretched in time due to the action of the field. This is a transient phenomena and as $t \to \pm\infty$, the energy levels relax back to the bare state picture. This stretching is known as "transient light shifts" and this introduces new frequency components in the system. The field also introduces " non-adiabatic coupling"(NAC) between the new energy levels.

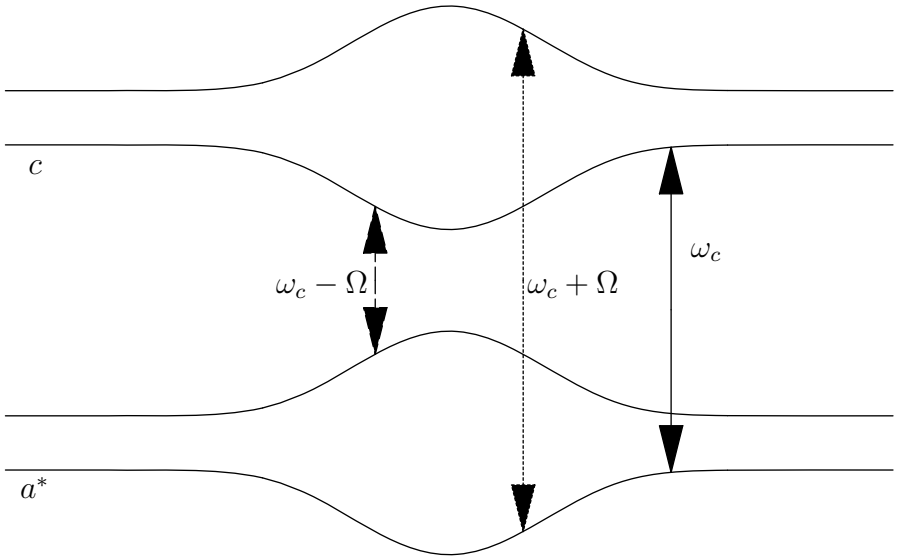

Figure 1.3: Coherence in adiabatic basis showing transient light shifts. In addition to ω_c, the system radiates at $\omega_c + \Omega$ and $\omega_c - \Omega$ frequencies during the transient time.

Coherence behavior

These new frequency components can be understood by looking at the coherence in the adiabatic basis. The coherence that is responsible for the radiated field is a^*c (as will be discussed in the next Section), and can be visualized in adiabatic basis as in Fig. 1.3. In addition to ω_c, the system radiates at frequencies $\omega_c + \Omega$ and $\omega_c - \Omega$ during the action of light shifts, provided that there is some population in excited adiabatic level. These new frequency components can be seen in the amplitude spectrum of the coherence are shown in Fig. 1.4 for a resonant strong field. The new components are similar to Mollow triplet [Mollow72] obtained when a strong non-resonant monochromatic field interacts with a two-level system. In the present case the Mollow triplet moves in time as the system is interacting with a pulse. Each new frequency component is generated twice during the interaction which causes these to interfere and result in the fringes shown in the Figure. The cutoff frequencies are given by $\omega_c - \Omega_{max}$ and $\omega_c + \Omega_{max}$, where Ω_{max} is the maximum separation between the light-shifted energy levels. These new frequency components can enrich the spectrum of another pulse that propagates in the medium, and can be used for wave-shaping of a weak ultrashort pulse. This will be discussed in Chapter. 2.

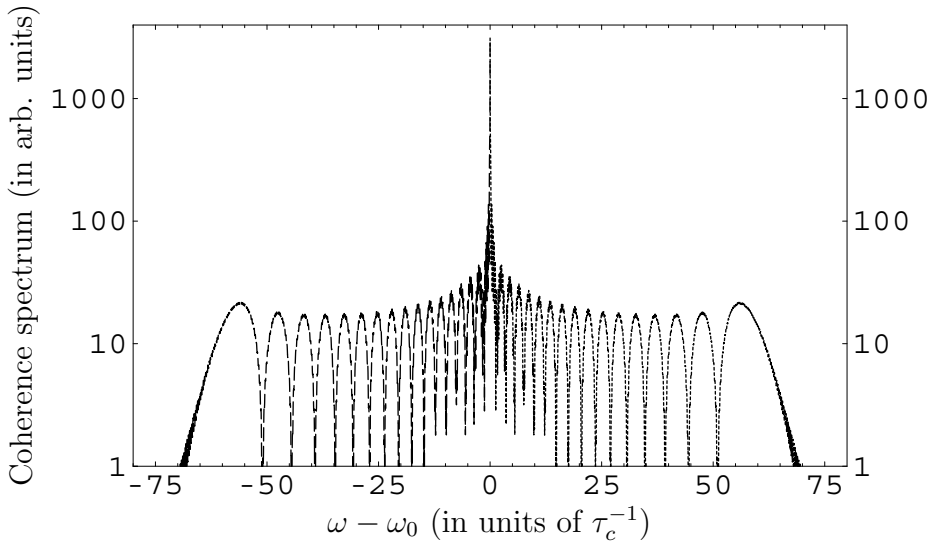

Figure 1.4: New frequency components generated during the action of light shifts with $\omega_c = \omega_0$. Each new component is generated twice, once when the levels are being stretched, and the second time when levels are relaxing back. The components at these two times interfere to give the modulated structure. The field is $\Omega_c(t) = \Omega_{c0} e^{-(t/\tau_c)^2}$ with $\Omega_{c0} = 60\tau_c^{-1}$, $\Delta_c = 0$.

Adiabatic vs non-adiabatic evolution

In this dressed picture one can distinguish between adiabatic and non-adiabatic evolution. For resonant excitation, or when the pulse is smooth enough such that $\Omega \gg |\partial_t \theta|$, the Hamiltonian in (1.14) is diagonal. The two amplitudes evolve freely and accumulate different phases. The solution of (1.14) is given by

$$\alpha(t) = \alpha(-\infty) \int_{-\infty}^{t} e^{\frac{\Delta_c - \Omega(\acute{t})}{2}\acute{t}} d\acute{t}, \tag{1.18a}$$

$$\gamma(t) = \gamma(-\infty) \int_{-\infty}^{t} e^{\frac{\Delta_c + \Omega(\acute{t})}{2}\acute{t}} d\acute{t}. \tag{1.18b}$$

This is adiabatic evolution of the system, and in this case there is no population transfer to the excited adiabatic state. However, if adiabatic levels correspond to different bare states before and after the interaction, then a complete population transfer in bare states is possible. This happens for example in the case of chirped pulse adiabatic passage [Broers92]. For pulses such that $\Omega \gg |\partial_t \theta|$ is not satisfied, the non-adiabatic coupling becomes important. The population transfer to the excited state depends strongly on the shape of the pulse [Berman98], and is no longer determined by the spectral components at resonance. Significant population can be transfered to the excited state even when there are no resonant frequency components in the spectrum of the field. This is in complete contrast with the simplified view of the light-matter interaction, in which a photon can only be absorbed if it is resonant with the system. This simplified version turns out to be true only in the limit of weak field regime. For strong pulses non-adiabatic effects make the interaction possible even with the non-resonant photons. For suitably shaped pulses the non-adiabatic coupling can even be made into a sudden jump which abruptly and suddenly transfers all the population to the adiabatic excited state [Vasilev06]. A scheme to observe and control these non-adiabatic jumps will also be presented in Chapter. 2.

1.1.3 Long pulse regime

For pulses having time duration of the order of nanoseconds or larger, the relaxation processes have generally to be taken into account in atomic systems. The formalism more adapted to study the interaction in this long pulse regime is that of density matrix. We define a density matrix ρ for the system as

$$\rho(t) = \begin{pmatrix} \rho_{aa} & \rho_{ac} e^{i\omega_c t} \\ \rho_{ca} e^{-i\omega_c t} & \rho_{cc} \end{pmatrix} (t). \tag{1.19}$$

The diagonal elements of ρ correspond to the populations in two states and off-diagonal elements stand for the coherence. The trace of ρ is unity — $Tr(\rho) = 1$, and the elements of the matrix satisfy $\rho_{ij} = \rho^*_{ji}$. The time evolution of the system is given by

$$i\hbar\partial_t\rho = [H, \rho] + \text{relaxations}, \tag{1.20}$$

where relaxation terms are added phenomenologically. Using the definition of ρ and of Hamiltonian (from 1.2) in the above equation, and after carrying out RWA, we get following time evolution equations

$$i\partial_t\rho_{cc} = (\Omega^*_c\rho_{ca} - \Omega_c\rho_{ac}) - i\Gamma\rho_{cc}, \tag{1.21a}$$
$$i\partial_t\rho_{ca} = \Omega_c\left(\rho_{cc} - \rho_{aa}\right) + \bar{\Delta}^*_c\rho_{ca}, \tag{1.21b}$$

where $\bar{\Delta}_c = \Delta_c + i\Gamma_d$. We have used the following relaxation terms: Γ is the excited state population damping rate, and Γ_d is the rate at which the coherence is destroyed. In the absence of non-radiative homogeneous dephasing processes Γ_d reduces to $\Gamma/2$.

For the long pulse regime the adiabatic description of interaction does not remain very useful. Relaxation processes introduce new channels through which adiabatic levels can exchange populations and thus, the distinction between "adiabatic" and "non-adiabatic" evolution becomes obscure. The perturbative solutions in the limit of weak field can still be worked out. At *zeroth order* with respect to field amplitude, the solution of (1.21) is given by

$$\rho^{(0)}_{cc}(t) = \rho^{(0)}_{cc}(-\infty)e^{-\Gamma t} \tag{1.22a}$$
$$\rho^{(0)}_{ca}(t) = \rho^{(0)}_{ca}(-\infty)e^{-i\bar{\Delta}^*_c t} \tag{1.22b}$$

For a short transient time, the solution depends on the initial conditions. But since the system is damped, as $t \to \infty$, the system attains a stationary state that is independent of the initial condition (for the present example). At *first order* the solution becomes

$$i\rho^{(1)}_{cc}(t) = Ce^{-\Gamma t} + e^{-\Gamma t}\int_0^t \Omega_c\left[\rho^{(0)}_{ca}(\acute{t}) - cc\right]e^{\Gamma\acute{t}}d\acute{t} \tag{1.23a}$$
$$i\rho^{(1)}_{ca}(t) = De^{-i\bar{\Delta}^*_c t} + e^{-i\bar{\Delta}^*_c t}\int_0^t \Omega_c\left[2\rho^{(0)}_{cc}(\acute{t}) - 1\right]e^{i\bar{\Delta}^*_c\acute{t}}d\acute{t} \tag{1.23b}$$

here $C = i\rho^{(1)}_{cc}(-\infty) - \Omega_c\left[\rho^{(0)}_{ca}(-\infty) - cc\right]$, $D = i\rho^{(1)}_{ca}(-\infty) - \Omega_c\left[2\rho^{(0)}_{cc}(-\infty) - 1\right]$, *cc* stands for complex conjugate, and for simplicity we have considered real

field. Again, for a short transient time perturbative solution depends on initial conditions, but as $t \to \infty$, a steady state solution is reached. The steady state solution at all orders can be worked out by putting the left hand side of Eqs. (1.21) equal to *zero*, and solving the resulting algebraic equations. This gives

$$\rho_{ca} = \frac{\Omega_c \bar{\Delta}_c}{4|\Omega_c|^2 \Gamma_d \Gamma^{-1} + |\bar{\Delta}_c|^2}, \tag{1.24a}$$

$$\rho_{cc} = \frac{2|\Omega_c|^2 \Gamma_d \Gamma^{-1}}{4|\Omega_c|^2 \Gamma_d \Gamma^{-1} + |\bar{\Delta}_c|^2}. \tag{1.24b}$$

Two extreme cases can be discussed here. For strong fields such that $|\Omega_c| \gg \sqrt{\Gamma_d \Gamma}$, the field saturates the system. The population is equally distributed between the ground and the excited states and the coherence vanishes. The system becomes transparent to the field, and is said to be bleached by the strong field.

In the weak field regime for $|\Omega_c| \ll \sqrt{\Gamma_d \Gamma}$, we get the linear response. In the linear response most of the population rests in the ground state and the coherence simplifies to $\rho_{ca} = \Omega_c / \bar{\Delta}_c^*$. The real and imaginary parts of this coherence determine the absorptive and dispersive response of the medium as we shall later see.

1.2 Propagation effects

The electric field interacting with an atomic system is modified by the absorptive and dispersive response of the medium. These effects can be accounted for by solving the Maxwell's equations. The atomic response is determined by the polarization that enters into the Maxwell's equation as a source term. The solution of Maxwell's equation determines how the field is modified as it propagates inside the medium. We will first derive the equation of propagation for the electric field, and then discuss the propagation effects in short and long pulse regimes separately.

1.2.1 Equation of propagation

We start from Maxwell's equation of propagation with source term (in 1 dimension).

$$\left(\partial_y^2 - \frac{1}{c^2}\partial_t^2\right) \vec{E}_c = \mu_0 \partial_t^2 \vec{P}, \tag{1.25}$$

here $\mu_0 = (c^2\epsilon_0)^{-1}$ is the permeability of free space, and we have neglected the transverse gradient $(\partial_x^2 + \partial_z^2)\,\vec{E}_c$. This approximation is in line for the laser beams that are not tightly focused, and hence are not strongly diverging. The variations along the transverse direction for such beams are negligible as compared to the variations along the propagation direction, and this justifies the one dimensional treatment. The polarization can be written as

$$\vec{P}\,(t,y) = \vec{e}_z\,\varrho\,(t,y)\,e^{-i(\omega_c t - k_c y)} + cc. \tag{1.26}$$

ϱ is the polarization amplitude. The expressions of the field (1.1), and the polarization (1.26) can be used in Eq. (1.25), and the terms containing second derivatives with respect to time and space can be simplified using following approximations:

$$|\partial_y^2 A_c| \ll k_c|\partial_y A_c|, \tag{1.27a}$$

$$|\partial_t^2 A_c| \ll \omega_c|\partial_t A_c|, \tag{1.27b}$$

$$|\partial_t^2 \varrho| \ll \omega_c|\partial_t \varrho| \ll \omega_c^2|\varrho|. \tag{1.27c}$$

The first two inequalities result from *slowly varying envelope approximation* which says that the pulse envelope varies slowly on the time scale of one period (ω_c^{-1}) and the length scale of unit wavelength (k_c^{-1}). The final inequality (1.27c) means that the atomic quantities also vary little over one optical period. This is in line with RWA approximation. These simplifications along with the dispersion relation $k_c \approx \omega_0/c$ lead us to the following equation of propagation for field amplitude

$$\left(\partial_y + \frac{1}{c}\partial_t\right) A_c = i\mu_0 c\omega_c\varrho/2. \tag{1.28}$$

ϱ can be calculated quantum mechanically. It is the mean expectation value of dipole moment operator and is given by

$$\varrho = Ntr\left(\hat{\vec{D}}\cdot\vec{e}_z\rho\right) = ND\rho_c. \tag{1.29}$$

Here N is the atomic density and ρ_c is the coherence that is responsible for the radiated field. For the present example of two-level system ρ_c is given by ρ_{ca} and that simplifies to a^*c in the absence of relaxations. The Eq. (1.28) can be further simplified if we place ourselves in a frame of reference that is moving along the pulse with the velocity of light. This can be done by making $t \to t - y/c$. In this new frame of reference, and using the definition of Rabi frequency ($\Omega_c = DA_c/\hbar$), the propagation equation for the field can be written as

$$\partial_y\Omega_c = i\frac{ND^2\omega_c}{2c\epsilon_0\hbar}\rho_c. \tag{1.30}$$

The above equation determines how the field is modified as it propagates in the medium and this equation along with equation set (1.7) or (1.24) completely determines the evolution of the system. The propagation effects are very different for short and long pulse regimes and will be taken separately in the following discussion.

1.2.2 Propagation effects for ultrashort pulses

For ultrashort pulses having time duration $\tau_c \ll \Delta_{dop}^{-1}$, where Δ_{dop} is the Doppler broadened linewidth, the propagation Eq. (1.30) can be written in a more useful form. We define a dimension-less parameter for the field as $\theta_c = DA_c\tau_c/\hbar$. This is usual pulse area and it characterizes the strength of the field. It is related to the Rabi frequency through the relation $\Omega_c(t) = \theta_c f_c(t)/\tau_c$. The propagation equation for an ultrashort pulse can now be written as [From Eq. (1.30)]

$$\partial_{(y/L)} f_c = i\frac{e_{disp}}{\theta_c} a^* c. \tag{1.31}$$

L is the length of the medium and $e_{disp} = ND^2\omega_c L\tau_c/(2c\epsilon_0\hbar)$ is an important parameter that characterizes the severity of dispersion effects. We first note some important considerations for the propagation of ultrashort pulses.

Negligible absorption with vanishing pulse area

The key element for the propagation of ultrashort pulse in resonant or near-resonant atomic media is the famous McCall&Hahn theorem [McCall67, McCall69]. For a weak pulse with $\theta_c < \pi$, it states that the pulse area $\propto \int_{-\infty}^{\infty} f_c(t,y)\,dt$ decreases exponentially with the propagation distance y. However, the pulse energy $\propto \int_{-\infty}^{\infty} f_c^2(t,y)\,dt$ can exhibit different behavior. Indeed, for ultrashort pulses — having time duration of the order of femtoseconds or picoseconds — the pulse spectrum τ_c^{-1} is much wider than the Doppler broadened linewidth Δ_{dop} that lies in GHz at room temperature. Therefore, no significant absorption can take place and the pulse energy remains unaltered as the pulse propagates. The pulse envelope thus either develops an oscillatory structure [Crisp70, Rothenberg84] or a long negative tail [Delagnes08] to satisfy both the vanishing pulse area and negligible pulse absorption.

Population dynamics

A consequence of the pulse area theorem is the vanishing excited state population with propagation. As the pulse area $\propto \int_{-\infty}^{\infty} f_c(t,y)\,dt$ goes to

zero, the excited state population, that is given in the resonant case as $\sin^2\left[\int_{-\infty}^{\infty} f_c(t,y)\,dt\right]$ also vanishes. This is in spite of the fact that no relaxation processes enter into the dynamics at these short time scales. Any energy transferred to the medium is temporary and it coherently comes back to the field as the field propagates in the medium. This is shown in Fig. 1.5. A near π area resonant pulse transfers all the population to the excited state

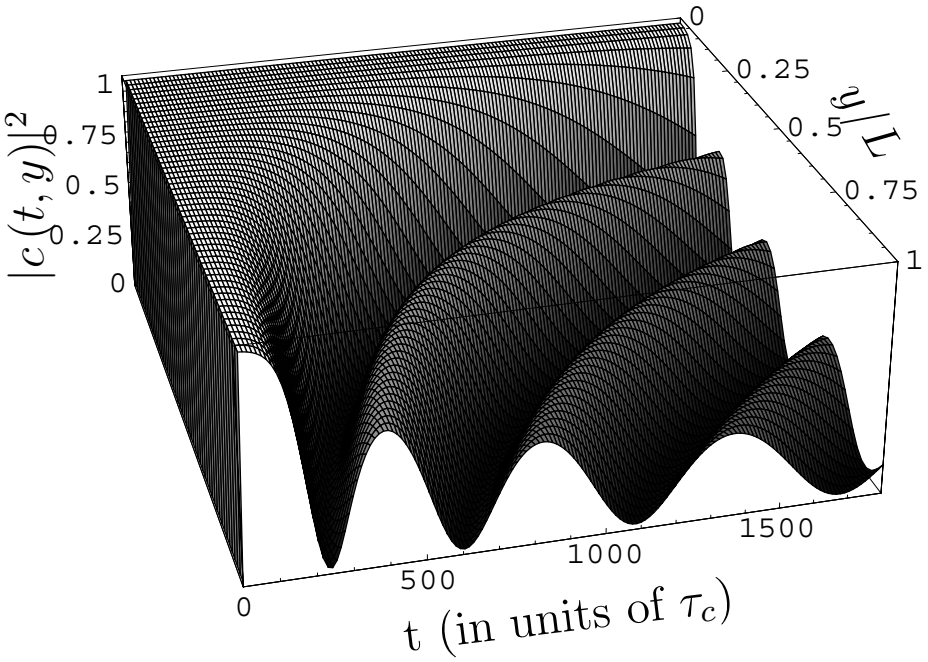

Figure 1.5: Population dynamics during propagation of ultrashort pulses. Excited state population comes back to the ground state with the propagation over a very long time scale. The field is given by $f_c(t,0) = e^{-(t/\tau_c)^2}/\sqrt{\pi}$. The parameters are $\theta_c = (\pi - 0.01)$, $\Delta_c = 0$, and $e_{disp} = 0.1$.

at $t = 0$. At the input of the medium at $y = 0$, the population remains in the excited state as the relaxation processes are not significant. But as the pulse propagates along y, the population comes back to the ground state in accordance with the vanishing pulse area. It eventually oscillates because of the dispersion effects. The Figure also suggests that the pulse area vanishes over a very large time scale.

Severity of dispersion effects

The severity of dispersion effects are quantified by the dispersion parameter e_{disp} used in Eq. (1.31). It is related to the better known parameter optical depth $\alpha_{dop}L$ by the relation $e_{disp} = \alpha_{dop}L\Delta_{dop}\tau_c$ ($\omega_c \approx \omega_0$ in RWA). α_{dop} is the field absorption coefficient at Doppler broadened linewidth and is given by $\alpha_{dop} = ND^2\omega_0/\left(2c\epsilon_0\hbar\Delta_{dop}\right)$. $\alpha_{dop}L\Delta_{dop}$ is the spectral domain over which the dispersion is important [Delagnes08]. $\alpha_{dop}L\Delta_{dop}\tau_c$ becomes the ratio of this spectral domain and the spectrum of the field (τ_c^{-1} is the spectral width of the field) and thus the dispersion parameter e_{disp} quantifies the dispersion effects. $e_{disp} \ll 1$ means that the pulse spectrum is much wider than the spectral domain over which dispersion is important. The dispersion can thus be neglected; the absorption is already negligible for ultrashort pulses. Hence, $e_{disp} \ll 1$ suggests counter-intuitive distortion-less propagation of the ultrashort pulses even in the presence of large optical depth $\alpha_{dop}L \gg 1$. In this case the pulse envelope develops a long negative tail to satisfy McCall&Hahn pulse area theorem as shown in Fig. 1.6.

For $e_{disp} \geq 1$, $\alpha_{dop}L\Delta_{dop}$ is as wide or wider than the pulse spectrum and the dispersion effects all the frequency components of the pulse. The dispersion effects in this case can not be neglected, and the pulse is severely distorted as it propagates in the medium. The absorption is still negligible and the pulse develops an oscillatory structure as shown in Fig. 1.7, and demonstrated in many studies. A complete discussion of the dispersion parameter and its effects on the spectral and temporal behavior of a weak resonant ultrashort pulse — propagating in a dense atomic media — can be found in [Delagnes08].

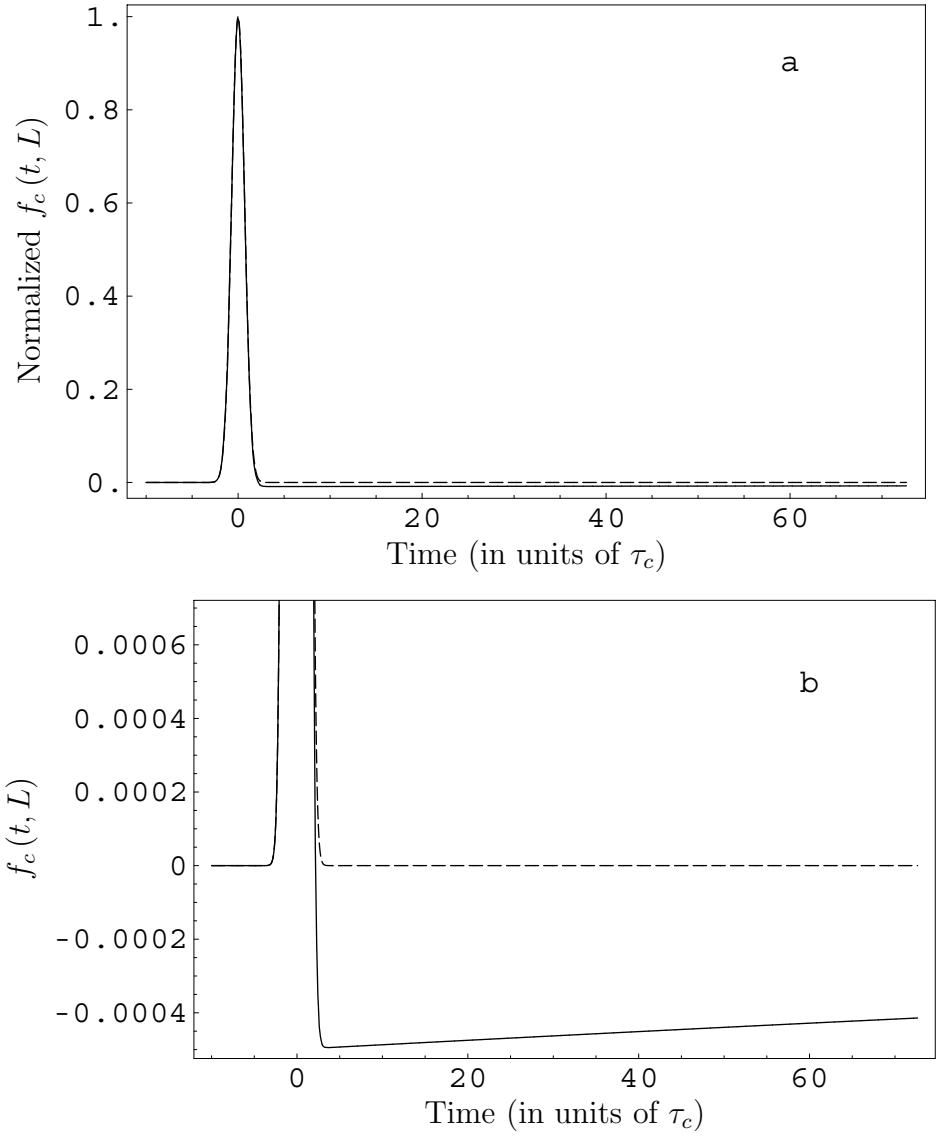

Figure 1.6: (a) Normalized field envelope at $y = 0$ (dashed) and at $y = L$ (solid). For $e_{disp} \ll 1$, the ultrashort pulse experiences distortion-less propagation, and develops a long negative tail to satisfy the vanishing pulse area theorem. (b) is a zoom to show the long negative tail. The field is given by $f_c(t, 0) = e^{-(t/\tau_c)^2}/\sqrt{\pi}$. The parameters are $\theta_c = 0.1$, $\Delta_c = 0$, and $e_{disp} = 0.01$. For $\Delta_{dop} = 0.6GHz$ and $\tau_c = 100fs$, this corresponds to $\alpha_{dop}L \simeq 160$.

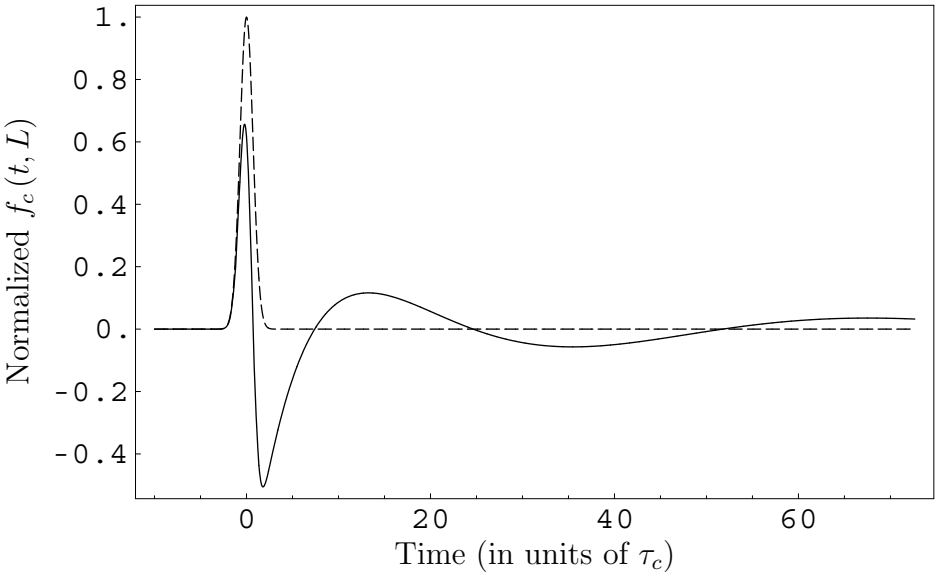

Figure 1.7: Normalized field envelope at $y = 0$ (dashed) and at $y = L$ (solid). For $e_{disp} = 1$, the ultrashort pulse experiences severe distortion, and develops an oscillatory structure to satisfy the vanishing pulse area theorem. The field is given by $f_c(t, 0) = e^{-(t/\tau_c)^2}/\sqrt{\pi}$. The parameters are $\theta_c = 0.1$, $\Delta_c = 0$, and $e_{disp} = 1$. For $\Delta_{dop} = 0.6GHz$ and $\tau_c = 100fs$, this corresponds to $\alpha_{dop}L \simeq 16500$.

1.2.3 Propagation effects for long pulses

We now consider the situation of long pulses and homogeneous broadening. The optical response is determined by optical susceptibility χ. It is defined by the relation

$$\vec{P} = \chi \epsilon_0 \vec{E}_c. \tag{1.32}$$

For the present case of two-level system, the susceptibility is given as

$$\chi = \chi' + i\chi'' = \frac{2\alpha_0 \Gamma_d}{k} \frac{\rho_{ca}}{\Omega_c}, \tag{1.33}$$

where $k = \omega_0/c$. The susceptibility is related to the refractive index $n(\omega)$, and the absorption coefficient $\alpha(\omega)$ through the relation

$$\left[n(\omega) + i\frac{\alpha(\omega)}{k} \right]^2 = 1 + \chi(\omega), \tag{1.34}$$

and thus it determines the absorptive and dispersive response of the medium. The propagation Eq. (1.30) can be written as

$$\partial_y \Omega_c(t, y) = i\alpha_0 \Gamma_d \rho_{ca}(t, y). \tag{1.35}$$

Here $\alpha_0 = (ND^2\omega_0)/(2c\epsilon_0\hbar\Gamma_d)$ is the field absorption coefficient at line center — $2\Gamma_d$ is the linewidth in the absence of Doppler broadening. Using Eq. (1.33), the propagation equation can be formally solved to give

$$\Omega_c(t, y) = \Omega_c(t, 0)\, e^{-\frac{ky}{2}\chi''} e^{i\frac{ky}{2}\chi'}. \tag{1.36}$$

The first exponent involving the imaginary part of the susceptibility accounts for the attenuation or absorption of the field, whereas the second exponent represents dispersive effects. The absorption is negligible if $(ky/2)\chi'' \ll 1$. An expression for the susceptibility can be written using the stationary state solution (1.24). Using the first order expression for ρ_{ca}, the linear susceptibility can be written as

$$\chi_{lin} = \frac{2\alpha_0 \Gamma_d}{k} \frac{\bar{\Delta}_c}{|\bar{\Delta}_c|^2}. \tag{1.37}$$

The plots of real and imaginary parts of the linear susceptibility are shown in Fig. 1.8. The imaginary or absorption part is a Lorentzian centered at resonance with FWHM given by $2\Gamma_d$. This is the linewidth in the absence of non-homogeneous dephasing processes. The real part follows anomalous dispersion (Δ_c is defined as $\omega_0 - \omega_c$). The real part also determines the velocity of pulse propagation as we will see in the next section.

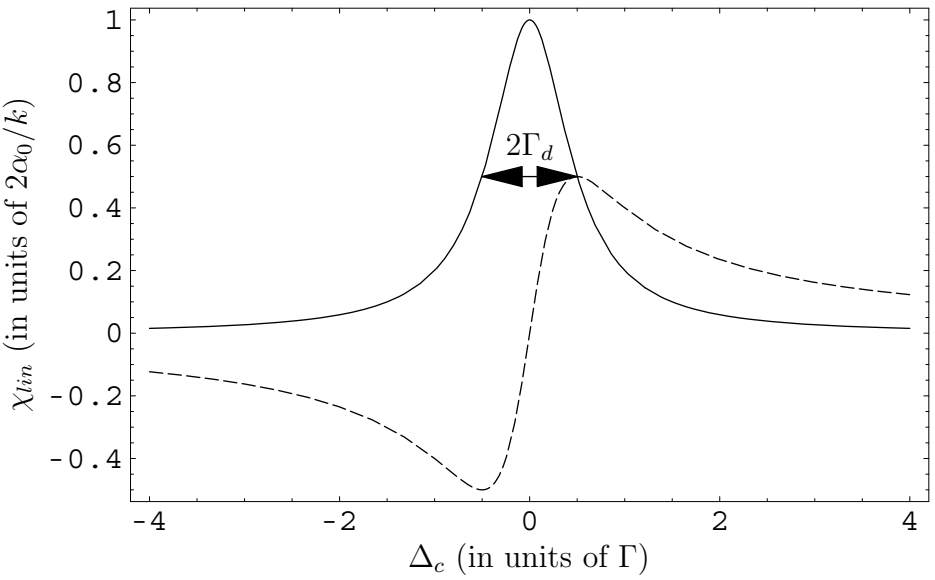

Figure 1.8: Linear susceptibility for a two-level system. Imaginary part (solid) suggests strong absorption at resonance. The real part (dashed) follows anomalous dispersion (for $\omega_c - \omega_0 = -\Delta_c$). Parameters are $\Gamma_d = 0.5\Gamma$.

1.3 Velocity of propagation

The velocity at which a light pulse propagates inside the medium has been at the center of some controversy. The confusion arises because pulse propagation inside the medium can be characterized by many different velocities, and some of these can acquire "abnormal" values. This is the case with the notion of group velocity. Group velocity characterizes the movement of pulse peak inside the medium with no pulse distortion. It can be greater or less than the velocity of light in vacuum — c, infinite, and can even have a negative value. At first sight, it seems in contradiction with the special theory of relativity, however, the contradiction is removed by noting that the group velocity is in general not the signal velocity. And although the group velocity does correspond with the energy transport, one has to take into account the energy stored in the medium for a short time, and look at the total energy flow, which is always less than or equal to c. A detailed text on this topic can be found in [Milonni05].

1.3.1 Group velocity

The light pulse results from the constructive interference of a large number of spectral components. The peak of the constructive interference moves with

the velocity c in vacuum. Inside a medium, the interference is affected by the interaction with the matter. This can either result in the distortion of pulse/splitting of the pulse into multiple fragments or the pulse can retain its shape. In the second case we can assign a velocity with the propagation of the pulse inside the medium. This is the group velocity, defined at the central laser frequency ω_c as

$$v_g = \left(dk/d\omega\right)_{\omega_c}. \tag{1.38}$$

I will next show that in the case of linear dispersive medium with constant absorption/gain, the pulse is not distorted as it propagates inside the medium, and the peak of the pulse moves with the group velocity given in the above expression.

The field given by the expression (1.1), written as $\vec{E}_c = E_c\vec{e}_z$, can be decomposed into its spectral components at the entrance of the medium (at $y = 0$) as

$$E_c(0,t) = A_c(0,t)e^{-i\omega_c t} = \int_\infty^\infty \tilde{A}_c\left(\omega\right) e^{-i\omega t} d\omega, \tag{1.39}$$

where $\tilde{A}_c\left(\omega\right)$ are different spectral components. During propagation, each spectral component is multiplied by $e^{i\tilde{k}y}$ where $\tilde{k} = \omega n(\omega)/c + i\alpha(\omega)$. $n(\omega)$ and $\alpha(\omega)$ are refractive index and absorption coefficients respectively. The field at a point y inside the medium is given by

$$E_c(y,t) = \int_\infty^\infty \tilde{A}_c\left(\omega\right) e^{-i\omega t} e^{i\omega n(\omega)y/c} e^{-\alpha(\omega)y} d\omega. \tag{1.40}$$

$n(\omega)$ can be expanded in a Taylor series as

$$n(\omega) = n(\omega_c) + \left.\frac{dn}{d\omega}\right|_{\omega_c} (\omega - \omega_c) + \left.\frac{d^2n}{d\omega^2}\right|_{\omega_c} (\omega - \omega_c)^2/2! + \ldots \tag{1.41}$$

In a region where refractive index changes linearly with frequency with vanishing $d^2n/d\omega^2$ and higher order derivatives, and where the absorption (or gain) is constant for all frequencies $\alpha(\omega) = \alpha(\omega_c)$, the expression in (1.40) can be simplified as

$$E_c(y,t) = e^{-\alpha(\omega_c)y} e^{-i(\omega_c t - k_c y)} \int_\infty^\infty \tilde{A}_c\left(\omega\right) e^{-i(\omega-\omega_c)(t-y/v_g)} d\omega, \tag{1.42}$$

with

$$v_g = \frac{c}{n(\omega_c) + \omega \left.\frac{dn}{d\omega}\right|_{\omega_c}}. \tag{1.43}$$

The integrand in (2.32) is the Fourier transform of $A_c(0, t - y/v_g)$. Hence the field inside the medium can be written as

$$E_c(y,t) = e^{-\alpha(\omega_c)y} A_c(0, t - y/v_g) e^{-i(\omega_c t - k_c y)}. \tag{1.44}$$

The field propagates inside the medium without any distortion of the envelope except for overall absorption or gain. Moreover, the velocity of the propagation is given by Eq. (1.43), which is the same as Eq. (3.4b).

1.3.2 Slow, fast, and backward propagating light

The group velocity inside a medium, given by the expression (1.43), is strongly affected by the dispersion profile of the medium. The first term in the denominator — the refractive index $n(\omega)$ — is almost unity in dilute atomic gases. And the second term which depends on the dispersion profile determines the velocity of propagation. For $\omega dn/d\omega > 0$, we get a light pulse that moves slower in the medium than its velocity in vacuum. Ultraslow light can be achieved by making $\omega dn/d\omega \gg 1$. For $\omega dn/d\omega < 0$, the velocity of light in the medium is greater than its velocity in vacuum. This is fast light — light covers a given distance inside the medium in less time than it takes to cover the same distance in vacuum. Fast light has been experimentally observed in cesium gas by Wang *et al.* [Wang00]. For $\omega dn/d\omega < -1$, we get backward propagating light. In this case the pulse peak leaves the system before even entering it, and inside the medium the pulse starts at the far end of the system and moves toward the near end. Backward propagating light has also been experimentally observed in erbium doped optical fiber by Gehring et al. [Gehring06]. This rich behavior of group velocity can be represented in a graph as shown in Fig. 1.9.

1.3.3 Slow and fast light with linear response

The linear response in the two-level system can give rise to slow and fast light. Using $\sqrt{1+\chi} \approx 1 + \chi/2$, using the expression of linear susceptibility from (1.37), and using the relation (1.34), the refractive index can be written as

$$n(\Delta_c) \approx 1 + \frac{\alpha_0}{k} \frac{\Gamma_d \Delta_c}{\Gamma_d^2 + \Delta_c^2}. \tag{1.45}$$

Using this expression in (1.43), the group velocity can be written as

$$v_g(\Delta_c) \approx \frac{c}{1 - \frac{c\alpha_0}{\Gamma_d} \frac{\Gamma_d^2 - \Delta_c^2}{\left(\Gamma_d^2 + \Delta_c^2\right)^2} \Gamma_d^2}. \tag{1.46}$$

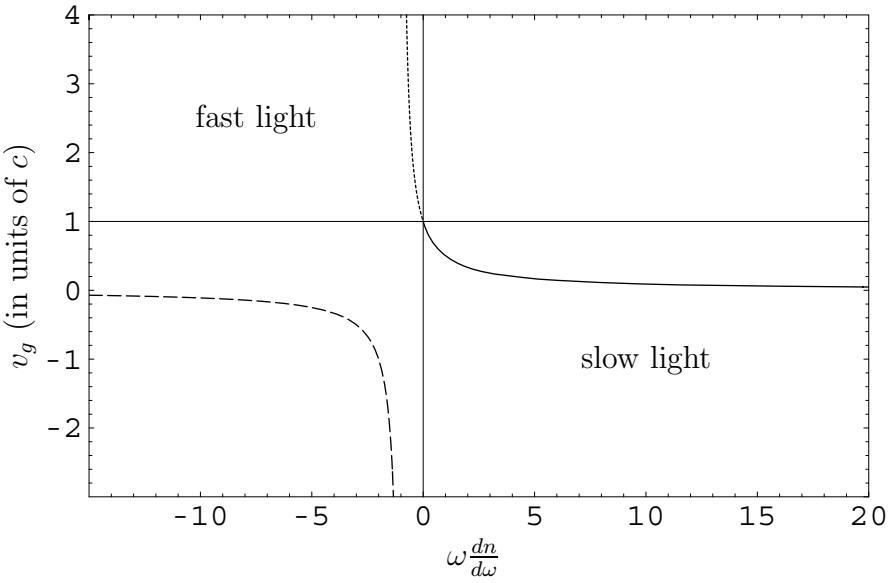

Figure 1.9: Slow, fast and backward propagating light. The origin is at $(0, c)$. The slow light regime is shown in solid, the fast light in dotted and dashed. The backward propagating is in dashed. For ultraslow light we need to have $\omega dn/d\omega \gg 0$.

The group velocity is equal to velocity in vacuum for $\Delta_c = \pm\Gamma_d$. Between these two limits we have fast light with $v_g > c$. The fastest light is $(1 - c\alpha_0/\Gamma_d)^{-1}$ times faster than c at $\Delta_c = 0$, and for $c\alpha_0/\Gamma_d > 1$ we can get backward propagating light. However, at $\Delta_c = 0$ the field is resonant and is strongly absorbed which makes the observation of fast or backward propagating light very difficult. Finally for $|\Delta_c| > \Gamma_d$, we can get slightly slower light propagation. This slow and fast light ranges can be seen in Fig 1.10. In order to obtain ultraslow light we need to have abrupt normal dispersion with $\omega dn/d\omega \gg 1$. This is not possible in the present case of the linear response in a two-level system. However techniques exist that modify the response of the atomic systems dramatically and produce huge normal dispersion. Some of these techniques will be discussed in Chapter. 3.

1.4 Summary of the chapter

In this chapter I have presented a summary of light interaction and propagation in a two-level system. Both short and long pulse regimes were discussed. For short pulse regime, adiabatic levels were presented which are more suited to study non-resonant, strong field interaction with the system. The strong

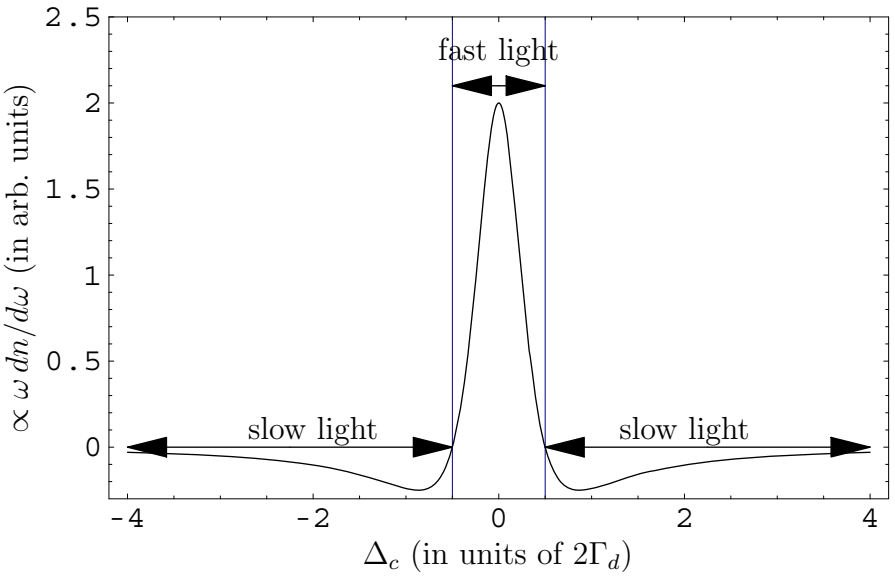

Figure 1.10: Slow and fast light with linear response. Close to absorption peak we get fast light with strong absorption, away from the resonance slow light can be achieved.

field introduces light shifts and non-adiabatic coupling. These light shifts and the coupling can be used to shape another weak pulse that propagates in the medium. This will be shown in the next chapter. Also, a scheme where non-adiabatic coupling appears in the form of a sudden jump, and the phase control of this jump will be discussed.

In long pulse regime the linear response of the medium, and the group velocity were discussed. The group velocity can be significantly modified by changing the dispersion profile of the medium. In Chapter. 3, some methods to introduce abrupt normal dispersion, and to produce ultraslow light will be presented.

Chapter 2

A Driven Two-level system in Ultrashort pulse regime

In the previous Chapter I have presented coherent light interaction with a two-level system. It was shown that a strong, non-resonant field can introduce important light shifts in the system, and if the envelope of the field is rapidly changing, the light shifts are accompanied by significant non-adiabatic coupling— which is proportional to the derivative of the field amplitude. In the present Chapter I will discuss how these changes — light shifts and non-adiabatic coupling— can be probed by introducing a weak pulse in the system, and how can these be used for important applications.

Dans le chapitre précédent, j'ai présenté l'interaction cohérente de la lumière avec un système à deux niveaux. On a montré qu'un champ fort, non résonant pouvait introduire des déplacements lumineux importants dans le système, et que si l'enveloppe du champ variait rapidement, ces déplacements lumineux étaient accompagnés par des transitions non-adiabatiques importantes (proportionnelles à la dérivée de l'amplitude du champ). Dans ce chapitre, je montrerai comment ces changements (déplacements lumineux et couplages non-adiabatiques) peuvent être sondés en introduisant une impulsion faibles dans le sytème et comment ils peuvent être utilisés pour des applications importantes.

The first part of the Chapter deals with bi-chromatic excitation of a two-level system in ultrashort pulse regime. A strong, non-resonant pulse introduces light shifts in the system which are probed by a weak resonant

La première partie de ce chapitre traite de l'excitation bi-chromatique d'un système à deux niveaux en régime d'impulsion ultracourte. Une impulsion intense, non résonante induits des déplacements lumineux

pulse. The weak pulse, as it propagates in the medium develops an oscillatory structure that maps out the light-shifts in real time. This can also be seen as "shaping" of the weak ultrashort pulse. The study is the extension of an idea first discussed in a three-level system where the light shifts on a transition were probed by a weak propagating pulse resonant on an adjacent transition [Delagnes04]. The present case of two-level system is paradoxically more complex as both the driving and the probe fields act on the same transition.

dans le système qui est sondée par une impulsion résonante faible. L'impulsion faible, développe en se propageant dans le milieu une structure oscillante qui fait ressortir les déplacements lumineux en temps réel. Ceci peut être vu comme une mise en forme de l'impulsion faible. Cette étude représente une extension d'une idée discutée en premier dans un système à trois niveaux où les déplacements lumineux sur une transition sont sondés par une impulsion faible résonante se propageant sur une transition adjacente [Delagnes04]. Le cas présent du système à deux niveaux est paradoxalement plus compliqué à analyser car les champs pompe et sonde agissent sur la même transition.

In the second part of the Chapter we focus on non-adiabatic coupling. A strong, non-resonant, asymmetric field causes significant non-adiabatic transitions. Under suitable conditions the non-adiabatic coupling can take the form of a resonant, π area, δ like function that abruptly transfers all the population to the excited adiabatic state [Vasilev06]. We consider the case where the exciting field consists of two time delayed, phase locked, and identical pulses. This scheme renders phase control of non-adiabatic jumps.

Dans la seconde partie de ce chapitre, nous nous focalisons sur les couplages non-adiabatiques. Un champ asymétrique, non résonant et intense produit des transitions non adiabatiques. Sous des conditions adaptées, le couplage non-adiabatique prend la forme d'une fonction résonante en forme de pic de Dirac, d'aire qui transfère de manière abrupte toute la population dans l'état adiabatique excité [Vasilev06]. On considèrera le cas où le champ excitateur consiste en deux impulsions identiques décalées dans le temps, verrouillées en phase. Ce schéma va permettre le contrôle par la phase des sauts non adiabatiques.

The last part of the Chapter deals with the observation of non-adiabatic jump. The jump takes place in adiabatic basis and can get unnoticed in

La dernière partie de ce chapitre traite de l'observation des sauts non-adiabatiques. Le saut se produit dans la base adiabatique et ne se voit

real populations. We propose the observation of the jump in real time, on the temporal profile of a weak probe, that propagates in the medium and couples resonantly the excited adiabatic state to a third level in the system. The probe develops an oscillatory structure with the oscillations starting at the time of non-adiabatic jump. This can again be seen as pulse shaping of the probe with non-adiabatic jump acting as a "turn on" switch for the shaping process.

pas dans les populations réelles. On va proposer une méthode permettant l'observation du saut en temps réel sur le profil temporel d'une impulsion sonde peu intense qui se propage dans le milieu en couplant de manière résonante l'état adiabatique excité à un troisième niveau dans le système. La sonde développe une structure oscillante avec des oscillations qui commencent au moment précis où se produit le saut non-adiabatique. Cet effet peut être vu à nouveau comme une mise en forme temporelle de l'impulsion avec le saut non-adibatique jouant le rôle d'un commutateur pour le processus.

2.1 Bi-chromatic excitation of a two-level system

Consider the two-level system discussed in Chapter. 1 Section. 1.1, interacting with a strong, non-resonant, ultrashort field $\vec{e}_z A_c f_c(t,y)\, e^{-i(\omega_c t - k_c y)} + cc$; and probed by a weak, resonant pulse $\vec{e}_z A_p f_p(t,\vec{r})\, e^{-i\left(\omega_0 t - \vec{k}_p\cdot\vec{r}+\phi\right)} + cc$, as shown in Fig. 2.1. The detuning of the strong "control" field is $\Delta_c = \omega_0 - \omega_c$; the Rabi frequencies associated with the two fields are $\Omega_c(t) = DA_c f_c(t)/\hbar$ and $\Omega_p(t) = DA_p f_p(t)/\hbar$ with $|\Omega_c| \gg |\Omega_p|$. The two pulse envelopes are given by

$$f_c(t) = \frac{1}{\sqrt{\pi}} e^{-(t/\tau_c)^2}, \tag{2.1}$$

$$f_p(t) = \frac{1}{\sqrt{\pi}} e^{-(t/\tau_p)^2}. \tag{2.2}$$

τ_c and τ_p are respectively the time durations of the control and the probe and their ratio is given by $\tau_{pc} = \tau_p/\tau_c$. The pulse envelopes are normalized to unity with $\int f_p\, d(t/\tau_p) = \int f_c\, d(t/\tau_c) = 1$. The dephasing between the two fields is

$$\Phi(t,\vec{r}) = \Delta_c t - \delta\vec{k}\cdot\vec{r} + \phi, \tag{2.3}$$

where $\delta\vec{k} = \vec{k}_p - k_c\vec{e}_y$ is the spatial dephasing and ϕ is the phase shift between the two fields. A small angle between the two fields is necessary. Firstly,

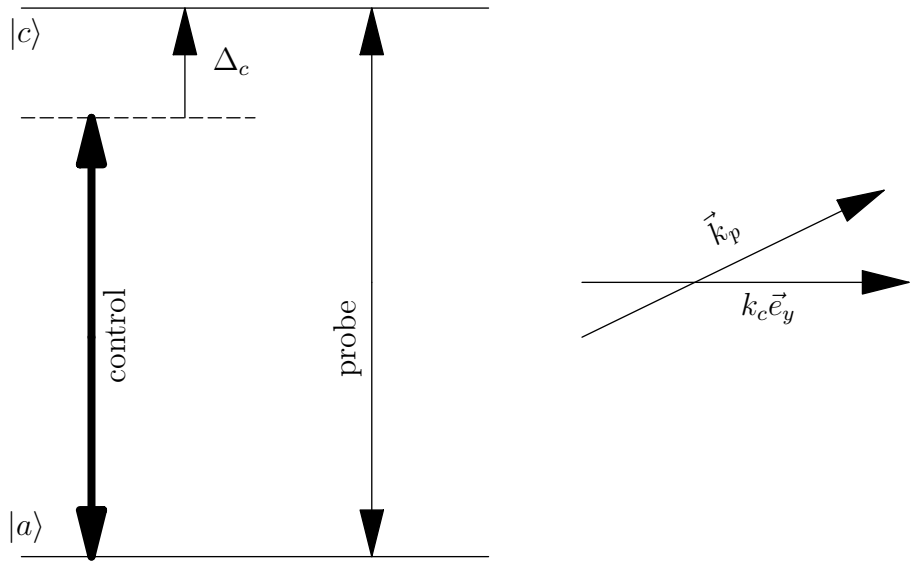

Figure 2.1: Bi-chromatic excitation of a two level system. The two fields propagate with a small angle between them.

it separates the two fields at the exit of the medium. Secondly, in this configuration the probe is immune to non-adiabatic effects, and probes only the light-shifts, as will be shown in the discussion.

The time evolution of the system in adiabatic basis [see Section. 1.1.2] after carrying out RWA is given by

$$i\hbar\partial_t \begin{pmatrix} \alpha \\ \gamma \end{pmatrix} = \hbar \left[A + V\right] \begin{pmatrix} \alpha \\ \gamma \end{pmatrix}. \tag{2.4}$$

A is the part of the Hamiltonian due to the control field and is given by

$$A\left(t\right) = \frac{1}{2} \begin{pmatrix} \Delta_c - \Omega\left(t\right) & 2i\left(\partial_t\theta\right)\left(t\right) \\ -2i\left(\partial_t\theta\right)\left(t\right) & \Delta_c + \Omega\left(t\right) \end{pmatrix}. \tag{2.5}$$

The diagonal terms with $\Omega = \sqrt{4\Omega_c^2 + \Delta_c^2}$ are light-shifted energy levels, and the off-diagonal terms are non-adiabatic coupling. The perturbation due to the weak probe is contained in V. It is given by

$$V\left(t, \vec{r}\right) = R \begin{pmatrix} 0 & -\frac{\theta_p f_p^*}{\tau_p} e^{i\Phi(\vec{r},t)} \\ cc & 0 \end{pmatrix} R^\dagger, \tag{2.6}$$

$\theta_p = DA_p\tau_p/\hbar$ is the pulse area of the probe and the rotation matrix R is the same as given by Eq. 1.9. The matrix V can be written as

$$V = V^{(-)}e^{-i\Phi(\vec{r},t)} + V^{(+)}e^{i\Phi(\vec{r},t)}, \tag{2.7}$$

with $V^{(+)} = V^{(-)^\dagger}$ and

$$V^{(-)} = \frac{\theta_p f_p}{2\tau_p} \begin{pmatrix} -\sin 2\theta & 2\sin^2\theta \\ -2\cos^2\theta & \sin 2\theta \end{pmatrix}. \tag{2.8}$$

V contains both the diagonal and off-diagonal terms that depend on both the control and the probe field. The diagonal terms induce modulation in the light-shifted energy levels, but these effects are small as long as the probe is weak. For $\theta_p \ll 1$, only the off-diagonal terms in matrix V are important and these describe the interaction of the probe with light-shifted energy levels.

2.1.1 Floquet like expansion

The spatial periodicity allows the use of Floquet methods. The atomic quantities can be expanded in Floquet series and that latter can be truncated at the *first order* with respect to the probe amplitude in the limit of weak probe. We write the amplitudes as

$$\alpha\left(t,\vec{r}\right) = \alpha^{(0)}\left(t,y\right) + \alpha^{(-)}\left(t,y\right)e^{-i\Phi(\vec{r},t)} + \alpha^{(+)}\left(t,y\right)e^{i\Phi(\vec{r},t)}, \tag{2.9a}$$

$$\gamma\left(t,\vec{r}\right) = \gamma^{(0)}\left(t,y\right) + \gamma^{(-)}\left(t,y\right)e^{-i\Phi(\vec{r},t)} + \gamma^{(+)}\left(t,y\right)e^{i\Phi(\vec{r},t)}. \tag{2.9b}$$

The time evolution of the system at the *first order* is given as

$$i\hbar\partial_t \begin{pmatrix} \alpha^{(0)} \\ \gamma^{(0)} \end{pmatrix}(t,y) = \hbar A \begin{pmatrix} \alpha^{(0)} \\ \gamma^{(0)} \end{pmatrix}(t,y). \tag{2.10}$$

In the adiabatic limit with vanishing off-diagonal elements of matrix A in Eq. (2.5), and with initially all the population in the ground state $|\alpha\rangle$, the solution of the above equations is given as

$$\alpha^{(0)}\left(t,0\right) = e^{-i\int_{-\infty}^{t}\frac{\Delta_c-\Omega(t')}{2}dt'}, \tag{2.11a}$$

$$\gamma^{(0)}\left(t,0\right) = 0. \tag{2.11b}$$

The ground state amplitude accumulates phase in accordance with light-shifted level but the excited state amplitude remains *zero* as there is no population in the excited state. At *first order* with respect to the probe amplitude, the evolution of the system is given by

$$i\hbar\partial_t \begin{pmatrix} \alpha^{(\pm)} \\ \gamma^{(\pm)} \end{pmatrix}(t,y) = \hbar A \begin{pmatrix} \alpha^{(\pm)} \\ \gamma^{(\pm)} \end{pmatrix}(t,y) + \hbar V^{(\pm)} \begin{pmatrix} \alpha^{(0)} \\ \gamma^{(0)} \end{pmatrix}(t,y). \tag{2.12}$$

Only the amplitude $\gamma^{(-)}$ will be relevant for the discussion that follows, and it is given at $y = 0$ as

$$\gamma^{(-)}\left(t,0\right) = i\frac{\theta_p}{\tau_p}\, e^{-i\int_{-\infty}^{t}\frac{\Delta_c-\Omega(t')}{2}dt'} \int_{-\infty}^{t} \cos^2\theta f_p\ \left(t',0\right) e^{-i\int_{t'}^{t}\Omega(t'')dt''}dt'. \tag{2.13}$$

2.1.2 Coherence behavior

The coherence responsible for the radiated field is a^*c. We can write it as

$$a^*c \approx \rho_c + \rho_p e^{-i\Phi(\vec{r},t)} + \rho_p' e^{i\Phi(\vec{r},t)}, \tag{2.14}$$

different terms in the above expression radiate in different directions. ρ_c radiates along the control field direction $k_c\vec{e}_y$, and it contains all the contribution from the non-adiabatic effects. ρ_p radiates in the direction of the probe, and ρ_p' radiates in the symmetric direction $k_c\vec{e}_y - \delta\vec{k}$. Having a small angle between the probe and the control ensures that any small non-adiabatic effects due to the control field do not influence the radiated probe, and the probe only experiences the light-shifts. In another geometry where the control and the probe are propagating co-linearly and have sufficient delay between the two, the probe is immune to light-shifts and experiences only the non-adiabatic effects [Delagnes05]. The coherence ρ_p in the adiabatic basis, and using the Floquet expansion (2.9), is given by

$$\begin{aligned}\rho_p = \cos^2\theta \left[\alpha^{(0)^*}\gamma^{(-)} + \alpha^{(+)^*}\gamma^{(0)}\right] - \sin^2\theta \left[\gamma^{(0)^*}\alpha^{(-)} + \gamma^{(+)^*}\alpha^{(0)}\right] \\ + \frac{\sin 2\theta}{2}\left[\alpha^{(0)^*}\alpha^{(-)} + \alpha^{(+)^*}\alpha^{(0)} - \gamma^{(0)^*}\gamma^{(-)} - \gamma^{(+)^*}\gamma^{(0)}\right].\end{aligned} \tag{2.15}$$

Eight terms in the above expression correspond to eight quantum paths available to the probe field in the dressed representation as shown in Fig. 2.2. Four correspond to the absorption of the probe from level 1 and 2 to level 3 and 4, and the other four correspond to stimulated emission on the same transition. The associated oscillation frequencies are shown in the Figure. The system can be considerably simplified as the probe interacts resonantly only on the transition $1 \leftrightarrow 4$, and that also for the time durations when the light shifts are not important. We next consider the coherence corresponding to $1 \leftrightarrow 4$ transition.

The coherence K_{14}

The probe is resonant only on the transition $1 \leftrightarrow 4$ in Fig. 2.2, and for the times outside the interval $[-T_r, T_r]$. This interval is the solution of $\Omega(t) - \Delta_c > \tau_p^{-1}$ and marks the region where the light shifts make the probe non-resonant with the system. Outside this interval, the probe interacts resonantly with the system. With initially all the population in the ground level 1, the level 4 is not populated during adiabatic evolution. Hence only the path corresponding to the absorption along $1 \rightarrow 4$ is important in

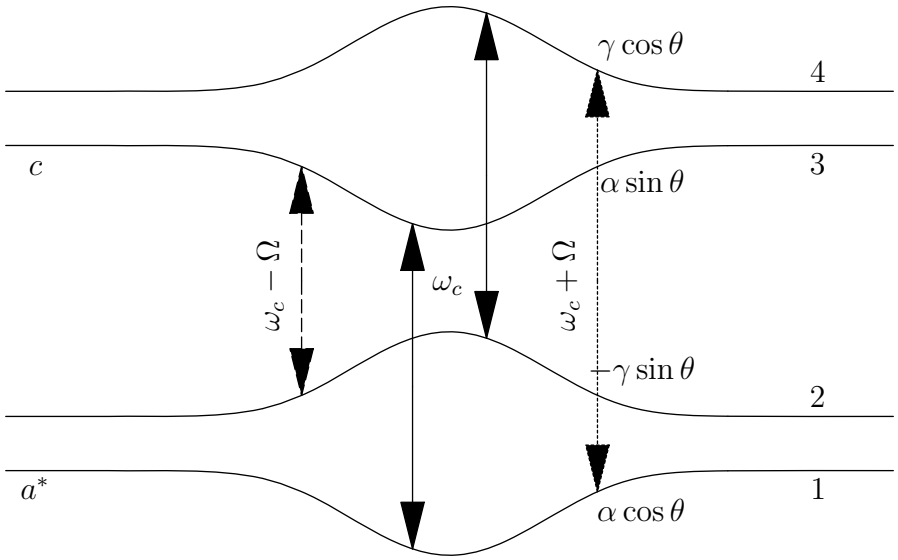

Figure 2.2: Coherence in adiabatic basis. Eight quantum paths — four for absorption and other four for emission — are available to the probe. However, during adiabatic evolution, with all the population initially in the state 1, only absorption on $1 \rightarrow 4$ is significant. $\alpha\cos\theta$, $\alpha\sin\theta$, $\gamma\cos\theta$, and $\gamma\sin\theta$ are the relative contributions of adiabatic levels to the bare state amplitudes.

the expression (2.15). This contribution is given by

$$K_{14} = \cos^2\theta\ \alpha^{(0)^*}\gamma^{(-)}, \tag{2.16}$$

and using Eq. (2.11) and Eq. (2.13), it can be written at $y = 0$ as

$$K_{14}\,(t,0) = i\frac{\theta_p}{\tau_p}\ \cos^2\theta \int_{-\infty}^{t} \cos^2\theta\ f_p\,(t',0)\, e^{-i\int_{t'}^{t}\Omega(t'')dt''}dt'. \tag{2.17}$$

We further distinguish between the resonant and the non-resonant contribution to K_{14}. Resonant contribution is for the time $-\infty$ to $-T_r$ and for the time T_r to ∞ with $\cos^2\theta \simeq 1$ during this time. Neglecting the non-resonant contribution, the coherence during the action of light-shifts (for $-T_r \leq t \leq T_r$) can be written as

$$K_{14}\,(t,0) \approx i\frac{\theta_p}{\tau_p}\ \cos^2\theta\ e^{-i\Delta_c t}\ e^{-i\int_{-\infty}^{t}(\Omega(t')-\Delta_c)dt'} \int_{-\infty}^{-T_r} f_p\,(t',0)\,dt'. \tag{2.18}$$

This relation will be used later to work out the expression for the radiated probe intensity.

Effects of light-shifts on the radiating coherence

The effects of the light shifts on the coherence $\rho_p \simeq K_{14}$ can be seen in Fig. 2.3(b). It shows $|\rho_p\,(t,0)|$ for different pulse duration widths. The plots should be compared with Fig. 2.3(a) which shows the evolution of the coherence in the absence of light-shifts. In (b) the coherence increases initially due to the resonant interaction. At $t = -T_r$ the light-shifts come into action and stop any further increase in the coherence. The non-resonant contribution to the coherence can be seen in this region in the form of oscillations. The oscillation arise because of the interference of the resonant contribution to the coherence for times $t < -T_r$ and the non-resonant contribution for time t between $[-T_r, T_r]$. The oscillations thus mark the region where the light-shifts are important. At the end of the light shifts at $T = T_r$, the coherence again continues to rise and reaches a maximum at the end of the probe. The maximum reached however, is considerably reduced as compared to that in Fig. 2.3(a), where the probe is propagating alone in the system and is never affected by the light-shifts. Moreover, by changing the ratio of the time duration of the control and the probe τ_{pc}, the action of light-shifts on the probe, and thus on the coherence can be controlled. For example in Fig. 2.3(b), for $\tau_{pc} = 2$, the probe is twice as long as the control and gets

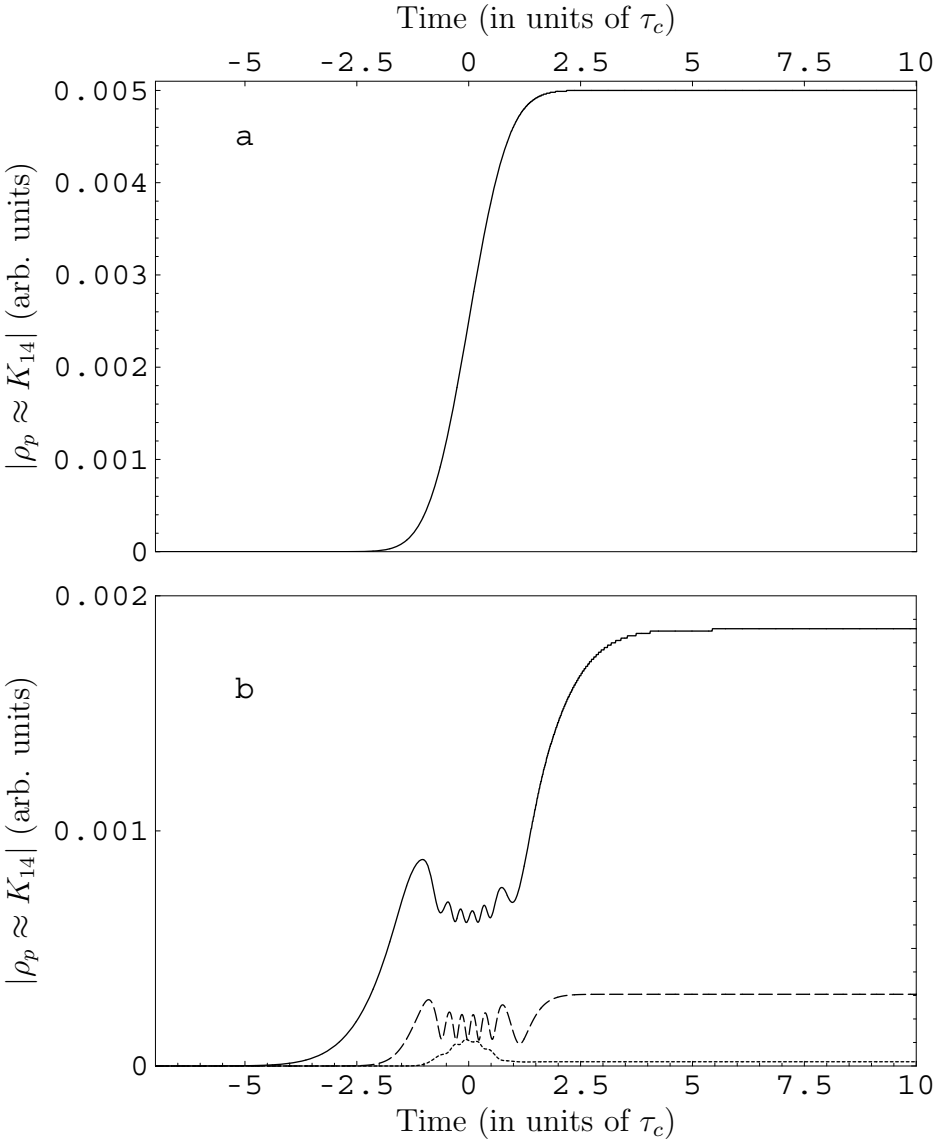

Figure 2.3: The coherence $|\rho_p \approx K_{14}|$ at $y = 0$. (a) The probe is propagating alone in the medium with $\Omega_c = 0$ and $\tau_{pc} = 1$. (b) Propagation in the presence of the control with $\Omega_c = 60\tau_c^{-1}$ for $\tau_{pc} = 1$ (dashed), $\tau_{pc} = 2$ (solid), and $\tau_{pc} = 0.5$ (dotted). Light-shifts suppress the coherence and induce modulations. Other parameters are $\theta_p = 0.01$ and $\Delta_c = 10\tau_c^{-1}$.

ample time to interact resonantly with the system. The coherence resulted in this case is significantly more than that of $\tau_{pc} = 0.5$, for which the light shifts are always present during the action of the probe and the latter gets very little time to act resonantly.

2.1.3 Behavior of the probe during propagation

Expression for transmitted probe intensity

The probe obeys the following equation of propagation

$$\partial_{y/L} f_p = i \frac{e_{disp}}{\theta_p} \tau_{pc} \rho_p. \tag{2.19}$$

e_{disp} is the dispersion parameter discussed in Section. 1.2.2. For $e_{disp}\tau_{pc} \geq \theta_p$, the dispersion affects the entire probe spectrum and the probe is significantly modified as it propagates. The control field obeys a similar equation of propagation, but is only slightly modified for $\theta_c = DA_c\tau_c/\hbar \gg e_{disp}$.

An approximate analytical solution for the transmitted probe intensity can be worked out for the case when the radiated field is small in comparison with the incident field. This condition is satisfied if the dispersion parameter is small and/or the population transfered to the excited state by the probe is substantially reduced by the action of the control. In this case the atoms experience only the incident field and the space dependence of atomic quantities can be neglected. Approximating the coherence ρ_p by the resonant part of K_{14} and using the Eq. (2.18) in Eq. (2.19), the transmitted intensity $I_p(t, L) \propto |A_p f_p(t, L)|^2$, can be approximated for $-T_r \leq t \leq T_r$ by the expression:

$$I_p(t, L) \simeq |A_p|^2 \left[|f_p(t, 0)|^2 - g(t, 0) \cos\left(\int_{-\infty}^{t} (\Omega - \Delta_c) dt' - \phi \right) \right], \tag{2.20}$$

with $g(t, 0) = -e_{disp} \cos^2\theta(t, 0) \left| \int_{-\infty}^{-T_r} f_p(t', 0)\, dt' \right|$. The above expression shows that the transmitted pulse intensity is time modulated with an interference pattern which depends on the light shifts. These oscillations may be shifted by changing the relative phase ϕ. The contrast of the oscillations can be controlled through the dispersion parameter e_{disp}. Another independent parameter to control the oscillations amplitude is the pulse durations ratio τ_{pc} as we see in the next Section.

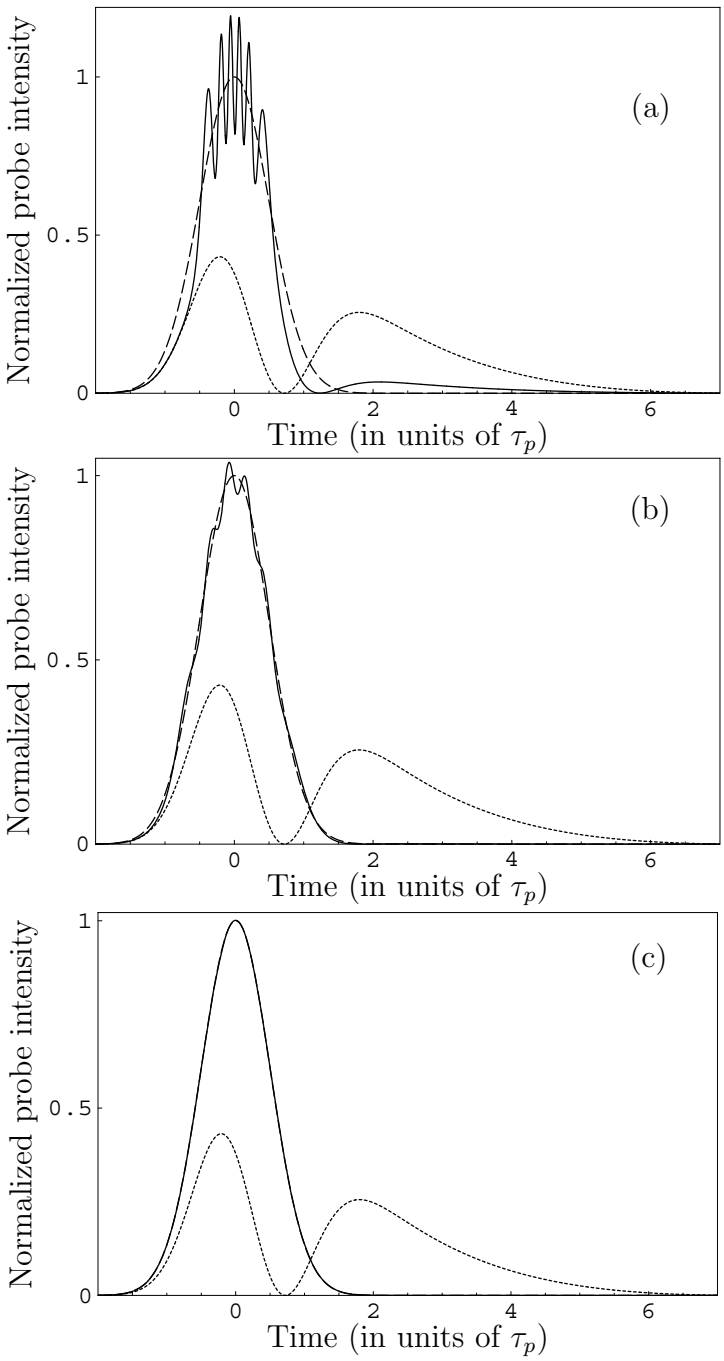

Figure 2.4: Normalized temporal profiles of the probe at $y = 0$ (dashed), at $y = L$ with $\Omega_c = 0$ (dotted), and at $y = L$ with $\Omega_c = 60\tau_c^{-1}$ (solid). The light shifts suppress the long dispersion tail and induce modulations in the central peak. The modulation depth varies for (a) $\tau_{pc} = 2$, (b) $\tau_{pc} = 1$, and (c) $\tau_{pc} = 0.5$. In the last case the probe propagates unaltered. Other parameters are $\theta_p = 0.01$, $\Delta_c = 10\tau_c^{-1}$, and $e_{disp} = 1/\tau_{pc}$.

Effects of light-shifts on the temporal profile

The transmitted probe intensity in the presence and the absence of the control field is shown in Fig. 2.4. In the absence of the control the probe develops a long dispersive tail due to the phenomena discussed in the previous Chapter. In the presence of the control field (and due to the light shifts) this long dispersion tail is significantly suppressed. This is in line with the coherence at $y = 0$ shown in Fig. 2.3(b). Light-shifts greatly reduce the coherence at the end of the probe and this causes the dispersion tail to vanish. As a result, the energy is concentrated in the central peak and the peak exhibits tiny oscillations. The origin of these oscillations is different from the ones seen in the coherence in Fig. 2.3. Here these arise due to the interference between the incident field whose frequency is fixed in time (at ω_0), and the radiated field whose frequency is time dependent ($\omega_c + \Omega$) through the light-shifts. These can be compared with the interference observed in the temporal profile of a chirped pulse as it propagates in a two-level system [Rothenberg85], or ringing effects in a Fabry-perot cavity [Poirson97]. In chirped case the interference between the incident field and the radiated field reveals the sweeping of the instantaneous frequency, whereas in the present case the interference reveals the light-shift induced sweeping of the atomic resonance frequency. The interference on the probe field intensity thus maps the light-shifted region, and can be used to probe the effects due to light-shifts.

The amplitude of the oscillations is modified by changing the relative pulse duration τ_{pc} as is shown in Fig. 2.4. This provides another control in addition to e_{disp} to control the modulation depth. The control arises because τ_{pc} determines $\pm T_r$ that mark the boundary of resonant interaction. For $\tau_{pc} = 2$ in Fig. 2.4(b), the probe gets ample time to interact resonantly with the system. The coherence created resonantly before the onset of the light-shifts is more than the other cases ($\tau_{pc} = 1$ and $\tau_{pc} = 0.5$), hence the radiation during the action of light-shifts is stronger, and causes more prominent oscillations. In the extreme opposite case of $\tau_{pc} = 0.5$, the light-shifts are important throughout the action of the probe, and the latter gets very little time to interact resonantly with the system. The coherence is severely suppressed as is clear in Fig. 2.3, and the probe passes through the system unaltered. This is similar to *electromagnetic induced transparency* [Fleischhauer05], however, in the present case the transparency is due to the action of light-shifts, and not due to the destructive interference of quantum paths (or the dark states).

Effects of light-shifts on the probe spectrum

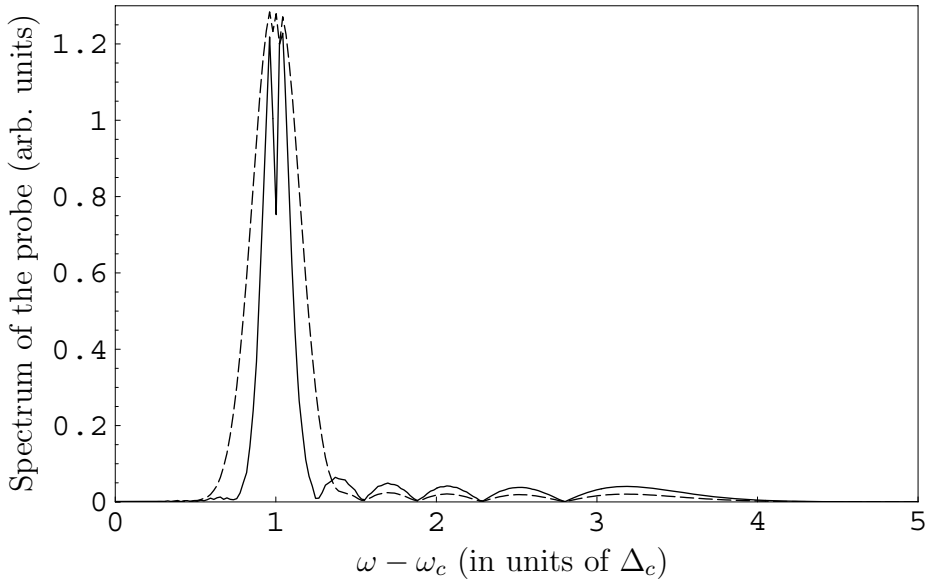

Figure 2.5: The spectrum of the probe gets enriched as it propagates in the driven atomic media. The new frequency components correspond to $1 \leftrightarrow 4$ transitions in the Fig. 2.2. The components are more pronounced for $\tau_{pc} = 2$ (solid) than $\tau_{pc} = 1$ (dashed). The cutoff in both cases is the same. Other parameters are $\Omega_c = 60\tau_c^{-1}$, $\theta_p = 0.01$, $\Delta_c = 10\tau_c^{-1}$, and $e_{disp} = 1/\tau_{pc}$.

The spectrum of the probe gets enriched during propagation in the strongly driven media. The light-shifts introduce new frequency components to the probe. This enriched spectrum of the transmitted probe is shown in Fig. 2.5 for $\tau_{pc} = 1$ and $\tau_{pc} = 2$ ($\tau_{pc} = 0.5$ exhibits similar features at a very reduced scale). In addition to the absorption features at resonance, a modulated structure can be seen in higher frequency range. This corresponds to the transition between the light-shifted levels 1 and 4 in Fig. 2.2 with frequencies $\omega_c + \Omega(t)$. Each new frequency is generated twice in time — once when the levels are being stretched and a second time when the levels are relaxing back — and this leads to the interference pattern shown in the figure. The oscillations in the case of $\tau_{pc} = 2$ are more pronounced as in this case the excited level 4 is more populated than for $\tau_{pc} = 1$. The cut-off frequency in both cases is the same and is given by $\omega_c + \Omega_{max}$.

2.1.4 The two-level system as a pulse shaper

We have seen that propagation of a weak probe in a strongly driven atomic media can probe the light-shifts. The temporal profile of the probe maps out in real time the light-shifted region, and develops an oscillatory structure due to the interference between the incident field, and the radiated field during the action of light-shifts. A smooth pulse at the entrance of the medium thus gets modulated, and the spectrum of the probe gets enriched with new frequency components. This can have a possible application in pulse-shaping that is important for the study and control of many physical processes and chemical pathways [Assion98]. Moreover, the present method provides advantage over the traditional pulse-shaping techniques like liquid crystal displays [Wefers95], accousto-optic modulators [Tull97], and deformable mirrors [Zeek99]; that it can act both for long pulses (picosecond pulses) and in ultraviolet domain.

2.1.5 Experimental considerations

The effects presented here can be observed for picosecond pulses in a two-level system with a large dipole moment,ensuring the induction of light-shifts without ionizing the atomic system. For instance in Rb atoms on the transition $5s\ ^2S_{1/2} \rightarrow 5p\ ^2P_{1/2}$ with $\lambda = 794.76nm$ and $D \simeq 1.7a.u.$ and assuming Gaussian incident pulses with $\tau_c = 10ps$, a beam waist $w_0 = 2mm$ and an energy of $7.2\mu J$, we get $\theta_c = 60$. A wavelength detuning of $0.33nm$ gives $\Delta_c = 10$. The peak intensity is then $I \simeq 3 \times 10^6 W/cm^2$, sufficiently low to avoid direct ionization or multiphoton processes in this system. The optical depths used in the simulations can easily be reached. For instance for a cell with length $L = 1cm$ (smaller than the Rayleigh length $z_0 = \pi w_0^2/\lambda \simeq 15.8m$), we have $e_{disp} \simeq 1$ at $N = 1.1 \times 10^{13} atoms/cm^3$. The atomic density is obtained for the cell temperature $T = 100°C$. The Doppler width $\Delta_{dop} = \sqrt{2k_BT/\left(m_{Rb}\lambda^2\right)}$ has a value of $0.37GHz$. The dipole dephasing time is then $\Delta_{dop}^{-1} \simeq 0.86\pi ns$ much larger than the typical characteristic time considered here ($\tau_c = 10ps$) ensuring that the energy deposition in the medium is small as has been assumed. The approximations used in this section also rely on the use of the one-dimensional model for the propagation. The two beams cross with a small angle that is just higher than the natural divergence angle of the beams so that the spatial separation is possible. The treatment is valid if this angle is very small (so $\theta_{div} = \lambda/\left(\pi w_0\right) \ll 1$) and the spatial overlap between the two beams is perfect along the sample with $\theta_{div} L \ll w_0$. This latter condition is equivalent to having a Rayleigh length $z_0 = \pi w_0^2/\lambda$ higher than the sample length ($z_0 \gg L$). In conclusion, one has to use the beams

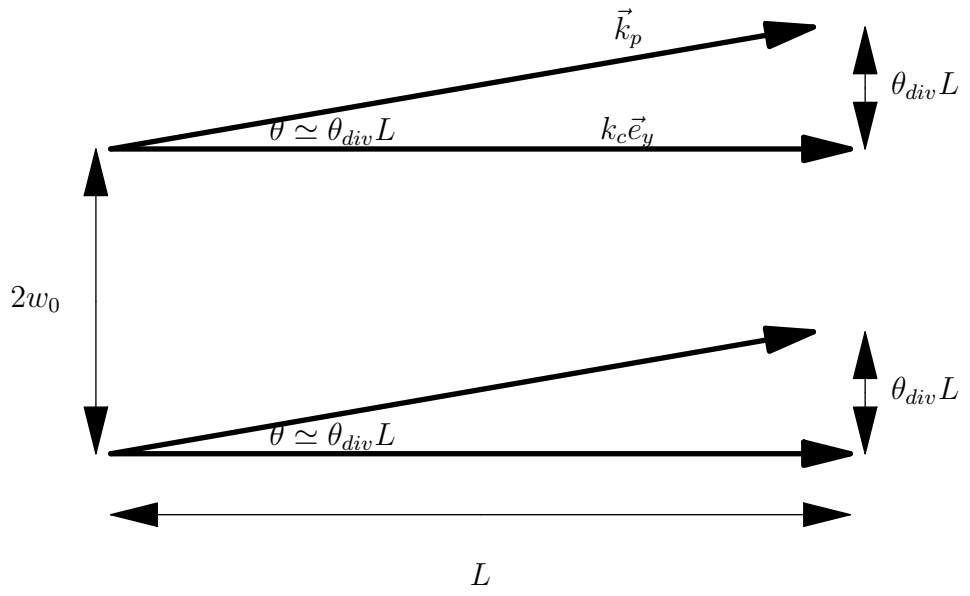

Figure 2.6: Spatial configuration taking into account for the spatial extent of the beams

with large transversal dimensions and to introduce a separation angle of the same order as the natural divergence. With the parameters given above, we get $\theta_{div} = 0.13mrad$ and the ratio z_0/L is 1.58×10^{-3}.

2.2 Phase control of Non-Adiabatic Jumps

Non-adiabatic transitions are another aspect of strong field interaction with the system which has no counterpart in weak field regime. These can lead to significant population transfer to the excited state even when the field does not contain any resonant photons. A complete population inversion in a two-level system interacting with asymmetric, non-resonant, zero-area pulses has been proposed [Vasilev06]. The phenomena is attributed to non-adiabatic jump (NAJ) that takes place in adiabatic basis and transfers suddenly and abruptly all the population to the excited state. We consider a scheme in which the two-level system is excited by two strong, non-resonant, phase locked, identical pulses. The coupling and the energy levels become phase dependent in the adiabatic basis, and for certain phase value NAJ can be invoked in the system. By slightly changing the phase, NAJ is destroyed. This renders phase control of NAJ. For still different values of the phase a double *adiabatic rapid passage*(ARP) [Allen75, Liedenbaum89, Melinger92] comes into action. This leads to transient population in the excited state but

the asymptotic population transfer is vanishing. Thus a very sensitive phase control of the asymptotic population transfer is achieved.

In the following, I will first present the system, introduce the adiabatic basis that are better suited to study the system, and then discuss NAJ and the control of NAJ.

2.2.1 A two-level system driven by a strong asymmetric field

Consider again the two-level system $\{|a\rangle, |c\rangle\}$ interacting with a strong, non-resonant, ultrashort field $A_c f_c(t) e^{-i\omega_c t} + cc$. The Rabi frequency for the field is $\Omega_c(t) = DA_c f_c(t)/\hbar$ and we write it as $\Omega_c(t) = \vartheta_c f_c(t)$. The detuning of the field is $\Delta_c = \omega_0 - \omega_c$, and the field envelope is given by

$$f_c(\phi, t) = \frac{1}{\sqrt{\pi}} \left[e^{-\left(\frac{t+\tau/2}{\tau_c}\right)^2} + e^{i\phi} e^{-\left(\frac{t-\tau/2}{\tau_c}\right)^2} \right]. \tag{2.21}$$

The envelope consists of two time delayed Gaussians each having the time duration τ_c. The delay between the two Gaussians is τ, and the two are dephased by the relative phase difference ϕ. This can arise for example in an interferometer where a field is split by a beam splitter and the two parts of the field propagate along different paths before recombining. The wavefunction of the system can be written as

$$|\Psi(\phi, t)\rangle = a(\phi, t)|a\rangle + c(\phi, t) e^{-i\omega_c t} |c\rangle. \tag{2.22}$$

Schrödinger equation with *rotating wave approximation* (RWA) leads to the following equations for the evolution of the system

$$i\hbar\partial_t \begin{pmatrix} a \\ c \end{pmatrix} (\phi, t) = \hbar \begin{pmatrix} 0 & -\vartheta_c f_c{}^* \\ -\vartheta_c f_c & \Delta_c \end{pmatrix} \begin{pmatrix} a \\ c \end{pmatrix} (\phi, t). \tag{2.23}$$

2.2.2 Adiabatic basis

The interaction can be better studied by transforming the system into adiabatic basis. The choice of the basis is, however, arbitrary. One can try to define the basis for general ϕ, but this makes the problem more complicated by making the phase of total effective field time-dependent. A better strategy is to define the basis for one particular ϕ, and then study how the light shifts and the coupling are modified by changing ϕ. We define the adiabatic basis for $\phi = \pi$. This choice of transformation will prove to be much more adapted

to the present situation, as the physics of the obtained results will be very elegantly highlighted with this basis change. We write the field envelope as

$$f_c(\phi,t) = f_c(\pi,t) + f_v(\phi,t), \tag{2.24}$$

where

$$f_c(\pi,t) = \frac{1}{\sqrt{\pi}}\left[e^{-\left(\frac{t+\tau/2}{\tau_c}\right)^2} - e^{-\left(\frac{t-\tau/2}{\tau_c}\right)^2}\right], \tag{2.25a}$$

$$f_v(\phi,t) = \frac{1}{\sqrt{\pi}}\left(1+e^{i\phi}\right)e^{-\left(\frac{t-\tau/2}{\tau_c}\right)^2}. \tag{2.25b}$$

The rotation matrix is

$$R(t) = \begin{pmatrix} \cos\theta & \sin\theta \\ -\sin\theta & \cos\theta \end{pmatrix}(t), \tag{2.26}$$

and the mixing angle $\theta(t)$ is defined as

$$\theta(t) = \frac{1}{2}\arctan\left[2r f_c(\pi,t)\right]. \tag{2.27}$$

Here $r = \vartheta_c/\Delta_c$ is an important parameter that characterizes the non-adiabatic coupling. The amplitudes of the wavefunction (2.22) are transformed into adiabatic basis as

$$\begin{pmatrix}\alpha\\ \gamma\end{pmatrix}(\phi,t) = R(t)\begin{pmatrix}a\\ c\end{pmatrix}(\phi,t). \tag{2.28}$$

The time evolution of the amplitudes is given by

$$i\hbar\partial_T\begin{pmatrix}\alpha\\ \gamma\end{pmatrix}(\phi,t) = \hbar\left[A(t)+V(\phi,t)\right]\begin{pmatrix}\alpha\\ \gamma\end{pmatrix}(\phi,t). \tag{2.29}$$

$A(t)$ represents the Hamiltonian for $\phi=\pi$. It is given by

$$A(t) = \frac{1}{2}\begin{pmatrix}\Delta_c-\Omega & 2i\partial_T\theta \\ -2i\partial_T\theta & \Delta_c+\Omega\end{pmatrix}. \tag{2.30}$$

The diagonal terms are the light shifted adiabatic energy levels with $\Omega(t) = \Delta_c\sqrt{1+4r^2f_c^2(\pi,t)}$ being the instantaneous separation between the levels, and the off-diagonal term $\partial_T\theta$ represents the non-adiabatic coupling. $V(\phi,t)$ in (2.29) represents the correction to the energy levels and the coupling when $\phi\neq\pi$. It is given by:

$$V(\phi,t) = \frac{-2r\Delta_c e^{\left(\frac{t-\tau/2}{\tau_c}\right)}}{\sqrt{\pi}}\cos^2\left(\frac{\phi}{2}\right)\begin{pmatrix}\sin 2\theta & \cos 2\theta - i\tan(\phi/2)\\ \cos 2\theta + i\tan(\phi/2) & -\sin 2\theta\end{pmatrix}. \tag{2.31}$$

We next consider the population dynamics for different values of ϕ.

2.2.3 Non-adiabatic jump (NAJ) for $\phi = \pi$

For $\phi = \pi$, the matrix $V(\phi, t)$ is *zero*, and the dynamics is determined by the matrix $A(t)$ as given in (2.30). The two Gaussians are asymmetric with respect to each other and for $|\tau| \gg \tau_c$, the two dress the system independently. Each Gaussian induces local non-adiabatic transitions but these do not cause significant population transfer to the excited state. When the two Gaussians are brought near to each other — with $|\tau| \approx \tau_c$ — such that the falling edge of one Gaussian coincides with the rising edge of the other, the light shifts and the non-adiabatic coupling add up non-linearly. The energy levels in this case present a modulated structure with a node at $t = 0$, and the coupling acquires the shape of a delta function at the node. The field profile, the adiabatic energy levels, and the non-adiabatic coupling for $\tau = \tau_c$ are shown in Fig. 2.7. The non-adiabatic coupling causes significant population transfer at $t = 0$ which is shown in Fig. 2.8. This abrupt jump in the adiabatic

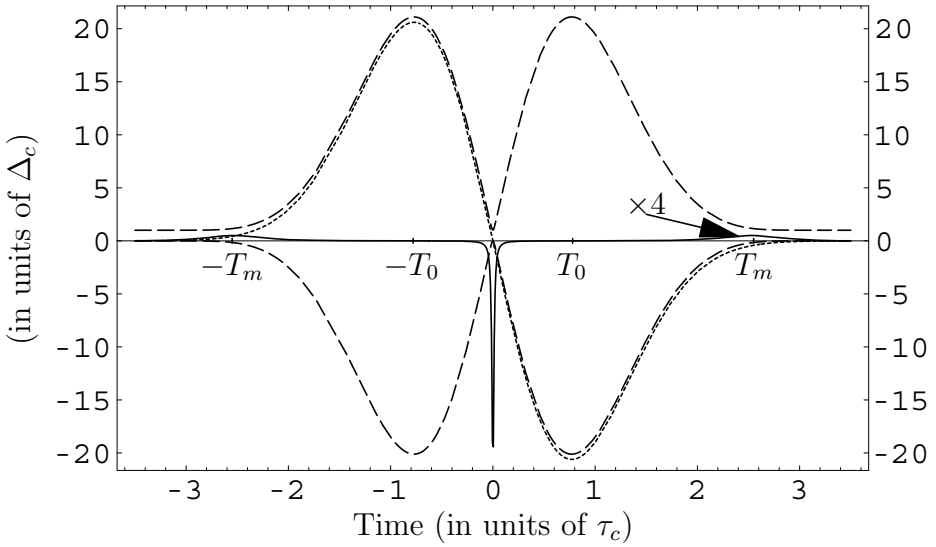

Figure 2.7: Field profile (dotted), adiabatic energy levels (dashed), and (4 times) magnified non-adiabatic coupling (solid). The coupling presents a minimum at $t = 0$, is 0 at $t = \pm T_0$, and presents two local maxima at $t = \pm T_m$.

populations can be understood by analyzing the behavior of non-adiabatic coupling. The coupling follows the derivative of the field profile and is given by

$$\partial_T \theta(t) = \frac{r \partial_T f_c(\pi, t)}{1 + 4r^2 f_c^2(\pi, t)}. \tag{2.32}$$

It presents a minimum at $t = 0$ where the light shifts vanish, and goes to *zero* at $\pm T_0$. $\pm T_0$ are the points where the light shifts are at maximum, and are the solutions of $2t \tanh(t\tau/\tau_c^2) = \tau$. The coupling presents two local maxima at $t = \pm T_m$. A small population disturbance at $\pm T_m$ can be seen in Fig. 2.7(b). We will next show that the non-adiabatic coupling behaves as a delta function near $t = 0$ for $r \to \infty$. At $t = 0$, the field vanishes $f_c(\pi, 0) = 0$, and from (2.32) we can see that the non-adiabatic coupling diverges for $r \to \infty$. However, the area beneath the coupling remains finite between $\pm T_0$. It is given by

$$\begin{aligned} A_{NC} &= 2\int_{-T_0}^{T_0} (\partial_T \theta)(t)\, dt, \\ &= 2\arctan\left[2r f_c(\pi, T_0)\right]. \end{aligned} \tag{2.33}$$

The factor 2 has been introduced to conform with the convention of "π area pulse causing complete population inversion". The area beneath the coupling behaves as $A_{NC}|_{r\to\infty} = -\pi$. The characteristic width of the coupling can be approximated as $\delta T = A_{NC}/\partial_T \theta(0)$. It behaves as $\delta T = 2\arctan\left[2r f_c(\pi, T_0)\right]/r\partial_T f_c(\pi, 0)$ and vanishes for $r \to \infty$. These results show that the central part of the non adiabatic coupling around $t = 0$ indeed behaves as a delta function with an area $-\pi$ (or π if the sequence of the two Gaussians is reversed). Moreover, near $t = 0$, the light shifts are at minimum with $\Omega \approx \Delta_c$, and in the limit of strong pulse ($r \gg 1$), the excitation can be considered as resonant. The transition probability to the excited adiabatic level is thus $\sin^2 \frac{A_{NC}}{2} \approx 1$. Complete population inversion in adiabatic basis with a sudden jump can be realized as shown in Fig. 2.8. A limitation to obtain a perfect 0 to 1 population jump in the adiabatic states is the population already transferred in the wing at $T = -T_m$. At $T = T_m$, the non-adiabatic coupling can again modify asymptotic population. This can be avoided if the evolution is adiabatic in the wings, requiring $\Omega(\pm T_m) \gg |\partial_T \theta(\pm T_m)|$. This condition can be easily fulfilled by making detuning large $\Delta_c \gg 1$, and maintaining $r \gg 1$ for obtaining the desired NAJ at $t = 0$.

2.2.4 Phase control of NAJ for $\phi \neq \pi$

When $\phi \neq \pi$, the additional contributions from the matrix $V(\phi, t)$ have to be taken into account. For arbitrary times and phase shift values, V contains both non-vanishing diagonal and off-diagonal terms. Light shifts and optical coupling between the adiabatic states are thus modified. As the total coupling is no longer a π area delta function, the transition probability to excited adiabatic state is dramatically affected. In Fig. 2.9, the excited state

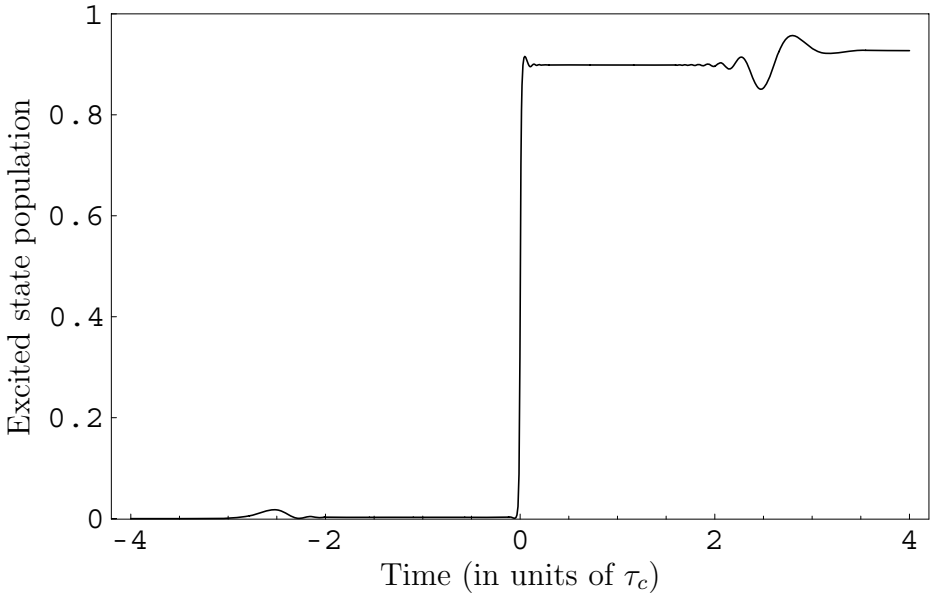

Figure 2.8: Excited state population in adiabatic basis exhibits a jump at $t = 0$. Parameters are $\Delta_c = 8\tau_c^{-1}$, $\vartheta_c = 400\tau_c^{-1}$ ($r = 50$), $\tau = \tau_c$, and $\phi = \pi$.

adiabatic population as a function of ϕ is shown just before and after the time when a non-adiabatic jump occurs for $\phi = \pi$. It can be seen that close to $\phi = \pi$, the jump retains some of it character in a very narrow window with rapidly losing its efficiency. Outside the narrow window around $\phi = \pi$, the population exhibits different behavior both before and after the jump. Before the jump in Fig. 2.9(a), the small population is due to the non-resonant coupling introduced by $V(\phi, t)$ that acts outside the interaction region δT. After the jump in Fig. 2.9(b), the rise in population away from $\phi = \pi$ is due to the level crossings introduced by $V(\phi, t)$. Both of these are the transient effects, and no permanent population transfer takes place in the wings, as can be verified in the plot of asymptotic excited state population in Fig. 2.10. This demonstrates the sensitive dependence of asymptotic transition probability on phase shift. The transient population dynamics will be discussed shortly.

Modification of NAJ for ϕ close to π

The behavior around $\phi = \pi$ in Fig. 2.10 can be explained by analyzing the matrix elements of $V(\phi, t)$. For small variations of ϕ around π with $\phi = \pi + \epsilon$, $\epsilon \ll 1$, we can neglect the additional light shifts as these are proportional to ϵ^2. The matrix V at $t = 0$ thus simplifies as $V \approx \frac{r\Delta_c\epsilon}{\sqrt{\pi}} e^{-\tau^2/(4\tau_c^2)} \left(\begin{smallmatrix} 0 & -i \\ i & 0 \end{smallmatrix}\right)$.

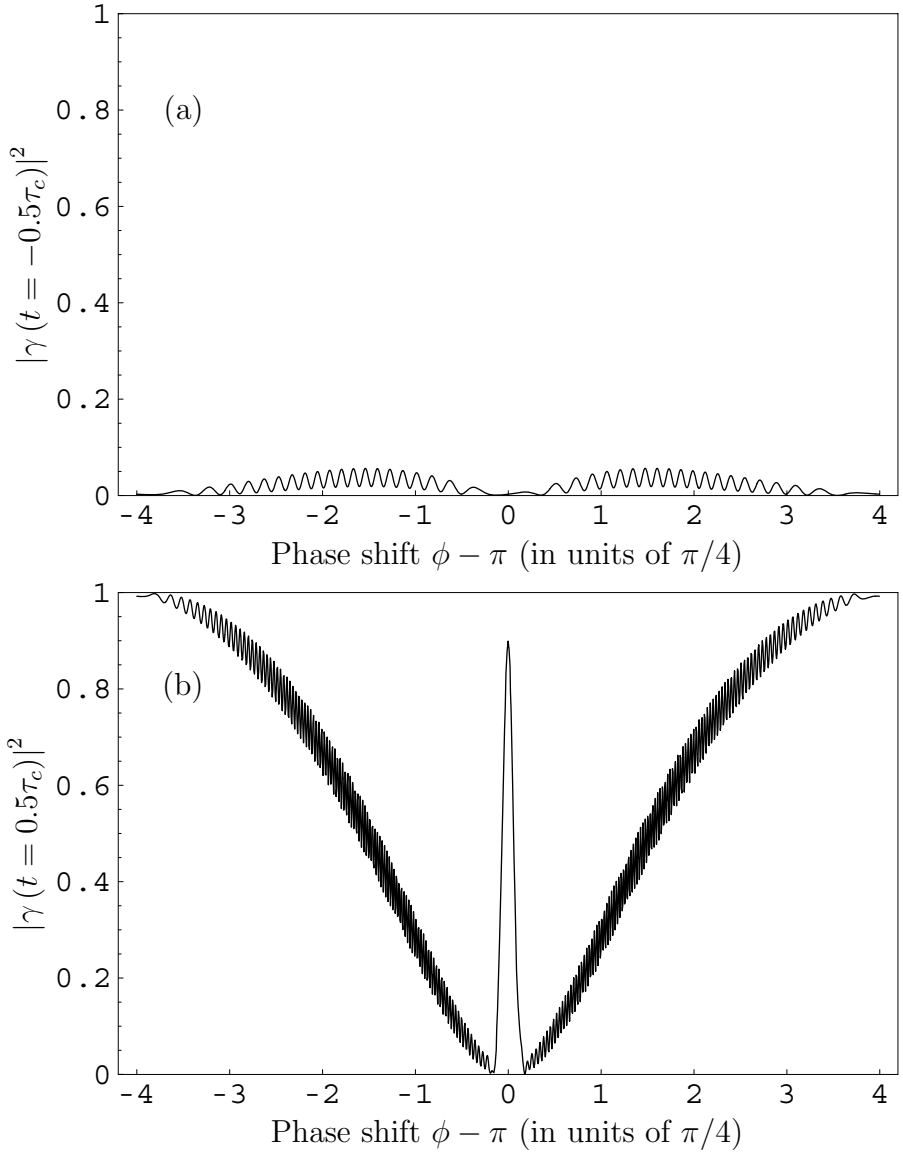

Figure 2.9: Adiabatic excited state population profile (a) before NAJ at $t=-0.5\tau_c$; (b) after NAJ at time $t=0.5\tau_c$. NAJ exists only for ϕ very close to π. Away from $\phi=\pi$, population in (a) is due to non-resonant coupling provided by $V(\phi,t)$; and in (b) because of level crossings. The oscillations are discussed in the text. Parameters are $\Delta_c=8\tau_c^{-1}$, $\vartheta_c=400\tau_c^{-1}$ ($r=50$), and $\tau=\tau_c$.

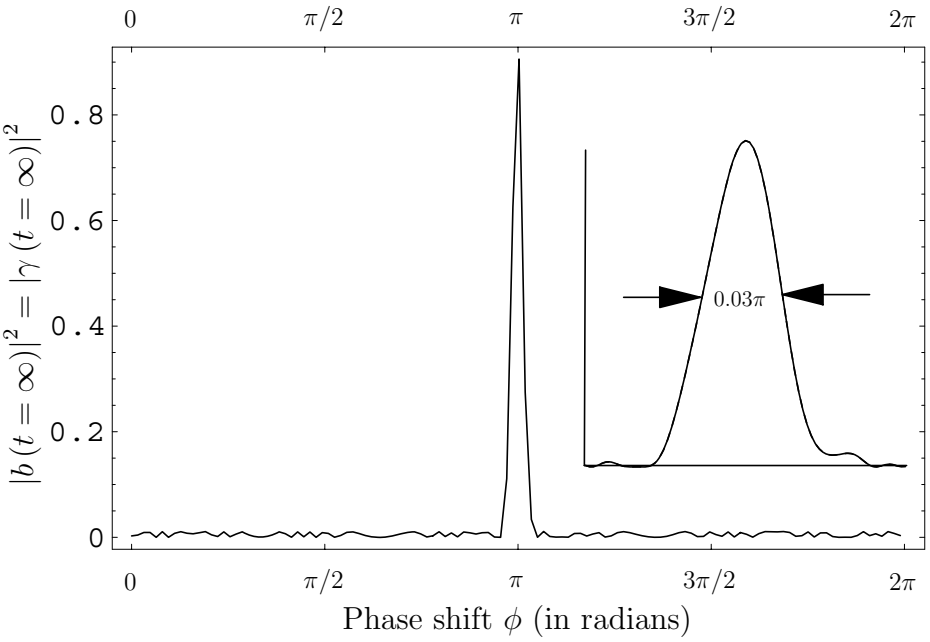

Figure 2.10: Asymptotic excited state population. In inset a zoom is made to show the narrow width of the peak. Parameters are $\Delta_c = 8\tau_c^{-1}$, $\vartheta_c = 400\tau_c^{-1}$ ($r = 50$), $\tau = \tau_c$, and $\phi = \pi$.

During the action of NAJ —in the time interval δT— the modification of the effective pulse area due to the presence of the additional coupling V is negligible provided $2\left|\frac{r\Delta_c\epsilon}{\sqrt{\pi}}e^{-\tau^2/(4\tau_c^2)}\delta T\right| \ll \pi$. This condition can be simplified to $\epsilon \ll \tau/(\Delta_c\tau_c^2)$, and it implies that for $\epsilon = \tau/(\Delta_c\tau_c^2)$, the contribution from $V(\pi, t)$ over the resonant-interaction region δT is as important as NAJ, and it completely washes out the effect of NAJ. For ϕ much closer to π, the perturbation due to the matrix V is small and NAJ retains some of its efficiency. This is shown in Fig. 2.11, where excited adiabatic state population is shown near $t = 0$ for different phase values. The vertical lines in the Figure mark the region δT. The asymmetry of the perturbation V modifies NAJ differently for different sign of ϵ. For $\phi = \pi + \epsilon$ the perturbation adds up to NAJ in the interaction region δT, and for $\phi = \pi - \epsilon$ it makes NAJ less efficient. An important feature is the modification of the population just outside the region δT. This is due to the fact that the perturbation V, unlike NAJ acts over a very wide region and can modify the populations when the energy levels are still close to each other.

Another interesting feature in Fig. 2.11 is the presence of oscillations both before and after NAJ, with the oscillations after NAJ much stronger and prominent. These arise because of the interference between the population transfered to the excited state at different times. Before NAJ, the small population transfered by $\partial_t\theta$ at $t = -T_m$ interferes with the population transfered non resonantly by $V(\phi, t)$. After the jump, the non-resonant contribution interferes with the population transfered resonantly by NAJ. These non-resonant contributions to the population are small, but these lead to observable effects because of the interference. Theses oscillations are different from Rabi oscillations and have been observed and reported in atomic systems driven by chirped pulses [Rothenberg85, Zamith01], or submitted to strong fields that induce light-shifts as discussed in the previous Section [Delagnes04, Delagnes06, Delagnes07e].

Adiabatic rapid passage

For $\phi \neq \pi$, the level crossings can appear in the system. Indeed, the diagonal elements of $V(\phi, t)$ in (2.31), are the corrections to the adiabatic energy levels for $\phi \neq \pi$. These corrections $\propto \cos^2(\phi/2)\sin 2\theta$ change sign at $t = 0$ because of the asymmetry of the field $f_c(\pi, t)$ (we have $\sin 2\theta = 2r f_c(\pi, t)$). If ϕ is such that these corrections become more important than the diagonal elements of $A(t)$, then the adiabatic energy levels exhibit a crossing near $t = 0$. Any small coupling at the crossing can cause significant population transfer through *adiabatic rapid passage* (ARP). This explains important

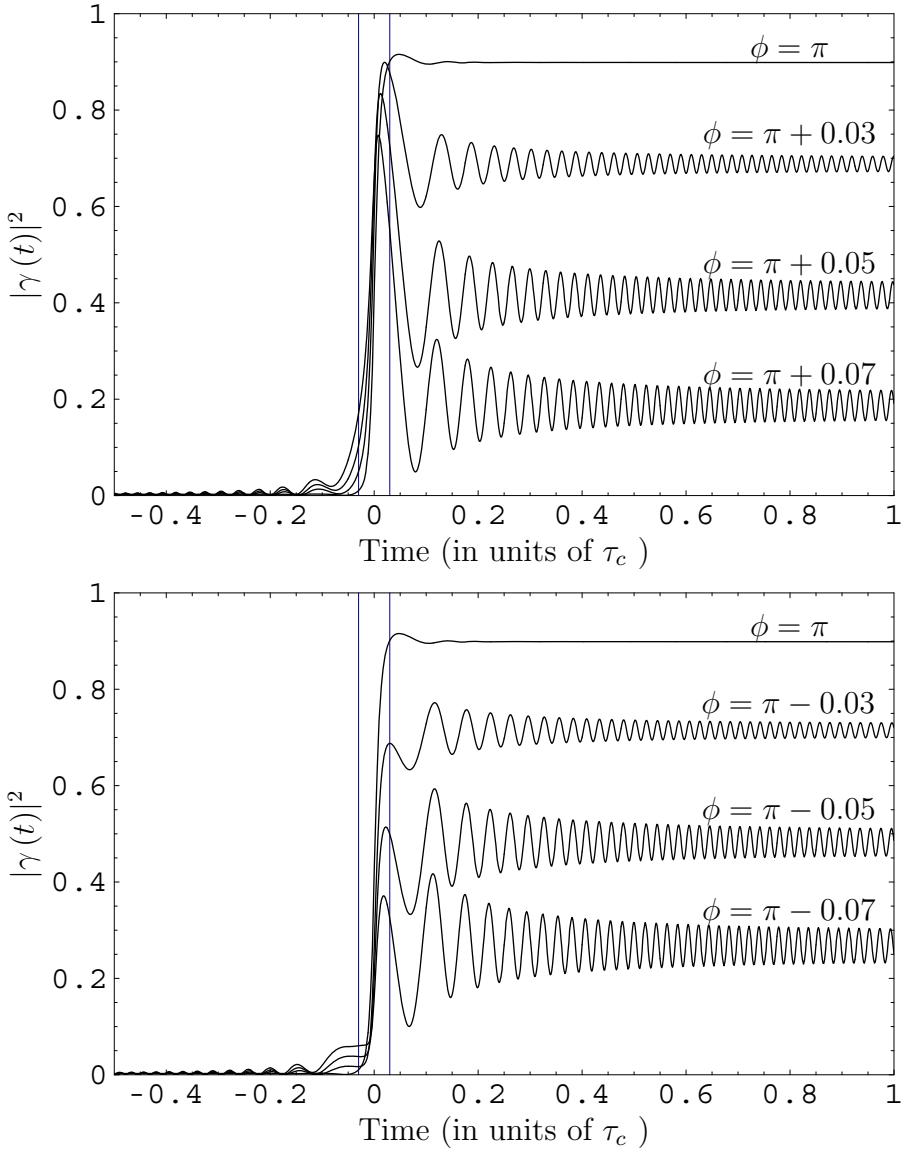

Figure 2.11: Adiabatic excited state population for various phase values. Vertical lines mark the region δT. NAJ survives for little variations around $\phi = \pi$. Parameters are $\Delta_c = 8\tau_c^{-1}$, $\vartheta_c = 400\tau_c^{-1}$ ($r = 50$), $\tau = \tau_c$, and $\phi = \pi$.

population transfer to the excited adiabatic state in Fig. 2.9(b) for ϕ away from π. However, this crossing is always accompanied by a second crossing when the contribution because of diagonal elements of $V(\phi, t)$ becomes negligible as compared to $\Omega(t)$. For $\phi = 0$, this second crossing appears near the end of the pulse when the adiabatic energy levels relax back to the bare state picture. The second crossings brings all the population back to the ground adiabatic level and explains vanishing asymptotic population for ϕ away from π in Fig. 2.10. These crossings and the population in the excited adiabatic state because of ARP for $\phi = 0$ are shown in Fig. 2.12. The transient oscillations are strongly attenuated in this case and appear only near the end of the pulse when the levels are close enough to cause non-resonant transitions.

Transient population dynamics

We can now understand the transient population dynamics in excited adiabatic level as shown in Fig. 2.9. For ϕ very close to π, the dynamics is determined by NAJ as has been already discussed. For ϕ away from π, and for times before the jump (at $t = -0.5\tau_c$ in the Figure), the small population in (a) is due to the non-resonant coupling provided by $V(\phi, t)$. The coupling has a component $\propto \sin\phi$ which acts over a very wide region, and a component $\propto \cos^2(\phi/2)$ which is localized near $t = 0$ (due to the profile of $\cos 2\theta$). Thus for times away from NAJ, and for phase close to $2n\pi$, the coupling vanishes and this explains the already small population in Fig. 2.9(a) going to *zero* in the wings.

The dynamics after the jump in Fig. 2.9(b) are governed by ARP and the level crossings. The crossings take place for $t \simeq 0$. In this region the additional coupling by $V(\phi, t)$ is resonant and non vanishing for all $\phi \neq \pi$. The interplay between the level stretching and the coupling leads to increased population transfer as we move away from $\phi = \pi$.

The oscillations in the Figure has the same origin as the one seen in the temporal profile in Fig. 2.11. The small population transfered by $\partial_t\theta$ at $t = -T_m$ interferes with the population transfered at later time by $V(\phi, t)$ and induces oscillations in the temporal profile. At a given time ($\pm 0.5\tau_c$ in the Figure), the change in the phase sweeps through these temporal oscillations by modifying the coupling. Hence oscillations appear in the phase profile as well as shown in the Figure. Moreover, the non-resonant population transfer in Fig. 2.9(a) is less sensitive to the phase variation than the one that takes place resonantly (at the crossing) with abruptly changing energy levels. This latter leads to more fast oscillations as seen in Fig. 2.9(b).

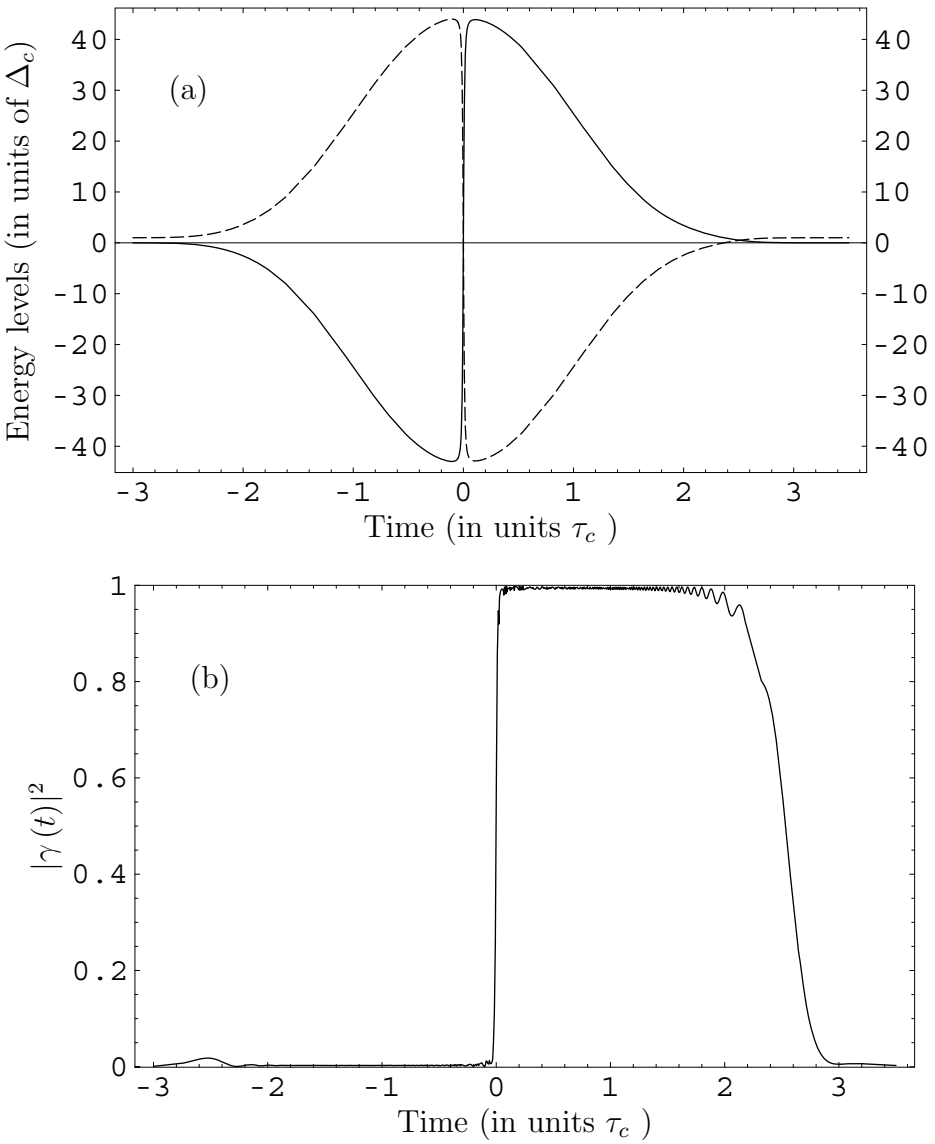

Figure 2.12: (a) Energy levels showing two crossings and (b) excited state adiabatic population. ARP results in complete but transient population transfer near $t = 0$, the population comes back when the adiabatic levels relax to bare state picture.

Sensitive phase dependence

The asymptotic population transfer to the excited state exhibits a very sensitive dependence with phase as shown in Fig. 2.10. In subsection 2.2.4, it was shown that NAJ is completely washed out by $V(\phi, t)$ for $|\phi - \pi| \geq \tau/(\Delta_c \tau_c^2)$. For ϕ inside this narrow window, the width of the central peak decreases further by increasing r. This is because of the population dynamics induced by by $V(\phi, t)$ outside the interaction region. This narrowing of the central peak for different field strengths is shown in Fig. 2.13.

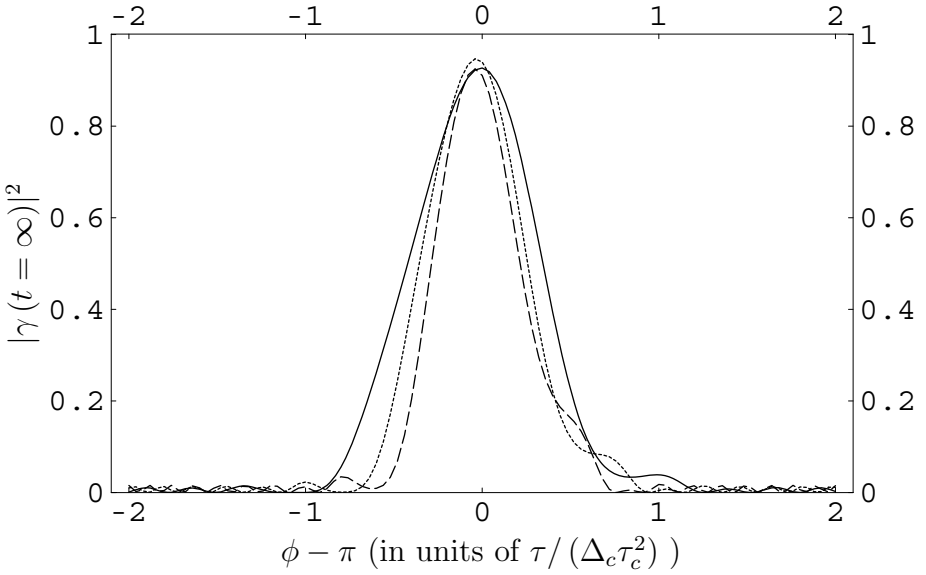

Figure 2.13: Sensitive phase dependence of NRJ. FWHM of the central peak decreases with increasing r. Parameters are $r = 50$ (solid) with width 0.031π , $r = 75$ (dotted) with width 0.025π, and $r = 100$ (100) with FWHM given by 0.019π

The realization of very sharp structures with ϕ is in line with a very good spatial and temporal sensitivity of interferometers. For instance when the sequence of two ultrashort pulses is obtained by sending a single pulse into an interferometer, we can write $\phi = \omega_c \delta t$, where δt is the delay between the two pulses. For pulses with 800 nm wavelength, we obtain from Fig. 2.10, $\delta t \sim 40\ as$ for field strength $\vartheta_c \tau_c = 400$. This correspond to spatial resolution $\delta x = c\delta t$ of 12 nm. Finally the large values of ϑ_c can be obtained by using long pulses. For instance, we have $\vartheta_c \tau_c \approx 110 \mu_{ab}(a.u.)\tau_c(ns)\sqrt{I(MW/cm^2)}$. For a transition with $\mu_{ab} = 4\ a.u.$, a laser pulse with a time duration $\tau_d = 10$ ns, and an energy of 1 μJ focused on 1 mm^2 spot, we can obtain a value for $\vartheta_c \tau_c$ as large as 440.

2.2.5 Observation of non-adiabatic jump

The observation of non-adiabatic transitions in bare state populations is not straightforward [Vasilev06]. Fig. 2.14 shows the bare state population corresponding to adiabatic populations shown in Fig. 2.8 and Fig. 2.12(b). In (a) with $\phi = \pi$, the population grows from *zero* to a maximum value exhibiting strong oscillations corresponding to off-resonance Rabi beating. The change associated with NAJ corresponds only to the modification of the oscillation amplitude at $t = 0$. These oscillations arise before the jump, near $-T_m$ where the residual non-adiabatic contribution populates the excited adiabatic state, and are modified at $T = 0$ due to abrupt re-distribution of population among adiabatic states. But the re-distribution of population among adiabatic levels does not always correspond to significant modifications in bare state. Indeed, in the case of an ideal jump with adiabatic population going from 0 to 1, these oscillations in the bare state disappear and the signature of the transition jump vanishes. This can be appreciated in the Fig. 2.14(b) for the case $\phi = 0$ where the adiabatic population show perfect population inversion [Fig. 2.12(b)], but the bare state picture does not reflect the change in adiabatic populations. It is thus hard to deduce the exact nature of the dynamics by measuring only the excited state population. We propose in the next section a method to observe these non-adiabatic jumps.

2.3 Probing NAJ by propagation effects

The non-adiabatic jump (NAJ) discussed in the previous Section takes place in adiabatic basis and can not always be detected in the bare state populations. However, the jump takes place for strong driving fields that also induce important light-shifts. These light-shifts can be probed using the technique discussed in Section. 2.1. The excited adiabatic level that is populated by NAJ, can be coupled resonantly by a weak probe to a third level in the system. The probe while propagating in the system maps out light-shifted region on its temporal profile (in the form of oscillations) only if the adiabatic level is populated. Before the jump, the excited adiabatic level is empty and the probe propagates unaltered in the system. At the onset of the jump, the level is populated and the probe develops an oscillatory structure starting at the time where the jump takes place. The position of the jump is thus marked in real time on the temporal profile of the probe.

Consider the three level system shown in Fig. 2.15. The state $|a\rangle$ and $|c\rangle$ are coupled by a strong, non-resonant, asymmetric pulse that induces NAJ at time $t = 0$ as discussed in the previous Section. We couple the excited level $|c\rangle$

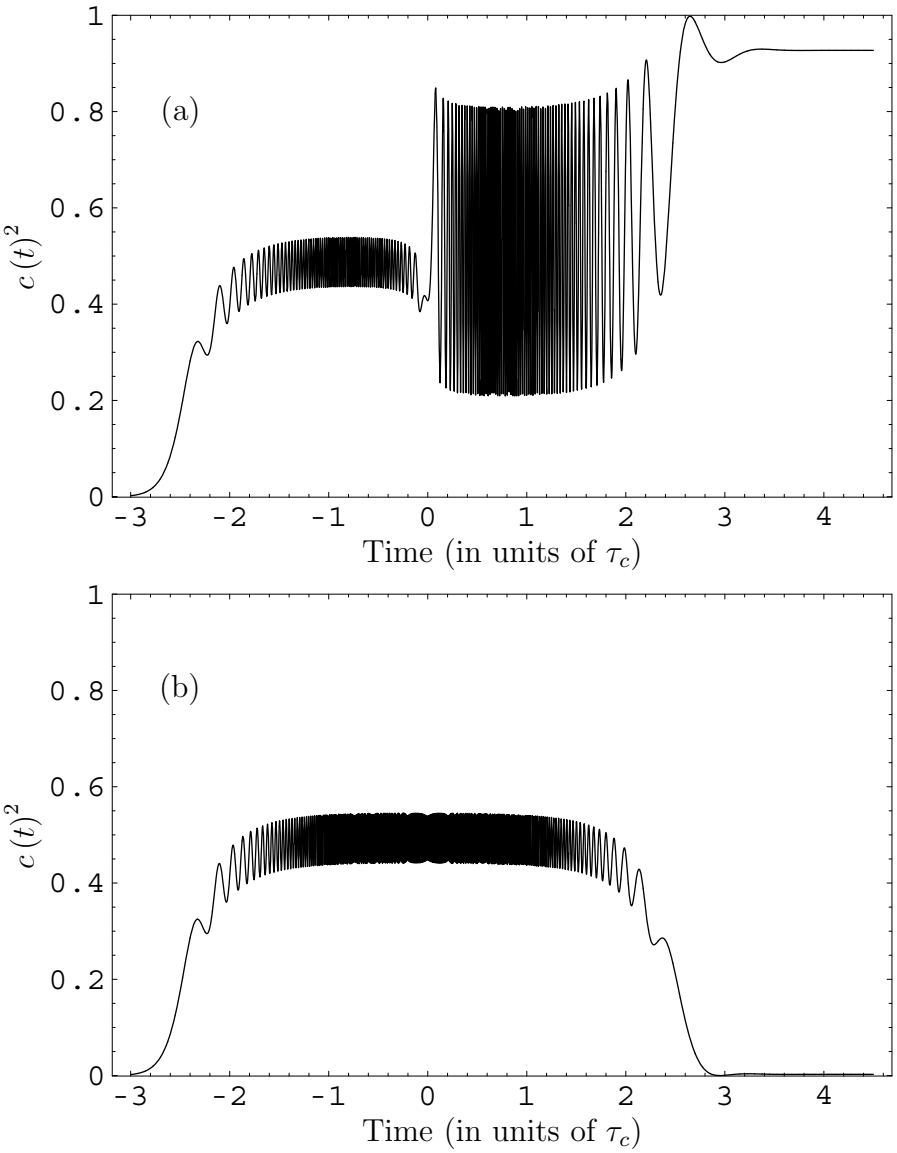

Figure 2.14: Excited bare state population corresponding to (a) NAJ in Fig. 2.8 with $\phi = \pi$, and (b) ARP in Fig. 2.12(b) with $\phi = 0$. In (a) the oscillation amplitude is changed with NAJ. In (b) the complete population inversion in adiabatic basis gets unnoticed in bare state representation. Parameters are $\Delta_c = 8\tau_c^{-1}$, $\vartheta_c = 400\tau_c^{-1}$ ($r = 50$), $\tau = \tau_c$, and $\phi = \pi$.

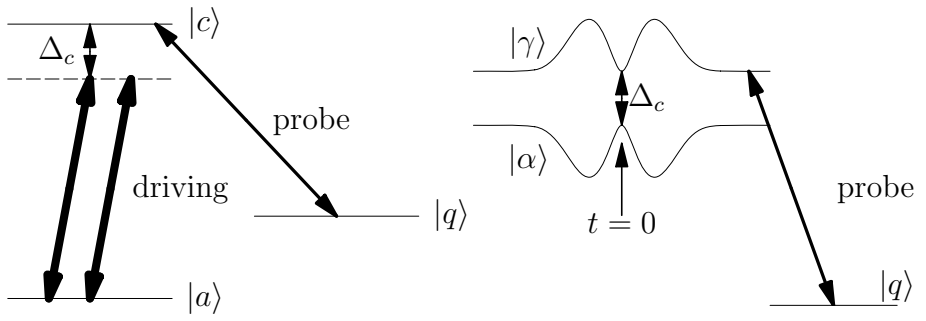

Figure 2.15: A sequence of two time delayed, non-resonant strong pulses excite a two level system. A weak probe resonant on an adjacent transition probes the non-adiabatic transitions.

to another level in the system $|q\rangle$ by a weak probe. The probe is resonant with the transition $|c\rangle \leftrightarrow |q\rangle$, and is given by $A_p f_p(t,y)\, e^{-i(\omega_{cq}t-ky)} + cc$. We define the dimension-less strength parameter for the probe as $\theta_p = D_{cq}A_p\tau_p/\hbar$. D_{cq} is the dipole matrix element for the concerned transition and τ_p^{-1} is the spectral bandwidth of the probe. The probe is propagating along y axis and the pulse envelope at $y=0$ is given by

$$f_p(t,0) = \frac{1}{\sqrt{\pi}} e^{-\left(\frac{t-t_p}{\tau_p}\right)^2}. \tag{2.34}$$

The system is transformed into adiabatic basis by the transformation

$$\begin{pmatrix} |\alpha\rangle \\ |\gamma\rangle \\ |q\rangle \end{pmatrix} = \begin{pmatrix} \cos\theta & \sin\theta & 0 \\ -\sin\theta & \cos\theta & 0 \\ 0 & 0 & 1 \end{pmatrix} \begin{pmatrix} |a\rangle \\ |c\rangle \\ |q\rangle \end{pmatrix}. \tag{2.35}$$

The mixing angle is the same as given by Eq. 2.27. The evolution of the the wave function

$$|\Psi\rangle = \alpha\,|\alpha\rangle + \gamma\,|\gamma\rangle + q\,|q\rangle\,, \tag{2.36}$$

is given by

$$i\partial_t \begin{pmatrix} \alpha \\ \gamma \\ q \end{pmatrix} = \begin{pmatrix} \frac{\Delta_c - \Omega(t)}{2} & i\partial_T\theta & -\theta_p\tau_p^{-1} f_p^* \sin\theta \\ -i\partial_T\theta & \frac{\Delta_c+\Omega(t)}{2} & -\theta_p\tau_p^{-1} f_p^* \cos\theta \\ -\theta_p\tau_p^{-1} f_p \sin\theta & -\theta_p\tau_p^{-1} f_p \cos\theta & \Delta_c \end{pmatrix} \begin{pmatrix} \alpha \\ \gamma \\ q \end{pmatrix}. \tag{2.37}$$

Here $\partial_T\theta$ is the non-adiabatic coupling given by Eq. 2.32 and causes NAJ at $t=0$. Here we have neglected the contribution due to $V(\phi,t)$ from (2.31) as it is not relevant for the present discussion.

In adiabatic basis the probe couples the state $|q\rangle$ with both the states $|\alpha\rangle$ and $|\gamma\rangle$. However for $\Delta_c \gg \tau_p^{-1}$, the coupling is resonant only with the excited adiabatic level $|\gamma\rangle$. Moreover, the coupling is resonant only for the time between $-T_r$ and T_r, which are the solutions of $\Omega - \Delta_c \leq \tau_p^{-1}$.

2.3.1 Coherence behavior

The coherence that radiates on on $|c\rangle \leftrightarrow |q\rangle$ is given by

$$\rho_p = q^* \left(\alpha \sin\theta + \gamma \cos\theta\right), \tag{2.38}$$

and can be simplified to $q^*\gamma\cos\theta$ because of the resonant-interaction consideration just discussed. We next work out the expression for the coherence and the transmitted probe intensity.

We assume that initially all the population is in the ground state $|\alpha\rangle$. With adiabatic evolution the population rests in the ground state until $t = 0$. At $t = 0$, there is a sudden jump and all the population is transfered to the excited state by NAJ. Subsequent evolution of the system at *zeroth order* with respect to the probe amplitude is given by

$$\alpha^{(0)}\left(t > 0\right) = e^{-i\int_0^t \frac{\Delta_c + \Omega(t')}{2} dt'}, \tag{2.39}$$

$$\gamma^{(0)}\left(t > 0\right) = 0. \tag{2.40}$$

For time $0 < t \leq T_r$, the probe is resonant on $|\gamma\rangle \leftrightarrow |q\rangle$ and can create the coherence ρ_p. The amplitude q at *first order* between the time 0 and T_r is given by:

$$q^{(1)}\left(0 < t \leq T_r\right) = i\frac{\theta_p}{\tau_p} e^{-i\Delta_c t} \int_0^t f_p dt'. \tag{2.41}$$

For $t > T_r$ we neglect the non-resonant contribution to the amplitude q and write it as

$$q^{(1)}\left(t > T_r\right) = i\frac{\theta_p}{\tau_p} e^{-i\Delta_c t} \int_0^{T_r} f_p dt'. \tag{2.42}$$

The coherence at $y = 0$ and for $t > 0$ can thus be approximated as

$$\rho_c \simeq= -i\frac{\theta_p}{\tau_p} e^{-i\int_0^t \frac{-\Delta_c + \Omega(t')}{2} dt'} \int_0^{T_r} f_p^* dt'. \tag{2.43}$$

2.3.2 Transmitted probe intensity

The probe follows the propagation equation

$$\partial_{y/L} f_p = i \frac{e'_{disp}}{\theta_p} \rho_p. \tag{2.44}$$

e'_{disp} is the dispersion parameter for the probe defined as $e'_{disp} = N D_{cq}^2 \omega_{cq} L \tau_p / (2c\epsilon_0 \hbar)$, and L is the length of the medium. The strong field that induces NAJ on $|a\rangle \leftrightarrow |c\rangle$ transition also obeys a similar equation of propagation, but is only slightly distorted because it is very strong. The above equation can be solved in the perturbative limit. Using the expression (2.43) we can write

$$f_p(t, y) \simeq f_p(t, 0) + g(t, 0)\, e^{-i \int_0^t \frac{-\Delta_c + \Omega(t')}{2} dt'}, \tag{2.45}$$

with $g(t, 0) = e'_{disp} \tau_p^{-1} \cos\theta(t, 0) \int_0^{T_r} f_p(t', 0)\, dt'$. The transmitted intensity $I_p(t, L) = |A_p f_p(t, L)|^2$ can thus be approximated for $t > T_r$, at the lowest order in e'_{disp} by the following expression:

$$I_p(t, L) \approx I_p(t, 0) + 2A_p^2 f_p(t, 0)\, g(t, 0)\, \cos \int_0^t \frac{\Omega(t') - \Delta_c}{2} dt'. \tag{2.46}$$

This formula shows that the transmitted pulse intensity is modulated with an interference pattern that depends on the light-shifts induced on the transition $|a\rangle \rightarrow |c\rangle$. These oscillations can be seen in the temporal profile of the transmitted probe intensity in Fig. 2.16. We represent the probe intensity as a function of time in three situations. In (a) and (b), NAJ occurs on the transition $|a\rangle \leftrightarrow |c\rangle$ at $t = 0$. The jump is revealed on the temporal profile of the probe. Before the jump for $t < 0$ the probe propagates into the medium without any distortion. At the jump, the excited adiabatic level is populated and a coherence develops between the states $|\gamma\rangle$ and $|q\rangle$. Subsequent radiation of the coherence during light shifted $|\gamma\rangle$ appears in the form of oscillations in the temporal profile. The jump is marked in real time by the onset of these oscillations. Moreover, it can be seen that by centering the probe at a different times, we can modulate different regions of the probe. The modulations always start at $t = 0$ with the onset of the jump. In Fig. 2.16(c) NAJ does not occur. In this case the matrix $V(\phi, t)$ from Eq. (2.31) has been taken into account in the time evolution. For $\phi = 0$, there is no NAJ and the adiabatic passage populates the excited level transiently as shown in Fig. 2.12. However, in this case the probe is made non-resonant by level crossings, and thus the transiently populated $|\gamma\rangle$ can not be probed. The probe propagates through the system unaltered as shown in the Figure.

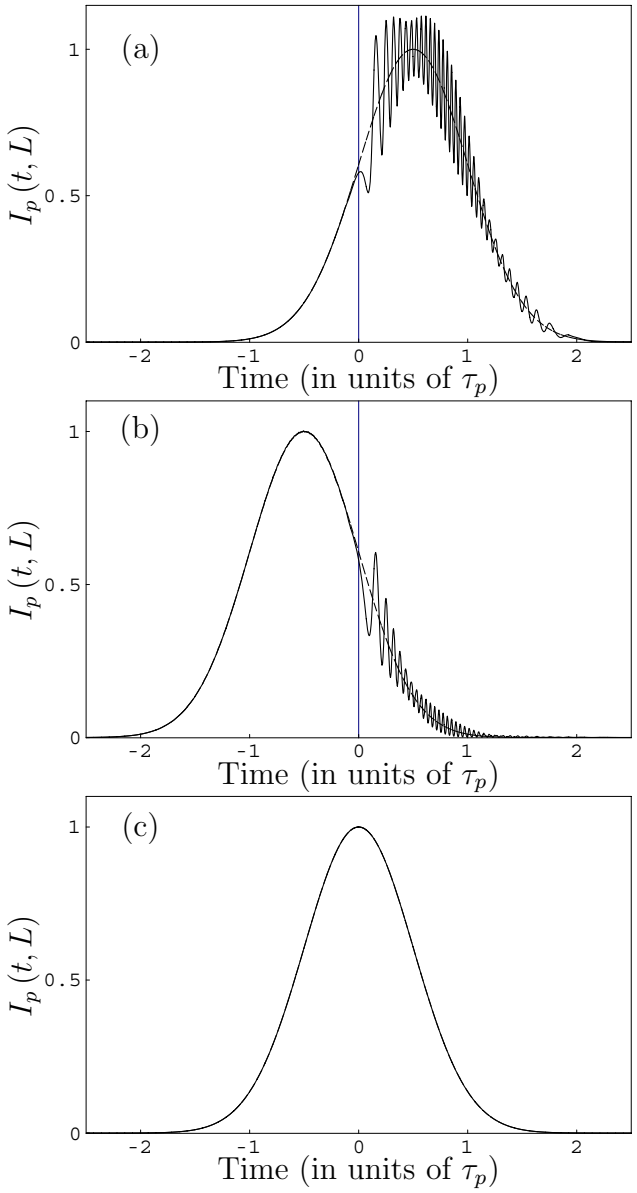

Figure 2.16: Normalized initial (dashed) and transmitted (solid) intensity profiles for the probe. In (a) and (b) $\phi = \pi$. The position of the non-adiabatic jump (shown by the vertical line) is marked by the beginning of oscillations. For (c) non-adiabatic jump does not occur and transiently populated $|\gamma\rangle$ state is always detuned from the probe because of level crossings. Parameters are (a) $t_p = 0.5\tau_p$, (b) $t_p = -0.5\tau_p$, and (c) $t_p = 0$. The other parameters are $\Delta_c = 8\tau_c^{-1}$, $\vartheta_c = 400\tau_c^{-1}$, $\theta_p = 0.2$, $\tau = 1$, $\tau_{pc} = 1$ and $e_{disp} = 2$

2.4 Conclusion

We have explored how strong field effects in an atomic medium in ultrashort regime can be probed by propagating a weak probe through the system. The light shifts induced by the strong field become visible on the temporal profile of the probe in the form of an oscillatory structure. The oscillations mark the region where light-shifts are important, and the oscillation period is determined by the strength of the light-shifts. This can have useful application in pulse shaping. We have also seen population dynamics due to non-adiabatic coupling. Asymmetric pulses can cause complete population inversion in adiabatic and the asymptotic bare state populations. The phase control of such transfer was presented. The very sensitive phase dependence of the population transfered by non-adiabatic jump can have important applications in interferometry. Finally a method to observe these jumps on the temporal profile of a weak propagating pulse was presented. The jump in this last case provides an additional control for the shaping of the weak field.

Chapter 3

Slow light

3.1 Introduction

Light travels at a tremendous velocity in vacuum and in thin media like air. In relatively dense media the velocity of light is reduced by a factor of $2 \sim 3$. This reduction in the velocity is determined by the refractive index of the material which is of the order of few units in dense materials. The term "slow light", however, does not refer to this marginal change in the velocity of light. Slow light means a reduction of many orders of magnitude in the propagation velocity of light. This is possible because the group velocity of light does not depend only on value of the refractive index of the material at the optical frequency. It also depends on dispersive property of the medium —on the manner how refractive index changes with the frequency. For very abrupt normal dispersion ultraslow group velocities can be realized as discussed in the first chapter. The key idea to produce ultraslow light is to induce a narrow transparency win-

La lumière se propage à une vitesse énorme dans le vide et dans des milieux dilués comme l'air. Dans un milieu relativement dense la vitesse de lumière est réduite d'un facteur 2 ou 3. Cette réduction est déterminée par l'indice de réfraction du milieu qui est de l'ordre de quelques unités dans des milieux denses. Le mot "lumière lente " toutefois ne désigne pas ce changement marginal dans la vitesse de la lumière. La lumière lente signifie une réduction de plusieurs ordres de grandeurs de la vitesse de propagation de la lumière. Ceci est possible car la vitesse de groupe de la lumière ne dépend pas seulement de la valeur de l'indice de réfraction à la fréquence optique. Il dépend aussi des propriétés dispersives du milieu c'est-à-dire sur la manière dont l'indice de réfraction varie avec la fréquence. Pour une variation abrupte de la dispersion normale, des vitesses de groupes très faibles peuvent être obtenus comme cela a été discuté dans

dow in the absorption spectrum of the medium. This narrow window is accompanied according to Kramers-Kronig relations by an abrupt normal dispersion with $\omega dn/d\omega \gg 1$. This leads to orders of magnitude reduction of the propagation velocity of light inside the medium as given be Eq. 1.43.

In this chapter I will first briefly present the two well known methods of slowing light— namely *electromagnetic induced transparency* (EIT) [Imamoğlu89, Fleischhauer05] and *coherent population oscillations* (CPO) [Schwarz67, Boyd81, Bigelow03b]. These two arise in different systems, present very different features, and are generally considered to be quite distinct from each other. Next I will present a new method that we have termed *coherent Zeeman oscillations* (CZO). It arises in a double two-level system interacting with two linearly polarized fields —having mutually orthogonal polarization— that propagate along slightly different directions, with one field much stronger than the other. This new technique, CZO, presents features that are intermediate between EIT and CPO. It may suggest that EIT and CPO are more close to each other than they are considered; and that EIT, CPO, and CZO can be considered as different manifestations of wave mixing phenomena. I will also present

le premier chapitre. L'idée clé pour la production de lumière ultra lente est d'induire une fenêtre de transparence étroite dans le spectre d'absorption du milieu. Cette fenêtre étroite est accompagnée selon les relations de Kramers-Krönig par une variation abrupte de la dispersion normale avec $\omega dn/d\omega \gg 1$. *Ceci conduit à une réduction de plusieurs ordres de grandeurs de la vitesse de propagation de la lumière dans le milieu comme cela est décrit par l'eq. 1.43.*

Dans ce chapitre je vais présenter brièvement deux méthodes bien connus de ralentissement de la lumière (basé nommément sur la transparence électromagnétique induite (TEI) [Imamoğlu89, Fleischhauer05] et les oscillations cohérentes de population (OCP) [Schwarz67, Boyd81, Bigelow03b]. Ces deux effets se produisent dans des systèmes différents, présentent des particularités différentes et sont en général considérés comme bien distinctes l'une de l'autre. Ensuite, je présenterai une nouvelle méthode basée sur ce que nous avons nominé comme des oscillations des cohérences Zeeman (OCZ). Elle se met en place dans un système à deux niveaux double interagissant avec deux champs polarisés linéairement (orthogonales entre eux), qui se propagent dans des directions différentes et dont l'un des champs est plus intense que l'autre. Cette nouvelle technique, basée sur les OCZ présente des particularités intermédiaires entre celles basées sur la TEI et les OCP. Cela suggère que la TEI (dans des systèmes lambda dégénérés) et les

the limitations of CZO, a short comparison of CZO with EIT and CPO, the possibility of storing light using CZO, and the conclusion.

OCP beaucoup sont plus proches que l'on ne croit, et que la TEI, les OCP et les OCZ peuvent être considérés comme des manifestations différentes du phénomène de mélange d'onde. Je présenterai aussi les limitations des OCZ, une courte comparaison de la méthode basée sur les OCZ avec ceux basées sur la TEI et les OCP, la possibilité de stocker la lumière en utilisant les OCZ et enfin je conclurai.

3.2 Slow light with EIT

Electromagnetic induced transparency or EIT is a quantum interference phenomena, traditionally seen in a three level Λ system, in which, the absorption of a weak resonant pulse on an atomic transition can be suppressed by applying a control field on an adjacent transition. In an exciting scheme where the two fields are detuned by the same amount from the common energy level, total destructive interference takes place and results in *zero* absorption, both for the weak field, and for the control. The optically opaque medium thus turns into a transparent one. The idea was first proposed by Harris *et al.* [Imamoğlu89], was experimentally verified by Boller *et al.* [Boller91], and has been discussed in great detail in topical review [Fleischhauer05, Marangos98].

In the following I will present a special treatment of EIT in a Λ system with degenerate ground states, that brings it closer to CPO and CZO. It will be followed by the traditional treatment of EIT in a general system in terms of the dark states, and some landmark experiments of slowing light using EIT. A more detailed discussion on EIT from the perspective of slowing light can be found in [Milonni05, Fleischhauer05, Milonni02].

3.2.1 The system for EIT

Consider a three level Λ system $\{|a\rangle, |b\rangle, |c\rangle\}$ with degenerate ground states interacting with a strong "control" field $A_c e^{-i\omega_c t} + cc$ on the transition $|a\rangle \leftrightarrow |c\rangle$, and with a weak "probe" field $A_p e^{-i\omega_p t} + cc$ on $|b\rangle \leftrightarrow |c\rangle$ transition as shown in Fig. 3.1. The control field is detuned by $\Delta_c = \omega_{ac} - \omega_c$ from the respective transition, and by $\Delta = \omega_p - \omega_c$ from the probe. The two Rabi frequencies are $\Omega_c(t) = DA_c/\hbar$ and $\Omega_p(t) = D_{cb}A_p/\hbar$ respectively where D and D_{cb} are the respective dipole matrix elements. The excited state $|c\rangle$ has the linewidth Γ and relaxes with the rate Γ_1 and Γ_2 into the ground states

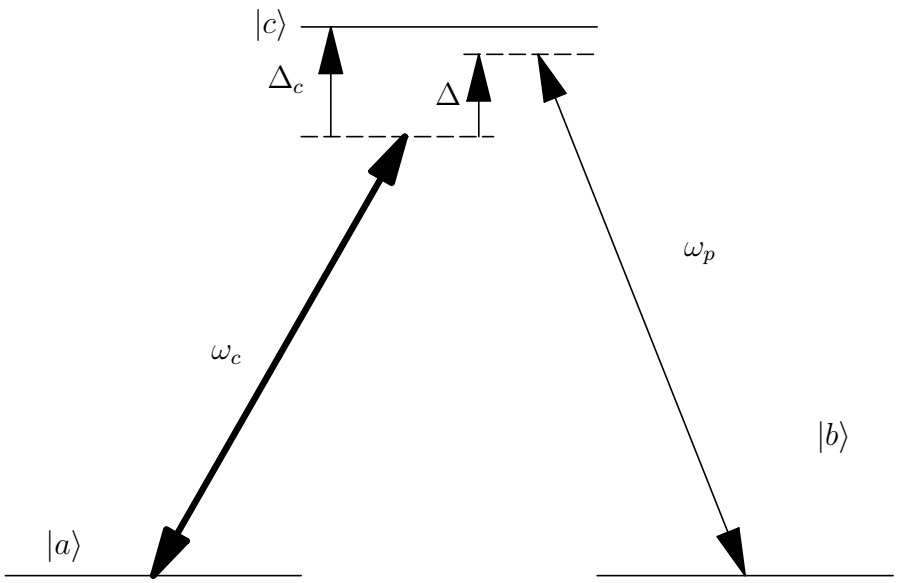

Figure 3.1: Three level Λ system for EIT.

$|a\rangle$ and $|b\rangle$ respectively. We have $\Gamma = \Gamma_2 + \Gamma_1$ and we use it as the unit of frequency in the following discussion. The coherences ρ_{ca} and ρ_{cb} relax with the rate Γ_d which reduces to $\Gamma/2$ in the absence of collisions. We place ourselves in the situation where the coherence ρ_{ab} does not relax.

The density matrix for the system is

$$\rho = \begin{pmatrix} \rho_{aa} & \rho_{ab} & \rho_{ac}e^{i\omega_c t} \\ \rho_{ba} & \rho_{bb} & \rho_{bc}e^{i\omega_p t} \\ \rho_{ca}e^{-i\omega_c t} & \rho_{cb}e^{-i\omega_p t} & \rho_{cc} \end{pmatrix}. \tag{3.1}$$

3.2.2 Time evolution of the system

The time evolution of the system is given by following equations:

$$i\partial_t \rho_{aa} = \Omega_c \rho_{ac} - \Omega_c^* \rho_{ca} + i\Gamma_1 \rho_{cc}, \tag{3.2a}$$
$$i\partial_t \rho_{bb} = \Omega_p e^{-i\Delta t} \rho_{bc} - \Omega_p^* e^{i\Delta t} \rho_{cb} + i\Gamma_2 \rho_{cc}, \tag{3.2b}$$
$$i\partial_t \rho_{cc} = -i\partial_t \rho_{aa} - i\partial_t \rho_{bb}, \tag{3.2c}$$
$$i\partial_t \rho_{ca} = \Omega_c \left(\rho_{cc} - \rho_{aa}\right) - \Omega_p e^{-i\Delta t} \rho_{ba} + \bar{\Delta}_c^* \rho_{ca}, \tag{3.2d}$$
$$i\partial_t \rho_{ab} = -\Omega_c^* \rho_{cb} + \Omega_p e^{-i\Delta t} \rho_{ac}, \tag{3.2e}$$
$$i\partial_t \rho_{cb} = -\Omega_c \rho_{ab} e^{i\Delta t} + \Omega_p e^{-i\Delta t} \left(\rho_{cc} - \rho_{bb}\right) + \left(\bar{\Delta}_c^* - \Delta\right) \rho_{cb}, \tag{3.2f}$$

where $\bar{\Delta}_c = \Delta_c + i\Gamma_d$.

The periodicity of the excitation allows the use of Floquet methods and we write

$$\rho_{ij} = \rho_{ij}^{(0)} + \rho_{ij}^{(-)} e^{-i\Delta t} + \rho_{ij}^{(+)} e^{i\Delta t}, \tag{3.3}$$

in the limit of $|\Omega_p| \ll |\Omega_c|$. The coherences responsible for the radiated field at control and probe laser frequencies are respectively $\rho_{ca}^{(0)}$ and $\rho_{cb}^{(-)}$.

3.2.3 Transparency for the control

At *zeroth order* with respect to probe amplitude, the stationary state solution of the system yields $\rho_{bb}^{(0)} = 1$. All other density matrix elements vanish at this order. This is the consequence of *coherent population trapping* (CPT) [Arimondo96]. The population is coherently trapped in the ground state $|b\rangle$ by the action of the control field. The field transfers the population from the ground state $|a\rangle$ to the excited state $|c\rangle$. Some of the population relaxes into state $|b\rangle$ and is trapped there since that level is not coupled to any other level (at *zeroth order*), and some population relaxes back into state $|a\rangle$ — only to be subsequently transfered to the excited state. This cycle keeps on going until all the population is transfered into the ground state $|b\rangle$ and system becomes transparent to the control.

3.2.4 Transparency for the probe

At *first order*, the relevant time evolution equations are

$$i\partial_t \rho_{ab}^{(-)} = -\Omega_c^* \rho_{cb}^{(-)} + \Omega_p \rho_{ac}^{(0)} - \Delta \rho_{ab}^{(-)}, \tag{3.4a}$$

$$i\partial_t \rho_{cb}^{(-)} = -\Omega_c \rho_{ab}^{(-)} + \Omega_p \left(\rho_{cc}^{(0)} - \rho_{bb}^{(0)} \right) + \left(\bar{\Delta}_c^* - \Delta \right) \rho_{cb}^{(-)}. \tag{3.4b}$$

The coherence ρ_{cb} results from the diffraction of the control from the oscillating ground coherence $\rho_{ab}^{(-)}$ [first term in Eq. (3.4b)], and the absorption of the probe by the populations $\rho_{bb}^{(0)} - \rho_{cc}^{(0)}$ [second term in Eq. (3.4b)]. These two phenomena compete with each other and the diffraction compensates for the absorption. Indeed the oscillating ground coherence produces a grating in time and the control can be diffracted from this grating into the probe. This compensation for the absorption produces a transparency window in the absorption profile for the probe.

The stationary state solution for above equations are $\rho_{ab}^{(-)} = -\Omega_c^* \rho_{cb}^{(-)} / \Delta$ ($\Delta \neq 0$) and

$$\rho_{cb}^{(-)} = \frac{\Delta}{|\Omega_c|^2 + \Delta \left(\bar{\Delta}_c^* - \Delta \right)} \Omega_p. \tag{3.5}$$

The coherence responsible for the radiated field at the probe frequency vanishes for $\Delta \to 0$. The compensation for the absorption is perfect when the two fields have the same frequency.

This description in terms of grating is particularly relevant if an angle is introduced between the control and the probe fields. Indeed, $\rho_{cb}^{(-)}$ is the only component in this case which is responsible for the modification of the probe. Note that $\rho_{cb}^{(+)} = \rho_{cb}^{(0)} = 0$, no radiation is emitted in any other directions.

3.2.5 Susceptibility for the probe

The effective susceptibility for the probe is given by $\chi_{eff} = \chi'_{eff} + i\chi''_{eff} = (2\alpha_{0p}\Gamma_d/k_p)\rho_{cb}^{(-)}/\Omega_p$, where $\alpha_{0p} = ND_{cb}^2\omega_p/(2c\hbar\epsilon_0\Gamma_d)$ is the field absorption coefficient at probe frequency and $k_p = \omega_p/c$. The susceptibility is shown in Fig. 3.2 in the presence and the absence of the control field. The control field opens up a narrow transparency window in the absorption profile. The absorption peak splits into two and the separation between the two is given by $\sqrt{4\Omega_c^2 + \Delta_c^2}$. The width of the window can be controlled by the control field intensity. The minimum of the window is at *zero*, signifying perfect transparency for $\Delta = 0$. The dispersion profile In Fig. 3.2(b) changes to normal dispersion in the presence of the control field. It can be very abrupt for a very narrow transparency window, and can lead to ultraslow light propagation velocities in the medium.

When the control field is made stronger $|\Omega_c| \geq \Gamma$, the two absorption peaks move apart, and no structure appears in between the peaks. The transparency in this case can be explained in terms of light-shifts (as was the case in Fig. 2.4(c) in ultrashort pulse regime), however, in this case the dispersion profile can not lead to ultraslow velocities. For low control field intensities, the quantum interference phenomena results in vanishing absorption of the probe. This interference effect can either be interpreted in terms of control field diffraction off the ground coherence (and thus the compensation for the absorption of the probe), or in terms of dark state that can be realized in the system and the CPT that traps all the population in the dark state as we see next.

3.2.6 Transparency due to CPT in a general Λ system

For a general Λ system, the transparency in the EIT scheme is provided by *coherent population trapping* (CPT) of all the population in a dark state. Note that CPT and EIT are related phenomena but some authors distinguish between the two depending on the initial and the relative field strengths [Fleischhauer05, Marangos98]. For a non-degenerate Λ system where the

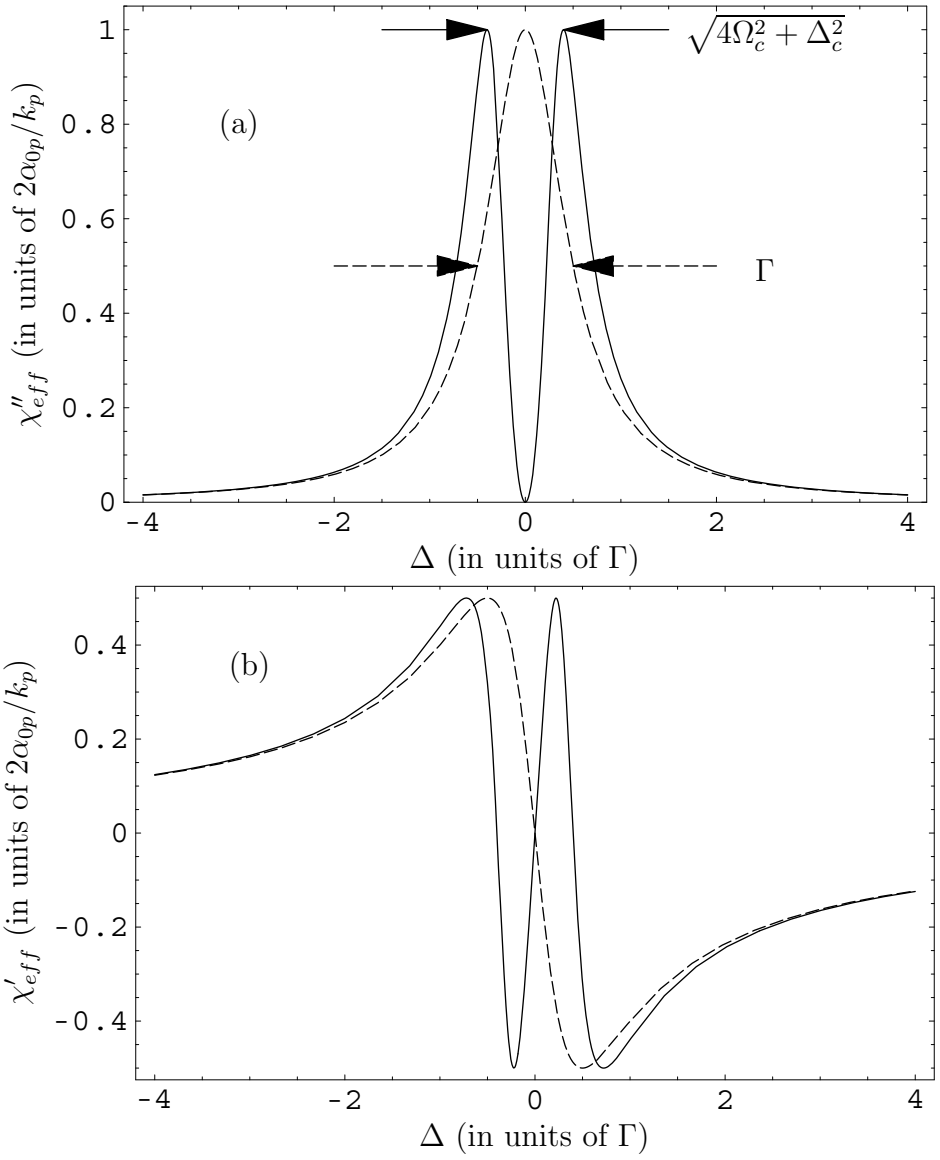

Figure 3.2: (a) Absorptive and (b) dispersive response of the medium for the probe in the presence $\Omega_c = 0.4\Gamma$ (solid), and absence $\Omega_c = 0$ (dashed) of the control. Other parameters are: $\Delta_c = 0$ and $\Gamma_d = 0.5\Gamma$.

two ground states $|a\rangle$, and $|b\rangle$ have energy difference $\hbar\omega_{ab}$, we can define the detuning between the probe and the control as $\Delta' = \omega_{ab} + \omega_p - \omega_c$. The effective Hamiltonian (after RWA) in the bare states $\{|a\rangle, |b\rangle, |c\rangle\}$ can be written as

$$H = \hbar \begin{pmatrix} 0 & 0 & -\Omega_c \\ 0 & \Delta' & -\Omega_p \\ -\Omega_c & -\Omega_p & \Delta_c \end{pmatrix}. \tag{3.6}$$

Here we have taken the fields to be real for simplicity, and have used the convention $\rho_{ca} \propto e^{-i\omega_c t}$, $\rho_{cb} \propto e^{-i\omega_p t}$, and $\rho_{ba} \propto e^{-i(\omega_c - \omega_p)t}$ for RWA. The system can be transformed into dressed states $\{|bright\rangle, |dark\rangle, |c\rangle\}$ by the rotation matrix

$$R = \begin{pmatrix} \cos\theta & \sin\theta & 0 \\ -\sin\theta & \cos\theta & 0 \\ 0 & 0 & 1 \end{pmatrix}. \tag{3.7}$$

The mixing angle θ is defined by the relation $\tan\theta = \Omega_p/\Omega_c$. The dressed Hamiltonian is given by

$$H_d = RHR^\dagger = \hbar \begin{pmatrix} \Delta' \sin^2\theta & \Delta' \sin 2\theta/2 & -\sqrt{\Omega_c^2 + \Omega_p^2} \\ \Delta' \sin 2\theta/2 & \Delta' \cos^2\theta & 0 \\ -\sqrt{\Omega_c^2 + \Omega_p^2} & 0 & \Delta_c \end{pmatrix}. \tag{3.8}$$

The system in the dressed basis is shown in Fig. 3.3. The two ground states $|a\rangle$ and $|b\rangle$ give rise to the $|bright\rangle$ and the $|dark\rangle$ state where the $|dark\rangle$ state is not coupled to the excited level $|c\rangle$. The only coupling of the dark state is to the bright state and this coupling is proportional to the detuning between the two fields Δ'. The bright state is coupled to the excited level through modified field, and in the presence of Δ', the two ground states are slightly shifted in the dressed basis.

For $\Delta' = 0$, the dark state is not coupled to any other state in the system. It can still receive population from the excited level $|c\rangle$ through relaxations, or if initially all the population is in the ground state $|b\rangle$, then this state corresponds to the dark state for $|\Omega_p| \ll |\Omega_c|$. However, once the population is in the dark state, it is trapped, and ceases to interact with the laser fields. The medium thus becomes transparent for $\Delta' = 0$ and this explains vanishing ρ_{cb}.

3.2.7 Slowing light with EIT

The first calculation of slow light propagation in an EIT medium was provided by Harris *et al.* [Harris92]. The group velocity in an EIT medium

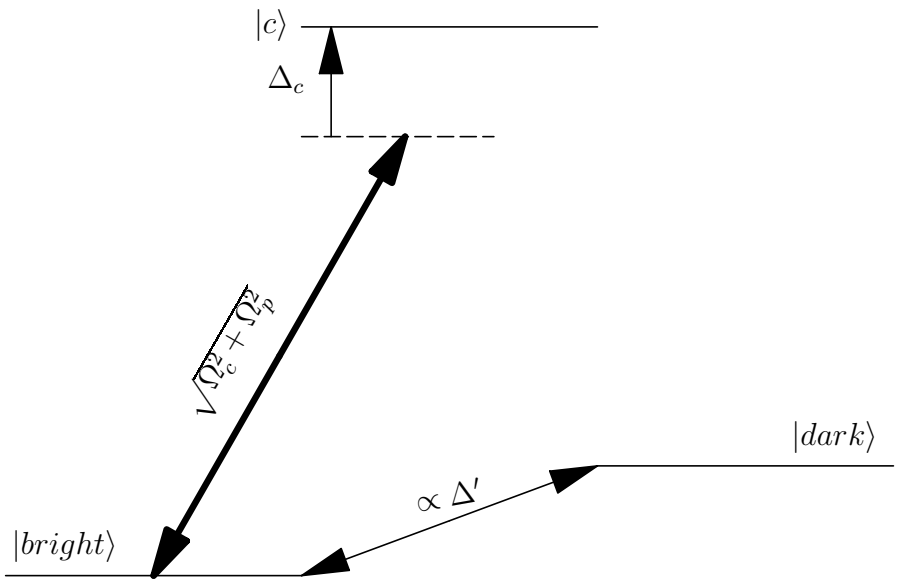

Figure 3.3: Dressed bases for the Λ system. Coherent population trapping of the population in the dark state induces transparency for $\Delta = 0$.

is determined by the control field intensity, the probe wavelength and the density of the atomic medium [Milonni05]. Harris *et al.* considered the propagation of 283 nm probe in ^{208}Pb vapor cell at an atomic density of 7×10^{15} $atoms/cm^3$. The control was provided by 405.9 nm field with the intensity 283 kW/cm^2. With these parameters they calculated the group velocity $v_g = c/250$ and a group delay of $\simeq 83ns$. The realization came 3 years later when a group delay of 55 ns corresponding to $v_g = c/165$ in a $10cm$ cell, was observed[Kasapi95]. This was the first realization of slow light through EIT and the result is shown in Fig. 3.4.

The most remarkable experiment of ultraslow light was reported by Hau *et al* [Hau99] in 1999. They used ultracold sodium atoms at the temperature of 450 nk having peak atomic density of 3.3×10^{12} $atoms/cm^3$. A weak control field with intensity 12 $mWcm^{-2}$ produced an extremely narrow transparency window and slowed down the probe to 32 m/s group velocity. Their result is shown in Fig. 3.5. They measured a series of pulse delays and corresponding atom cloud sizes in the temperature range between 2.5 μk and 50 nK, and obtained a light speed of 17 m/s for pulse propagation in an atom cloud initially prepared as an almost pure Bose – Einstein condensate.

However, ultracold atoms are not required to produce ultraslow lights, as was experimentally demonstrated by Kash *et al*[Kash99] by slowing down light to 90 m/s in ^{87}Rb atoms at the temperature of 360 K. Very narrow

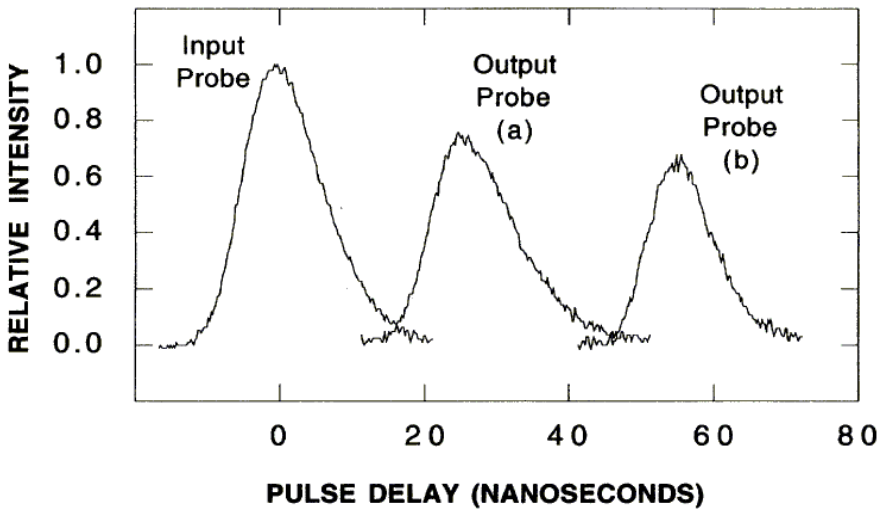

Figure 3.4: First realization of slow light in EIT medium (taken from [Kasapi95]). The probe in (b) is delayed by 55 ns.

transparency windows can be induced even in Doppler broadened hot media. The reason for this is the dependence of transparency on the difference of frequencies of two fields (on $\Delta = \omega_p - \omega_c$), as is evident by the expression (3.5). In hot media an atom moving with velocity $\vec{v}$ sees the probe as having frequency $\omega_p - \vec{k}_p \cdot \vec{v}$, and the control with the frequency $\omega_c - \vec{k}_c \cdot \vec{v}$. The detuning of the two fields in Doppler broadened media thus modifies $\Delta_{dop} = \omega_p - \omega_c - (\vec{k}_p - \vec{k}_c) \cdot \vec{v}$. In the Λ system with nearly degenerate ground states, the two fields have $k_p \simeq k_c$. Δ_{dop} reduces to Δ in this case and the transparency survives Doppler averaging. In fact the only velocity dependence of the transparency is through $\Delta_c \rightarrow \Delta_c - \vec{k}_c \cdot \vec{v}$ which arises in the denominator of (3.5). For $|\Omega_c| \gg |\vec{k}_c \cdot \vec{v}|$ the effect of the Doppler broadening for all velocity distributions is negligible.

3.3 Slow light with CPO

Another method to produce slow light makes use of *Coherent Population Oscillations* or CPO. Here the absorption of a weak probe in a two level system shows a narrow dip when a strong slightly detuned field is applied on the same transition. The dip is centered at the strong field frequency and its width is given by the population relaxation rate. This dip as " a hole burned" in the homogeneously broadened absorption spectrum, was first suggested by Schwarz and Tan [Schwarz67]. Later the phenomena was treated in great

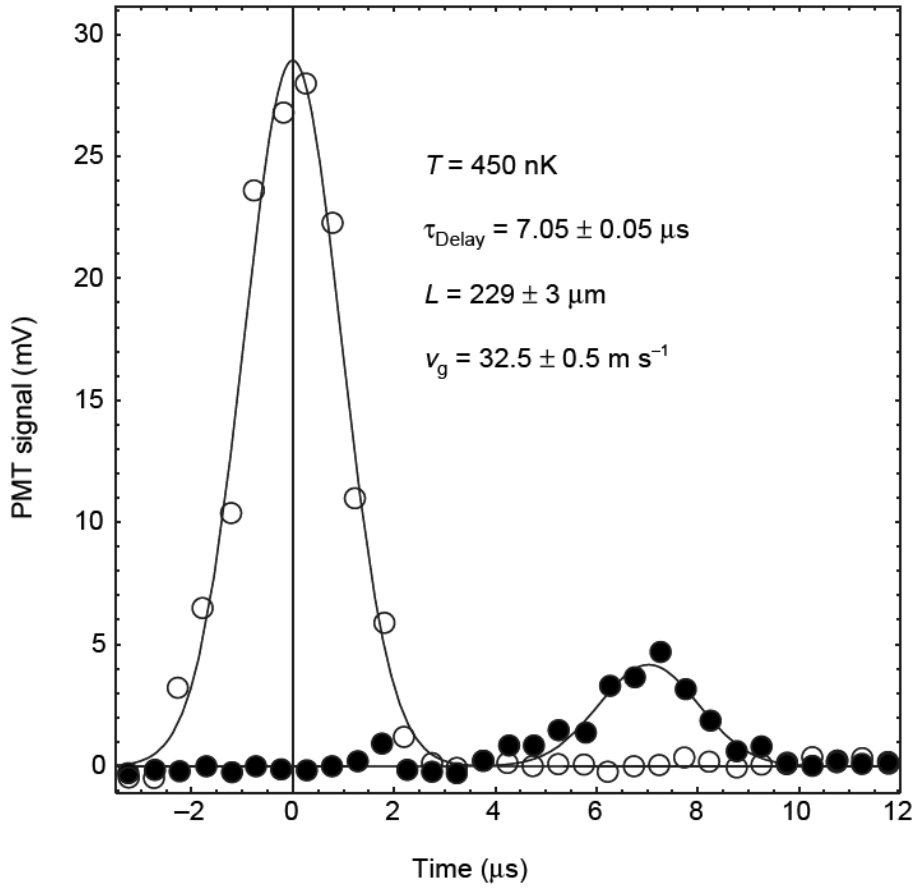

Figure 3.5: Slow light in ultracold sodium atoms(taken from [Hau99]). Open circles represent the reference probe when no atoms are present. Filled circles represent the probe delayed by 7 μs in a 229 μm medium, corresponding to $v_g = 32.5\ m/s$.

detail by Boyd *et al* [Boyd81] and was experimentally observed by Hillman *et al* [Hillman83].

3.3.1 The system for CPO

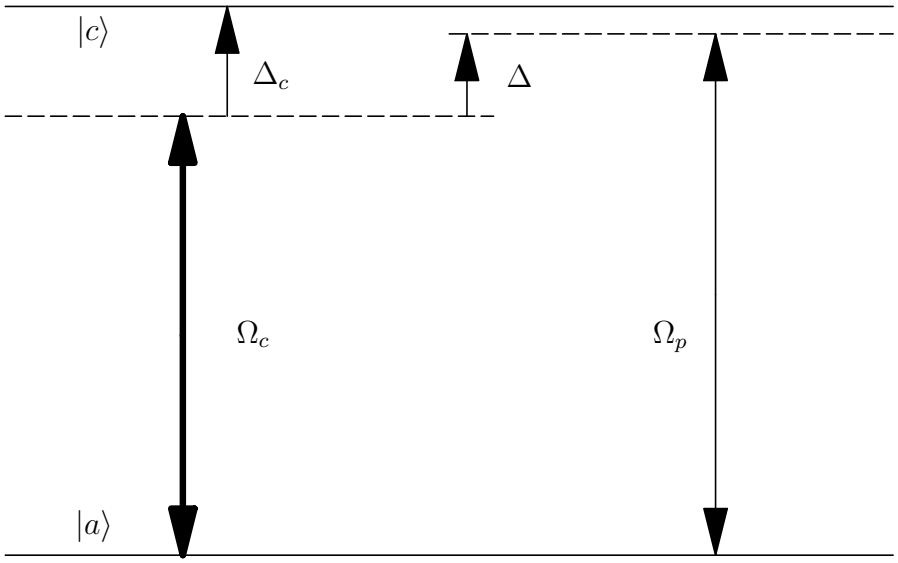

Figure 3.6: A two level system interacting with bi-chromatic field.

Consider a two-level system interacting with a weak probe $A_p e^{-i\omega_p t} + cc$ and a strong control field $A_c e^{-i\omega_c t} + cc$ as shown in Fig. 3.6. The two Rabi frequencies are $\Omega_c = DA_c/\hbar$ and $\Omega_p = DA_p/\hbar$ with $|\Omega_p| \ll |\Omega_c|$. The control field is detuned by $\Delta_c = \omega_0 - \omega_c$ from the resonance, and by $\Delta = \omega_p - \omega_c$ from the probe. The time evolution equations of the system are written as

$$i\partial_t \rho_{cc} = \left(\Omega_c^* + \Omega_p^* e^{i\Delta t}\right) \rho_{ca} - \left(\Omega_c + \Omega_p e^{-i\Delta t}\right) \rho_{ac} - i\Gamma \rho_{cc}, \tag{3.9a}$$

$$i\partial_t \rho_{ca} = \left(\Omega_c + \Omega_p e^{-i\Delta t}\right) (\rho_{cc} - \rho_{aa}) + \bar{\Delta}_c^* \rho_{ca}. \tag{3.9b}$$

Γ is the population relaxation rate and $\bar{\Delta}_c = \Delta_c + i\Gamma_d$ where Γ_d is the rate at which the coherence ρ_{ca} relaxes. In the absence of homogeneous dephasing processes Γ_d reduces to $\Gamma/2$.

The periodicity of the excitation allows the use of Floquet like expansion

$$\rho_{ij} = \rho_{ij}^{(0)} + \rho_{ij}^{(+)} e^{i\Delta t} + \rho_{ij}^{(-)} e^{-i\Delta t}, \tag{3.10}$$

in Eqs. (3.9). At *zero order* with respect to probe amplitude the system simplifies to a two-level system interacting with a single field as discussed in

Section. 1.1.3, and the stationary state solution is given by Eq. (1.24). At *first order* the time evolution equations are

$$i\partial_t \rho_{cc}^{(-)} = \left(\Omega_c^* \rho_{ca}^{(-)} - \Omega_c \rho_{ac}^{(-)}\right) - \Omega_p \rho_{ac}^{(0)} - \left(\Delta + i\Gamma\right) \rho_{cc}^{(-)}, \tag{3.11a}$$

$$i\partial_t \rho_{ca}^{(-)} = \Omega_c \left(\rho_{cc}^{(-)} - \rho_{aa}^{(-)}\right) + \Omega_p \left(\rho_{cc}^{(0)} - \rho_{aa}^{(0)}\right) + \left(\bar{\Delta}_c^* - \Delta\right) \rho_{ca}^{(-)}, \tag{3.11b}$$

$$i\partial_t \rho_{ca}^{(+)} = \Omega_c \left(\rho_{cc}^{(+)} - \rho_{aa}^{(+)}\right) + \left(\bar{\Delta}_c^* + \Delta\right) \rho_{ca}^{(+)}. \tag{3.11c}$$

$\rho_{cc}^{(+)}$ can be worked out using the identity $\left(\rho_{ij}^{(+)}\right)^* = \rho_{ji}^{(-)}$. Moreover we have the relations $\rho_{cc}^{(0)} + \rho_{aa}^{(0)} = 1$ and $\rho_{cc}^{(\pm)} + \rho_{aa}^{(\pm)} = 0$.

The coherence $\rho_{ca}^{(-)}$ radiates at the probe frequency, whereas $\rho_{ca}^{(+)}$ radiates at $2\omega_c - \omega_p$. If an angle is introduced between the probe and the control, then these two radiate in different directions with $\rho_{ca}^{(-)}$ radiating in the direction of the probe. For $\Delta = 0$, such geometry is necessary to separate different radiating components. The stationary state solution for the two coherences is given by

$$\rho_{ca}^{(-)} = \frac{\bar{\Delta}\bar{\Delta}_c \left(\Delta + \bar{\Delta}_c\right) + 2\Delta|\Omega_c|^2}{\left(\Gamma|\bar{\Delta}_c|^2 + 4\Gamma_d|\Omega_c|^2\right)\left[-\bar{\Delta}\left(\Delta + \bar{\Delta}_c\right)\left(\Delta - \bar{\Delta}_c^*\right) + 4\left(\Delta + i\Gamma_d\right)|\Omega_c|^2\right]} \Gamma \bar{\Delta}_c^* \Omega_p, \tag{3.12a}$$

$$\rho_{ca}^{(+)} = \frac{-2\Gamma\left(\Delta - 2i\Gamma_d\right)\Omega_c^2}{\left(\Gamma|\bar{\Delta}_c|^2 + 4\Gamma_d|\Omega_c|^2\right)\left[-\bar{\Delta}^*\left(\Delta + \bar{\Delta}_c^*\right)\left(\Delta - \bar{\Delta}_c\right) + 4\left(\Delta - i\Gamma_d\right)|\Omega_c|^2\right]} \Gamma \bar{\Delta}_c \Omega_p^*, \tag{3.12b}$$

with $\bar{\Delta} = \Delta + i\Gamma$, and $\bar{\Delta}_c = \Delta_c + i\Gamma_d$. Here we have used the *zero order* results from Eq. (1.24).

The response for the probe is determined by $\chi_{eff} = \chi'_{eff} + i\chi''_{eff} = (2\alpha_0\Gamma_d/k)\rho_{ca}^{(-)}/\Omega_p$, where $\alpha_0 = ND^2\omega_0/\left(2c\hbar\epsilon_0\Gamma_d\right)$ and $k = \omega_0/c$. The imaginary part of the susceptibility corresponding to the absorption profile is shown in Fig. 3.7. For strong dephasing $\Gamma_d \gg \Gamma$, the presence of the control opens up a narrow transparency window. The minimum of the width is determined by the population relaxation rate Γ (shown in a zoom in Fig. 3.7(b)), and can not be arbitrarily decreased. For strong control fields the saturation becomes important as shown in Fig(a). For still higher control fields the transparency window splits into two with new structure appearing in the center [Boyd81]. Finally, the minimum of the transparency depth does not reach *zero* signifying that the transmission can not be perfect.

The transparency is explained as follows. The interference of the probe and the control field causes the total field to modulate at beat frequency. If the beat frequency is lower than the population relaxation rate, the population starts to oscillate at the beat frequency. This produces a grating in

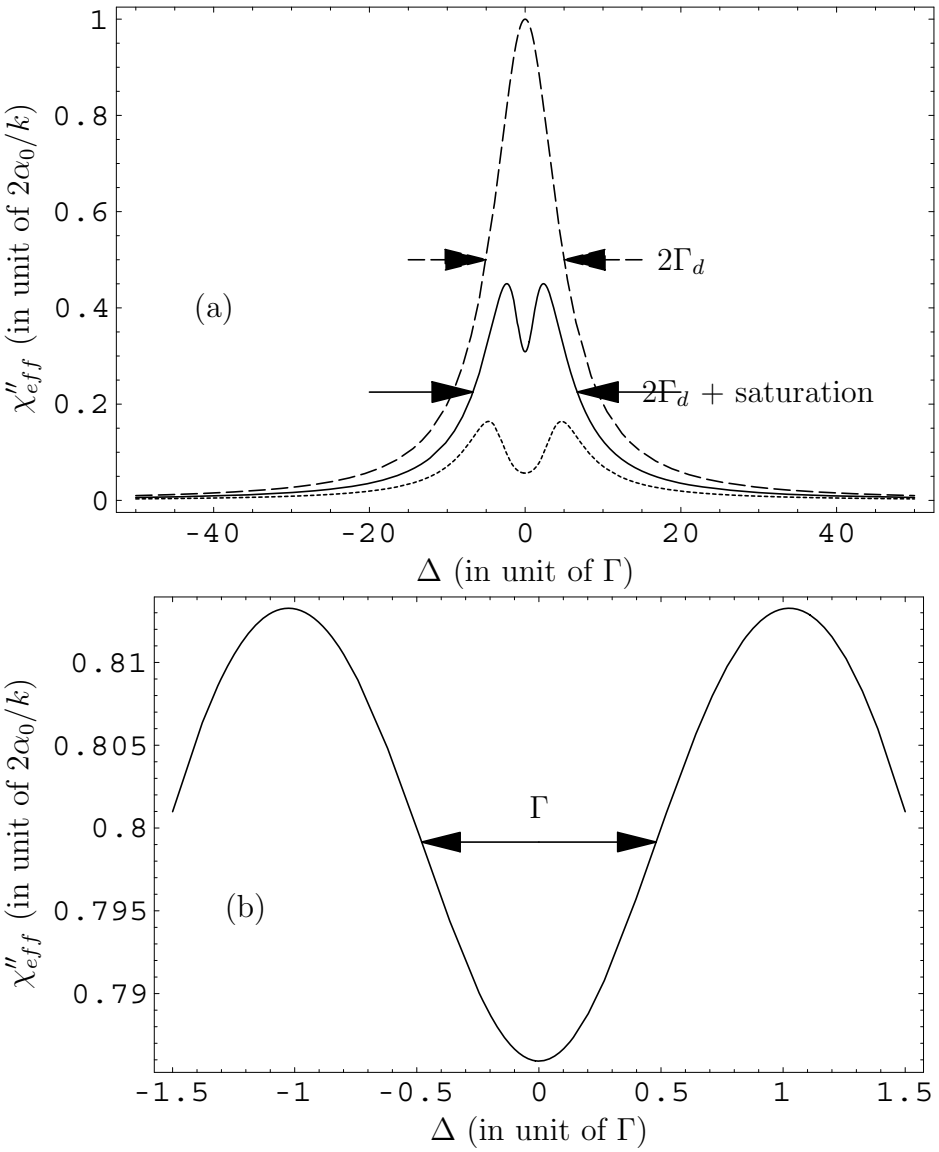

Figure 3.7: Absorption profile of the medium in CPO. A narrow transparency window appears in the presence of the control field. In (a) the window is power broadened. In (b) a zoom shows the width of the window for a weak control field.

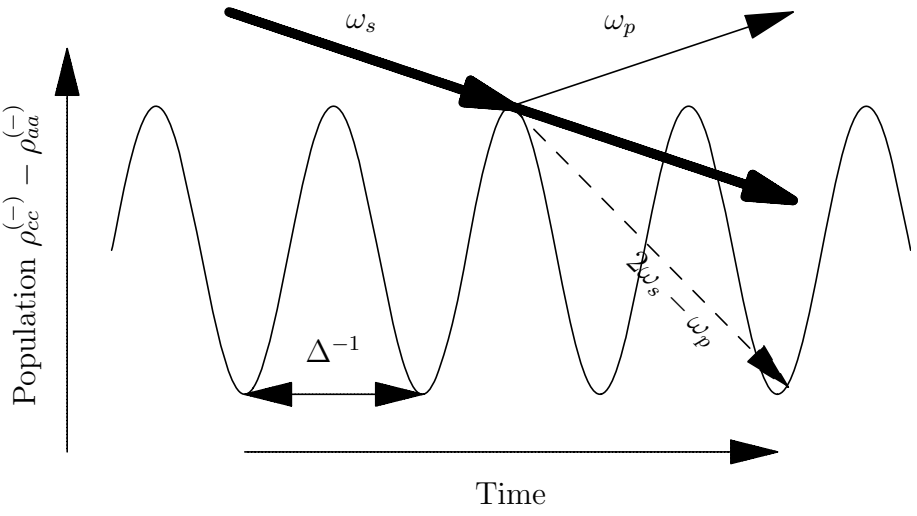

Figure 3.8: Compensation for the absorption of probe. Diffraction of the control field from the population grating compensates for the absorption of probe. A small angle between the control and the probe is required (for $\Delta = 0$) to separate spatially the component that radiates at $2\omega_s - \omega_p$ frequency.

time and the control field is diffracted off this grating into the probe field, compensating for the absorption of the latter. The diffraction of the control is accounted for by the first term in Eq. (3.11b) where as the second term represents the absorption of the probe by the static population. The interplay between these two processes produces a narrow transparency window in the absorption profile.

3.3.2 Slowing light with CPO

The first experiment to slow light using this technique was reported by Bigelow *et al* [Bigelow03a]. They propagated an amplitude modulated argon ion laser operating at 514.5 nm through a 7.25 cm long ruby rod, which could be modeled as an effective two level system. This modulated field caused a dip in the absorption spectrum which in turn delayed the modulation. A group velocity of 57.5 m/s was inferred in their experiment. In another experiment [Bigelow03b] they reported the group velocity of 91 m/s in Alexendarite crystal. The CPO has also been used to slow light upto $2.7m/s$ by Baldit *et al.* [Baldit05].

3.4 Slow light with CZO

Now I present a new method to produce slow light that can be realized in a double two-level system interacting with two linearly polarized fields. The fields are mutually orthogonally polarized and propagate with a small angle between them. One of the field "the control" is much stronger than the other "the probe". The control field turns the system into a slow light medium for the weak probe by inducing a narrow transparency window. The transparency window presents features that resemble to the one obtained by traditional EIT in a Λ system. However, unlike the traditional EIT, there is no dark state in the present system. The transparency in the present system arises because of the diffraction of the control from the space/time grating induced by the total polarization. In this regard it resembles more to CPO and to the non-standard description of EIT presented in Section. 3.2.

3.4.1 The double two-level system I

Consider a double two-level system consisting of degenerate ground states $|a\rangle$ and $|b\rangle$ and degenerate excited states $|c\rangle$ and $|d\rangle$ as shown in Fig. 3.9. The energy difference between the ground and excited states is $\hbar\omega_0$. The system is excited by two linearly polarized fields which are mutually orthogonally polarized. The expressions for the two fields are

$$\vec{E}_c\left(t,\vec{r}\right) = \vec{e}_z A_c e^{-i\left(\omega_c t - \vec{k}_c\cdot\vec{r}\right)} + cc, \tag{3.13a}$$

$$\vec{E}_p\left(t,y\right) = \vec{e}_x A_p e^{-i\left(\omega_p t - k_p y\right)} + cc. \tag{3.13b}$$

The control field is π polarized with $\vec{e}_z = \vec{e}_\pi$, and connects the transitions with identical m_F —state $|a\rangle$ with $|c\rangle$ and state $|b\rangle$ with $|d\rangle$. The weak probe is σ polarized with $\vec{e}_x = \left(\vec{e}_- - \vec{e}_+\right)/\sqrt{2}$. The probe connects the levels that have different m_F. The excitation scheme and the polarization axis are shown in Fig. 3.9.

The Rabi frequencies associated with the two fields are $\Omega_c = DA_c/\hbar$ and $\Omega_p = DA_p/\hbar$ with $|\Omega_p| \ll |\Omega_c|$ and $D = \left\langle a|\hat{\vec{D}}\cdot\vec{e}_\pi|c\right\rangle$ ($\hat{\vec{D}}$ is the dipole moment). The control is detuned by $\Delta_c = \omega_0 - \omega_c$ from the resonance and by $\Delta = \omega_c - \omega_p$ from the probe. The two fields propagate with a small angle ϑ between them and give rise to space/time dephasing $\Phi\left(t,\vec{r}\right) = \Delta t - \delta\vec{k}\cdot\vec{r}$ where we have $\delta\vec{k} = k_p\vec{e}_y - \vec{k}_c$. The propagation geometry is shown in Fig. 3.9(b).

The Hamiltonian in $\{|a\rangle, |b\rangle, |c\rangle, |d\rangle\}$ basis is given by

$$H = H_0 - \hat{\vec{D}}\cdot\left(\vec{E}_c + \vec{E}_p\right). \tag{3.14}$$

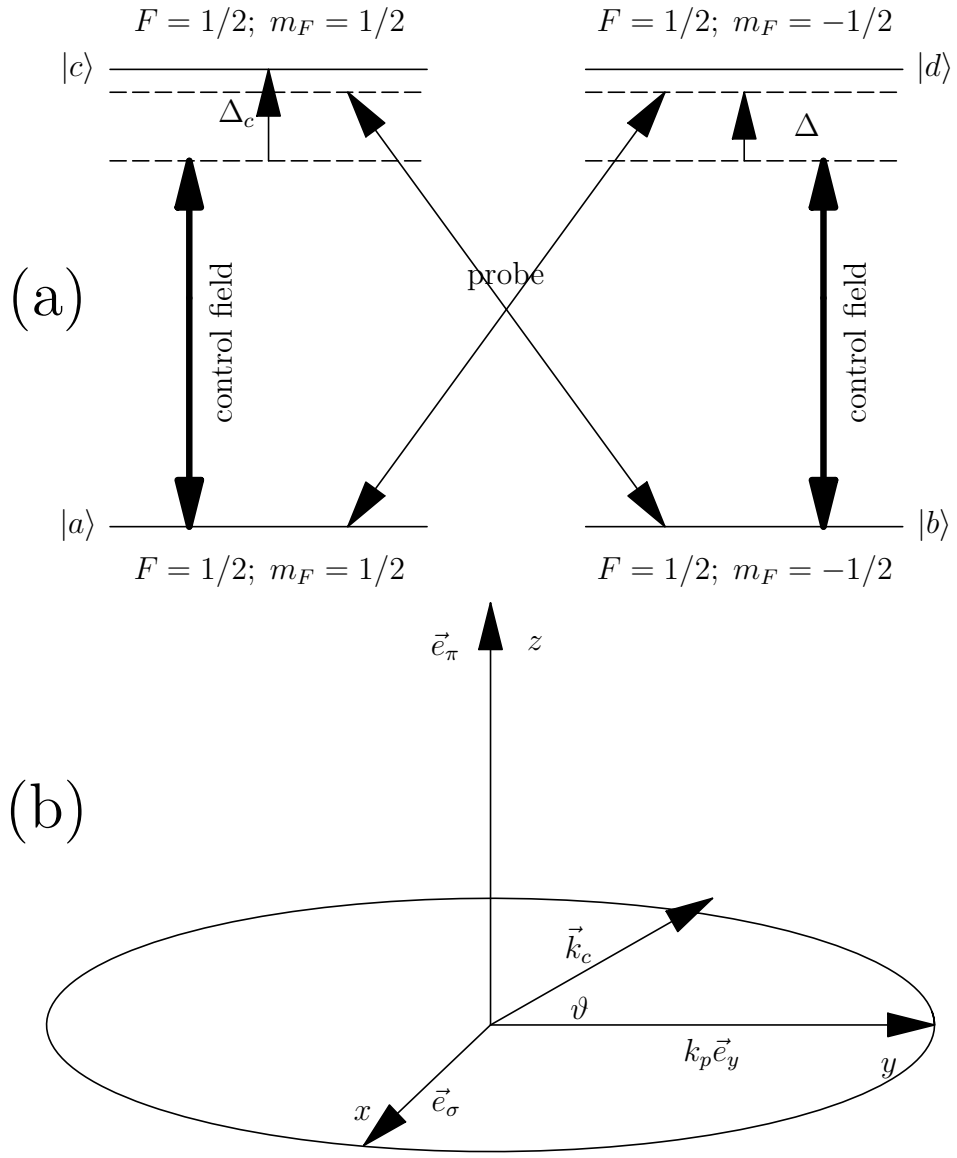

Figure 3.9: (a) A Double two-level system for slowing light. The π polarized control field drives each single two-level system, and the σ polarized probe connects crossed transitions. (b) Propagation and polarization axis.

H_0 is the free Hamiltonian and the dipole matrix elements are given by [Sobelman92]

$$\hat{\vec{D}}\cdot\vec{e}_\pi = D\begin{pmatrix}0&0&1&0\\0&0&0&-1\\1&0&0&0\\0&-1&0&0\end{pmatrix};\hat{\vec{D}}\cdot\vec{e}_- = \sqrt{2}D\begin{pmatrix}0&0&0&0\\0&0&1&0\\0&0&0&0\\1&0&0&0\end{pmatrix};\quad \hat{\vec{D}}\cdot\vec{e}_+ = -\left(\hat{\vec{D}}\cdot\vec{e}_-\right)^\dagger. \tag{3.15}$$

We define the density matrix for the system as

$$\rho = \begin{pmatrix} \rho_{aa} & \rho_{ab} & \rho_{ac}e^{i\left(\omega_c t-\vec{k}_c\cdot\vec{r}\right)} & \rho_{ad}e^{i\left(\omega_c t-\vec{k}_c\cdot\vec{r}\right)} \\ \rho_{ba} & \rho_{bb} & \rho_{bc}e^{i\left(\omega_c t-\vec{k}_c\cdot\vec{r}\right)} & \rho_{bd}e^{i\left(\omega_c t-\vec{k}_c\cdot\vec{r}\right)} \\ \rho_{ca}e^{-i\left(\omega_c t-\vec{k}_c\cdot\vec{r}\right)} & \rho_{cb}e^{-i\left(\omega_c t-\vec{k}_c\cdot\vec{r}\right)} & \rho_{cc} & \rho_{cd} \\ \rho_{da}e^{-i\left(\omega_c t-\vec{k}_c\cdot\vec{r}\right)} & \rho_{db}e^{-i\left(\omega_c t-\vec{k}_c\cdot\vec{r}\right)} & \rho_{dc} & \rho_{dd} \end{pmatrix}. \tag{3.16}$$

3.4.2 Time evolution of the system

The time evolution of the system is given by $i\hbar\partial_t\rho = [H,\rho]$+relaxations where the relaxation terms are added phenomenologically. Using the definitions of the density matrix (3.16) and the expression for the Hamiltonian (3.14) along with (3.15), and after carrying out *rotating wave approximation* we get following equations for the time evolution of the system:

$$i\partial_t\rho_{aa} = \left[\left(\Omega_c\rho_{ac}+\Omega_p\rho_{ad}e^{-i\Phi(t,\vec{r})}\right)-cc\right]+i\Gamma\left(\rho_{cc}+2\rho_{dd}\right)/3, \tag{3.17a}$$

$$i\partial_t\rho_{bb} = \left[\left(-\Omega_c\rho_{bd}+\Omega_p\rho_{bc}e^{-i\Phi(t,\vec{r})}\right)-cc\right]+i\Gamma\left(\rho_{dd}+2\rho_{cc}\right)/3, \tag{3.17b}$$

$$i\partial_t\rho_{cc} = \left[-\left(\Omega_c\rho_{ac}+\Omega_p\rho_{bc}e^{-i\Phi(t,\vec{r})}\right)-cc\right]-i\Gamma\rho_{cc}, \tag{3.17c}$$

$$i\partial_t\rho_{dd} = \left[\left(\Omega_c\rho_{bd}-\Omega_p\rho_{ad}e^{-i\Phi(t,\vec{r})}\right)-cc\right]-i\Gamma\rho_{dd}, \tag{3.17d}$$

$$i\partial_t\rho_{ca} = \Omega_c\left(\rho_{cc}-\rho_{aa}\right)+\Omega_p e^{-i\Phi(t,\vec{r})}\left(\rho_{cd}-\rho_{ba}\right)+\bar{\Delta}_c^*\rho_{ca}, \tag{3.17e}$$

$$i\partial_t\rho_{db} = \Omega_c\left(\rho_{bb}-\rho_{dd}\right)+\Omega_p e^{-i\Phi(t,\vec{r})}\left(\rho_{dc}-\rho_{ab}\right)+\bar{\Delta}_c^*\rho_{db}, \tag{3.17f}$$

$$i\partial_t\rho_{ab} = -\left(\Omega_c\rho_{ad}+\Omega_c^*\rho_{cb}\right)+\left(\Omega_p e^{-i\Phi(t,\vec{r})}\rho_{ac}-\Omega_p^* e^{i\Phi(t,\vec{r})}\rho_{db}\right)-i\Gamma_{zg}\rho_{ab}, \tag{3.17g}$$

$$i\partial_t\rho_{cd} = -\left(\Omega_c\rho_{ad}+\Omega_c^*\rho_{cb}\right)+\left(-\Omega_p e^{-i\Phi(t,\vec{r})}\rho_{bd}+\Omega_p^* e^{i\Phi(t,\vec{r})}\rho_{ca}\right)-i\Gamma_{ze}\rho_{cd}, \tag{3.17h}$$

$$i\partial_t\rho_{da} = \Omega_c\left(\rho_{ba}+\rho_{dc}\right)+\Omega_p e^{-i\Phi(t,\vec{r})}\left(\rho_{dd}-\rho_{aa}\right)+\bar{\Delta}_c^*\rho_{da}, \tag{3.17i}$$

$$i\partial_t\rho_{cb} = -\Omega_c\left(\rho_{ab}+\rho_{cd}\right)+\Omega_p e^{-i\Phi(t,\vec{r})}\left(\rho_{cc}-\rho_{bb}\right)+\bar{\Delta}_c^*\rho_{cb}, \tag{3.17j}$$

with $\bar{\Delta}_c = \Delta_c + i\Gamma_d$. We have used the following relaxation terms. The transitions have the Doppler free linewidth Γ. This will also be used in

the following as the unit of frequency. The excited sates populations relax into the ground states with the rates that are proportional to the square of respective transition dipole moments [Sobelman92]. Thus the states relax with $\Gamma/3$ in the ground state with identical m_F and with the rate $2\Gamma/3$ in the ground state with different m_F. All the coherences except the ones between Zeeman levels relax with the rate Γ_d. In the absence of non-radiative dephasing processes, Γ_d reduces to $\Gamma/2$. The excited state Zeeman coherence ρ_{cd} relaxes with the rate Γ_{ze} and the ground Zeeman coherence ρ_{ab} relaxes with Γ_{zg}. In pure radiative dephasing $(\Gamma_{ze}, \Gamma_{zg})$ reduces to $(\Gamma, 0)$.

3.4.3 Simplification due to the symmetry

The system described by Eqs. (3.17) can be simplified by a change of variables. We write $n_g = \rho_{aa} + \rho_{bb}$ for the total ground state population. The excited state population is given by $n_e = 1 - n_g = \rho_{cc} + \rho_{dd}$. The coherences responsible for the radiated σ and π polarized fields are given respectively by $\rho_p = \rho_{cb} + \rho_{da}$ and $\rho_c = \rho_{ca} - \rho_{db}$. Finally, the imaginary parts of the ground and excited Zeeman coherences are $\rho_{zg} = \rho_{ab} - \rho_{ba}$ and $\rho_{ze} = \rho_{cd} - \rho_{dc}$. with these definitions the Eqs. (3.17) reduce to

$$i\partial_t n_g = \left(\Omega_c \rho_c^* + \Omega_p e^{-i\Phi(t,\vec{r})}\rho_p^* - cc\right) + i\Gamma\left(1 - n_g\right), \tag{3.18a}$$

$$i\partial_t \rho_c = \Omega_c\left(n_e - n_g\right) + \Omega_p e^{-i\Phi(t,\vec{r})}\left(\rho_{zg} + \rho_{ze}\right) + \bar{\Delta}_c^* \rho_c, \tag{3.18b}$$

$$i\partial_t \rho_p = -\Omega_c\left(\rho_{zg} + \rho_{ze}\right) + \Omega_p e^{-i\Phi(t,\vec{r})}\left(n_e - n_g\right) + \bar{\Delta}_c^* \rho_p, \tag{3.18c}$$

$$i\partial_t \rho_{zg} = \left(-\Omega_c \rho_p^* + \Omega_p e^{-i\Phi(t,\vec{r})}\rho_c^* + cc\right) - i\Gamma_{zg}\rho_{zg}, \tag{3.18d}$$

$$i\partial_t \rho_{ze} = \left(-\Omega_c \rho_p^* + \Omega_p e^{-i\Phi(t,\vec{r})}\rho_c^* + cc\right) - i\Gamma_{ze}\rho_{ze}. \tag{3.18e}$$

It is remarkable that only fewer equations are required to describe the dynamics of the system. This is the consequence of the symmetry of the system (of special relations between dipole moments), and of the excitation. Indeed a complementary set of equations can be written that includes the real parts of the Zeeman coherences; the difference of populations between the left and right two-level sub-systems $\rho_{aa} - \rho_{bb}$ and $\rho_{cc} - \rho_{dd}$;and the coherences $\rho_{da} - \rho_{cb}$ and $\rho_{ca} + \rho_{db}$, but this second set does not describe the dynamics of the system and vanishes in the steady state regime.

It is also interesting that only imaginary parts of the Zeeman coherences ρ_{ab} and ρ_{cd} are involved in the dynamics. This is again the consequence of the symmetry of the system. From (3.17e) we see that the action of the probe $\Omega_p e^{-i\Phi(t,\vec{r})}$ on the coherence ρ_{ba} creates the coherence ρ_{ca}, but ρ_{db} is created by the action of the probe on $(\rho_{ba})^*$ as we can see in (3.17f). Hence for $\rho_c = \rho_{ca} - \rho_{db}$, the contribution of real part of ρ_{ba} vanishes. Similarly ρ_{da} and

ρ_{cb} are created by the action of control field on ρ_{ba} and $(-\rho_{ba})^*$ respectively as shown by (3.17i) and (3.17j). Thus, again only the imaginary part of ρ_{ba} contribute in the evolution of the coherence $\rho_p = \rho_{cb} + \rho_{da}$. Similar argument holds for the contribution of ρ_{cd} in the evolution of ρ_c and ρ_p.

3.4.4 Steady state solution

The periodicity of the excitation allows for the use of Floquet methods. We expand the density matrix elements as

$$\rho_{ij}\left(\vec{r},t\right) = \sum_{m=-\infty}^{\infty} \rho_{ij}^{(m)} e^{im\Phi(\vec{r},t)}. \tag{3.19}$$

Using this expansion in Eqs. (3.18), order by order steady state solution of the system (with respect to probe amplitude) can be worked out. The coherences ρ_c and ρ_p are now given as :

$$\rho_c = \frac{1}{2\pi}\int_{-\infty}^{\infty} \left(\rho_{ca} - \rho_{db}\right) du, \tag{3.20a}$$

$$\rho_p = \frac{1}{2\pi}\int_{-\infty}^{\infty} e^{-iu}\left(\rho_{cb} + \rho_{da}\right) du, \tag{3.20b}$$

with $u = \delta\vec{k}\cdot\vec{r}$. The component of the coherence ρ_p given by $\int e^{iu}\left(\rho_{cb} + \rho_{da}\right) du$ radiates a field in the direction conjugate to the probe field direction (i. e. in $2\vec{k}_c - k_p\vec{e}_y$ direction).

Zero order solution: Absorption of the control

In the limit of weak σ field, ρ_p can be approximated at *first order* with respect to probe amplitude as $\rho_p^{(-)} = \rho_{cb}^{(-)} + \rho_{da}^{(-)}$. Similarly ρ_c can be approximated as $\rho_c^{(0)} = \rho_{ca}^{(0)} - \rho_{db}^{(0)}$. The Floquet expansion (3.19) can thus be truncated at *first order*. Using this truncated Floquet expansion in (3.18), we write the *zeroth order* equations in two sets. The first set consists of populations and the ρ_c coherence. It is given as:

$$i\partial_t n_g^{(0)} = \Omega_c \rho_c^{(0)^*} - \Omega_c^* \rho_c^{(0)} + i\Gamma\left(1 - n_g^{(0)}\right), \tag{3.21a}$$

$$i\partial_t \rho_c^{(0)} = \Omega_c\left(n_e^{(0)} - n_g^{(0)}\right) + \bar{\Delta}_c^* \rho_c^{(0)}. \tag{3.21b}$$

The stationary state solution of these two equations is:

$$n_e^{(0)} = \frac{2|\Omega_c|^2\Gamma_d\Gamma^{-1}}{4|\Omega_c|^2\Gamma_d\Gamma^{-1} + |\bar{\Delta}_c|^2}, \tag{3.22a}$$

$$n_g^{(0)} = 1 - n_e^{(0)} = \frac{2|\Omega_c|^2\Gamma_d\Gamma^{-1} + |\bar{\Delta}_c|^2}{4|\Omega_c|^2\Gamma_d\Gamma^{-1} + |\bar{\Delta}_c|^2}, \tag{3.22b}$$

$$\rho_c^{(0)} = \frac{\bar{\Delta}_c}{2\Omega_c^*\Gamma_d\Gamma^{-1}} n_e^{(0)} = \frac{\Omega_c}{\bar{\Delta}_c^*}\left(n_g^{(0)} - n_e^{(0)}\right) = \frac{\Omega_c\bar{\Delta}_c}{4|\Omega_c|^2\Gamma_d\Gamma^{-1} + |\bar{\Delta}_c|^2}. \tag{3.22c}$$

This is the same as given in Section. 1.1.3 by Eqs. 1.24 for a two-level system interacting with a single field. Indeed, in the absence of the probe, the system simplifies to an effective two-level system.

The other set of equations involve ρ_p and the Zeeman coherences. It is given by

$$i\partial_t\rho_p^{(0)} = -\Omega_c\left(\rho_{zg}^{(0)} + \rho_{ze}^{(0)}\right) + \bar{\Delta}_c^*\rho_p^{(0)}, \tag{3.23a}$$

$$i\partial_t\rho_{zg}^{(0)} = -\Omega_c\rho_p^{(0)^*} - \Omega_c^*\rho_p^{(0)} - i\Gamma_{zg}\rho_{zg}^{(0)}, \tag{3.23b}$$

$$i\partial_t\rho_{ze}^{(0)} = -\Omega_c\rho_p^{(0)^*} - \Omega_c^*\rho_p^{(0)} - i\Gamma_{ze}\rho_{ze}^{(0)}. \tag{3.23c}$$

It can be verified that no non-trivial stationary state solution exists for these equations, and we have $\rho_p^{(0)} = \rho_{zg}^{(0)} = \rho_{ze}^{(0)} = 0$. This shows that the control field alone can not create Zeeman and ρ_p coherences.

System at *first order*

The *first order* equations of (3.18) can again be written in two independent subsets. The first set, consisting of populations and ρ_c coherences, is given as:

$$i\partial_t n_g^{(-)} = \Omega_c\rho_c^{(+)^*} - \Omega_c^*\rho_c^{(-)} + \Omega_p\rho_p^{(0)^*} - (i\Gamma + \Delta)\, n_g^{(-)}, \tag{3.24a}$$

$$i\partial_t\rho_c^{(-)} = -2\Omega_c n_g^{(-)} + \Omega_p\left(\rho_{zg}^{(0)} + \rho_{ze}^{(0)}\right) + \left(\bar{\Delta}_c^* - \Delta\right)\rho_c^{(-)}, \tag{3.24b}$$

$$i\partial_t n_g^{(+)} = \Omega_c\rho_c^{(-)^*} - \Omega_c^*\rho_c^{(+)} - \Omega_p^*\rho_p^{(0)} - (i\Gamma - \Delta)\, n_g^{(+)}, \tag{3.24c}$$

$$i\partial_t\rho_c^{(+)} = -2\Omega_c n_g^{(+)} + \left(\bar{\Delta}_c^* + \Delta\right)\rho_c^{(+)}, \tag{3.24d}$$

Here we have used the relation $n_e^{(\pm)} = -n_g^{(\pm)}$. It can be shown that no non-trivial steady state solution exists for these equations. The weak probe at *first order* can not change populations or the ρ_c coherence. This is in contrast with CPO, where the *first order* populations are not zero.

The Zeeman and σ coherences at *first order* evolve as:

$$i\partial_t \rho_p^{(-)} = -\Omega_c \left(\rho_{zg}^{(-)} + \rho_{ze}^{(-)}\right) + \Omega_p \left(n_e^{(0)} - n_g^{(0)}\right) + \left(\bar{\Delta}_c^* - \Delta\right) \rho_p^{(-)}, \tag{3.25a}$$

$$i\partial_t \rho_{zg}^{(-)} = -\Omega_c \rho_p^{(+)^*} - \Omega_c^* \rho_p^{(-)} + \Omega_p \rho_c^{(0)^*} - \left(i\Gamma_{zg} + \Delta\right) \rho_{zg}^{(-)}, \tag{3.25b}$$

$$i\partial_t \rho_{ze}^{(-)} = -\Omega_c \rho_p^{(+)^*} - \Omega_c^* \rho_p^{(-)} + \Omega_p \rho_c^{(0)^*} - \left(i\Gamma_{ze} + \Delta\right) \rho_{ze}^{(-)}, \tag{3.25c}$$

$$i\partial_t \rho_p^{(+)} = -\Omega_c \left(\rho_{zg}^{(+)} + \rho_{ze}^{(+)}\right) + \left(\bar{\Delta}_c^* + \Delta\right) \rho_p^{(+)}, \tag{3.25d}$$

$$i\partial_t \rho_{zg}^{(+)} = -\Omega_c \rho_p^{(-)^*} - \Omega_c^* \rho_p^{(+)} - \left(i\Gamma_{zg} - \Delta\right) \rho_{zg}^{(+)}, \tag{3.25e}$$

$$i\partial_t \rho_{ze}^{(+)} = -\Omega_c \rho_p^{(-)^*} - \Omega_c^* \rho_p^{(+)} - \left(i\Gamma_{ze} - \Delta\right) \rho_{ze}^{(+)}. \tag{3.25f}$$

Coherent Zeeman oscillations

The most relevant equation in Eqs. (3.25) is (3.25a). It determines the response of the medium for the probe. The equation has remarkable similarity with Eq. (3.4b) for the EIT scheme, with the difference that here the ground and the excited Zeeman coherences are involved. It can also be compared with (3.11b) for the CPO scheme. However, in contrast to the CPO here the populations are stationary and the Zeeman coherences are oscillating.

All the three equations (3.4b) for EIT, (3.11b) for CPO, and (3.25) for CZO can be interpreted in the same manner. The diffraction of the control off some grating compensates for the absorption of the probe by the population. In EIT, the coherence between two ground states provides the grating through temporal dephasing of the two fields; in CPO the grating is provided by the oscillating populations; and in the present case, the space/time dephasing of the two fields makes the Zeeman coherences to oscillate and to provide the grating from which the control field is diffracted into the probe.

We can write Zeeman coherences as

$$\rho_{zg} = \rho_{zg}^{(0)} + \rho_{zg}^{(-)} e^{-i\Phi(\vec{r},t)} + \rho_{zg}^{(+)} e^{i\Phi(\vec{r},t)}. \tag{3.26}$$

The oscillations arise because the total field and hence the polarization is a modulated structure. The total polarization can be written as

$$e_T = \vec{e}_z + \vec{e}_x \frac{A_p}{A_c} e^{-i\Phi(\vec{r},t)}. \tag{3.27}$$

It is an oscillating structure due to the space/time dephasing of the two fields. This modulated polarization is graphically represented in Fig. 3.10. The diffraction of the control from the oscillating Zeeman coherence is shown in Fig. 3.11.

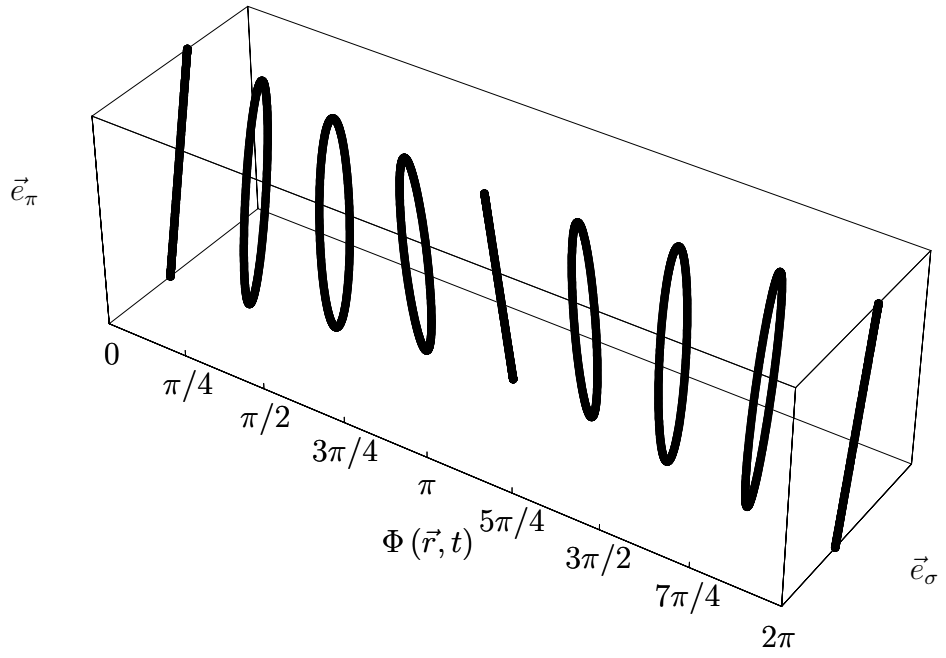

Figure 3.10: Polarization as a modulated structure in space and time.

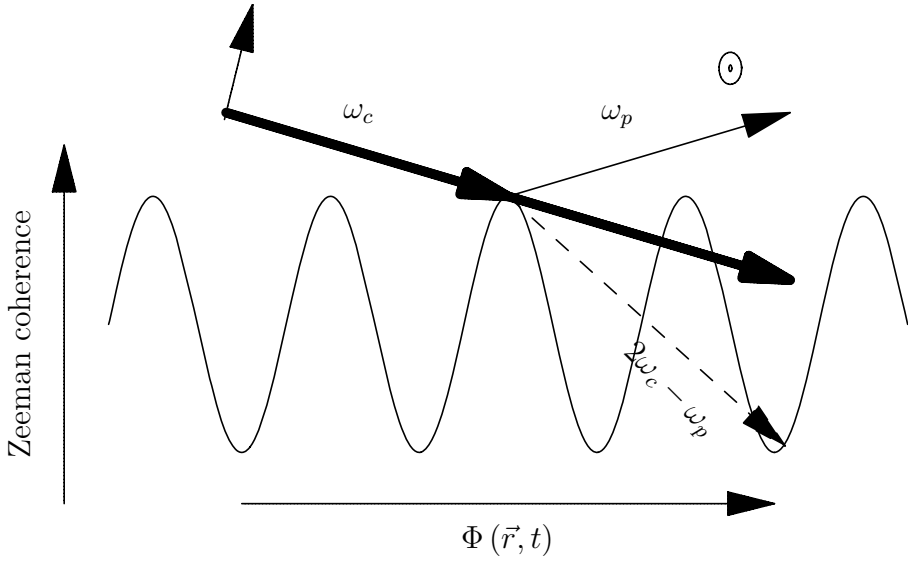

Figure 3.11: The absorption of the probe being compensated by the diffraction of the control off the oscillating Zeeman coherences.

Quantum excitations paths

The quantum excitation paths involved in the generation of $\rho_p^{(-)}$ (3.25a), can be shown for the two constituent components of the coherence $\rho_{cb}^{(-)}$ and $\rho_{da}^{(-)}$ as in Fig. 3.12 (the paths involving the excited Zeeman coherence are not shown). The path (a) and (b) in the figure correspond to the absorption of the probe by the static populations as given by the second term in Eq. (3.25a). The path (c) and (d) represent the diffraction of the control from the ground Zeeman coherence. The Zeeman coherence is established by the combined action of the control and the probe fields, and the subsequent diffraction of the control from the Zeeman coherence compensates for the absorption of the probe. The paths in (c) and (d) resemble the ones encountered in cross-Kerr effect [Boyd92].

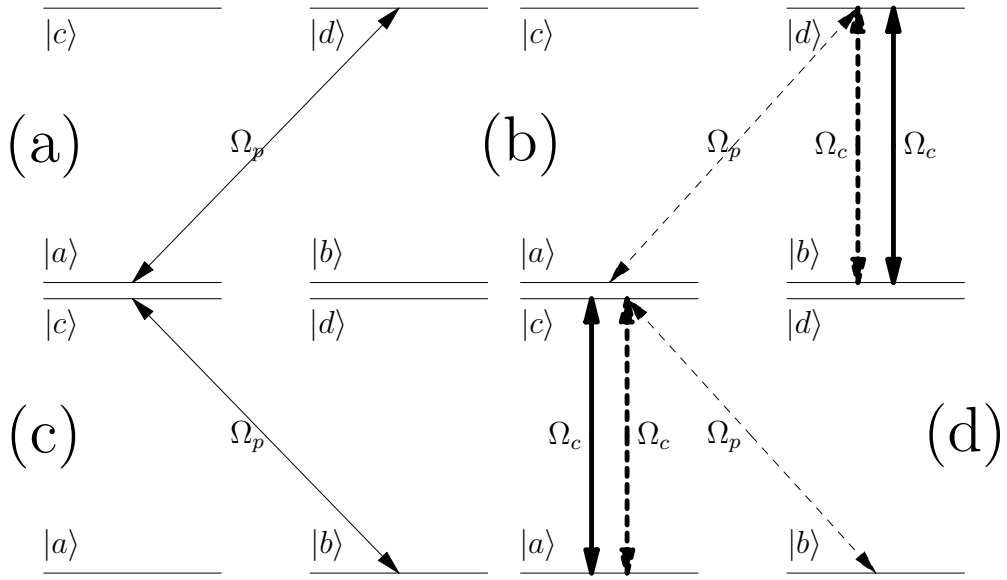

Figure 3.12: Quantum paths that contribute to generation of $\rho_p^{(-)}$. (a) Absorption path for $\rho_{da}^{(-)}$, (b) compensation path for $\rho_{da}^{(-)}$, (c) absorption path for $\rho_{cb}^{(-)}$, and (d) compensation path for $\rho_{da}^{(-)}$.

First order solution: Transparency for the probe

The stationary state solution of equation set (3.25) can be easily worked out. Using the Hermitian property of density matrix ($\rho_{ij} = {\rho_{ji}}^*$), we can work out the relations $\rho_{ze}^{(-)} = -\rho_{ze}^{(+)^*}$ and $\rho_{zg}^{(-)} = -\rho_{zg}^{(+)^*}$. Using these relations the

steady state solution of (3.25) can be written as:

$$\rho_{ze}^{(-)} = \frac{\Delta}{\bar{\Delta}_c}\rho_{zg}^{(-)}, \tag{3.28a}$$

$$\rho_{p}^{(-)} = \frac{\Omega_c M \rho_{zg}^{(-)} + \Omega_p \left(n_g^{(0)} - n_e^{(0)}\right)}{\bar{\Delta}_c^* - \Delta} \tag{3.28b}$$

$$\rho_{p}^{(+)} = \frac{\Omega_c M^* \rho_{zg}^{(+)}}{\bar{\Delta}_c^* + \Delta}, \tag{3.28c}$$

$$\rho_{zg}^{(-)} = \frac{\Omega_c^* \Omega_p \left(n_g^{(0)} - n_e^{(0)}\right)\left[\frac{1}{\Delta_c} - \frac{1}{\Delta_c^* - \Delta}\right]}{(\Delta + i\Gamma_{zg}) + |\Omega_c|^2 M \left[\frac{1}{\Delta_c^* - \Delta} - \frac{1}{\Delta_c + \Delta}\right]}, \tag{3.28d}$$

with

$$M = \frac{2\Delta + i\left(\Gamma_{zg} + \Gamma_{ze}\right)}{\Delta + i\Gamma_{ze}}. \tag{3.29}$$

The Eq. (3.28b) determines the response of the medium for the weak probe. The expression suggests that the coherence is the result of two processes as has already been discussed. For long-lived ground Zeeman coherence with $\Gamma_{zg} = 0$, and when the two fields are detuned to the same value with $\Delta = 0$, we have $\Omega_c M \rho_{zg}^{(-)} = -\Omega_p \left(n_g^{(0)} - n_e^{(0)}\right)$. The diffraction of the control completely compensates for the absorption of the probe, and the coherence $\rho_p^{(-)}$ vanishes. This is in spite of the fact that the modulation depth of the grating is weak as $\rho_{zg}^{(-)} \propto \Omega_p/\Omega_c$ (for $\Gamma_{zg} = \Delta = 0$). However, the diffraction of the control from the grating is of the same order as the absorption of the probe.

A transparency window for the probe is thus obtained, and the transparency is perfect for $\Gamma_{zg} = \Delta = 0$. The characterization of this transparency window and of the resulting slow light will be discussed in detail in the next pages.

3.4.5 A double Λ system with No dark state

The system shown in Fig. 3.9 can be seen as consisting of two Λ systems $\{|a\rangle, |c\rangle, |b\rangle\}$ and $\{|a\rangle, |d\rangle, |b\rangle\}$. These two Λ systems are shown in 3.13. Such double Λ systems have been extensively studied [Morigi02, Korsunsky99, Lukin98, Cerboneschi96] and electromagnetic induced transparency has been demonstrated [Park05] in such systems using dark states. Deng *et. al.* have proposed a scheme in which the dark state is realized after certain propagation inside the medium [Deng05]. However, the dark state exists only for

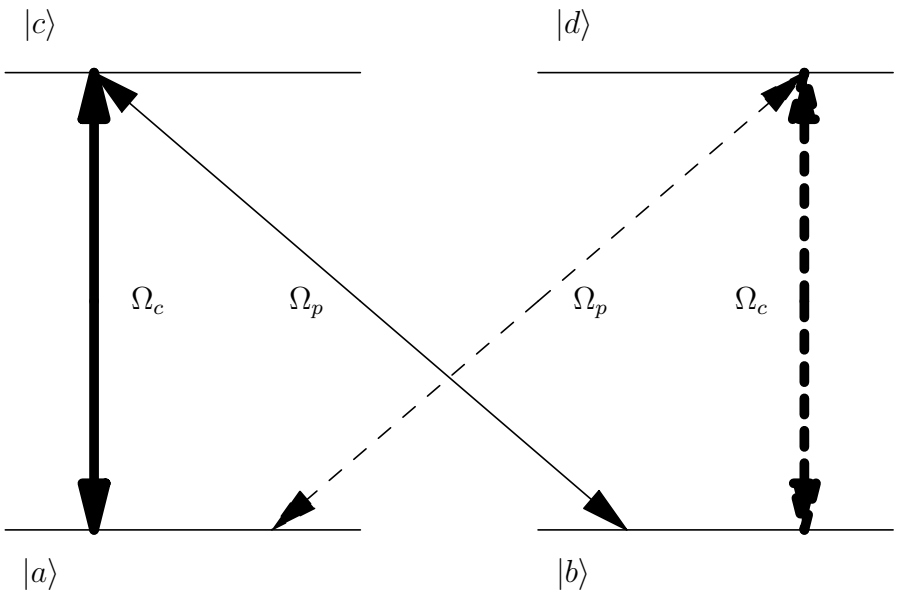

Figure 3.13: The double two-level system seen as a double Λ system. The control and the probe field in solid form one Λ system. The second system is shown with the control and the probe field in dashed.

special matching conditions when the control and the probe have specific intensity relationships.

We can define the dark states for two Λ sub-systems in Fig. 3.13 as:

$$|D_{acb}\rangle = -\Omega_p e^{-i\Phi(\vec{r},t)} |a\rangle + \Omega_c |b\rangle , \tag{3.30}$$

$$|D_{adb}\rangle = \Omega_c |a\rangle + \Omega_c e^{-i\Phi(\vec{r},t)} |b\rangle . \tag{3.31}$$

It can be seen that when the the matching condition

$$\Omega_c^2 + i\Omega_p^2 e^{-2i\Phi(t,\vec{r})} \tag{3.32}$$

is satisfied, we get $|D_{adb}\rangle = i\,|D_{acb}\rangle$. The two Λ sub-systems share a common dark state. All the population can be coherently trapped in the dark state and the medium becomes transparent.

However, this dark state can not be realized in our system in the present configuration. The two fields are real and we have $|\Omega_p| \ll |\Omega_c|$. Therefore the transparency in the present system can not be explained in terms of CPT or dark states. Interestingly, in a different excitation scheme, the present system can give rise to the dark state after certain propagation in the system. This will be discussed in the next Chapter in Section. 4.5.

3.4.6 Transparency window for the probe

For the discussion that follows we place ourselves in the situation where the ground Zeeman coherences are long lived, with $\Gamma_{zg} = 0$. This is the case where non-radiative dephasing processes like collisions are absent. The case with non-vanishing Γ_{zg} is a limitation to the present scheme of slowing light and will be discussed in the limitations in Section. 3.4.8.

The response of the medium for the probe is determined by

$$\chi_{eff} = \chi'_{eff} + i\chi''_{eff}, \tag{3.33}$$

$$= \frac{2\alpha_0\Gamma_d}{k}\frac{\rho_p^{(-)}}{\Omega_p}. \tag{3.34}$$

Here $\alpha_0 = ND^2\omega_0/\left(2c\hbar\epsilon_0\Gamma_d\right)$ and $k = \omega_0/c$. Using the expression of $\rho_p^{(-)}$ from Eq. (3.28b) (for $\Gamma_{zg} = 0$), the susceptibility can be written as

$$\chi_{eff}\left(\Delta, \bar{\Delta}_c\right) = \Delta\frac{2\alpha_0\Gamma_d}{k}\left(n_g^{(0)} - n_e^{(0)}\right)\frac{|\Omega_c|^2 M\bar{\Delta}_c^{-1} + \left(\Delta + \bar{\Delta}_c\right)}{2|\Omega_c|^2 M\left(\Delta + i\Gamma_d\right) + \Delta\left(\bar{\Delta}_c^* - \Delta\right)\left(\bar{\Delta}_c + \Delta\right)} \tag{3.35}$$

It vanishes for $\Delta = 0$ as has been discussed. For $\Delta \neq 0$, the susceptibility is shown in the Fig. 3.14, in the presence and the absence of the control field.

In the absence of the control, the system exhibits linear behavior for the probe, with strong absorption and anomalous dispersion at resonance. The control field opens up a transparency window in the absorption profile and changes the dispersion profile to normal dispersion. The minimum of the window is at *zero* for $\Delta = 0$, signifying perfect transparency and the complete compensation for the absorption of the probe. This is similar to what is obtained in EIT with a dark state, and in contrast to CPO where the transmission is not perfect.

The width of the transparency window

The width of the transparency window decreases by decreasing the control field intensity as shown in Fig. 3.14. A simplified expression for the width can be worked out. For resonant control field $\Delta_c = 0$, and in the limit $|\Omega_c|, \Delta \ll \Gamma_d, \Gamma_{ze}$, the imaginary part of the susceptibility [from (3.35)] simplifies to

$$\chi''_{eff}\left(\Delta\right) \approx \frac{\alpha_0}{k}\frac{2\left(\frac{\Gamma_d\Delta}{2|\Omega_c|^2}\right)^2}{1 + \left(\frac{\Gamma_d\Delta}{2|\Omega_c|^2}\right)^2}. \tag{3.36}$$

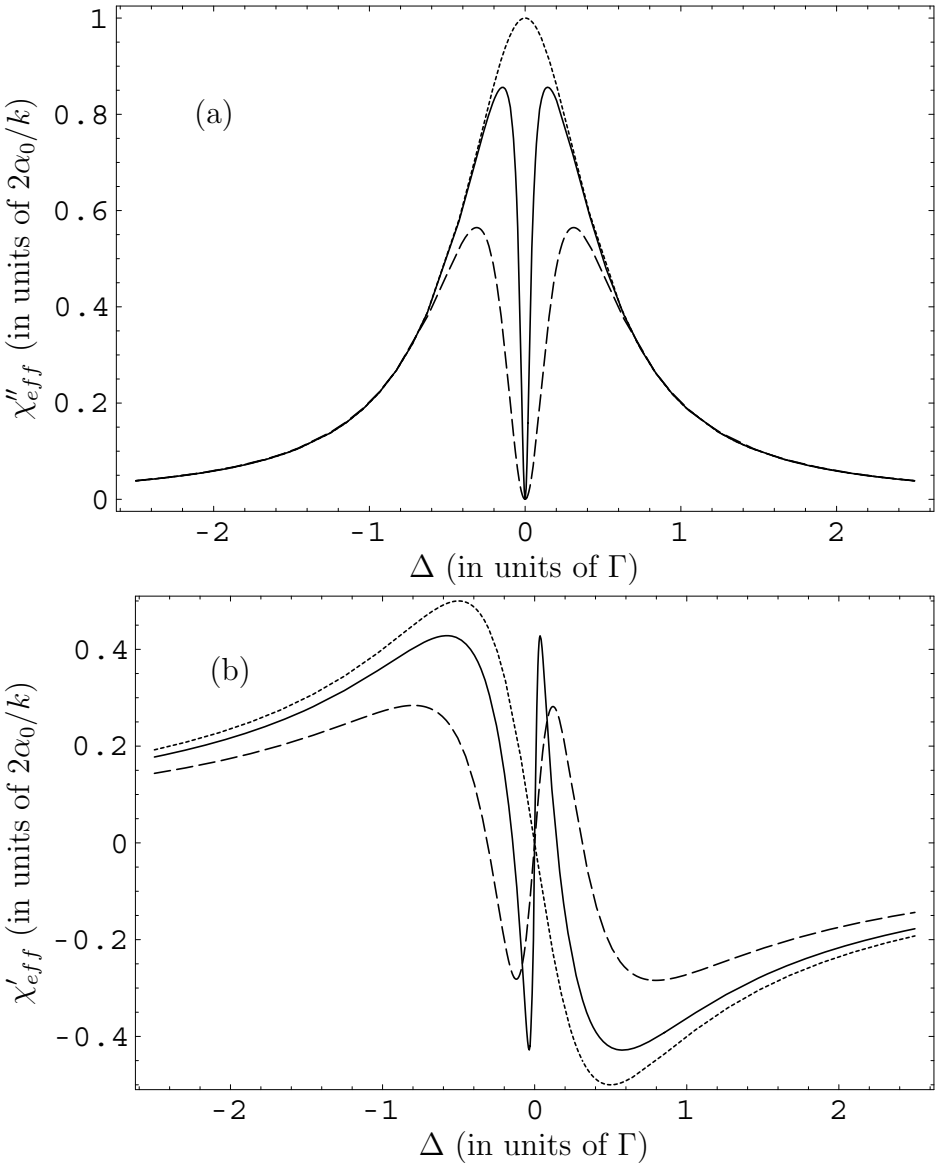

Figure 3.14: Effective susceptibility for the probe as the function of the detuning $\Delta = \omega_p - \omega_c$ in CZO scheme. (a) Absorption profile, (b) dispersion profile. Parameters are $\Omega_c = 0$ (dotted), $\Omega_c = 0.2\Gamma$ (dashed), and $\Omega_c = 0.1\Gamma$ (solid). Other parameters are $\Delta_c = 0$, $\Gamma_d = 0.5\Gamma$, $\Gamma_{zg} = 0$, and $\Gamma_{ze} = \Gamma$.

This is an inverted Lorentzian with the full width at half minimum given by $4|\Omega_c^2|/\Gamma_d$. The width of the absorption profile is given by $2\Gamma_d$. The relative width of the transparency with respect to the absorption profile is thus given as $2|\Omega_c/\Gamma_d|^2$, and it can be significantly reduced by decreasing the control field intensity. This is similar to the behavior found in EIT, and in contrast to CPO.

Robustness against control field detuning

The transparency at $\Delta = 0$ is robust against the control field detuning Δ_c, as is clear from the expression for the susceptibility in (3.35). This is shown in the Fig. 3.15.

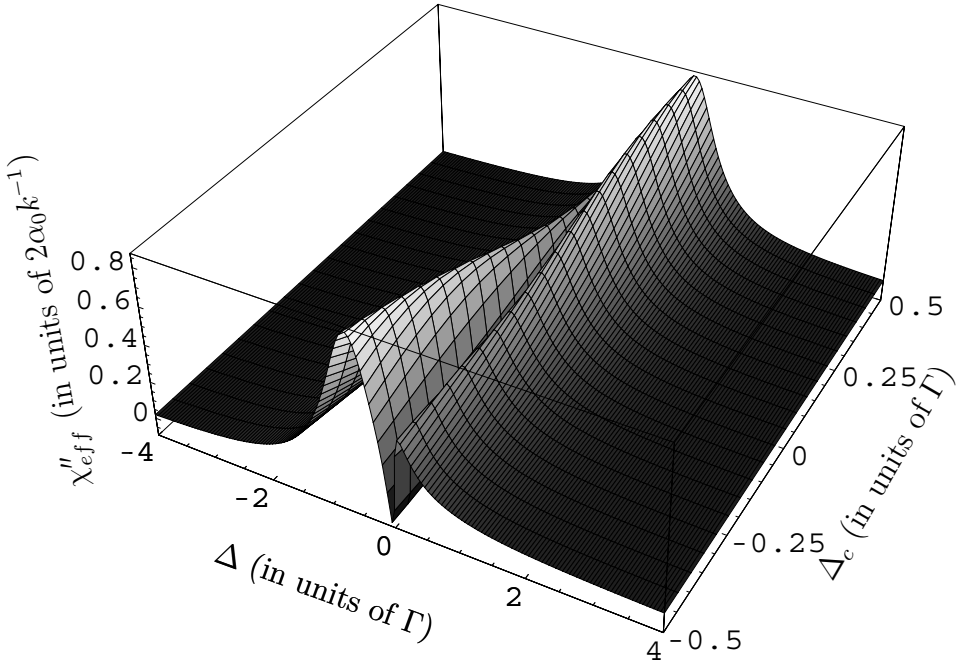

Figure 3.15: The transparency is robust against the control field detuning. Parameters are $\Omega_c = 0.2\Gamma$, $\Gamma_d = 0.5\Gamma$, $\Gamma_{zg} = 0$, and $\Gamma_{ze} = \Gamma$.

Saturation with the control field

The maximum of the absorption peaks in the Fig. 3.14 does not reach the same limit in the presence of the control as is the absence of the control. This is the saturation effects because of the control field and is shared between CPO and CZO. In EIT however, the two absorption peaks just move apart by the action of the control and no saturation of the absorption takes place.

Possibility of fast light

For control field strength such that $|\Omega_c| \geq \Gamma_d$, the light shifts induced by the control field become important. The absorption peaks move apart and unlike EIT, new structure appears in the center as shown in the Fig. 3.16. This is similar to the the splitting of an absorption peak into *three* because

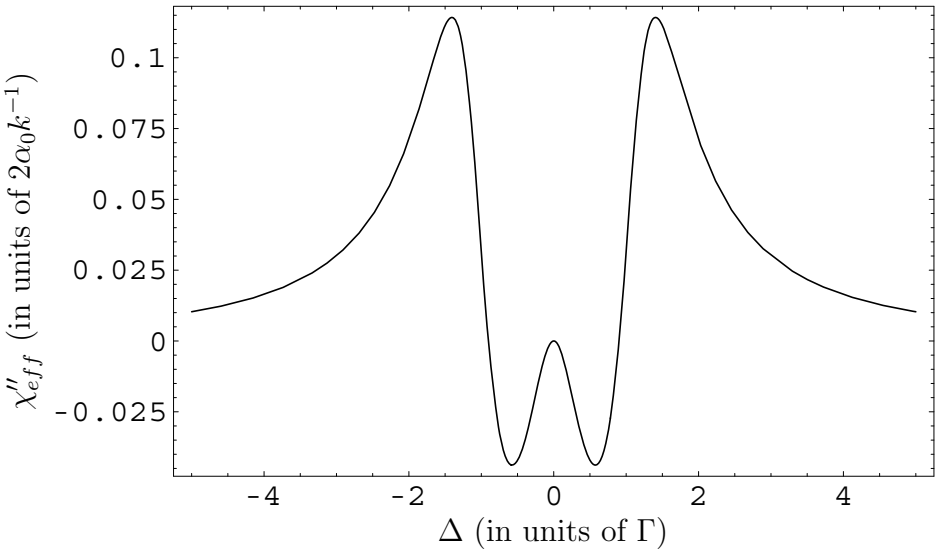

Figure 3.16: Splitting of the transparency window with a gain region in the center. Parameters are $\Delta_c = 0$, $\Omega_c = 0.6\Gamma$, $\Gamma_d = 0.5\Gamma$, $\Gamma_{zg} = 0$, and $\Gamma_{ze} = \Gamma$.

of the induced energy levels in a strongly driven two level atomic system [Boyd81]. However, in the present case the central absorption peak is being compensated for by the diffraction of the probe. This produces regions of gain around $\Delta = 0$, where the control field overcompensates for the absorption of probe. This can be used to produce fast light in the medium.

Strong saturation

For $|\Omega_c| \gg \Gamma_d$, the control field saturates the system. The populations in the excited and the ground levels become equal with $n_g^{(0)} - n_e^{(0)} \to 0$, and from Eq. (3.28d) and Eq. (3.28a), we see that the Zeeman coherences vanish. In this case the system reduces to a strongly driven two-level system being probed by a weak probe. It presents the well known absorption spectra [Boyd92, Boyd88, Boyd81] for a strongly driven two level system. For non-resonant control, we observe a one photon absorption peak at $\omega_c + \Omega_{max}$, a three photon gain peak at $\omega_c - \Omega_{max}$, and dispersion like resonance at ω_c

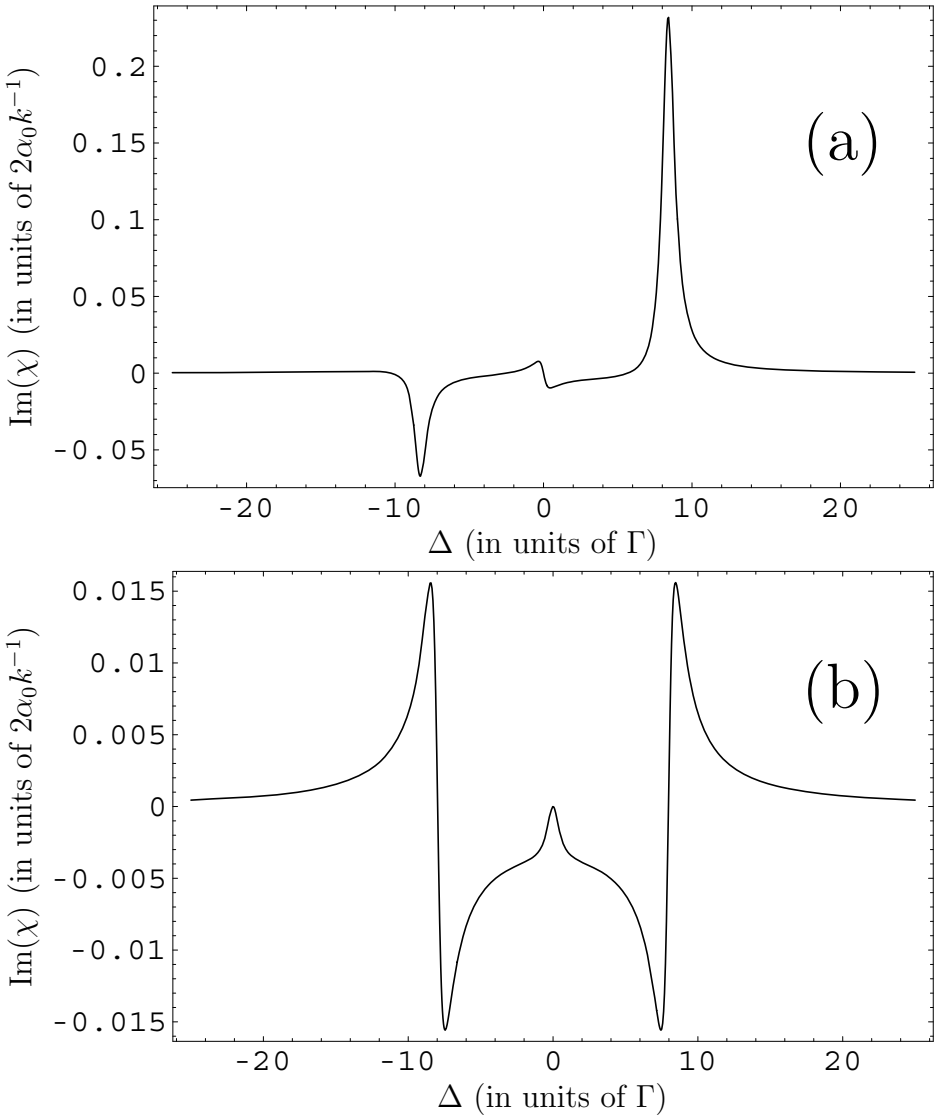

Figure 3.17: Absorption spectra when the system reduces to an effective (strongly driven) two-level system. Parameters are (a) $\Delta_c = 2.5$, (b) $\Delta_c = 0$. Other parameters are $\Omega_c = 4\Gamma$, $\Gamma_d = 0.5\Gamma$, $\Gamma_{zg} = 0$, and $\Gamma_{ze} = \Gamma$

[Boyd92, Boyd88] as shown in Fig. 3.17(a). For the resonant excitation, the spectrum exhibits two mixed gain/absorption peaks at $\omega_c \pm \Omega_{max}$ and a broad region of gain in between [Boyd81] and is shown in Fig. 3.17(b).

3.4.7 Light propagation

Narrow transparency windows with abrupt normal dispersion profiles as shown in Fig. 3.14 (with $|\Omega_c| < \Gamma_d$) can lead to slow light propagation in the medium. The equation of propagation for the probe in a frame of reference that is moving with the velocity of light in vacuum, c, can be written as (see Section. 1.2.1)

$$\partial_y \Omega_p (t, y) = i\alpha_0 \Gamma_d \rho_p^{(-)} (t, y) . \tag{3.37}$$

The control field follows a similar equation of propagation, but for $|\Omega_c| \gg |\Omega_p|$, the control field is not affected by the presence of the probe. However, the control does experience the absorption and dispersion effects of the medium as the transparency is not achieved for the control. This effect can be minimized either by restricting the propagation to short distances (with low optical thickness), or by making the control field cross the medium transversely as shown in Fig. 3.18. Such crossed propagation geometry has also been proposed to reduce the propagation effects on the control field in the case of CPO [Piredda07].

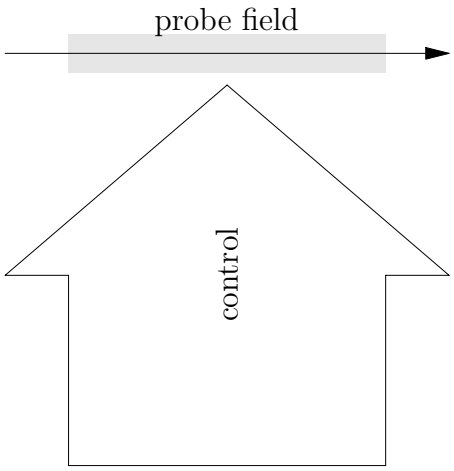

Figure 3.18: Field configuration. The control field crosses the medium transversely in order to reduce the propagation effects.

Group velocity

The group velocity for the probe is given by $v_g = c\left[n + \omega_c dn/d\omega_c\right]^{-1}$. Using $n \approx 1 + \chi'_{eff}/2$ and using the expression of susceptibility from Eq. (3.35), the group velocity at $\Delta = 0$ is given by

$$v_g = c\left[1 + \frac{c\alpha_0\Gamma_d}{2|\Omega_c|^2}\frac{|\bar{\Delta}_c|^2 - |\Omega_c|^2}{4|\Omega_c|^2\Gamma_d\Gamma^{-1} + |\bar{\Delta}_c|^2}\right]^{-1}. \tag{3.38}$$

In the limit of weak control field with $|\Omega_c| \ll \Gamma_d$, this expression reduces to $v_g = 2|\Omega_c|^2/\left(\alpha_0\Gamma_d\right)$. Very small group velocities can be reached by either decreasing the control field intensity,or by increasing the atomic density. However, if the atomic density is increased then a distributed configuration as shown in Fig. 3.18 has to be used.

A numerical example of slow light can be worked out as follows. Using the definition of Rabi frequency for the control field $\Omega_c = DA_c/\hbar$, the definition of field absorption coefficient $\alpha_0 \simeq ND^2\omega_c/(2c\hbar\epsilon_0\Gamma_d)$, and the relation between the field amplitude and the field intensity $I_\pi = 2c\epsilon_0|A_c|^2$, the group velocity can be written in terms of control field intensity as

$$v_g = \frac{2I_\pi}{\hbar\omega_p N}. \tag{3.39}$$

For the control field intensity of 1 mW/cm^2, the atomic density of $N = 10^{12}$ at/cm^3, a probe at 800 nm will experience the group velocity $v_g \approx 75$ m/s.

Slow light

In order to observe such slow lights, the entire pulse spectrum should be contained inside the transparency window. This requires that the pulse duration τ_p should be much larger than the inverse of the transparency window. At the entrance of the medium (at $y = 0$), it can be ensured by having $\tau_p \gg \Gamma_d/\left(4\Omega_c^2\right)$. However, during propagation any components outside the transparency window (in the wings of the pulse spectrum) can be significantly absorbed.

Th absorption in the wings is given by $e^{-ky\chi''_{eff}}$ where y is the propagation distance. Hence the effective transparency window is reduced to $4\Omega_c^2/\left(\Gamma_d\sqrt{\alpha_0 y}\right)$, and we need to have $\tau_p \gg \Gamma_d\sqrt{\alpha_0 y}/\left(4\Omega_c^2\right)$.

The delay introduced by the slow propagation for a distance L is $\tau = L\left(v_g^{-1} - c^{-1}\right)$ and is given as

$$\tau = \frac{\alpha_0 L\Gamma_d\left(|\bar{\Delta}_c|^2 - \Omega_c^2\right)}{2\Omega_c^2\left(4\Omega_c^2\Gamma_d\Gamma^{-1} + |\bar{\Delta}_c|^2\right)}. \tag{3.40}$$

For $|\Omega_c| \ll \Gamma_d$, the delay simplifies to $\alpha_0 L\Gamma_d/\left(2\Omega_c^2\right)$. The fractional delay is given as τ/τ_p and because of the restraint on pulse duration it is always much less than $2\sqrt{\alpha_0 L}$. Thus in order to have good fractional delays $\alpha_0 L$ has to be much greater than few units and a distributed field configuration has to be used to avoid the absorption of the control field.

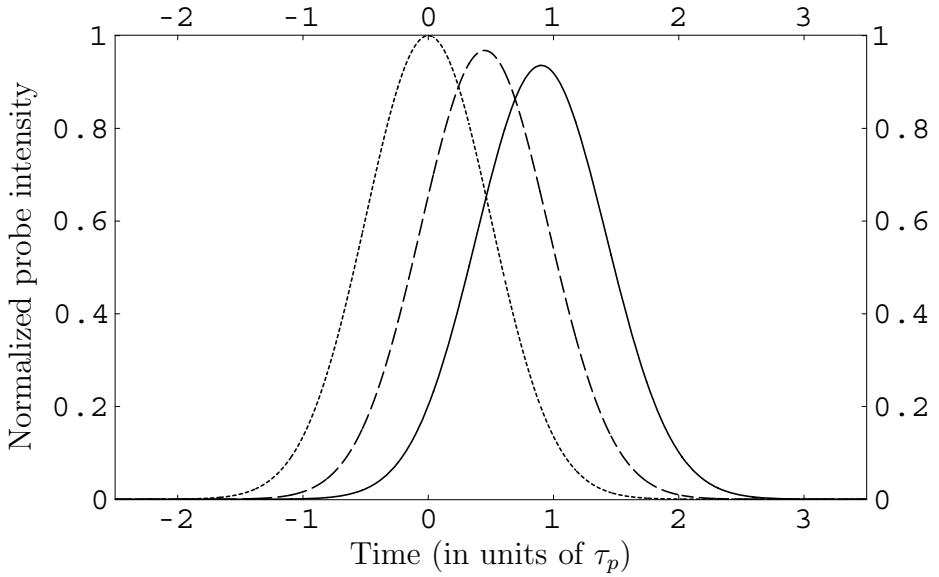

Figure 3.19: Slow light in dense atomic media. Probe is a Gaussian given by $\Omega_p = \Omega_{\sigma 0} e^{-(t/\tau_p)^2}$ with $\Omega_{\sigma 0} = 0.001\Gamma$, and $\tau_p = 2500\Gamma^{-1}$. Dotted curve shows initial pulse intensity. Dashed and solid curves show pulse intensity profiles after propagation for $\alpha_0 L = 50$, and $\alpha_0 L = 100$ respectively. Other parameters are $10\Omega_c = 2\Gamma_d = \Gamma_{ze} = \Gamma$, and $\Delta = \Delta_c = \Gamma_{zg} = 0$. In a system with $L = 1\ cm$, and $\Gamma = 37\ MHz$, this corresponds to a $\sim 67\ \mu s$ pulse propagating at $\sim 300\ m/s$ (dashed), and $160\ m/s$ (solid).

The slow light using CZO in dense optical medium is shown in Fig. 3.19. The absorption is due to the fact that the probe duration τ_p is just $20 \sim 28$ times larger than the reduced transparency window. The optical depth is large and a distributed control must be used. The length of the medium L is thus limited by the transverse dimension of the control beam.

An example of slow light in low optical thickness is given in Fig. 3.20. Here $\alpha_0 L = 1$, The pump can propagate along with the probe in the medium and only a small angle between the two is required to remove the conjugate wave. This minimum angle is given by $\sqrt{\lambda/L}$ where λ is the wavelength of the probe.

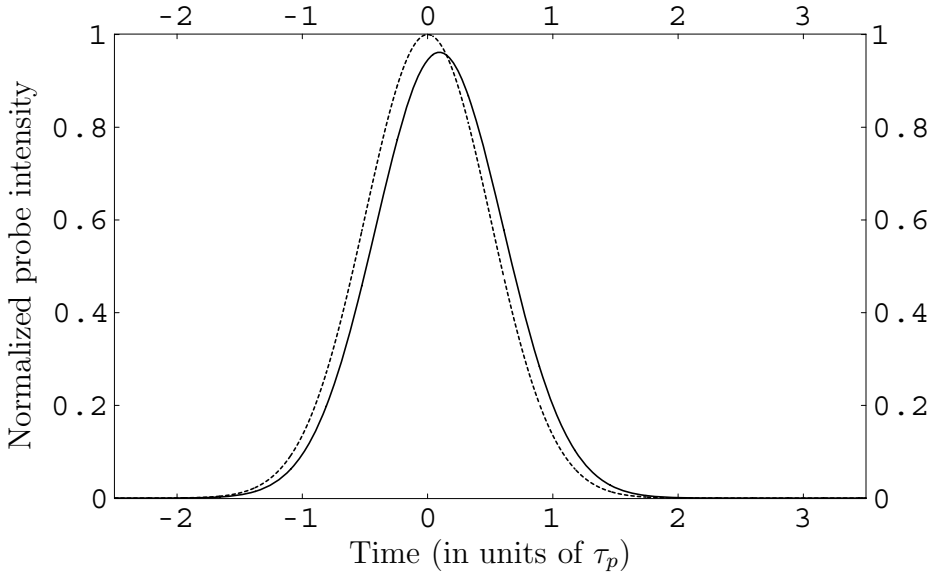

Figure 3.20: Slow light in low optical thickness. Probe is a Gaussian given by $\Omega_p = \Omega_{\sigma 0} e^{-(t/\tau_p)^2}$ with $\Omega_{\sigma 0} = 0.001\Gamma$, and $\tau_p = 1000\Gamma^{-1}$. Dotted curve shows initial pulse intensity. Solid curve shows pulse intensity profiles after propagation for $\alpha_0 L = 1$. Other parameters are $20\Omega_c = 2\Gamma_d = \Gamma_{ze} = \Gamma$, and $\Delta = \Delta_c = \Gamma_{zg} = 0$. In a system with $L = 1\ cm$, and $\Gamma = 37\ MHz$, this corresponds to a $\sim 27\ \mu s$ pulse propagating at $\sim 3700\ m/s$ (solid).

Fast light

For resonant control field with $\bar{\Delta}_c = i\Gamma_d$, and for $\Omega_c \geq \Gamma_d$, the expression Eq. (3.38) suggests a group velocity for the probe that is larger than the c. The medium can thus turn into a fast light medium. Correspondingly the real part of the probe susceptibility exhibits anomalous dispersion near $\Delta = 0$ and is shown in Fig. 3.21. For $|\Omega_c| \gg \Gamma_d$, the group velocity expression simplifies to $v_g = 8|\Omega_c|^2 c/\left(8|\Omega_c|^2 - c\alpha_0\Gamma\right)$.

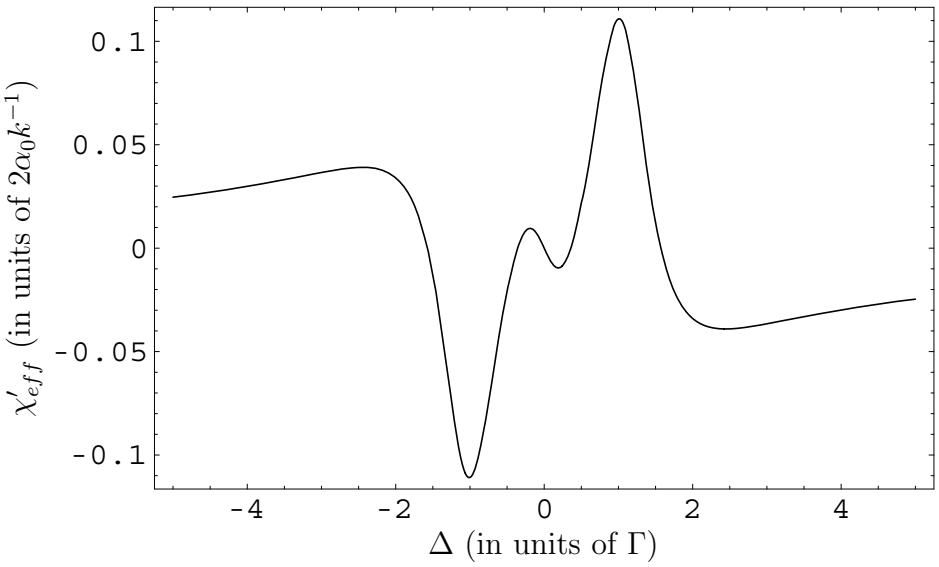

Figure 3.21: Anomalous dispersion at $\Delta = 0$ suggests fast light propagation. Parameters are $\Delta_c = 0$, $\Omega_c = 0.6\Gamma$, $\Gamma_d = 0.5\Gamma$, $\Gamma_{zg} = 0$, and $\Gamma_{ze} = \Gamma$

3.4.8 Limitations of CZO

Now I discuss the important limitations of CZO technique. In addition to the absorption of control which severely limits propagation in dense atomic media in a non-distributed configuration, three effects have to be discussed. These include the Doppler broadening in hot atomic vapors, the dephasing of the ground Zeeman coherence in the presence of depolarizing collisions, and the non-linear effects with respect to the probe amplitude.

The Doppler effect

In hot atomic gases the Doppler broadening of transitions has to be taken into account. The need arises because different atoms moving with different velocities experience the control and the probe lasers with different frequencies.

The detunings thus change as $\Delta_c \rightarrow \Delta_c - \vec{k}_c \cdot \vec{v}$ and $\Delta \rightarrow \Delta - \left(k_p \vec{e}_y - \vec{k}_c\right) \cdot \vec{v}$, and the susceptibility has to be averaged over a distribution of atomic velocities. This velocity distribution can be written as:

$$f\left(\vec{v}\right) = \prod_{i=x,y,z} f_i\left(v_i\right) \tag{3.41}$$

where each component of $f\left(\vec{v}\right)$ follows a Maxwellian distribution

$$f_i\left(v_i\right) = \frac{e^{-\left(v_i/u\right)^2}}{\sqrt{\pi}u}. \tag{3.42}$$

Here we have $u = \sqrt{\frac{2k_BT}{m}}$, k_B is the Boltzman constant, T is the temperature, and m is the mass of the atoms. The Doppler averaged susceptibility can now be written as:

$$\chi_{avg}\left(\Delta, \Delta_c\right) = \int_x \int_y \int_z \chi\left(\Delta - k_p \vec{e}_y \cdot \vec{v} + \vec{k}_c \cdot \vec{v}, \Delta_c - \vec{k}_c \cdot \vec{v}\right) f\left(\vec{v}\right) dxdydz \tag{3.43}$$

For a large angle ϑ between the control and the probe beams, and for $|\vec{k}_c| = k_p$, the susceptibility has to be averaged around Δ over a range $k_p v_y \left(1 - \cos\vartheta\right) - k_p v_x \sin\vartheta$, and around Δ_c over a range $k_p v_y \cos\vartheta + k_p v_x \sin\vartheta$.

From Eq. (3.35) and Fig. 3.15, it can be seen that the transparency at $\Delta = 0$ is robust against averaging across Δ_c. However, any averaging across Δ over a window broader than the transparency window can spoil the transparency. $k_p v_y \sim k_p v_w$ at room temperature lies in GHz, whereas the transparency window $4\Omega_c^2/\Gamma_d$ lies in MHz or few tens of MHz. The averaging thus spoils the transparency even for a Doppler width as small as $\Delta_{dop} = uk = \Gamma$ as shown in Fig. 3.22(a)

However, in a non distributed configuration, with only a very small angle between the two beams, the Doppler averaging can be overcome. If the angle ϑ is such that $\vartheta << 4\Omega_c^2/\left(k_p v_y \Gamma_d\right)$, the averaging across Δ still lies within the transparency window. In this case the Eq. (3.43) simplifies to

$$\chi_{avg}\left(\Delta, \Delta_c\right) = \int_y \chi\left(\Delta, \Delta_c - k_p v_y\right) f\left(v_y\right) dy. \tag{3.44}$$

From Eq. (3.35) and Fig. 3.15 we see that the transparency is ensured at $\Delta = 0$ for all the different velocity classes. The transparency thus survives the Doppler-averaging of the susceptibility and only its width can be modified. This robust behavior against Doppler averaging is shown in Fig. 3.22(b,c) This robustness, however, comes with a price. A small angle between the control and the probe means that the optical depth $\alpha_0 L$ is limited—because of the absorption of the control—to only few units.

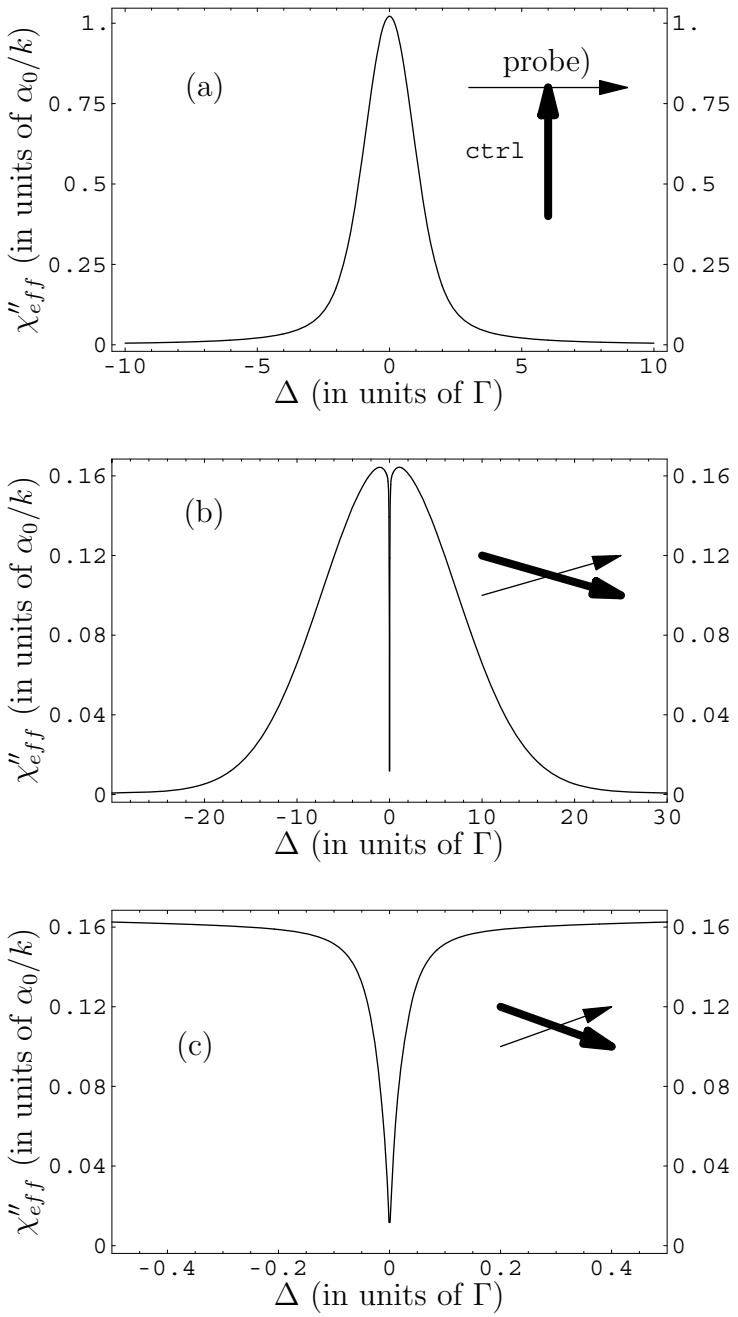

Figure 3.22: Doppler broadening of CZO. In a distributed configuration (a), the Doppler averaging washes out the transparency whereas in a near collinear geometry (b) and (c), the transparency window is robust against Doppler broadening. (c) is a zoom of (b). Parameters are (a) $\vartheta = \pi/2$, $\delta_{dop} = \Gamma$; (b) $\vartheta = 0.0001$, $\delta_{dop} = 10\Gamma$. Other parameters are $\Omega_c = 0.1\Gamma$, $2\Gamma_d = \Gamma_{ze} = \Gamma$, and $\Delta_c = \Gamma_{zg} = 0$

Ground state Zeeman decoherence $\Gamma_{zg} \neq 0$

The relaxation of the ground state Zeeman coherence is another limitation to slowing light using CZO. When the coherence is destroyed, the strong field can no longer be diffracted into the probe. With $\Gamma_{zg} \neq 0$, the compensation of the absorption of the probe is not perfect at $\Delta = 0$. This can be seen from Eq. (3.28d) where $\Omega_c M \rho_{zg}^{(-)}$ no longer equals $-\Omega_p \left(n_g^{(0)} - n_e^{(0)} \right)$. The minimum of the transparency dip does not go to zero, and hence the absorption of the probe presents a limitation to slowing light. This limitation can be quantified by the ratio $\Gamma_{zg} / \left(2\Omega_c^2 M / \Gamma_d \right)$, where for simplicity we have taken $\Delta_c = 0$. For $\Gamma_{zg} \ll \Gamma_{ze}$, M is almost unity and we need to satisfy $\Gamma_{zg} \ll 2\Omega_c^2 / \Gamma_d$ in order to minimize the absorption of the probe.

The effective susceptibility for $\Gamma_{zg} \neq 0$ can be written as

$$\chi\left(\Delta, \bar{\Delta}_c\right) = 2\frac{\alpha_0 \Gamma_d}{k}\left(n_g^{(0)} - n_e^{(0)}\right) \frac{\Delta\Omega_c^2 M \bar{\Delta}_c^{-1} + \left(\Delta + i\Gamma_{zg}\right)\left(\Delta + \bar{\Delta}_c\right)}{2\Omega_c^2 M\left(\Delta + i\Gamma_d\right) + \left(\Delta + i\Gamma_{zg}\right)\left(\bar{\Delta}_c^* - \Delta\right)\left(\bar{\Delta}_c + \Delta\right)}. \tag{3.45}$$

It no longer vanishes at $\Delta = 0$ and the absorption at the minimum of the width is determined by $\Gamma_{zg} / \left(2\Omega_c^2 \Gamma_d^{-1}\right)$. The real and imaginary parts of

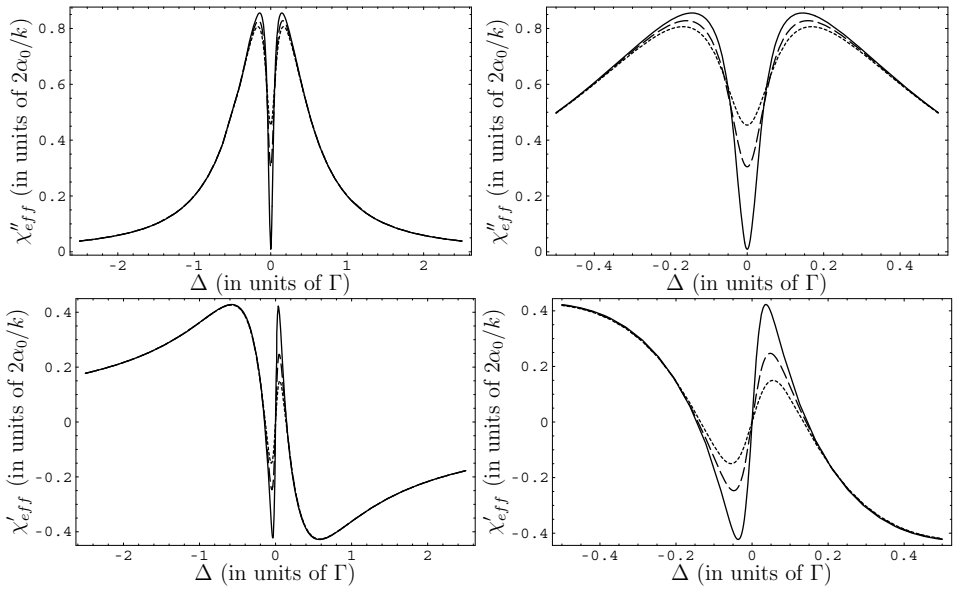

Figure 3.23: Decoherence between the ground Zeeman states spoils the transparency. Parameters for the four figures are (dotted) $\Gamma_{zg} = 2\Omega_c^2/\Gamma_d$, (dashed) $\Gamma_{zg} = \Omega_c^2/\Gamma_d$, and (solid) $\Gamma_{zg} = 0.02\Omega_c^2/\Gamma_d$. Other parameters are $\Omega_c = 0.1\Gamma$, $\Delta_c = 0$, and $2\Gamma_d = \Gamma_{ze} = \Gamma$.

the effective susceptibility in the presence of non-vanishing Γ_{zg} are shown in Fig. 3.23.

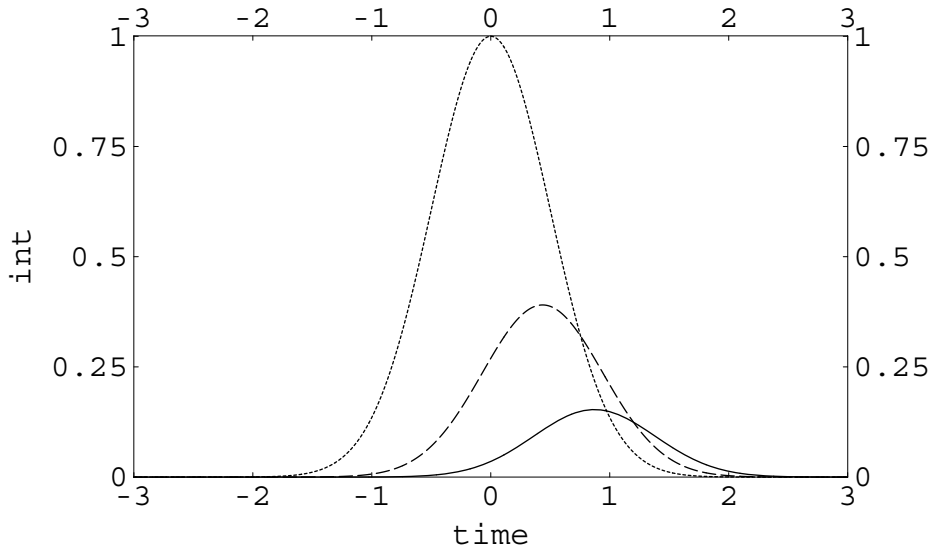

Figure 3.24: Probe is distorted when $\alpha_0 L\Gamma_{zg} \ll 2\Omega_c^2/\Gamma_d$ is not respected. Probe is a Gaussian given by $\Omega_p = \Omega_{\sigma 0} e^{-(t/\tau_p)^2}$ with $\Omega_{\sigma 0} = 0.001\Gamma$, and $\tau_p = 2500\Gamma^{-1}$. Dotted curve shows initial pulse intensity. Dashed and solid curves show intensity profile for propagation for $\alpha_0 L = 50$ and $\alpha_0 L = 100$ respectively. Other parameters are $10\Omega_c = 2\Gamma_d = \Gamma_{ze} = \Gamma$, and $\Delta = \Delta_c = \Gamma_{zg} = 0$.

For realizing slow light in the presence of ground Zeeman decoherence, the propagation effects have to be taken into account. Although $\Gamma_{zg} \ll 2\Omega_c^2/\Gamma_d$ ensures the transparency at the entrance of the medium, it is no longer true during propagation in a thick optical medium. The decoherence can be neglected only if $kL\chi''_{eff} \ll 1$. This requires $\alpha_0 L\Gamma_{zg} \ll 2\Omega_c^2/\Gamma_d$. The ground-state-Zeeman-coherence relaxation rate, magnified by the optical depth, should be smaller than the width of the spectral hole created in the susceptibility profile. The distortion of the probe, if this condition is not respected, is shown in Fig. 3.24.

Non-linear effects

The results presented in Eq. (3.35) with vanishing susceptibility, is correct up to the first order with respect to the probe amplitude only. Higher order effects can modify this ideal behavior. We have said that for $|\Omega_p|/\Omega_c \ll 1$,

the truncation of the Floquet expansion in Eq. (3.19) at first order can be justified. But it might not be always the case. Secondly the probe field strengths for which the inequality $|\Omega_p| \ll \Omega_c$ can not be justified, necessitates the inclusion of higher order terms in the Floquet expansion. The analytical solution for the susceptibility in this case can not be worked out; however, an expression for the minimum of the transparency width is possible. The equation set (3.18) can be solved exactly for the stationary state solution for $\Delta = 0$. In this case $\Phi(\vec{r}, t)$ reduces to $\Phi(\vec{r})$ and ρ_p in stationary state is given by

$$\rho_p = \frac{\bar{\Delta}_c \left(\Omega_c^2 + \Omega_p^2 e^{-2i\Phi(\vec{r})} \Omega_p^* e^{i\Phi(\vec{r})}\right)}{4\Gamma_d \Gamma^{-1} |\Omega_c^2 + \Omega_p^2 e^{-2i\Phi(\vec{r})}|^2 + |\bar{\Delta}_c|^2 \left(|\Omega_c|^2 + |\Omega_p|^2\right)} \tag{3.46}$$

The coherence that radiates in the direction of the probe, $\rho_p^{(-)}$, can be worked out using the Fourier transform given in the Eq. (3.20b). At the first non vanishing order, it is given by

$$\rho_p^{(-)} \approx \frac{\left(\Omega_p/\Omega_c\right)^2}{\bar{\Delta}_c^* \left(1 + 4\Gamma_d \Gamma^{-1} |\bar{\Delta}_c|^{-2} \Omega_c^2\right)} \tag{3.47}$$

It can be seen that the effects associated with this higher order contribution are small as long as $\Omega_p << \Omega_c$. However, the condition $\Omega_p \ll \Omega_c$ alone does not ensure distortion-less slow light propagation in an optically thick medium. The propagation effects magnify any small absorption and we need to have $\alpha_0 L |\Omega_p/\Omega_c|^2 \ll 1$. This poses another limitation on the slow light process using CZO. The distortion of the probe due to the higher order effects is shown in Fig. 3.25.

3.4.9 Comparison with EIT

CZO technique of producing transparency in the system and inducing slow light presents some features that are similar to the traditional EIT method in a Λ system. These include (for CZO with $\alpha_0 L |\Omega_p/\Omega_c|^2 \ll 1$) perfect transparency at $\Delta = 0$, control-field-intensity dependent transparency-width, and thus, the possibility to reduce the transparency window arbitrarily. Both CZO and EIT are affected by the decoherence of the ground states, with perfect transparency ensured only when the Raman coherence between the ground states do not relax [Milonni05, Marangos98, Fleischhauer05]. EIT is robust against the Doppler broadening in a collinear geometry whereas CZO is very sensitive.

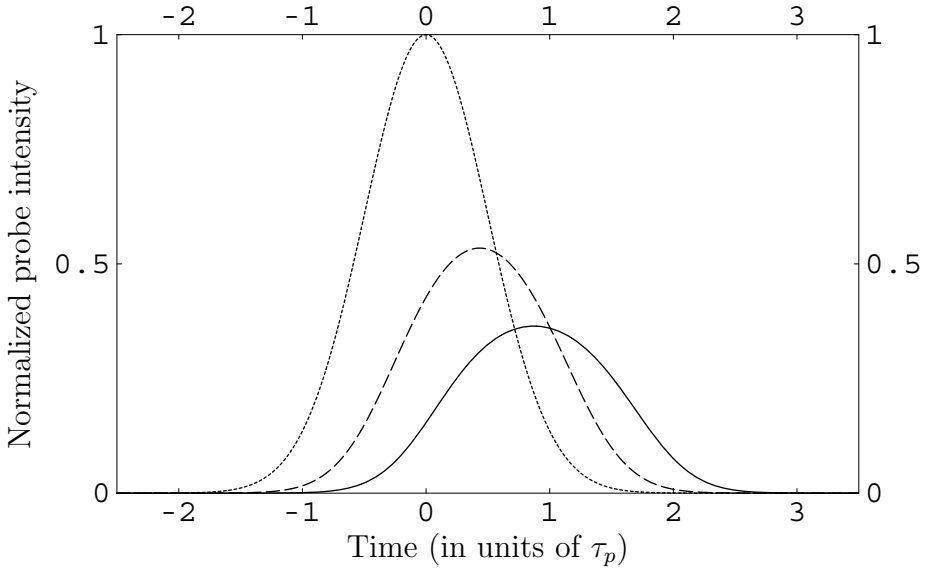

Figure 3.25: Distortion due to non-linear effects. Probe is distorted when $\alpha_0 L|\Omega_p|/\Omega_c \ll 1$ is not respected. Probe is a Gaussian given by $\Omega_p = \Omega_{\sigma 0} e^{-(t/\tau_p)^2}$ with $\Omega_{\sigma 0} = 0.01\Gamma$, and $\tau_p = 2500\Gamma^{-1}$. Dotted curve shows initial pulse intensity. Dashed and solid curves show intensity profile for propagation for $\alpha_0 L = 50$ and $\alpha_0 L = 100$ respectively. Other parameters are $10\Omega_c = 2\Gamma_d = \Gamma_{ze} = \Gamma$, and $\Delta = \Delta_c = \Gamma_{zg} = 0$.

However, an important difference between CZO and EIT is the absence of any dark state in the former. In EIT, a dark state is realized that ensures the transparency for all probe strengths [Krmpot05], and for the control as well. In CZO on the other hand, there is no dark state. The transparency in CZO is achieved only for the probe, and that also only at the *first order* with respect to probe amplitude. The absorption of the control is thus a limitation in CZO.

As it was discussed, large optical thickness, $\alpha_0 L \gg 1$, is important for obtaining good fractional delays. In EIT the optical depth can be made as large as required thanks to the transparency for both fields, whereas in CZO, it is not possible.

Finally, the behavior of the transparency window in CZO and in EIT is different. In EIT, strong fields introduce light shifts and move the two absorption peaks apart, with no new structure in between. On the other hand, in CZO, the strong control field saturates the absorption, and the region of gain appears close to $\Delta = 0$ with the possibility of fast light. Fast light is not possible with EIT.

3.4.10 Comparison with CPO

In a qualitative manner CZO is more like a CPO phenomena. The absorption of the probe is being compensated by the diffraction of the control off some grating. However, in contrast to CPO where the grating is formed by the oscillating populations, in CZO, it is the Zeeman coherence that is oscillating.

CPO does not offer much control on the width of the transparency window whereas in CZO, the width can be reduced arbitrarily due to its control-field-intensity dependence. The minimum of the width in CPO is not *zero* whereas in CZO perfect transparency for the probe is achieved at $\Delta = 0$.

A small angle between the exciting fields is required in both the CZO and CPO to separate the radiated field with $2\omega_c - \omega_p$ frequency (for $\omega_p \simeq \omega_c$). Distributed configuration is required in both CZO and CPO to overcome the absorption of the control. In gas phase, this distributed configuration washes out transparency in the Doppler broadened media for both CPO and CZO. In CPO the Doppler broadening can be overcome by using counter propagating fields [Agarwal03].

3.5 Stored light with CZO

An important application of the slow light is the possibility to store the light by switching off the control field and making the group velocity of

the probe go to *zero* [Fleischhauer02, Liu01, Phillips01]. In this process the probe is coherently absorbed and its properties are transferred to the atomic coherences. The stored light survives as long as the decoherence can be neglected. By switching the control field again, before the decoherence, the coherence properties can again be transferred to the light, and the probe pulse is re-generated in the medium. This storage and retrieval of the light is possible with the CZO scheme.

The stored light using CZO is shown in the Fig. 3.26. For the ideal conditions for the slow light with no ground Zeeman decoherence $\Gamma_{zg} = 0$, no non-linear effects $\alpha_0 L|\Omega_p/\Omega_c| \ll 1$, and for the entire probe spectrum contained inside the transparency window $\tau_p \gg \sqrt{\alpha_0 L}/\left(4|\Omega_c|^2\right)$, the slow light is realized in the medium. For $|\Omega_c| \ll \Gamma_d$, the group velocity is given by $v_g = 2|\Omega_c|^2/\left(\alpha_0 \Gamma_d\right)$, and the spatial extent of the probe is $v_g \tau_p$. The propagation has to continue until $v_g \tau_p \ll L$, to ensure that the entire probe field is contained inside the medium. At this point the control field can be adiabatically switched off, and a transfer of energy from the probe to the ground Zeeman coherence takes place as can be seen in the steady state solution $\rho_{zg}^{(-)} \simeq -\Omega_p/\Omega_c$ Eq. (3.28d). The probe is absorbed and the information is written on the oscillating ground Zeeman coherence. After some delay, when the control field is turned on, a reverse process takes place and the probe field is rebuilt from the information stored on the coherence.

This is shown in Fig. 3.26. The probe is a Gaussian given by $\Omega_p\left(t,0\right) = \Omega_{p0} e^{-(t/\tau_p)^2}$ with $\Omega_{p0} = 0.0001\Gamma$, and the probe pulse duration $\tau_p = 22500\Gamma^{-1}$. The control is a hyper Gaussian given by $\Omega_c\left(t\right) = \Omega_{c0}\left[1 - e^{-\left(\frac{t-10^5\Gamma^{-1}}{4\times10^4\Gamma^{-1}}\right)^4}\right]$ with $\Omega_{c0} = 0.1\Gamma$. The other parameters are $\Delta_c = 0\Gamma_{zg} = 0$, $\Gamma_{ze} = 2\Gamma_d = \Gamma$. The Figure shows that the probe field is stored in the medium by switching off of the control field and retrieved at a latter time by turning on the control field.

3.6 Summary

I have presented a new method to slow light that introduces transparency in the system without invoking dark states. This can be realized in a double two-level-system interacting with a strong control and a weak probe field. The two fields propagate with a small angle between the two, and have mutually orthogonal and linear polarizations. The transparency is achieved only for the probe pulse and is limited by numerous factors that include Doppler broadening, ground-Zeeman-coherence relaxation, and higher order effects. The technique presents features that are intermediate between the

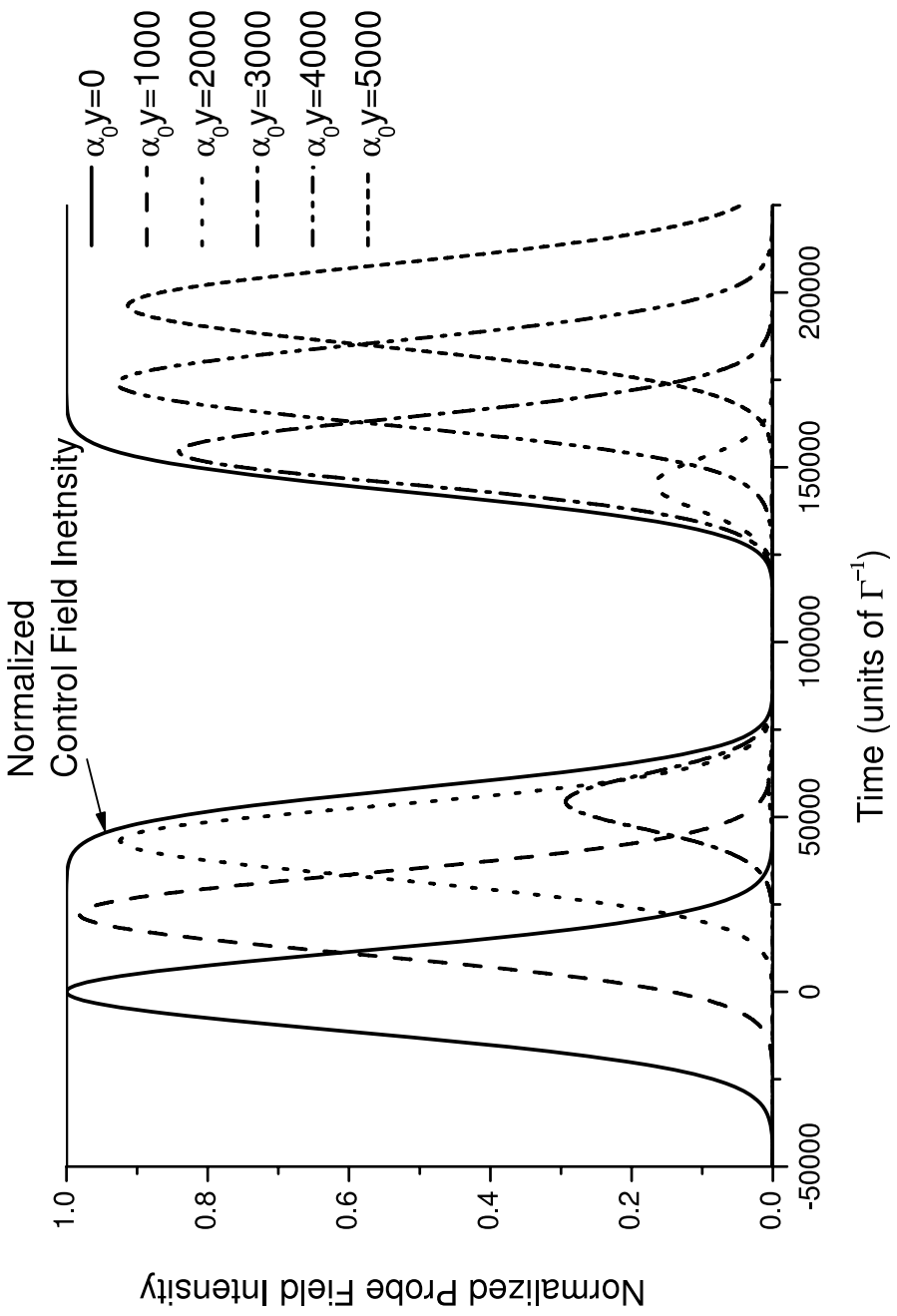

Figure 3.26: Storing light with CZO. The parameters are given in the text.

already existing techniques CPO and EIT, and can be thought of as a hybrid between the two. This also suggests that all three techniques: EIT (in a degenerate case), CPO, and CZO are different manifestations of the same underlying phenomena, and can be discussed using the same formalism. All of the three can be seen as the compensation of the absorption of the probe by the diffraction of the control off some grating. The presence of the dark state, however, remains a peculiarity of EIT.

Chapter 4

Coherent Control of the Optical Response

In this Chapter we consider again the duplicated two-level system discussed in the previous Chapter in Section. 3.4. In the previous Chapter it was shown that the linear response to a weak, σ polarized field can be canceled by applying a strong, π polarized field to the system. This canceled absorption is accompanied by the emergence of phase-conjugate, non-linear response for the probe which I present in the present Chapter.

I will discuss the behavior of the system both in ultrashort and long pulse regimes. In the ultrashort regime, phase control of the gain for the resonant weak pulse has already been reported [Delagnes07b]. Here, I show that such a control can be achieved for non-resonant excitations as well. In the long pulse regime the system offers some very exotic phenomena depending upon the relative phase shift ϕ between the weak probe

Dans ce chapitre nous considérons à nouveau le système à deux niveaux dupliqué discuté précédemment en section. 3.4. Dans le chapitre précédent, on a montré que la réponse linéaire à un champ faible de polarisation σ peut être annulée en appliquant au système un champ fort de polarisation π. Cette annulation de l'absorption est accompagnée par l'émergence d'une réponse linéaire conjuguée en phase pour le champ sonde, ce qui sera détaillé dans ce chapitre.

Je discuterai du comportement du système dans les deux régimes ultracourt et long. En régime ultracourt, le contrôle par la phase du gain du milieu pour une impulsion résonante faible a été déjà rapporté [Delagnes07b]. Ici, je montrerai comment un tel contrôle peut être réalisé pour des excitations non résonantes aussi. En régime d'impulsions longues, des phénomènes originaux se produisent dans le système

and the strong control field. For low optical thickness the system behaves as a tunable medium whose absorptive and dispersive response to the probe can be coherently controlled with the relative phase ϕ. Moreover, for sufficiently weak control field, the response can be made independent of the control field characteristics. In this case the effective susceptibility for the probe behaves as $\chi_{lin}e^{2i\phi}$ where χ_{lin} is the linear susceptibility. For higher optical depths, phase saturation takes place, and the susceptibility for the probe behaves as χ^*_{lin}. The absorptive properties are dramatically changed without effecting the dispersive response. For still higher optical depths a dark state is realized after certain propagation into the system and electromagnetic induced transparency makes the system transparent to both the control and the probe.

selon la valeur de la phase relative ϕ entre la sonde faible et le champ contrôle intense. Pour des épaisseurs optiques faibles, le système se comporte comme un milieu accordable dont la réponse vis-à-vis de l'absorption et de la dispersion de la sonde peut être contrôlée de manière cohérente par la phase relative ϕ. De plus, pour des champs contrôles suffisamment faibles, la réponse peut être indépendante des caractéristiques du champ contrôle. Dans ce cas, la susceptibilité effective pour la sonde s'écrit comme $\chi_{lin}e^{2i\phi}$ où χ_{lin} est la susceptibilité linéaire. Pour des densités plus élevés, la saturation de la phase se produit et la susceptibilité du système s'écrit comme χ^*_{lin}. Les propriétés d'absorption changent de manière spectaculaire sans affecter la réponse dispersive. En augmentant encore plus la densité optique, un état noir est dans le milieu après une certaine distance de propagation. Le phénomène de transparence électromagnétique induite rend alors le système transparent aux champs contrôle et sonde.

In the following, I will first present the system and then discuss the coherent control in ultrashort and long pulse regimes separately.

Dans ce qui suit, je présenterai en premier le système et discuterai alors le contrôle cohérent en régimes d'impulsions ultracourtes et longues.

4.1 The double two-level system II

Consider a duplicated two-level system consisting of states $\{|a\rangle, |b\rangle, |c\rangle, |d\rangle\}$ as shown in Fig. 4.1. The strong, π polarized control field connects the level $|a\rangle$ with $|c\rangle$, and the level $|b\rangle$ with $|d\rangle$; and the weak, σ polarized probe connects crossed transitions. The expressions for the fields are $\vec{e}_z A_c e^{-i(\omega_c t - k_c y)} + cc$ and $\vec{e}_x A_p e^{-i(\omega_c t - k_c y + \phi)} + cc$. It is important to note that the two fields

have the same frequency and are propagating co-linearly. There is no spatio-temporal dephasing between the fields, as was the case in the previous Chapter, and the only dephasing between the two is the relative phase shift ϕ. The two fields have linear polarizations, and the polarizations of the two are orthogonal to each other. The polarization axis are chosen such that $\vec{e}_z = \vec{e}_\pi$ and $\vec{e}_x = \vec{e}_\sigma$, and the two fields propagate along y axis. Experimentally this configuration can be realized by splitting a single laser beam into two, and by rotating the polarization of one component by $\pi/2$. The phase difference is then related to the delay τ between the two components by $\phi = \omega_c \tau$.

The Rabi frequencies associated with the two fields are $\Omega_c = DA_c/\hbar$ and $\Omega_p = DA_p/\hbar$. The detuning from the resonance is given by $\Delta_c = \omega_0 - \omega_c$, and the effective Hamiltonian of the system (after carrying out RWA) can be written in $\{|a\rangle, |b\rangle, |c\rangle, |d\rangle\}$ states as

$$H = \hbar \begin{pmatrix} 0 & 0 & -\Omega_c^* & -\Omega_p^* e^{i\phi} \\ 0 & 0 & -\Omega_p^* e^{i\phi} & \Omega_c^* \\ -\Omega_c & -\Omega_p e^{-i\phi} & \Delta_c & 0 \\ -\Omega_p e^{-i\phi} & \Omega_c & 0 & \Delta_c \end{pmatrix}. \tag{4.1}$$

The time evolution of the system is given by [from Eqs. (3.18)]:

$$i\partial_t n_g = \left(\Omega_c \rho_c^* + \Omega_p e^{-i\phi} \rho_p^* - cc\right) + i\Gamma\left(1 - n_g\right), \tag{4.2a}$$

$$i\partial_t \rho_c = \Omega_c \left(n_e - n_g\right) + \Omega_p e^{-i\phi} \left(\rho_{zg} + \rho_{ze}\right) + \bar{\Delta}_c^* \rho_c, \tag{4.2b}$$

$$i\partial_t \rho_p = -\Omega_c \left(\rho_{zg} + \rho_{ze}\right) + \Omega_p e^{-i\phi} \left(n_e - n_g\right) + \bar{\Delta}_c^* \rho_p, \tag{4.2c}$$

$$i\partial_t \rho_{zg} = \left(-\Omega_c \rho_p^* + \Omega_p e^{-i\phi} \rho_c^* + cc\right) - i\Gamma_{zg} \rho_{zg}, \tag{4.2d}$$

$$i\partial_t \rho_{ze} = \left(-\Omega_c \rho_p^* + \Omega_p e^{-i\phi} \rho_c^* + cc\right) - i\Gamma_{ze} \rho_{ze}. \tag{4.2e}$$

Here $\bar{\Delta}_c = \Delta_c + i\Gamma_d$; $n_g = \rho_{aa} + \rho_{bb}$ and $n_e = \rho_{cc} + \rho_{dd}$ are respectively the ground and the excited state populations; $\rho_c = \rho_{ca} - \rho_{db}$ and $\rho_p = \rho_{cb} + \rho_{da}$ are the coherences responsible for π and σ polarized radiated fields; and $\rho_{zg} = \rho_{ab} - \rho_{ba}$ and $\rho_{ze} = \rho_{cd} - \rho_{dc}$ are the imaginary parts of ground and excited state Zeeman coherences. Only imaginary parts of the Zeeman coherences are relevant to the dynamics due to the symmetry of the system as already discussed in Section. 3.4.3. The propagation equations for the two fields are given as

$$\partial_y \Omega_p e^{-i\phi} = i\alpha_0 \Gamma_d \rho_p, \tag{4.3a}$$

$$\partial_y \Omega_c = i\alpha_0 \Gamma_d \rho_c. \tag{4.3b}$$

$\alpha_0 = ND^2\omega_0/(2c\hbar\epsilon_0)\Gamma_d$ is the field absorption coefficient at resonance, and $\alpha_0 L$—for a medium of length L—is thus the optical thickness.

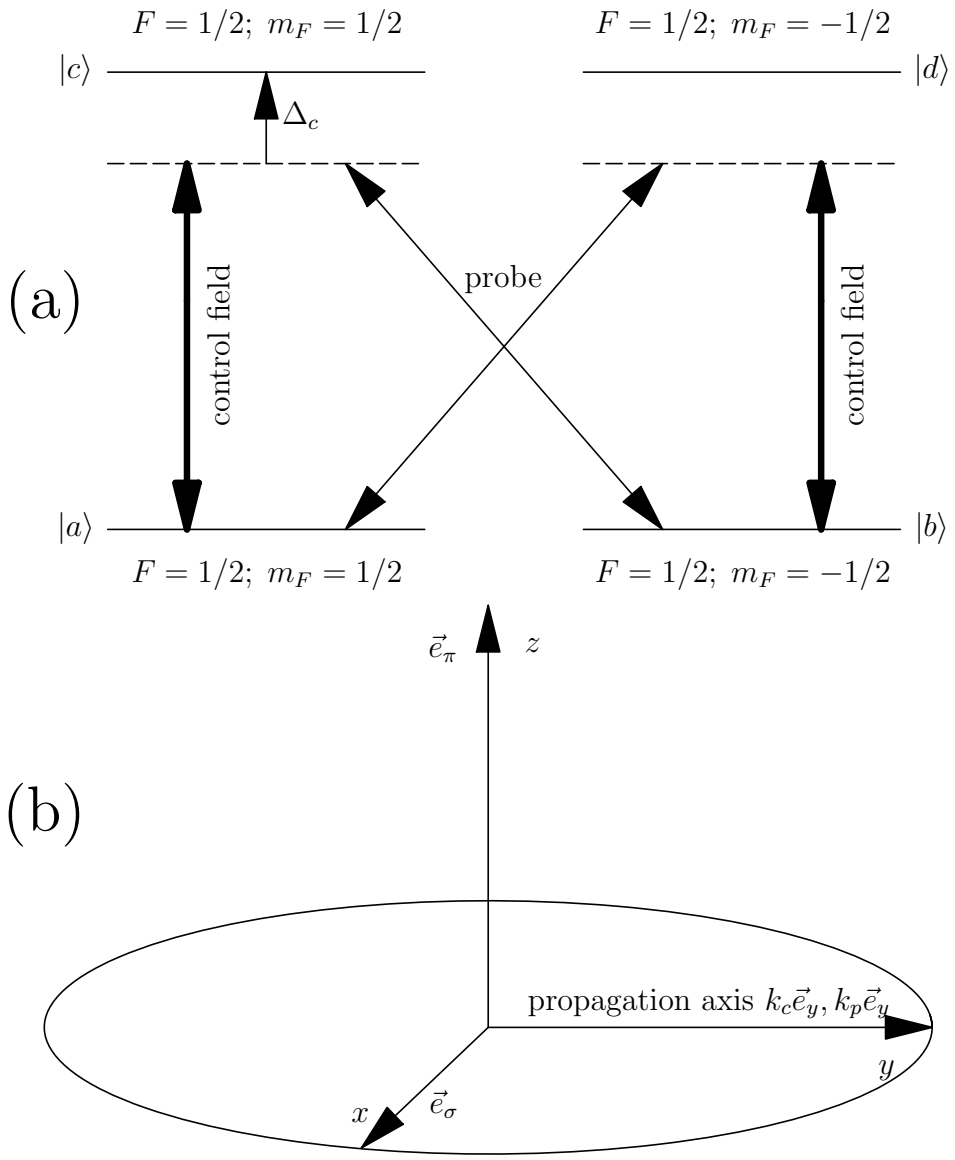

Figure 4.1: (a) A Double two-level system for the control of optical response of the medium. The π polarized control field drives each single two-level system, and the σ polarized probe connects crossed transitions. (b) Propagation and polarization axis.

4.2 Control in the ultrashort pulse regime

The control in the ultrashort pulse regime comes from the action of the probe with light shifted energy levels. Light shifts induced by the strong control field play a very important role in a lot of physical processes. The control of the action of light shifts is however limited to the one provided by modifying the control field intensity and the detuning [Niikura03]. In a duplicated two-level system the control of the action of light shifts on the probe has been demonstrated experimentally in the ultrashort pulse regime [Delagnes07b]. The system changes from being transparent to an amplifier for the probe, as the relative phase shift between the the probe and the control is modified (Fig. 4.3). The control comes from the interference between different quantum paths accessible to the probe in light shifted system, and can be better understood in adiabatic basis.

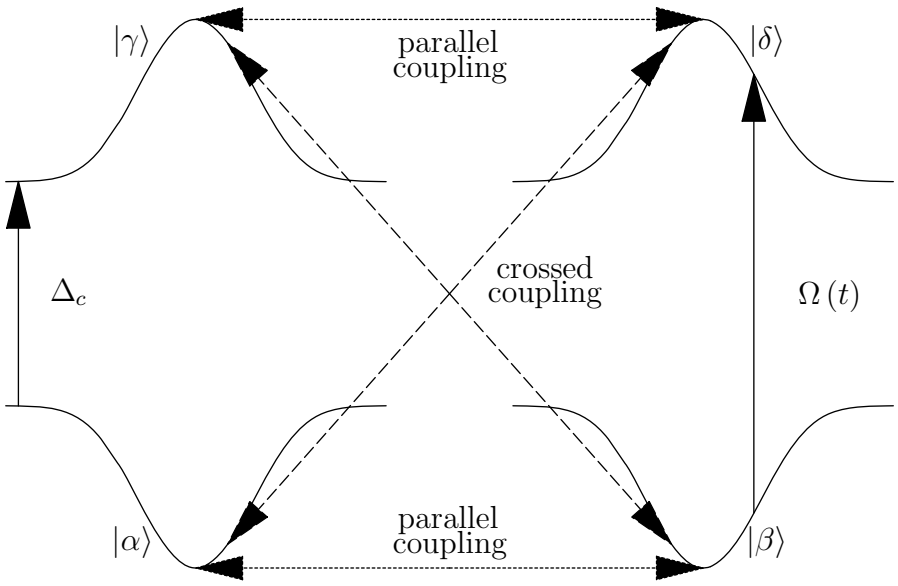

Figure 4.2: Double two-level system in adiabatic basis. Light shifted adiabatic energy levels (solid), parallel coupling (dotted), and crossed coupling (dashed) of the probe.

Adiabatic basis

We define the rotation matrix for the effective Hamiltonian in (4.1) as

$$R = \begin{pmatrix} \cos\theta & 0 & \sin\theta & 0 \\ 0 & \cos\theta & 0 & -\sin\theta \\ -\sin\theta & 0 & \cos\theta & 0 \\ 0 & \sin\theta & 0 & \cos\theta \end{pmatrix}, \tag{4.4}$$

with $\tan 2\theta = 2\Omega_c/\Delta_c$. The adiabatic states are defined by

$$\begin{pmatrix} \langle\alpha| & \langle\beta| & \langle\gamma| & \langle\delta| \end{pmatrix}^\dagger = R \begin{pmatrix} \langle a| & \langle b| & \langle c| & \langle d| \end{pmatrix}^\dagger, \tag{4.5}$$

and the adiabatic Hamiltonian is given as

$$H_d = RHR^\dagger = A + V, \tag{4.6}$$

where

$$A = \frac{\hbar}{2} \begin{pmatrix} \Delta_c - \Omega & 0 & 0 & 0 \\ 0 & \Delta_c - \Omega & 0 & 0 \\ 0 & 0 & \Delta_c + \Omega & 0 \\ 0 & 0 & 0 & \Delta_c + \Omega \end{pmatrix}, \tag{4.7}$$

with $\Omega = \sqrt{4\Omega_c^2 + \Delta_c^2}$ are the light shifted energy levels. The two ground states are shifted downward in energy and the excited states are shifted upward by the action of the control field. The perturbation due to the weak probe is given by

$$V = \hbar\Omega_p \times \begin{pmatrix} 0 & i\frac{2\Omega_c}{\Omega}\sin\phi & 0 & -\cos\phi - i\frac{\Delta_c}{\Omega}\sin\phi \\ -i\frac{2\Omega_c}{\Omega}\sin\phi & 0 & -\cos\phi - i\frac{\Delta_c}{\Omega}\sin\phi & 0 \\ 0 & -\cos\phi + i\frac{\Delta_c}{\Omega}\sin\phi & 0 & i\frac{2\Omega_c}{\Omega}\sin\phi \\ -\cos\phi + i\frac{\Delta_c}{\Omega}\sin\phi & 0 & -i\frac{2\Omega_c}{\Omega}\sin\phi & 0 \end{pmatrix}. \tag{4.8}$$

Control of the interaction

In the adiabatic picture the probe field introduces two types of couplings as given in the matrix V, and shown in Fig. 4.2. The two ground (and the excited) levels are coupled through the *parallel* coupling which is proportional to $\sin\phi$. This coupling is always resonant but vanishes for $\phi = n\pi$; n is an integer. The other coupling is between the levels that are stretched in the

opposite sense. Between the ground level of one m_F state and the excited level of different m_F state. This is *crossed* coupling and it can be made non-resonant by introducing strong light shifts. Thus, important light shifts with $\sin\phi = 0$ make the system transparent to the probe whereas the probe interacts resonantly with the system for $\cos\phi = 0$, no matter how important the light shifts are. This renders coherent phase control of the interaction of the probe with the system.

The control can be seen in Fig. 4.3 taken from [Delagnes07b]. Two ultrashort resonant pulses— a weak probe and a strong control, having linear and mutually orthogonal polarizations excite $S_{1/2} \rightarrow P_{1/2}$ transition of rubidium atoms resonantly at 794.76 nm. The transmitted intensity of the probe as a function of delay ($\tau = \phi/\omega_c$) between the control and the probe is shown. The intensity profile exhibits oscillations corresponding to alternate regions of medium being transparent at $\phi = n\pi$, and being an amplifier at $\phi = (2n+1)\,\pi/2$.

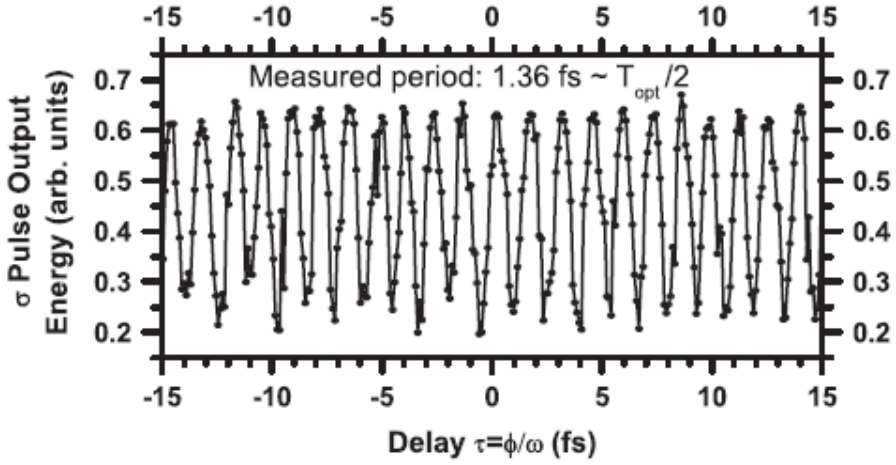

Figure 4.3: Coherent control of the interaction in the ultrashort regime— taken from [Delagnes07b]. The output probe intensity oscillates as the function of delay (and thus the relative phase) with the control. The parameters are $\Delta_c = 0$, $\Omega_c \simeq 1.1\pi\tau_c^{-1}$, and $\Omega_p \simeq 0.2\pi\tau_c^{-1}$ with $\tau_c = 90\ fs$.

4.3 Control in the long pulse regime

In the long pulse regime, the relaxation processes come into action and introduce new channels through which adiabatic levels can exchange populations,

and the interaction can proceed. The phase control of the interaction presented in the previous Section thus no longer remains valid. However, the control of the optical response of the medium is still possible as we discuss below.

4.3.1 Stationary state solution

We first work out the stationary state solution of Eqs. (4.2) for long pulse regime. It can be made easy by first simplifying the relations between various density matrix elements in the stationary regime. We note from (4.2d) and (4.2e) that in the stationary regime

$$\Gamma_{ze}\rho_{ze} = \Gamma_{zg}\rho_{zg}. \tag{4.9}$$

The two Zeeman coherences are created by the combined action of the control and the probe through identical processes and only relax differently. This leads to the above relation between the two, and for long lived ground Zeeman coherence , the excited Zeeman coherence vanishes. We now eliminate first $\rho_{zg} + \rho_{ze}$ and then $n_e - n_g$ from (4.2b) and the complex conjugate of (4.2c) to get:

$$\left(|\Omega_c|^2 - |\Omega_p|^2\right)(n_e - n_g) = -\Omega_c^*\bar{\Delta}_c^*\rho_c + \Omega_p e^{-i\phi}\bar{\Delta}_c\rho_p^*, \tag{4.10a}$$

$$\left(|\Omega_c|^2 - |\Omega_p|^2\right)(\rho_{zg} + \rho_{ze}) = -\Omega_c\bar{\Delta}_c\rho_p^* + \Omega_p^* e^{i\phi}\bar{\Delta}_c^*\rho_c. \tag{4.10b}$$

The left hand sides of the two equations are either purely real or purely imaginary. Comparing the two with their complex conjugates and using (4.2a) in (4.10a), and (4.2d) in (4.10b), we get :

$$\Omega_c^*\rho_c + \Omega_p^* e^{i\phi}\rho_p = \frac{\Gamma\bar{\Delta}_c}{2\Gamma_d}n_e, \tag{4.11a}$$

$$\Omega_c^*\rho_p - \Omega_p^* e^{i\phi}\rho_c = -\frac{\Gamma_{zg}\bar{\Delta}_c}{2\Gamma_d}\rho_{zg}. \tag{4.11b}$$

Finally, from (4.2b) and (4.2c), we have:

$$\rho_c = -\frac{1}{\bar{\Delta}_c^*}\left[\Omega_c\left(2n_e - 1\right) + \Omega_p e^{-i\phi}\frac{\Gamma_{zg} + \Gamma_{ze}}{\Gamma_{ze}}\rho_{zg}\right], \tag{4.12a}$$

$$\rho_p = -\frac{1}{\bar{\Delta}_c^*}\left[\Omega_p e^{-i\phi}\left(2n_e - 1\right) - \Omega_c\frac{\Gamma_{zg} + \Gamma_{ze}}{\Gamma_{ze}}\rho_{zg}\right]. \tag{4.12b}$$

Relations (4.11) and (4.12) can be used to work out the stationary state solution for this general configuration. We place ourselves in the situation

where the ground Zeeman coherences do not relax. In this case $\Gamma_{zg} = 0$, and the stationary state solution of the system is given by

$$n_e = 2\Gamma_d\Gamma^{-1}|\Omega_c^2 + \Omega_p^2 e^{-2i\phi}|^2/X, \tag{4.13a}$$

$$n_g = 1 - n_e, \tag{4.13b}$$

$$\rho_c = \bar{\Delta}_c \left(\Omega_c^2 + \Omega_p^2 e^{-2i\phi}\right) \Omega_c^*/X, \tag{4.13c}$$

$$\rho_p = \bar{\Delta}_c \left(\Omega_c^2 + \Omega_p^2 e^{-2i\phi}\right) \Omega_p^* e^{i\phi}/X, \tag{4.13d}$$

$$\rho_{zg} = |\bar{\Delta}_c|^2 \left(\Omega_c \Omega_p^* e^{i\phi} - \Omega_c^* \Omega_p e^{-i\phi}\right)/X, \tag{4.13e}$$

$$\rho_{ze} = 0, \tag{4.13f}$$

with the denominator given by:

$$X = 4\Gamma_d\Gamma^{-1}|\Omega_c^2 + \Omega_p^2 e^{-2i\phi}|^2 + \left(|\Omega_c|^2 + |\Omega_p|^2\right)|\bar{\Delta}_c|^2. \tag{4.13g}$$

The individual density matrix elements can also be worked out from Eq. Set (3.17) (for $\Phi\left(t, \vec{r}\right) = \phi$), and it can be shown that $\rho_{aa} = \rho_{bb}$, $\rho_{cc} = \rho_{dd}$, $\rho_{ca} = -\rho_{db}$, $\rho_{cb} = \rho_{da}$, $\rho_{cd} = 0$, and ρ_{ab} is purely imaginary in the stationary regime.

4.3.2 Phase control in low optical thickness

For long lived ground Zeeman coherence with $\Gamma_{zg} = 0$, and for a weak probe with $|\Omega_p| \ll |\Omega_c|$, the stationary state solution of ρ_p simplifies to [from Eq. (4.13d)]

$$\rho_p = \left(\frac{\Omega_c^2}{|\Omega_c|^2}\right)^2 \frac{\bar{\Delta}_c \Omega_p^* e^{i\phi}}{4\Gamma_d\Gamma^{-1}|\Omega_c|^2 + |\bar{\Delta}_c|^2}. \tag{4.14}$$

At *first order* ρ_p has no component $\propto e^{-i\phi}$ (which represent the linear response). This is due to the fact that the absorption of the probe at *first order* is compensated by the control field. Moreover, by introducing an angle between the control and the probe — so that the two fields have spatial dephasing— the component given in the above expression can be spatially separated, and the transparency can be induced for the probe. This is how the transparency and the slow light were achieved in this system in the previous Chapter.

The effective susceptibility for the probe is $\chi_{eff} = \left(2\alpha_0\Gamma_d/k\right)\rho_p e^{i\phi}/\Omega_p$ with $k = \omega_0/c$, and can be written as

$$\begin{aligned}\chi_{eff} &= \chi'_{eff} + i\chi''_{eff} \\ &= \frac{2\alpha_0\Gamma_d}{k}\left(\frac{\Omega_c^2}{|\Omega_c|^2}\right)^2 \left(\frac{\Omega_p^*}{\Omega_p}\right) \frac{\bar{\Delta}_c e^{2i\phi}}{4\Gamma_d\Gamma^{-1}|\Omega_c|^2 + |\bar{\Delta}_c|^2}.\end{aligned} \tag{4.15}$$

It vanishes for $|\Omega_c| \gg \sqrt{\Gamma_d \Gamma}$ because of the saturation effects. A strong control field saturates the system with equal populations in the ground and the excited state, and vanishing coherences.

For $|\Omega_c| \ll \sqrt{\Gamma_d \Gamma}$, and for small optical depths $\alpha_0 L \ll 1$, the phase accumulated by the fields during propagation can be ignored. The fields remain real and the susceptibility simplifies to

$$\chi_{eff} = \chi_{lin} e^{2i\phi}, \tag{4.16}$$

where $\chi_{lin} = 2\alpha_0 \Gamma_d / (k \bar{\Delta}_c^*)$ is the linear susceptibility. The medium turns into a linear medium with phase dependent susceptibility that is independent of the control field intensity. This phase control of the absorptive (χ''_{eff}) and dispersive properties (χ'_{eff}) of the medium is shown in Fig. 4.4 at the entrance of the medium, and in Fig. 4.5 for an optical thickness $\alpha_0 L = 0.2$. The medium turns from an absorber at $\phi = 0$ to an amplifier at $\phi = \pi/2$ with the change in the dispersion profile accordingly. Moreover, For $\phi = \pi/4$ and $\phi = 3\pi/4$, the absorption becomes "dispersion like ", and the dispersion takes the form of a gain dip or an absorption peak.

In dense atomic media the propagation leads to the accumulation of the phase by the two fields and the control of the optical response is lost. This propagation effects will be discussed in the next Section and a precise condition on the optical thickness to observe the phase control will be given in [4.4.3].

Control field intensity dependence

The important condition to realize the phase control of the optical response is $|\Omega_p| \ll |\Omega_c|$ which allows the simplification from Eq. (4.13d) to Eq. (4.14) — in addition to $\Gamma_{zg} = 0$ and $\alpha_0 L \ll 1$. The condition $|\Omega_c| \ll \sqrt{\Gamma_d \Gamma}$ is required only to obtain a response independent of control field characteristics. If this latter condition is not satisfied, Eq. (4.16) is not true and the response is determined by Eq. (4.15). The control field modifies the response but the phase control of the response is still present. This control-field-intensity-dependent phase control of the optical susceptibility is shown in Fig. 4.6

Explanation in terms of quantum paths

This phase control can be understood in terms of the quantum paths that give rise to $\rho_p = \rho_{da} + \rho_{cb}$ coherence and which are shown in Fig. 4.7. We will focus only on ρ_{da}; equivalent features hold for ρ_{cb}. The concerned time

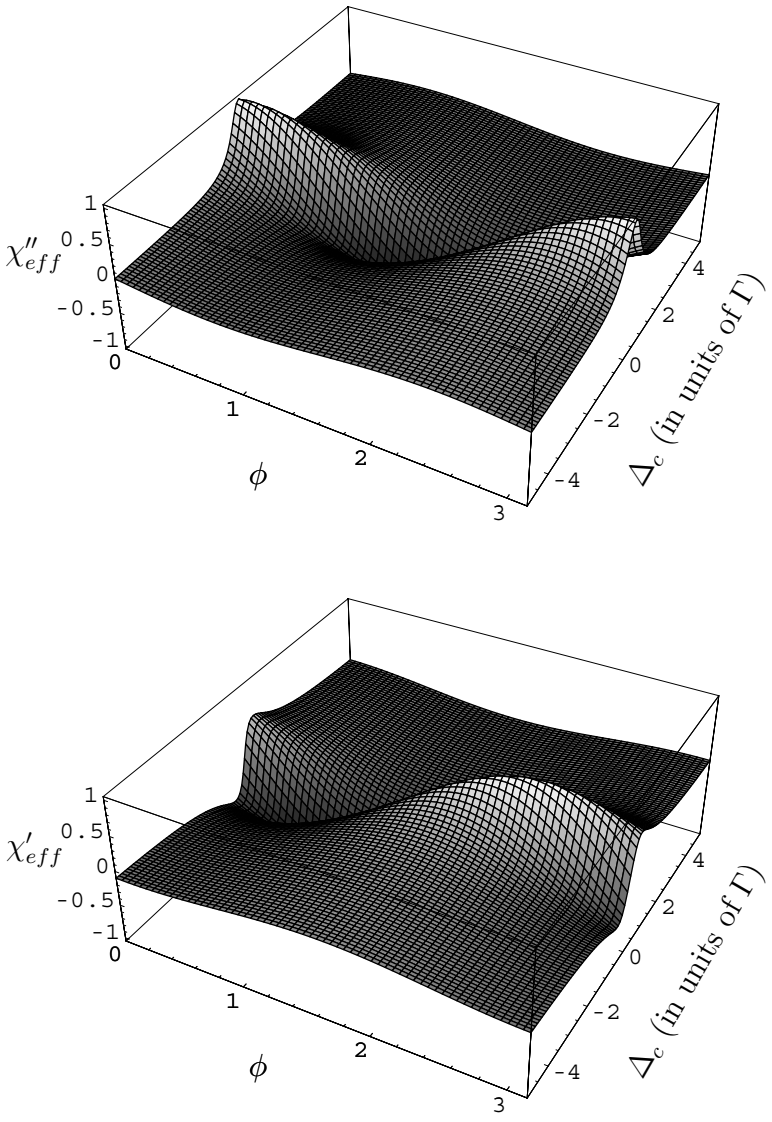

Figure 4.4: Phase control of the medium response. The absorptive (χ''_{eff}) and dispersive (χ'_{eff}) properties of the medium change dramatically with the phase. Parameters are $\Gamma_d = 0.5\Gamma$.

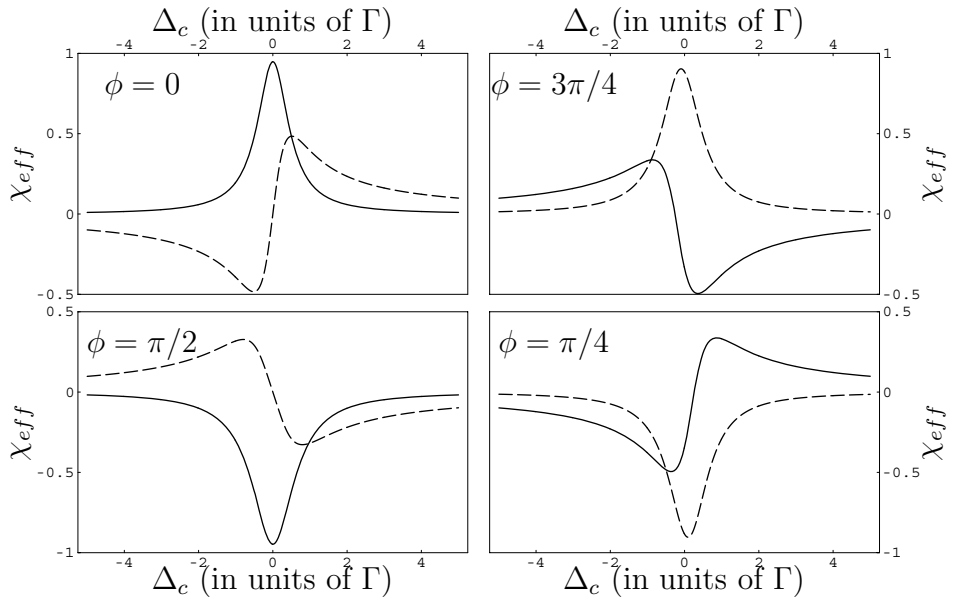

Figure 4.5: Real (dashed), and imaginary (solid) parts of the effective susceptibility (in units of $2\alpha_0/k$), showing phase control of the medium response. Parameters are $\Omega_c = 100\Omega_p = 0.1\Gamma$, $\Gamma_{ze} = 2\Gamma_d = \Gamma$, $\Gamma_{zg} = 0$, and $\alpha_0 L = 0.2$.

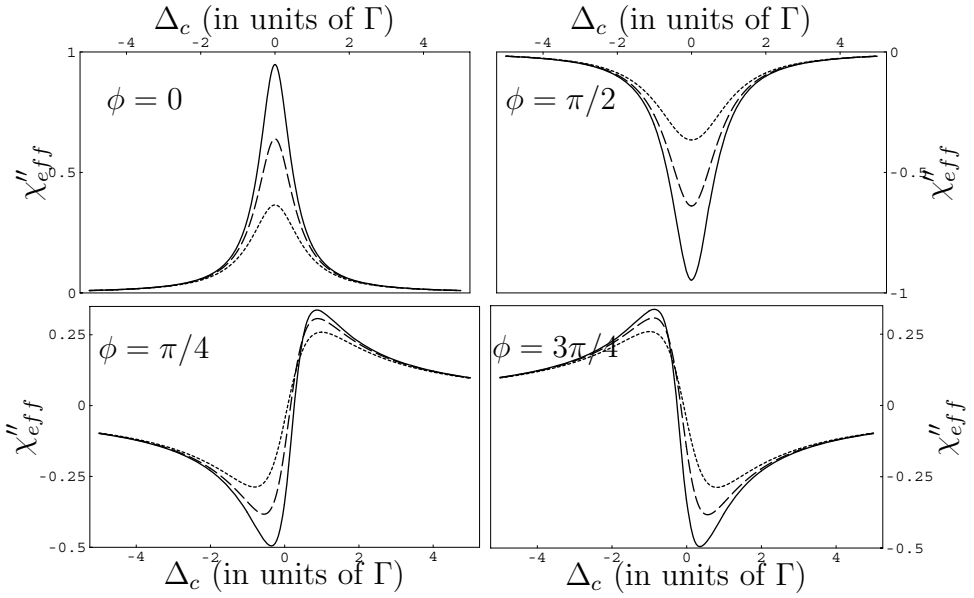

Figure 4.6: Imaginary parts of the effective susceptibility χ''_{eff} (in units of $2\alpha_0/k$) showing phase control of the medium response when $|\Omega_c| \ll \sqrt{\Gamma_d \Gamma}$ is not satisfied. Parameters are $\Omega_c = 0.1\Gamma$ (solid), 0.3Γ (dashed), and 0.5Γ (dotted). Other parameters are $\Omega_p = 0.001\Gamma$, $\Gamma_{ze} = 2\Gamma_d = \Gamma$, $\Gamma_{zg} = 0$, and $\alpha_0 L = 0.2$.

evolution equations are [From (3.17)]

$$i\partial_t\rho_{ba} = -\left(\Omega_c^*\rho_{da} + \Omega_c\rho_{bc}\right) + \left(\Omega_p^* e^{i\phi}\rho_{ca} - \Omega_p e^{-i\phi}\rho_{bd}\right) - i\Gamma_{zg}\rho_{ba}, \quad (4.17a)$$

$$i\partial_t\rho_{da} = \Omega_c\left(\rho_{ba} + \rho_{dc}\right) + \Omega_p e^{-i\phi}\left(\rho_{dd} - \rho_{aa}\right) + \left(\Delta_c - i\Gamma_d\right)\rho_{da}. \quad (4.17b)$$

At the lowest order with respect to probe amplitude, ρ_{da} results from the absorption of the probe by population difference on transition $|a\rangle \leftrightarrow |d\rangle$ Fig. 4.7(a), and the diffraction of the control from the ground Zeeman coherence (case b and c in the Figure). Note that $\rho_{cd} = 0$ in the stationary regime and does not contribute to the signal. The ground Zeeman coherence in turn involves excitation by the probe of the transition $|a\rangle \leftrightarrow |d\rangle$ with the phase $e^{-i\phi}$ (case b), and along $|b\rangle \leftrightarrow |c\rangle$ with the phase $e^{i\phi}$. The two paths resemble to "cross-Kerr" and "phase conjugate" type effects, however, the paths do not represent these effects. The Figure just represents different paths through which probe interacts with the system and the coherence ρ_p is generated; it does not corresponds to one or three photon processes. For $|\Omega_c| \gg |\Omega_p|$ and for $\Gamma_{zg} = 0$, the cross-Kerr type path completely compensates for the absorption. This is a quantum interference phenomena and can be explained in terms of the diffraction of the control off the Zeeman grating, as discussed in the previous Chapter. Thus, only the phase conjugate type path (c in the Figure) determines the response of the medium. The phase control of the effective susceptibility can thus be related to a wave mixing process where the only radiated field is the conjugate wave and that when added to the incident wave, gives rise to interference inducing a gain dispersion coupling seen in Fig. 4.5.

4.4 Phase saturation in large optical thickness

The above description is valid only in the regime of low optical thickness for $\alpha_0 L \ll 1$. For large optical depths, the phase accumulated during propagation by both the probe and the control can not be neglected. We consider next this phase evolution with the propagation of the fields in dense atomic media.

4.4.1 Evolution of the relative phase

The relative phase ϕ evolves during propagation to $\Delta\phi = \phi + \phi_p - \phi_c$. ϕ_p and ϕ_c are the phases accumulated by the two fields and are defined as

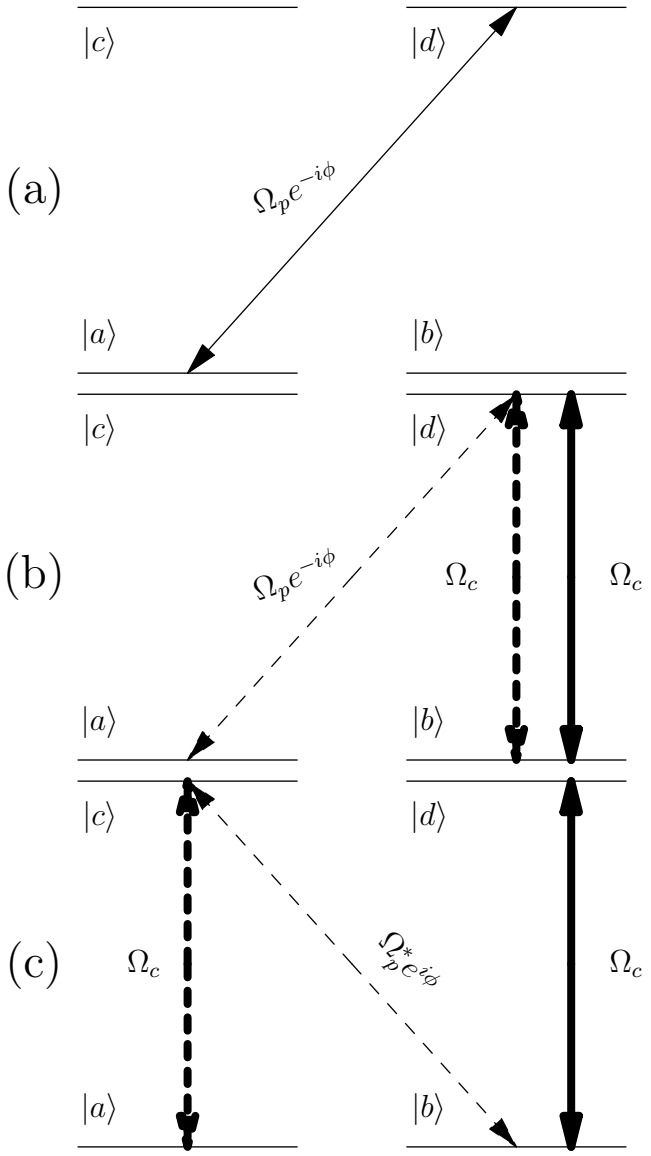

Figure 4.7: Quantum paths that give rise to ρ_{da}. (a) absorption by the population, (b) cross Kerr type path that compensates for the absorption , and (c) phase conjugate type path responsible for the phase dependence of the medium response.

$\Omega_c = |\Omega_c|e^{-i\phi_c}$ and $\Omega_p = |\Omega_p|e^{-i\phi_p}$. The propagation Eqs. (4.3) can now be written as

$$\partial_y|\Omega_p| - i|\Omega_p|\partial_y\phi_p = i\alpha_0\Gamma_d\ \rho_p e^{i(\phi+\phi_p)}, \tag{4.18a}$$

$$\partial_y|\Omega_c| - i|\Omega_c|\partial_y\phi_c = i\alpha_0\Gamma_d\ \rho_c e^{i\phi_c}. \tag{4.18b}$$

We are always in the regime where $|\Omega_p| \ll |\Omega_c|$, and $\Gamma_{zg} = 0$. For simplicity we first take the case of $|\Omega_c| \ll \sqrt{\Gamma_d\Gamma}$. In this case the response is independent of control field intensity and can be written as [From Eq. (4.15)]

$$\chi_{eff} = \chi_{lin}e^{2i\Delta\phi}. \tag{4.19}$$

Using $\chi_{eff} = (2\alpha_0\Gamma_d/k)\,\rho_p e^{i\phi}/\Omega_p$, and $\rho_p\left(\Omega_p e^{-i\phi}/\Omega_c\right)^*\rho_c$ — from[Eq. (4.13c) and Eq. (4.13d)], we can write

$$\rho_p = \frac{k}{2\alpha_0\Gamma_d}\chi_{lin}|\Omega_p|e^{2i\Delta\phi}e^{-i(\phi+\phi_p)}, \tag{4.20a}$$

$$\rho_c = \frac{k}{2\alpha_0\Gamma_d}\chi_{lin}|\Omega_c|e^{-i\phi_c}. \tag{4.20b}$$

We can use these expressions in Eqs. (4.18) to write following equations for phase evolution

$$\partial_y\phi_p = -\frac{k}{2}\left(\chi'_{lin}\cos 2\Delta\phi - \chi''_{lin}\sin 2\Delta\phi\right), \tag{4.21a}$$

$$\partial_y\phi_c = -\frac{k}{2}\chi'_{lin}. \tag{4.21b}$$

Here $\chi_{lin} = \chi'_{lin} + i\chi''_{lin}$. The phase of the control field evolves under the action of linear dispersion as the medium response to the strong control field is given by the linear susceptibility. The phase of the probe field evolves under the action of gain-dispersion coupling induced by the phase-dependent medium response. The two phases continue to grow with the propagation distance y, and the phase difference between the two evolves as

$$\partial_y\Delta\phi = k\sin\Delta\phi\left(\chi'_{lin}\sin\Delta\phi + \chi''_{lin}\cos\Delta\phi\right). \tag{4.22}$$

The analytical solution for the above equation is given by

$$\tan\Delta\phi(y) = \frac{\tan\phi_l}{\left(\frac{\tan\phi_l}{\tan\phi}+1\right)e^{-2\alpha_0 y\sin^2\phi_l} - 1}, \tag{4.23}$$

where ϕ_l is the phase of linear susceptibility defined as $\chi_{lin} = |\chi_{lin}|e^{i\phi_l}$. We next consider the solution for different cases.

4.4.2 Linear response for $\phi = 0$

For $\phi = 0$, the phase does not evolve. $\Delta\phi$ remains 0 and the susceptibility is given by $\chi_{eff} = \chi_{lin}$. Indeed the total field is linearly polarized and because both the probe and the control are weak with $|\Omega_p| \ll |\Omega_c| \ll \sqrt{\Gamma_d, \Gamma}$, the response of the medium is linear. The control field can modify the effective susceptibility for the probe only if the total field has elliptic polarization.

4.4.3 Phase control of the response

It was discussed in Section. 4.3.2 that for small optical thickness the medium behaves as a tunable medium with phase dependent optical response. A precise condition on the limit of optical thickness can be worked out from Eq. (4.23). For small optical depths such that $\alpha_0 L \sin^2 \phi_l \ll 1$ the phase behaves as $\Delta\phi = \phi$. No additional phase is introduced during propagation and the phase control discussed in the previous Section in realized.

4.4.4 Phase saturation and conjugate susceptibility

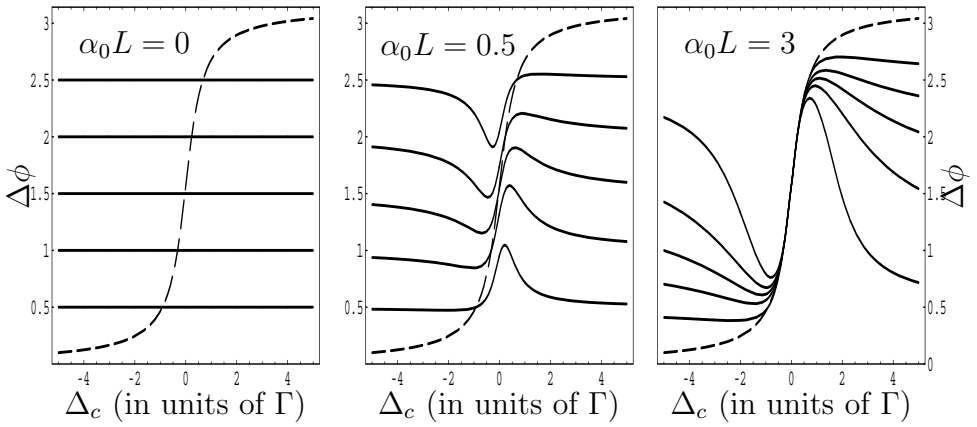

Figure 4.8: Phase saturation with propagation. Dashed curve shows the phase of χ^*_{lin}. Parameters are $\Omega_c = 10^4\Omega_p = 0.1\Gamma$ (at entrance), $\Gamma_{ze} = 2\Gamma_d = \Gamma$, and $\Gamma_{zg} = 0$.

For optical depths such as $\alpha_0 L \sin^2 \phi_l \gg 1$, the phase saturates to $\Delta\phi = -\phi_l$ and the effective susceptibility turns into

$$\chi_{eff} = \chi^*_{lin}. \tag{4.24}$$

The medium turns into an amplifier for the probe but the dispersive response of the medium is not changed. The saturation is reached after the propagation distance of the order of $y \approx 1/\left(\alpha_0 \sin^2 \phi_l\right)$. The two phases ϕ_c and ϕ_p still continue to grow according to Eqs. (4.21), but at saturation the two evolve at the same rate. Indeed at $\Delta\phi = -\phi_l$, $\chi'_{lin} \cos 2\Delta\phi - \chi''_{lin} \sin 2\Delta\phi = \chi'_{lin}$. Both phases evolve under the action of linear dispersion and the difference between the two stays at $-\phi_l$. This saturation is ensured as long as $|\Omega_p| \ll |\Omega_c|$ is true.

The phase saturation is shown in Fig. 4.8, and the resulting conjugate susceptibility in Fig. 4.9. The parameters used in the simulation are difficult to realize experimentally. Indeed the absorption of the control under the action of χ_{lin} and the amplification of the probe by χ^*_{lin} makes maintaining $|\Omega_p| \ll |\Omega_c|$ very difficult in dense optical media.

Connection with Kramers-Kronig relations

The principle of causality imposes well known Kramers-Kronig relations that relate the absorptive and dispersive response of a medium, interacting with electromagnetic fields. Eq. (4.24), where the the dispersive response of the medium is not changed and the medium is converted from an absorber to an amplifier, seems as an apparent contradiction. The contradiction is removed by noting that the effective susceptibility given by Eq. (4.24) is valid only for spectral components such that $\alpha_0 L \sin^2 \left[\phi_l \left(\Delta_c\right)\right] \gg 1$. This is a local phenomena and takes place only close to the resonance as can be seen in Fig. 4.9. The phase saturation and the relation (4.24) can not be satisfied for arbitrary large frequencies. Alternatively, the distance (and thus the time) required to establish linear response for a pulse with an arbitrary spectrum bandwidth diverges. The causality in this case no longer implies the well known Kramers-Krönig relations. This effects has already been identified in degenerate four-wave mixing [Bervas92] and resonance stimulated Raman scattering [Kircheva94].

Control field intensity dependence

The phase saturation discussed above with susceptibility changing to conjugate of linear susceptibility requires $|\Omega_p| \ll |\Omega_c|$, $\alpha_0 L \sin^2 \phi_l \gg 1$, $\Gamma_{zg} = 0$, and $|\Omega_c| \ll \sqrt{\Gamma_d \Gamma}$. The last condition is required only to have a response independent of the control field characteristics. If this last condition is not satisfied then Eq. (4.23) is not true, however, the phase saturation still occurs. The susceptibility is now given as

$$\chi_{eff} = \chi_{nlin} e^{2i\Delta\phi}, \tag{4.25}$$

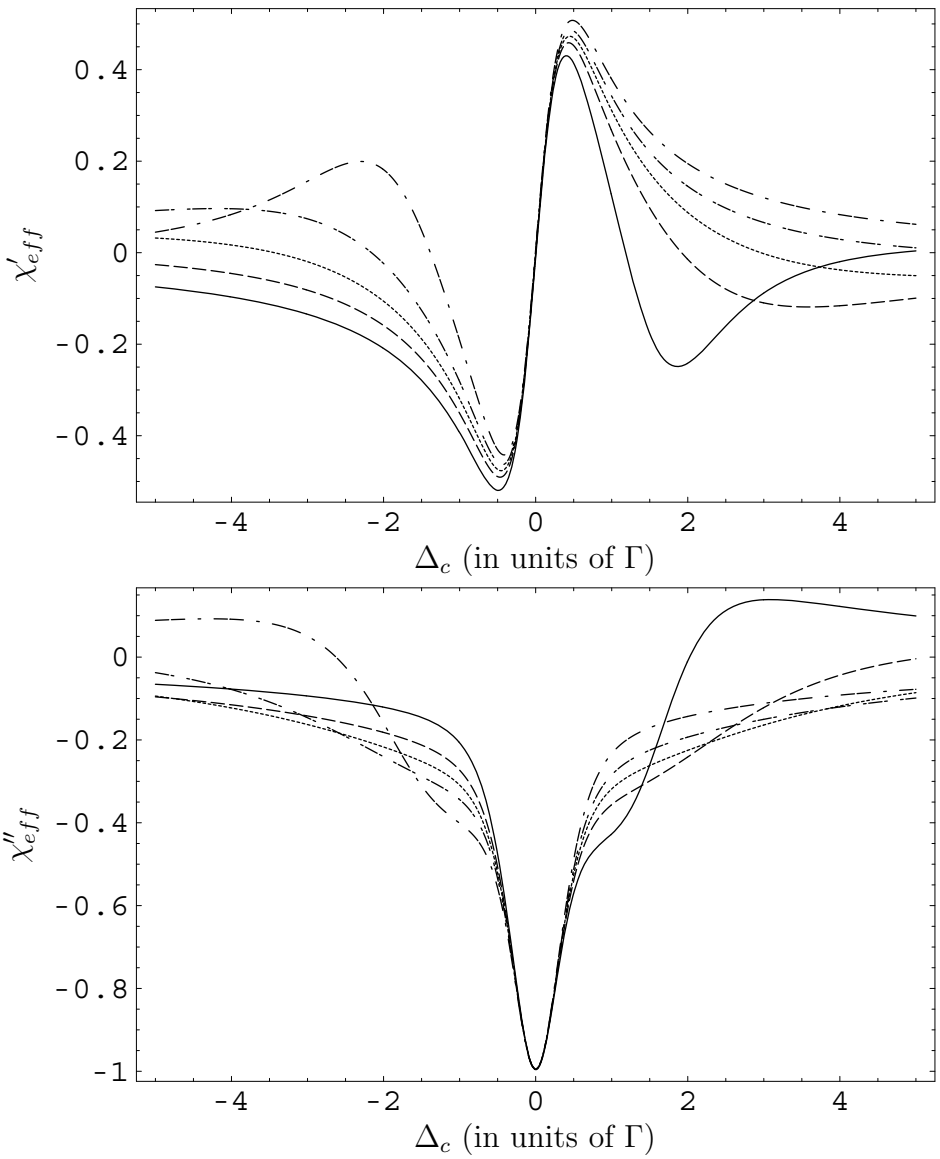

Figure 4.9: Susceptibility (in units of $2\alpha_0/k$) behaves as χ^*_{lin} close to resonance. Parameters are $\phi = 0.5$ (solid), $\phi = 1.0$ (dashed), $\phi = 1.5$ (dotted), $\phi = 2.0$ (dash dot dot), and $\phi = 2.5$ (dash dot dash). Other Parameters are $\Omega_c = 10^4\Omega_p = 0.1\Gamma$ (at entrance), $\Gamma_{ze} = 2\Gamma_d = \Gamma$, and $\Gamma_{zg} = 0$.

where

$$\begin{aligned}\chi_{nlin} &= \chi'_{nlin} + i\chi''_{nlin}, \\ &= \frac{2\alpha_0\Gamma_d}{k}\frac{\bar{\Delta}_c}{4\Gamma_d\Gamma^{-1}|\Omega_c|^2 + |\bar{\Delta}_c|^2}.\end{aligned} \tag{4.26}$$

This is the susceptibility for a saturated two-level system. The phase evolution is now given as

$$\partial_y\Delta\phi = k\sin\Delta\phi\left(\chi'_{nlin}\sin\Delta\phi + \chi''_{nlin}\cos\Delta\phi\right). \tag{4.27}$$

It can be seen that phase saturation still takes place and the phase again saturates as $\Delta\phi = -\phi_l$.However, the response of the medium is now determined by control-field-intensity-dependent χ^*_{nlin}.

4.5 Transparency for large optical thickness

We have seen that the double two-level system acts as a tunable medium for the probe with $\chi_{eff} = \chi_{lin}e^{2i\phi}$ in low optical thickness, and as an amplifier with $\chi_{eff} = \chi^*_{lin}$ in large optical depths. In this latter range, the probe is amplified under the action of χ^*_{lin} whereas the control is absorbed by the action of χ_{lin}. Eventually the two fields attain $|\Omega_c/\Omega_p| = 1$, and the phase saturation comes to an end. This behavior of field amplitudes is shown in Fig. 4.10.

When the condition $|\Omega_p| \ll |\Omega_c|$ is no longer satisfied, the relative phase $\Delta\phi$ continues to grow again. For $|\Omega_c/\Omega_p| = 1$, and for $\Delta\phi = \pm\pi/2$, the matching condition $\Omega_c^2 + \Omega_p^2 e^{-2i\Delta\phi} = 0$ is realized, and from Eq. (4.13c) and Eq. (4.13d), we see that the two coherences vanish. The system becomes transparent to both the control and the probe fields. The transparency can be seen in Fig. 4.10 where after certain propagation the two field amplitudes stop to grow or decrease any further. The behavior of the relative phase during propagation is shown in Fig. 4.11. The initial phase selected in the simulation is $\Delta\phi = \phi_l$ which becomes $-\phi_l$ for $\alpha_0\sin^2\phi_l \gg 1$. The phase saturation discussed in the previous Section can be seen here in the form of near-flat plateau. For still higher optical depths, the field amplitudes do not satisfy the required condition. The phase conjugation comes to end and the relative phase evolves again leading to transparency at $\Delta\phi = \pi/2$.

This transparency in this case is due to the dark state that is realized in the system, as discussed in the previous Chapter in Section. 3.4.5. The total polarization in this case —$\vec{e}_z \pm i\vec{e}_x$ — is circular, and the population is respectively trapped in the eigenstates of F_y with $m_y = \pm 1/2$. Interestingly,

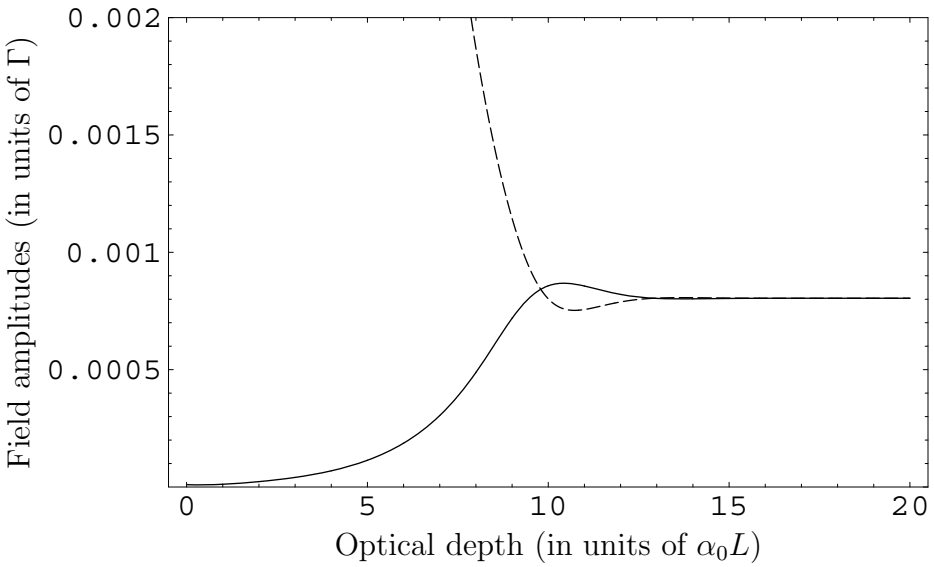

Figure 4.10: Field amplitudes $|\Omega_p|$ (solid), $|\Omega_c|$ (dashed) evolution with propagation for $\Delta_c = 0.5\Gamma$. At $y = 0$ we have $\phi = \phi_l$ and $\Omega_c = 10^4\Omega_p = 0.1\Gamma$. Strong absorption of the control and amplification of the probe leads to $|\Omega_c/\Omega_p| = 1$ at which point the transparency is reached and the fields do not grow any longer. Other parameters are $\Gamma_{ze} = 2\Gamma_d = \Gamma$, and $\Gamma_{zg} = 0$.

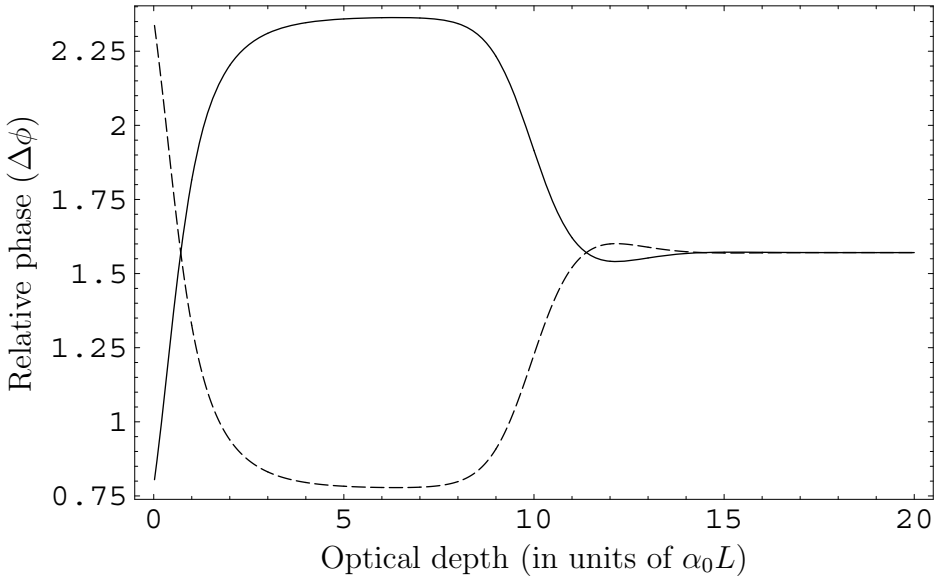

Figure 4.11: The relative phase evolution with propagation for $\Delta_c = -0.5\Gamma$ (Dashed) and $\Delta_c = 0.5\Gamma$(solid). At $y = 0$ we have $\phi = \phi_l$ and $\Omega_c = 10^4\Omega_p = 0.1\Gamma$. The phase attains conjugation for high optical depth and maintains it for as long as $|\Omega_p| \ll |\Omega_c|$. When the condition fails, the phase continues to grow again until $\Delta\phi = \pi/2$ at which point the transparency is reached. Other parameters are $\Gamma_{ze} = 2\Gamma_d = \Gamma$, and $\Gamma_{zg} = 0$.

there is no dark state in the system initially, and the dark state is realized only after a certain propagation in the system. Such behavior, where the dark state is realized during propagation has been discussed by Deng *at el.* [Deng05] for a a double Λ system.

4.6 Conclusion

A duplicated two-level system interacting with two linearly polarized fields , having mutually orthogonal polarizations, has been presented. The two fields have the same frequency, propagate co-linearly, and have relative phase difference ϕ. One of the field Ω_c is much stronger than the other Ω_p. In ultrashort pulse regime, the interaction of the weak probe field can be controlled by the phase difference ϕ. For vanishing ϕ the system becomes transparent to the probe in the limit of important light shifts, whereas the probe is always resonant for $\phi = \pi/2$ in the adiabatic picture leading to non-vanishing gain.

In the long pulse regime, for $|\Omega_p| \ll |\Omega_c|$, and in the low optical thickness, the system becomes a phase tunable medium for the probe. The absorption profile can exhibit normal absorption peak, or a gain dip, or normal or anomalous dispersion. For an additional condition $|\Omega_c| \ll \sqrt{\Gamma_d \Gamma}$, the response becomes independent of the control field characteristics and is given by $\chi_{lin} e^{2i\phi}$. For higher optical depths, the phase saturation takes place and the system turns either into χ^*_{lin} or control field intensity dependent χ^*_{nlin} depending on the control field intensity. At still higher optical depths, a dark state is realized and the system becomes transparent to the exciting fields.

Conclusions

I have presented the theoretical study of the propagation effects experienced by weak light pulses as they propagate through strongly driven atomic media. The propagation effects can be used to probe the driven system, and also to realize important applications. A variety of phenomena has been studied both in ultrashort and long pulse regime.

J'ai présenté dans cette thèse l'étude théorique des effets de propagation subis par des impulsions lumineuses de faible intensité lorsqu'elles se propagent à travers des systèmes atomiques pilotés par des champs forts. Les effets de propagation peuvent indifféremment être utilisés pour sonder le système ou pour réaliser des applications importantes. Divers phénomènes ont été étudiés en régime d'impulsions ultracourtes et en d'impulsions longues.

In ultrashort pulse regime the propagation effects were used to reveal the phenomena induced by strong pulses. The induced phenomena include important light shifts and non-adiabatic transitions. It was shown that the light shifts can be probed by propagating a resonant weak pulse through the system. The weak pulse in this case develops tiny oscillatory structure that reveals in time the light-shifted region, and by the modulation frequency, the strength of the light shifts. The modulation phase and amplitude can be controlled by a number of experimental parameters. The phenomena can be seen as wave shaping of

En régime d'impulsions ultracourtes, les effets de propagation furent utilisés pour révéler les phénomènes induits par des champs forts. Ceux-ci inclus les déplacements lumineux et les transitions non-adiabatiques. On a montré que les déplacements lumineux pouvaient être sondés en propageant une impulsion de faible intensité dans le milieu. L'impulsion faible révèle une zone affectée par le déplacement lumineux par l'existence d'une structure oscillante tandis que la fréquence de la modulation révèle l'importance de ces dplacements. La phase et l'amplitude modulées peuvent être contrôlées par un nombre de paramétres expérimentaux.

the probe and can have important applications in domains where traditional pulse shapers do not work well. I also presented the phase control of the asymptotic excited state population when two time delayed, phase locked, and identical strong pulses interact non-resonantly with a two-level system. The phenomena is interpreted in terms of non-adiabatic jumps and rapid adiabatic passage. The extreme sensitivity of non-adiabatic jump and the excited asymptotic populations was demonstrated.

In the long pulse regime, the modification of the optical response was discussed. A new method to produce slow light is proposed *coherent Zeeman oscillations*, that can be realized in a double two-level system interacting with two linearly polarized (mutually orthogonal) fields. It produces an *electromagnetic induced transparency* like transparency window without the need of a dark state, but acts in a manner which is close to *coherent population oscillations* technique of slowing light. An attempt was made to describe these three different phenomena by the same formalism which is particularly relevant if non-collinear geometries of excitations are used.

Le phénomène peut être interprété comme une mise en forme de l'impulsion sonde et peut avoir des applications importantes dans des domaines oú les " pulse shapers " classiques ne fonctionnent pas. J'ai aussi présenté dans ce manuscrit le contrôle par la phase de la partie asymptotique de la population excité quand deux impulsions identiques, décalées dans le temps, verrouillées en phase, et intenses interagissent avec un système à deux niveaux de manière non résonante. Le phénomène a été interprété en termes de sauts non-adiabatiques et de passage adiabatique rapide. L'extrême sensibilité en fonction de la phase relative a été mise en évidence.

En régime d'impulsions longues, la modification de la réponse optique a été discutée. Une nouvelle méthode basée sur les oscillations des cohérence Zeeman a été proposée pour ralentir la lumière, et peut être implémenter dans un système à deux niveaux interagissant avec deux champs polarisés linéairement et perpendiculairement entre eux. Ils créent une fenêtre de transparence spectrale comme dans le phénomène de transparence électromagnétique induite mais sans la présence d'un état noir. Ce type de fonctionnement est proche de la technique des oscillations cohérentes de population utilise pour ralentir la lumière. Une tentative a été effectuée pour décrire ces trois phénomènes différents dans un même formalisme qui s'est révélé particulièrement pertinent dans une

The coherent control of the optical response of the medium was also presented in the long pulse regime. In the presence of a strong, linearly polarized field, a double two-level systems acts as a tunable medium for a weak pulse that also has linear but orthogonal polarization. In the low optical thickness, the coherent control of the absorptive and dispersive properties of the medium is possible. The medium can be changed from being an absorber to an amplifier, and from slow light medium to fast light medium by changing the relative phase between the two fields; the weak field can also be subjected to normal or anomalous dispersion.

The experimental realization of the ideas presented in the thesis is one perspective. On theoretical side, the refinement of the interaction and application of the ideas to new domains is another perspective.

The wave shaping method that is presented, is limited to the phase introduced by light shifts. The excitation schemes can be explored that render the control of light-shifts. It will also be interesting to realize schemes where multiple non-adiabatic jumps are possible. This will provide the "turn on", "turn off" switch for the shaping method that is presented. The extreme sensitivity of excited state population on the relative phase, presented in the thesis, can lead to the realization of new techniques to stabilize interferome-

géométrie d'excitation non colinéaire.

Le contrôole cohérent de la réponse optique a été aussi étudié en régime d'impulsions longues. En présence d'un champ intense polarisé linéairement, un système à deux niveaux double se comporte comme un milieu accordable pour l'impulsion faible de polarisation linéaire et orthogonale. Pour de faibles épaisseurs optiques, le contrôle cohérent de l'absorption et de la dispersion est possible. En changeant la phase relative entre les champs, le milieu peut être modifié d'un absorbant en un amplificateur et d'un milieu ralentisseur de lumière à celui accélérateur. En outre, le champ faible peut subir une dispersion normale ou anormale.

Une perspective qui ressort de ce travail de thése est la réalisation expérimentale de ces idées. Sur le plan théorique, le raffinement de l'interaction et l'application de ces idées à de nouveaux domaines constituent une autre perspective.

La méthode de mise en forme qui a été présentée, est limitée à la l'introduction d'une phase induite par les déplacements lumineux. Différents schémas d'excitations peuvent être explorés pour mettre en place le contrôle. Il peut être aussi intéressant de réaliser des schémas oú de multiples sauts non-adiabatiques sont possibles. Cela fournit différentes possibilités de commutations "on - off " à la méthode de mise en forme présentée. L'extrême sensibilité de la population excitée à la phase relative présentée dans cette thése peut

ters and to obtain very high resolution displacement-measurements.

Regarding slow light methods, a more sound formalism to unite CPO, EIT and CZO is an interesting problem. In EIT like method, the relation between the dark state in a collinear geometry and the diffraction picture in a non-collinear geometry is another intriguing question. The modification of the optical response presented in the thesis can also be applied to different domains and opens many possibilities. For instance, the medium can switch from an absorber to an amplifier by adjusting the relative phase. The coherent control of the group velocity of light is possible by changing the medium from slow light medium to the fast light medium. It can also be used for optical switching and for the control of dipole force on atoms.

Finally the treatment presented is valid in semi-classical picture. In this picture, although the atomic system and field modifications are coupled, there is no entanglement of light and matter. The extension of the control of the atomic response to quantized fields is an open question. The quantized fields interacting with the atomic systems give rise to light matter entanglement. If the phenom-

conduire à la réalisation de nouvelles techniques de stabilisation d'interfromtres et peut conduire à des mesures de déplacement à trés haute résolution.

En ce qui concerne les méthodes de ralentissements de la lumière, la mise en place d'un formalisme unificateur entre les techniques basées sur les OCP, la TEI et les OCZ est un probléme intéressant. Dans la méthode TEI, la relation entre état noir dans une géométrie colinéaire et l'image de diffraction dans une géométrie non colinéaire est une question intrigante. La modification de la réponse optique présentée dans cette thèse peut être aussi appliquée à différents domaines et ouvrent la voie à diverses possibilités. Par exemple, le milieu peut commuter d'un absorbant à un amplificateur en ajustant simplement la phase relative. Le contrôle cohérent de la vitesse de groupe est aussi possible en faisant passer le système d'un milieu ralentisseur à un milieu accélérateur. Il peut être aussi utilisé pour la commutation optique et le contrôle de la force dipolaire qui agit sur les atomes.

Finalement, le traitement présenté ici est valable dans une image semiclassique. Dans cette image, bien que les modifications du système atomique et du champ soient couplées, il n'y a pas d'intrication entre la lumière et la matière. L'extension du contrôle de la réponse atomique à des champs quantifiés est une question ouverte. Les champs quantifiés interagissant avec le système

ena presented here is applicable to the quantized fields, then some very interesting and fundamental research problems can be investigated.

atomique donne lieu à une intrication rayonnement-matière. Si les phénomènes présentés ici sont applicables aux champs quantifiés, quelques problèmes fondamentaux trés intéressants peuvent être alors explorés.

A note on numerical technique

A number of numerical approaches and resources have been used to produce the simulations presented in this thesis. The atomic quantities at the entrance of the medium (Chapter 1. & Chapter 2.) are the numerical solution of the time evolution equations presented in the text. The filed and the atomic quantities inside the medium are worked out by solving the time evolution equations for atomic quantities, coupled with the Maxwell's equation for field propagation. The equation of propagation is derived in Chapter. 1 using standard approximations. The coupled equations are either solved using commercially available numerical routines (NAG routines for Chapter. 1 & Chapter 2.) or by the code I have written myself (Chapter 3. & Chapter 4). The approach is as follows. Given a field at $y = 0$ (y being the propagation distance), the atomic system can be solved for all times t. With this, one can work out the polarization at $y = 0$ for all times that determines the field at $y = y + \delta y$. With the field at $y = y + \delta y$, one can work out the atomic system for all times at this new point in space. By keeping on repeating this process until y reaches the length of the medium L, the problem can be solved.

To account for the non-collinear geometries (with only small angle between the fields so that the one dimensional treatment is valid), two approaches have been used and found to give the identical results. In the limit of weak probe, the atomic system can be expanded in a perturbative series and the resulting time evolution equations are solved coupled with the field propagation equations (Chapter 2). The second approach is to solve the atomic system at any given y for different k vectors. By taking the Fourier transform of atomic quantities, the coherence responsible for the radiating field in the right direction can be worked out. This value of the coherence can be used to solve the field propagation equation for subsequent y.

In Chapter 2, the non-adiabatic population profiles are solved first in bare state picture and then transformed into adiabatic basis. Similarly, although the time evolution equations in bare state picture are not given in the last section of the Chapter 2. the system is nevertheless solved in bare state. Finally for Chapter 4. dealing with monochromatic cases, the stationary

state result for the coherences is used in solving numerically the propagation equations for the fields.

Analytical solution for phase evolution Eq. (4.22)

In this Annex I present the analytical solution for the relative phase evolution Eq. (4.22) of Chapter. 4 Section. 4.4.1.

The relative phase evolves according to the equation

$$\frac{\partial}{\partial_y}\Delta\phi = k\sin\Delta\phi\left(\chi'_{lin}\sin\Delta\phi + \chi''_{lin}\cos\Delta\phi\right). \tag{28}$$

Denoting $\Delta\phi\,(y=0) = \phi$ and $\Delta\phi\,(y=y_i) = \phi_{y_i}$ (where y_i is some point inside the medium), the above expression can be written as

$$\int_{\phi}^{\phi_{y_i}} \frac{\csc\Delta\phi}{\chi'_{lin}\sin\Delta\phi + \chi''_{lin}\cos\Delta\phi} d\left(\Delta\phi\right) = k\int_0^{y_i} d\left(y\right). \tag{29}$$

We can use the identity

$$b\int \frac{\csc x}{a\sin x + b\cos x}dx = \ln\frac{\sin x}{b\cos x + a\sin x}, \tag{30}$$

to solve the expression (29). The solution can be written as

$$\ln\frac{\sin\phi_{y_i}}{\chi'_{lin}\sin\phi_{y_i} + \chi''_{lin}\cos\phi_{y_i}} - \ln\frac{\sin\phi}{\chi'_{lin}\sin\phi + \chi''_{lin}\cos\phi} = ky_i\chi''_{lin}, \tag{31}$$

or

$$\frac{\sin\phi_{y_i}}{\chi'_{lin}\sin\phi_{y_i} + \chi''_{lin}\cos\phi_{y_i}} = \frac{\sin\phi}{\chi'_{lin}\sin\phi + \chi''_{lin}\cos\phi} e^{ky_i\chi''_{lin}}. \tag{32}$$

We use $\tan\phi_l = \chi''_{lin}/\chi'_{lin}$ to write the above expression as

$$1 + \frac{\tan\phi_l}{\tan\phi_{y_i}} = \left[1 + \frac{\tan\phi_l}{\tan\phi}\right] e^{-ky_i\chi''_{lin}}. \tag{33}$$

Finally noting that $\chi''_{lin} = (2\alpha_0/k)\sin^2\phi_l$ with $\sin^2\phi_l = \Gamma_d^2/|\bar{\Delta}_c|^2$, the above expression simplifies to Eq. (4.23) given in the text.

Propagation equations for the fields in the double two-level system

In this Annex we work out the coherences responsible for the radiated fields, and the equations of propagation for the fields in the double two-level system discussed in Chapter. 3, Section. 3.4, and in Chapter. 4.

The propagation equation for a single field interacting with a two-level system was derived in Chapter. 1 in Section. 1.2.1. For the double two-level system interacting with the field given by

$$\vec{E}_T(t,\vec{r}) = \left(\vec{e}_z A_z + \vec{e}_x A_x e^{-i\Phi(t,\vec{r})}\right) e^{-i(\omega_c t - k_c y)} + cc, \tag{34}$$

and taking into account for the vectorial dependence of the polarization, the propagation equation (1.28) can be written as

$$\partial_y \left[A_z \vec{e}_z + A_x e^{-i\Phi(t,\vec{r})}\vec{e}_x\right] = i\mu_0 c\omega_c \vec{\varrho}/2. \tag{35}$$

Here we are in a frame of reference that is moving along y axis with the speed of light c with $t \to t - y/c$; and $\vec{\varrho}$ is the polarization amplitude related to the polarization as

$$\vec{P}_T(t,\vec{r}) = \vec{\varrho} e^{-i(\omega_c t - k_c y)} + cc. \tag{36}$$

$\vec{\varrho}$ can be evaluated by the expression

$$\vec{\varrho} = NTr\left(\hat{\vec{D}}\rho\right), \tag{37}$$

$$= ND\left[\vec{e}_z(\rho_{ca} - \rho_{db}) + \vec{e}_x(\rho_{da} + \rho_{cb}) + i\vec{e}_y(\rho_{da} - \rho_{cb})\right] e^{-i(\omega_c t - k_c y)} + cc, \tag{38}$$

where we have used the expression (3.16) for the density matrix ρ, Eq. (3.15) for $\hat{\vec{D}}$, and the identity $\vec{e}_\pm = \mp(\vec{e}_x \pm i\vec{e}_y)/\sqrt{2}$. Using the above expression in

Eq. (35), and with the definitions $\Omega_z = DA_z/\hbar$, $\Omega_x = DA_x/\hbar$, we can write the propagation equations for the fields as

$$\partial_y \Omega_z = i\alpha_0 \Gamma_d \left(\rho_{ca} - \rho_{db}\right), \tag{39}$$

$$\partial_y \Omega_x e^{-i\Phi(t,\vec{r})} = i\alpha_0 \Gamma_d \left(\rho_{da} + \rho_{cb}\right). \tag{40}$$

With $\alpha_0 = ND^2\omega_0/\left(2c\hbar\epsilon_0\Gamma_d\right)$ ($\omega_0 \approx \omega_c$ with RWA). We can identify the two coherences $\rho_c = \rho_{ca} - \rho_{db}$ and $\rho_p = \rho_{da} + \rho_{cb}$ responsible for the two radiated fields with $\vec{e}_z$ and $\vec{e}_x$ polarizations respectively.

In the case discussed in Chapter. 4, $\Phi\left(t, \vec{r}\right)$ reduces to ϕ and Eq. (40) simplifies to Eq. (4.3a) with $\Omega_z = \Omega_c$ and $\Omega_x = \Omega_p$.

In the case of non-collinear propagation discussed in Chapter. 3, we expand the coherence ρ_p as $\rho_p = \rho_p^{(0)} + \rho_p^{(-)} e^{-i\Phi(t,\vec{r})} + \rho_p^{(+)} e^{i\Phi(t,\vec{r})}$ and write the field as $\Omega_x = \Omega_x^{(0)} + \Omega_x^{(-)} e^{-i\Phi(t,\vec{r})} + \Omega_x^{(+)} e^{i\Phi(t,\vec{r})}$. Using these expressions in (40), we can write the propagation equation (3.37) for the component of the field radiating in the direction of the probe field with $\Omega_p = \Omega_x^{(0)}$.

Bibliography

[Agarwal03] Agarwal, G. S. and T. N. Dey. *Slow light in doppler-broadened two-level systems*. Physical Review A, **68**(6), page 063816 (2003). Copyright (C) 2008 The American Physical Society Please report any problems to prola@aps.org PRA.

[Allen75] Allen, L. and J. H. Eberly. *Optical Resonance and Two level Atoms*. Dover, New York (1975).

[Arimondo96] Arimondo, E. *Coherent population trapping in laser spectroscopy*. In E. Wolf, editor, *Progress in Optics*, volume 35. Elsevier, Amsterdam (1996).

[Arlt97a] Arlt, J., C. Weiss, G. Torosyan, and R. Beigang. *Coherent pulse propagation and the dynamics of rydberg wave packets*. Physical Review Letters, **79**(24), page 4774 (1997). Copyright (C) 2008 The American Physical Society Please report any problems to prola@aps.org PRL.

[Arlt97b] Arlt, J., C. Weiss, G. Torosyan, and R. Beigang. *Coherent pulse propagation and the dynamics of rydberg wave packets* (1997).

[Assion98] Assion, A., T. Baumert, M. Bergt, T. Brixner, B. Kiefer, V. Seyfried, M. Strehle, and G. Gerber. *Control of chemical reactions by feedback-optimized phase-shaped femtosecond laser pulses*. Science, **282**(5390), pages 919–922 (1998).

[Avenel83] Avenel, O., M. Rouff, E. Varoquaux, and G. A. Williams. *Resonant pulse propagation of sound in superfluid he3-b*. Phys. Rev. Lett., **50**(20), pages 1591–1594 (1983).

[Baldit05] Baldit, E., K. Bencheikh, P. Monnier, J. A. Levenson, and V. Rouget. *Ultraslow light propagation in an inhomogeneously broadened rare-earth ion-doped crystal*. Physical Review Letters, **95**(14), page 143601 (2005).

[Bass01] Bass, M., editor. *Handbook of Optics*, volume II and IV. McGraw-Hill, New York (2001).

[Berman98] Berman, P. R., L. Yan, K.-H. Chiam, and R. Sung. *Nonadiabatic transitions in a two-level quantum system: Pulse-shape dependence of the transition probability for a two-level atom driven by a pulsed radiation field*. Physical Review A, **57**(1), page 79 (1998). Copyright (C) 2008 The American Physical Society Please report any problems to prola@aps.org PRA.

[Bervas92] Bervas, H., B. Attal-Tretout, S. L. Boiteux, and J. P. Taran. *Oh detection and spectroscopy by dfwm in flames; comparison with cars*. Journal of Physics B: Atomic, Molecular and Optical Physics, **25**(5), pages 949–969 (1992).

[Bigelow03a] Bigelow, M. S., N. N. Lepeshkin, and R. W. Boyd. *Observation of ultraslow light propagation in a ruby crystal at room temperature*. Physical Review Letters, **90**(11), page 113903 (2003). Copyright (C) 2007 The American Physical Society Please report any problems to prola@aps.org PRL.

[Bigelow03b] Bigelow, M. S., N. N. Lepeshkin, and R. W. Boyd. *Superluminal and slow light propagation in a room-temperature solid*. Science, **301**(5630), pages 200–202 (2003).

[Blanchet97] Blanchet, V., C. Nicole, M.-A. Bouchene, and B. Girard. *Temporal coherent control in two-photon transitions: From optical interferences to quantum interferences*. Physical Review Letters, **78**(14), page 2716 (1997). Copyright (C) 2008 The American Physical Society Please report any problems to prola@aps.org PRL.

[Boller91] Boller, K. J., A. Imamolu, and S. E. Harris. *Observation of electromagnetically induced transparency.* Physical Review Letters, **66**(20), page 2593 (1991). Copyright (C) 2008 The American Physical Society Please report any problems to prola@aps.org PRL.

[Bouchène92] Bouchène, M. A., A. Débarre, J.-C. Keller, J.-L. L. Gouët, and P. Tchénio. *Observation of 0π-pulse formation with incoherent light.* J. Opt. Soc. Am. B, **9**(2), pages 281–289 (1992).

[Boyd81] Boyd, R. W., M. G. Raymer, P. Narum, and D. J. Harter. *Four-wave parametric interactions in a strongly driven two-level system.* Physical Review A, **24**(1), page 411 (1981). Copyright (C) 2008 The American Physical Society Please report any problems to prola@aps.org PRA.

[Boyd88] Boyd, R. W. and M. Sargent. *Population pulsations and the dynamic stark effect.* J. Opt. Soc. Am. B, **5**(1), page 99 (1988).

[Boyd92] Boyd, R. W. *Non Linear Optics.* Academic, San Diego (1992).

[Broers92] Broers, B., H. B. van Linden van den Heuvell, and L. D. Noordam. *Efficient population transfer in a three-level ladder system by frequency-swept ultrashort laser pulses.* Physical Review Letters, **69**(14), page 2062 (1992). Copyright (C) 2008 The American Physical Society Please report any problems to prola@aps.org PRL.

[Brumer86] Brumer, P. and M. Shapiro. *Control of unimolecular reactions using coherent light.* Chemical Physics Letters, **126**(6), page 541 (1986). 0009-2614 doi: DOI: 10.1016/S0009-2614(86)80171-3.

[Cerboneschi96] Cerboneschi, E. and E. Arimondo. *Propagation and amplitude correlation of pairs of intense pulses interacting with a double- lambda system.* Physical Review A, **54**(6), page 5400 (1996). Copyright (C) 2008 The

American Physical Society Please report any problems to prola@aps.org PRA.

[Christov98] Christov, I. P., M. M. Murnane, and H. C. Kapteyn. *Generation and propagation of attosecond x-ray pulses in gaseous media*. Phys. Rev. A, **57**(4), pages R2285–R2288 (1998).

[Cohen-Tannoudji98] Cohen-Tannoudji, C., J. Dupont-Roc, and G. Grynberg. *Atom-Photon Interactions: Basic Processes and Applications*. Wiley, New York (1998).

[Crisp69] Crisp, M. D. *Distortionless propagation of light through an optical medium*. Physical Review Letters, **22**(16), page 820 (1969). Copyright (C) 2008 The American Physical Society Please report any problems to prola@aps.org PRL.

[Crisp70] Crisp, M. D. *Propagation of small-area pulses of coherent light through a resonant medium*. Physical Review A, **1**(6), page 1604 (1970). Copyright (C) 2008 The American Physical Society Please report any problems to prola@aps.org PRA.

[Delagnes04] Delagnes, J. C. and M. A. Bouchene. *Effect of a transient light shift on the propagation of an ultrashort pulse in a resonant atomic medium*. Physical Review A (Atomic, Molecular, and Optical Physics), **69**(6), page 063813 (2004).

[Delagnes05] Delagnes, J. C. *Contrôle de la propagation d'implusions ultracourtes. Effets de déplacements lumineux*. Ph.D. thesis, Université Paul Sabatier, Toulouse (2005).

[Delagnes06] Delagnes, J. C., F. A. Hashmi, and M. A. Bouchene. *Spectral and temporal modifications of a weak resonant ultrashort pulse propagating in a two-level system driven by a strong nonresonant field*. Physical Review A (Atomic, Molecular, and Optical Physics), **74**(5), page 053822 (2006).

[Delagnes07a] Delagnes, J. C. and M. A. Bouchene. *Coherent control of light shifts in an atomic medium driven by two orthogonally polarized pulses: Effect of the pulse overlap.* Physical Review A (Atomic, Molecular, and Optical Physics), **76**(5), 053809 (2007).

[Delagnes07b] Delagnes, J. C. and M. A. Bouchene. *Coherent control of light shifts in an atomic system: Modulation of the medium gain.* Physical Review Letters, **98**(5), page 053602 (2007).

[Delagnes07c] Delagnes, J. C. and M. A. Bouchene. *Gain-dispersion coupling induced by transient light shifts in an atomic medium.* Physical Review A (Atomic, Molecular, and Optical Physics), **76**(2), 023422 (2007).

[Delagnes07d] Delagnes, J. C. and M. A. Bouchene. *Influence of wave-packet dynamics on the medium gain of an atomic system.* Physical Review A (Atomic, Molecular, and Optical Physics), **76**(4), 045805 (2007).

[Delagnes07e] Delagnes, J. C., F. A. Hashmi, and M. A. Bouchene. In M. Abdel-Aty, editor, *Aspects of Optical Sciences and Quantum Information*, pages 173–193. Research Signpost, Kerala (2007).

[Delagnes07f] Delagnes, J. C., A. Monmayrant, P. Zahariev, A. Arbouet, B. Chatel, B. Girard, and M. A. Bouchene. *Compensation of resonant atomic dispersion using a pulse shaper.* Applied Physics B: Lasers and Optics, **86**(4), page 573 (2007). 10.1007/s00340-006-2549-7.

[Delagnes08] Delagnes, J. C. and M. A. Bouchene. *Beyond the pulse-area theorem: Role of the absorption and the dispersion in the propagation of weak ultrashort resonant pulses.* Optics Communications, **281**(23), page 5824 (2008). 0030-4018 doi: DOI: 10.1016/j.optcom.2008.08.047.

[Demtröder96] Demtröder, W. *Laser Spectroscopy.* Springer-Verlag, Berlin (1996).

[Deng05] Deng, L. and M. G. Payne. *Achieving induced transparency with one- and three-photon destructive inter-*

ference in a two-mode, three-level, double-lambda system. Physical Review A (Atomic, Molecular, and Optical Physics), **71**(1), page 011803 (2005).

[Diels96] Diels, J. C. and W. Rudolph. *Ultrashort Laser Pulse Phenomena: Fundamentals, Techniques and Applications on a Femtosecond time scale*. Academic press, San Diego (1996).

[Dudovich02] Dudovich, N., D. Oron, and Y. Silberberg. *Coherent transient enhancement of optically induced resonant transitions*. Phys. Rev. Lett., **88**(12), page 123004 (2002).

[Eberly81] Eberly, J. H., S. R. Hartmann, and A. Szabo. *Propagation narrowing in the transmission of a light pulse through a spectral hole*. Phys. Rev. A, **23**(5), pages 2502–2506 (1981).

[Felinto04] Felinto, D., L. H. Acioli, and S. S. Vianna. *Accumulative effects in the coherence of three-level atoms excited by femtosecond-laser frequency combs*. Phys. Rev. A, **70**(4), page 043403 (2004).

[Fleischhauer02] Fleischhauer, M. and M. D. Lukin. *Quantum memory for photons: Dark-state polaritons*. Physical Review A, **65**(2), page 022314 (2002). Copyright (C) 2007 The American Physical Society Please report any problems to prola@aps.org PRA.

[Fleischhauer05] Fleischhauer, M., A. Imamoglu, and J. P. Marangos. *Electromagnetically induced transparency: Optics in coherent media*. Reviews of Modern Physics, **77**(2), page 633 (2005).

[Gauthier05] Gauthier, D. J. *Slow light brings faster communication*. Physics World, **18**(12), pages 30–32 (2005).

[Gauthier06] Gauthier, D. J., A. L. Gaeta, and R. W. Boyd. *Slow light: From basics to future prospects*. Photonics Spectra, pages 44–50 (2006).

[Gehring06] Gehring, G. M., A. Schweinsberg, C. Barsi, N. Kostinski, and R. W. Boyd. *Observation of backward pulse*

propagation through a medium with a negative group velocity. Science, **312**(5775), pages 895–897 (2006).

[Gersen05] Gersen, H., T. J. Karle, R. J. P. Engelen, W. Bogaerts, J. P. Korterik, N. F. v. Hulst, T. F. Krauss, and L. Kuipers. *Real-space observation of ultraslow light in photonic crystal waveguides*. Physical Review Letters, **94**(7), page 073903 (2005).

[Gibbs70] Gibbs, H. M. and R. E. Slusher. *Peak amplification and breakup of a coherent optical pulse in a simple atomic absorber*. Physical Review Letters, **24**(12), page 638 (1970). Copyright (C) 2008 The American Physical Society Please report any problems to prola@aps.org PRL.

[Gibbs71] Gibbs, H. M. and R. E. Slusher. *Optical pulse compression by focusing in a resonant absorber*. Applied Physics Letters, **18**(11), page 505 (1971).

[Gibbs73] Gibbs, H. M. *Incoherent resonance fluorescence from a rb atomic beam excited by a short coherent optical pulse*. Physical Review A, **8**(1), page 446 (1973). Copyright (C) 2008 The American Physical Society Please report any problems to prola@aps.org PRA.

[Grischkowsky72] Grischkowsky, D. and J. A. Armstrong. *Self-defocusing of light by adiabatic following in rubidium vapor*. Phys. Rev. A, **6**(4), pages 1566–1570 (1972).

[Grischkowsky73] Grischkowsky, D. *Adiabatic following and slow optical pulse propagation in rubidium vapor*. Phys. Rev. A, **7**(6), pages 2096–2102 (1973).

[Harris92] Harris, S. E., J. E. Field, and A. Kasapi. *Dispersive properties of electromagnetically induced transparency*. Physical Review A, **46**(1), page R29 (1992). Copyright (C) 2008 The American Physical Society Please report any problems to prola@aps.org PRA.

[Hashmi08a] Hashmi, F. A. and M. A. Bouchene. *Coherent control of the effective susceptibility through wave mixing in a duplicated two-level system*. Physical Review Letters, **101**(21), 213601 (2008).

[Hashmi08b] Hashmi, F. A. and M. A. Bouchene. *Slowing light through zeeman coherence oscillations in a duplicated two-level system.* Physical Review A (Atomic, Molecular, and Optical Physics), **77**(5), page 051803 (2008).

[Hau99] Hau, L. V., S. E. Harris, Z. Dutton, and C. H. Behroozi. *Light speed reduction to 17 metres per second in an ultracold atomic gas.* Nature, **397**(6720), page 594 (1999). 0028-0836 10.1038/17561 10.1038/17561.

[Hillman83] Hillman, L. W., R. W. Boyd, J. Krasinski, and C. R. Stroud. *Observation of a spectral hole due to population oscillations in a homogeneously broadened optical absorption line.* Optics Communications, **45**(6), page 416 (1983).

[Imamoğlu89] Imamoğlu, A. and S. E. Harris. *Lasers without inversion: interference of dressed lifetime-broadened states.* Optics Letters, **14**(24), page 1344 (1989).

[Kallmann99] Kallmann, U., S. Brattke, and W. Hartmann. *Propagation of resonant π pulses in rubidium.* Phys. Rev. A, **59**(1), pages 814–818 (1999).

[Kang03] Kang, H. and Y. Zhu. *Observation of large kerr nonlinearity at low light intensities.* Physical Review Letters, **91**(9), page 093601 (2003). Copyright (C) 2008 The American Physical Society Please report any problems to prola@aps.org PRL.

[Kapale05] Kapale, K., M. Sahari, H. Tajali, and Z. S. *Phase control of electromagnetically induced transparency and its applications to tunable group velocity and atom localization.* arXiv:quant-ph/0F02159v1 (2005).

[Kasapi95] Kasapi, A., M. Jain, G. Y. Yin, and S. E. Harris. *Electromagnetically induced transparency: Propagation dynamics.* Physical Review Letters, **74**(13), page 2447 (1995). Copyright (C) 2007 The American Physical Society Please report any problems to prola@aps.org PRL.

[Kash99] Kash, M. M., V. A. Sautenkov, A. S. Zibrov, L. Hollberg, G. R. Welch, M. D. Lukin, Y. Rostovtsev, E. S.

Fry, and M. O. Scully. *Ultraslow group velocity and enhanced nonlinear optical effects in a coherently driven hot atomic gas.* Physical Review Letters, **82**(26), page 5229 (1999). Copyright (C) 2007 The American Physical Society Please report any problems to prola@aps.org PRL.

[Kijoon01] Kijoon, L. and M. L. Nabil. *Optically induced pulse delay in a solid-state raman amplifier.* Applied Physics Letters, **78**(6), pages 703–705 (2001).

[Kircheva94] Kircheva, P. P. and G. B. Hadjichristov. *Kramers-kronig relations in fwm spectroscopy.* Journal of Physics B: Atomic, Molecular and Optical Physics, **27**(16), pages 3781–3793 (1994).

[Korsunsky99] Korsunsky, E. A. and D. V. Kosachiov. *Phase-dependent nonlinear optics with double- lambda atoms.* Physical Review A, **60**(6), page 4996 (1999). Copyright (C) 2007 The American Physical Society Please report any problems to prola@aps.org PRA.

[Krmpot05] Krmpot, A., M. Mijailović, B. Panić, D. Lukić, A. Kovačević, D. Pantelić, and B. Jelenković. *Sub-doppler absorption narrowing in atomic vapor at two intense laser fields.* Opt. Express, **13**(5), pages 1448–1456 (2005).

[Lamb71] Lamb, G. L. *Analytical descriptions of ultrashort optical pulse propagation in a resonant medium.* Reviews of Modern Physics, **43**(2), page 99 (1971). Copyright (C) 2008 The American Physical Society Please report any problems to prola@aps.org RMP.

[Liedenbaum89] Liedenbaum, C., S. Stolte, and J. Reuss. *Inversion produced and reversed by adiabatic passage.* Physics Reports, **178**(1), page 1 (1989).

[Liu01] Liu, C., Z. Dutton, C. H. Behroozi, and L. V. Hau. *Observation of coherent optical information storage in an atomic medium using halted light pulses.* Nature, **409**(6819), page 490 (2001). 0028-0836 10.1038/35054017 10.1038/35054017.

[Lukin98] Lukin, M. D., P. R. Hemmer, M. Lffler, and M. O. Scully. *Resonant enhancement of parametric processes via radiative interference and induced coherence*. Physical Review Letters, **81**(13), page 2675 (1998). Copyright (C) 2008 The American Physical Society Please report any problems to prola@aps.org PRL.

[Marangos98] Marangos, J. P. *Electromagnetically induced transparency*. Journal of Modern Optics, **45**(3), pages 471 – 503 (1998).

[McCall67] McCall, S. L. and E. L. Hahn. *Self-induced transparency by pulsed coherent light*. Physical Review Letters, **18**(21), page 908 (1967). Copyright (C) 2008 The American Physical Society Please report any problems to prola@aps.org PRL.

[McCall69] McCall, S. L. and E. L. Hahn. *Self-induced transparency*. Physical Review, **183**(2), page 457 (1969). Copyright (C) 2008 The American Physical Society Please report any problems to prola@aps.org PR.

[McCullough00] McCullough, E., M. Shapiro, and P. Brumer. *Coherent control of refractive indices*. Physical Review A, **61**(4), page 041801 (2000). Copyright (C) 2008 The American Physical Society Please report any problems to prola@aps.org PRA.

[Melinger92] Melinger, J. S., S. R. Gandhi, A. Hariharan, J. X. Tull, and W. S. Warren. *Generation of narrowband inversion with broadband laser pulses*. Physical Review Letters, **68**(13), page 2000 (1992). Copyright (C) 2008 The American Physical Society Please report any problems to prola@aps.org PRL.

[Milonni02] Milonni, P. W. *Controlling the speed of light pulses*. Journal of Physics B: Atomic, Molecular and Optical Physics, **35**(6), pages R31–R56 (2002).

[Milonni05] Milonni, P. W. *Fast Light, Slow Light and Left-Handed Light*. Series in Optics and Optoelectronics. Taylor & Francis, New York (2005).

[Mollow72] Mollow, B. R. *Stimulated emission and absorption near resonance for driven systems.* Physical Review A, **5**(5), page 2217 (1972). Copyright (C) 2008 The American Physical Society Please report any problems to prola@aps.org PRA.

[Morigi02] Morigi, G., S. Franke-Arnold, and G.-L. Oppo. *Phase-dependent interaction in a four-level atomic configuration.* Physical Review A, **66**(5), page 053409 (2002). Copyright (C) 2007 The American Physical Society Please report any problems to prola@aps.org PRA.

[Niikura03] Niikura, H., P. B. Corkum, and D. M. Villeneuve. *Controllng vibrational wave packet motion with intense modulated laser fields.* Physical Review Letters, **90**(20), page 203601 (2003). Copyright (C) 2008 The American Physical Society Please report any problems to prola@aps.org PRL.

[Okawachi05] Okawachi, Y., M. S. Bigelow, J. E. Sharping, Z. Zhu, A. Schweinsberg, D. J. Gauthier, R. W. Boyd, and A. L. Gaeta. *Tunable all-optical delays via brillouin slow light in an optical fiber.* Physical Review Letters, **94**(15), page 153902 (2005).

[Park05] Park, S. J., H. S. Lee, T. Y. Kwon, H. Cho, and J. D. Park. *Phase-sensitive probing of coherent superpositions of lower states in a double-[lambda] system.* Optics Communications, **251**(4-6), page 237 (2005).

[Patel67] Patel, C. K. N. and R. E. Slusher. *Self-induced transparency in gases.* Physical Review Letters, **19**(18), page 1019 (1967). Copyright (C) 2008 The American Physical Society Please report any problems to prola@aps.org PRL.

[Patel70] Patel, C. K. N. *Investigation of pulse delay in self-induced transparency.* Physical Review A, **1**(4), page 979 (1970). Copyright (C) 2008 The American Physical Society Please report any problems to prola@aps.org PRA.

[Pendry00] Pendry, J. B. *Negative refraction makes a perfect lens.* Physical Review Letters, **85**(18), page 3966 (2000). Copyright (C) 2008 The American Physical Society Please report any problems to prola@aps.org PRL.

[Phillips01] Phillips, D. F., A. Fleischhauer, A. Mair, R. L. Walsworth, and M. D. Lukin. *Storage of light in atomic vapor.* Physical Review Letters, **86**(5), page 783 (2001). Copyright (C) 2006 The American Physical Society Please report any problems to prola@aps.org PRL.

[Piredda07] Piredda, G. and R. W. Boyd. *Slow light by means of coherent population oscillations: laser linewidth effects.* Journal of the European Optical Society-Rapid Publications, **2**, page 07004 (2007).

[Poirson97] Poirson, J., F. Bretenaker, M. Vallet, and A. L. Floch. *Analytical and experimental study of ringing effects in a fabry–perot cavity. application to the measurement of high finesses.* J. Opt. Soc. Am. B, **14**(11), pages 2811–2817 (1997).

[Rabi37] Rabi, I. I. *Space quantization in a gyrating magnetic field.* Physical Review, **51**(8), page 652 (1937). Copyright (C) 2008 The American Physical Society Please report any problems to prola@aps.org PR.

[Rothenberg84] Rothenberg, J. E., D. Grischkowsky, and A. C. Balant. *Observation of the formation of the pi pulse.* Physical Review Letters, **53**(6), page 552 (1984). Copyright (C) 2008 The American Physical Society Please report any problems to prola@aps.org PRL.

[Rothenberg85] Rothenberg, J. E. and D. Grischkowsky. *Measurement of the phase of a frequency-swept ultrashort optical pulse.* J. Opt. Soc. Am. B, **2**(4), pages 626–633 (1985).

[Scherer90] Scherer, N. F., A. J. Ruggiero, M. Du, and G. R. Fleming. *Time resolved dynamics of isolated molecular systems studied with phase-locked femtosecond pulse*

pairs. The Journal of Chemical Physics, **93**(1), page 856 (1990).

[Schmidt96] Schmidt, H. and A. Imamogdlu. *Giant kerr nonlinearities obtained by electromagnetically induced transparency*. Optics Letters, **21**(23), pages 1936–1938 (1996).

[Schwarz67] Schwarz, S. E. and T. Y. Tan. *Wave interactions in saturable absorbers*. Applied Physics Letters, **10**(1), page 4 (1967).

[Shapiro03] Shapiro, M. and P. Brumer. *Principles of the quantum control of molecular processes*. Wiley, New Jersey (2003).

[Shelby01] Shelby, R. A., D. R. Smith, and S. Schultz. *Experimental verification of a negative index of refraction*. Science, **292**(5514), pages 77–79 (2001).

[Shore90] Shore, B. W. *The Theory of Coherent Atomic Excitation*. Wiley, New York (1990).

[Slusher72] Slusher, R. E. and H. M. Gibbs. *Self-induced transparency in atomic rubidium*. Physical Review A, **5**(4), page 1634 (1972). Copyright (C) 2008 The American Physical Society Please report any problems to prola@aps.org PRA.

[Sobelman92] Sobelman, I. *Atomic Spectra and radiative transitions*. Springer, Berlin (1992).

[Sun08] Sun, H., Y. Niu, S. Jin, and S. Gong. *Phase control of the kerr nonlinearity in electromagnetically induced transparency media*. Journal of Physics B: Atomic, Molecular and Optical Physics, **41**(6), page 065504 (6pp) (2008).

[Torosov07] Torosov, B. T. and N. V. Vitanov. *Coherent control of a quantum transition by a phase jump*. Physical Review A (Atomic, Molecular, and Optical Physics), **76**(5), page 053404 (2007).

[Tull97] Tull, J. X., M. A. Dugan, and W. S. Warren. *High resolution, ultrafast laser pulse shaping and its applications*. Advances in Magnetic and Optical Resonance, **20**, page 1 (1997).

[Vasilev06] Vasilev, G. S. and N. V. Vitanov. *Complete population transfer by a zero-area pulse*. Physical Review A (Atomic, Molecular, and Optical Physics), **73**(2), page 023416 (2006).

[Vitanov07] Vitanov, N. V. *Complete population inversion by a phase jump: an exactly soluble model*. New Journal of Physics, **9**(3), page 58 (2007).

[Wang00] Wang, L. J., A. Kuzmich, and A. Dogariu. *Gain-assisted superluminal light propagation*. Nature, **406**(6793), page 277 (2000). 0028-0836 10.1038/35018520 10.1038/35018520.

[Wefers95] Wefers, M. M. and K. A. Nelson. *Analysis of programmable ultrashort waveform generation using liquid-crystal spatial light modulators*. Journal of the Optical Society of America B, **12**(7), pages 1343–1362 (1995).

[Wu77] Wu, F. Y., S. Ezekiel, M. Ducloy, and B. R. Mollow. *Observation of amplification in a strongly driven two-level atomic system at optical frequencies*. Phys. Rev. Lett., **38**(19), pages 1077–1080 (1977).

[Zamith01] Zamith, S., J. Degert, S. Stock, B. de Beauvoir, V. Blanchet, M. Aziz Bouchene, and B. Girard. *Observation of coherent transients in ultrashort chirped excitation of an undamped two-level system*. Physical Review Letters, **87**(3), page 033001 (2001).

[Zeek99] Zeek, E., K. Maginnis, S. Backus, U. Russek, M. Murnane, G. Mourou, H. Kapteyn, and G. Vdovin. *Pulse compression by use of deformable mirrors*. Optics Letters, **24**(7), pages 493–495 (1999).

This thesis deals with the study of propagation effects experienced by weak light pulses as they propagate in atomic media driven by strong pulses. We explore both the ultra-short and long pulse regime and investigate the phenomena that arise at these different time scales. In the short pulse regime, a strongly driven two level atomic system presents transient light shifts, and non-adiabatic transitions occur between these adiabatic levels. We have studied a method to probe these light shifts in real time by propagating a weak probe through the medium. The light shifts enrich the spectrum of the probe and the probe gets shaped as a result. In this way a strongly driven two-level system can act as an active pulse shaper, and can introduce oscillations in the temporal profile of an ultra-short pulse at a time scale shorter than the pulse duration. We also show that by driving the system with two time delayed non-resonant strong fields, the non-adiabatic effects can be rendered phase dependent. This gives very sensitive phase control of the excited state population and can be used to formulate new techniques in interferometry. In the long pulse regime we present a new method of slowing light that can be realized in a double two-level system interacting with two orthogonally polarized light pulses that propagate along different axis. Spatio-temporal dependence of the total polarization induces a grating in the ground Zeeman coherence. The stronger of the two fields (the control field) is diffracted from this grating into the direction of the weak probe field compensating for the absorption of this latter field. A transparency window is thus created in the absorption spectrum of the probe leading to the slowing down of light. The transparency window exhibits characteristics similar to the one obtained by EIT (electromagnetic induced transparency) method. However, the important difference between our method and the traditional EIT method, is that ours doesn't rely on realizing dark state in the system. This may open the possibility of slowing down light in more complex atomic media. Moreover, when the linear absorptive response of the medium is cancelled in this manner, the nonlinear response becomes more important. In the situation where fields propagate in the same direction and have same frequency, two regimes have been investigated. For small optical depths, the effective susceptibility behaves as $\chi_{lin}e^{2i\phi}$ (with ϕ the phase difference between two fields). This renders phase control of the medium response, and the medium can be changed from an absorber to an amplifier, with normal or anomalous dispersion, by adjusting the relative phase ϕ. In the regime of large optical thickness, phase saturation takes place and the effective susceptibility turns into χ_{lin}^*, changing an absorber into an amplifier without effecting the dispersive response.

Keywords : propagation effects, coherent controle, wave shaping, non-adiabatic jumps, slow light

Cette thèse concerne l'étude des effets de propagation subis par des impulsions lumineuses de faible intensité lorsqu'elles se propagent dans des systèmes atomiques soumis à des champs intenses. Nous explorons aussi bien le régime d'impulsions longues que courtes et nous analysons les phénomènes qui se produisent à ces échelles de temps différents. En régime d'impulsions ultracourtes, un système atomique à deux niveaux soumis à un champ intense présente des déplacements lumineux transitoires, et des transitions non adiabatiques se produisent entre ces états. Nous avons étudié une méthode qui permette de sonder en temps réel ces déplacements lumineux en propageant un champ sonde de faible intensité. Les déplacements lumineux enrichissent le spectre de la sonde qui se trouve ainsi modifiée. Un système à deux niveaux peut se comporter alors comme un dispositif de mise en forme et peut induire sur le profil temporel d'une impulsion ultra courte des oscillations à une échelle de temps plus courte que la durée de l'impulsion. Nous montrons aussi qu'en excitant le système avec deux impulsions intenses non résonantes et décalées dans le temps, les effets non adiabatiques peuvent être dépendant de la phase. Ceci conduit à un contrôle très sensible par la phase de la population excitée. Cet effet peut être utilisée pour créer de nouvelles techniques en interférométrie. En régime d'impulsions longues, nous présentons une nouvelle méthode de ralentissement de la lumière qui peut être réalisée dans un système à deux niveaux double interagissant avec deux impulsions de lumière polarisées orthogonalement et se propageant selon des axes différents. La dépendance spatio-temporelle de la polarisation totale induit un réseau dans la cohérence Zeeman du fondamental. Le champ le plus intense (champ de contrôle) est diffracté par ce réseau dans la direction du champ sonde de faible intensité compensant l'absorption de ce dernier. Une fenêtre de transparence est alors créée dans le spectre d'absorption de ce champ conduisant au ralentissement de la lumière. La fenêtre de transparence exhibe alors des caractéristiques similaires à ceux obtenus par la méthode EIT (electromagnetic induced transparency). Toutefois la différence importante avec la méthode EIT est que dans notre cas aucun état noir n'est créé dans le système. Ceci ouvre la voie à la possibilité de ralentir la lumière dans des systèmes plus complexes. D'autre part, quand l'absorption (linéaire) du système est éliminée, la réponse non linéaire devient plus importante. Dans la situation où les champs se propagent dans la même direction et ont même fréquence, deux régimes d'interactions ont été étudiés. Pour de faibles épaisseurs optiques, la susceptibilité effective se comporte comme $\chi_{lin}e^{2i\phi}$ avec ϕ la différence de phase entre champs. Ceci rend alors possible le contrôle de la réponse du milieu par la phase. Le milieu peut se transformer d'un absorbant à un amplificateur avec une dispersion normale ou anormale en ajustant la phase relative ϕ. En régime de large épaisseur optique, la saturation de la phase se produit et la susceptibilité effective se trouve changée en χ_{lin}^*, modifiant un absorbant en un amplificateur sans affecter la réponse dispersive.

Mots clés : Effets de propagation, contrôle cohérent, mise en forme d'impulsions, transitions non adiabatiques, ralentissement de la lumière,